TRANSITIONAL CONTROLLER DESIGN FOR ADAPTIVE CRUISE CONTROL SYSTEMS

Zeeshan Ali

BEng Mechanical Engineering

**Thesis submitted to the University of Nottingham
for the degree of Doctor of Philosophy**

December 2010

This thesis is dedicated to my parents
Mumtaz and Ali
in love and gratitude

Abstract

Traffic congestion is an important reason for driver frustration which in turn is the main cause of human errors and accidents. Statistics reports have shown that over 90% of accidents are caused by human errors. Therefore, it is vital to improve vehicle controls to ensure adequate safety measures in order to decrease the number of accidents or to reduce the impact of accidents.

An application of mathematical control techniques to the longitudinal dynamics of a vehicle equipped with an adaptive cruise control (ACC) system is presented. This study is carried out for the detailed understanding of a complex ACC vehicle model under critical transitional manoeuvres (TMs) in order to establish safe inter-vehicle distance with zero range-rate (relative velocity) behind a preceding vehicle. TMs are performed under the influence of internal complexities from vehicle dynamics and within constrained operation boundaries. The constrained boundaries refer to the control input, states, and collision avoidance constraints.

The ACC vehicle is based on a nonlinear longitudinal model that includes vehicle inertial and powertrain dynamics. The overall system modelling includes: complex vehicle models, engine maps construction, first-order vehicle modelling, controllers modelling (upper-level and lower-level controllers for ACC vehicles). The upper-level controller computes the desired acceleration commands for the lower-lever controller which then provides the throttle/brake commands for the complex vehicle model.

An important aspect of this study is to compare four control strategies: proportional-integral-derivative; sliding mode; constant-time-gap; and, model predictive control for the upper-level controller analysis using a first-order ACC

vehicle model. The first-order model represents the lags in the vehicle actuators and sensor signal processing and it does not consider the dynamic effects of the vehicle's sub-models. Furthermore, parameter analyses on the complex ACC vehicle for controller and vehicle parameters have been conducted.

The comparison analysis of the four control strategies shows that model predictive control (MPC) is the most appropriate control strategy for upper-level control because it solves the optimal control problem on-line, rather than off-line, for the current states of the system using the prediction model, at the same time being able to take into account operation constraints.

The analysis shows that the complex ACC vehicle can successfully execute TMs, tracking closely the desired acceleration and obeying the constraints, whereas the constraints are only applied in the MPC controller formulation. It is found that a higher length of the prediction horizon should be used for a closed acceleration tracking. The effect of engine and transmission dynamics on the MPC controller and ACC vehicle performance during the gear shifting is studied. A sensitivity analysis for MPC controller and vehicle parameters indicates that a length of the control horizon that is too high can seriously disturb the vehicle behaviour, and this disturbance can be only removed if a higher value of control input cost weighting is used. Furthermore, the analysis indicates that a mass within the range of 1400-2000 kg is suitable for the considered ACC vehicle. It is recommended that a variable headway time should be used for the spacing control between the two vehicles. It is found that the vehicle response is highly sensitive to the control input cost weighting; a lower value (less than one) can lead to a highly unstable vehicle response. It is recommended that the lower-level controller must take into account the road gradient information because the complex ACC vehicle is unable to achieve the control objectives while following on a slope.

Based on the results, it is concluded that a first-order ACC vehicle model can be used for the controller design, but it is not sufficient to capture the complex vehicle dynamic response. Therefore, a complex vehicle model should be of use for the detailed ACC vehicle analysis. In this research study the first-order ACC vehicle model is used for the complex vehicle validation, whereas the complex ACC vehicle model can be used for the experimental validation in future work.

Acknowledgments

I would like to express my sincere thanks to Mehran University of Engineering and Technology, Pakistan for giving me an opportunity to pursue PhD studies at University of Nottingham, UK.

I would like to express my gratitude to Prof. Atanas Popov for his invaluable support and patience throughout this project. I am grateful for his consistent motivation, encouragement, both personal and academic, and for his continuous guidance during the write-up of my thesis. I am most indebted to Dr. Guy Charles for his valuable direction and technical support, without which it would have been difficult to progress with the project.

I am appreciative of all my friends in and outside the Department for their extended support. I would like to thank my colleagues from the Structural Integrity and Dynamics research group, especially Tanweer Hussain Phulpoto, Shakir Jiffri, and Rupesh Patel for providing support during my tough time.

I am eternally grateful to my wife Mehreen and my brothers Sharjeel and Adeel for their constant love and strength throughout the years.

My very special thanks to my best friend Sofi Ali, without her, and her ability to raise my spirits when I was most discouraged, I could never made it this far. Sofi, you are the wind beneath my wings.

Contents

List of Figures

xiii

List of Tables

Nomenclature

d	Relative distance between the two vehicles
e	Error signal
$\mathbf{e}_k$	Discrete-time state space error vector
err_k	Position error
$\dot{err}_k$	Range-rate error
$\ddot{err}_k$	ACC vehicle's acceleration
g	Gravitational acceleration
h	Headway time
k_i	Sample time
m	Mass of the vehicle
$\mathbf{m}$	Sliding mode design constant
m	Time step
$\dot{m}_{ai}$	Mass rate of air entering the intake manifold
$\dot{m}_{ao}$	Mass rate of air leaving the intake manifold
$\dot{m}_f$	Mass rate flow of fuel
m_{man}	Intake manifold mass
m_{man_des}	Desired mass in the intake manifold
p_{man}	Intake manifold pressure
p_{man_des}	Desired intake manifold pressure
r_{eff}	Effective tyre radius
$r(k_i)$	Given set point
r	Rolling radius of the free-rolling tire
s	Sliding mode surface
t	Time

u	Control input
$v_{preceding}$	Preceding vehicle's velocity
ω_e	Engine speed
ω_p	Angular speed of pump
ω_t	Angular speed of turbine
ω_w	Angular speed of the wheels
ω_{wf}	Front wheel angular speed
ω_{wr}	Rear wheel angular speed
x	Vehicle position
x	State variable
y	Position to be controlled
y	System output

A	Discrete-time state space matrix
A_F	Frontal area
B	Discrete-time state space matrix
C	Discrete-time state space matrix
C_d	Aerodynamic drag coefficient
C_{of}	Longitudinal tyre stiffness of the front wheel
C_{or}	Longitudinal tyre stiffness of the rear wheel
F	Prediction model state space outputs matrix
F_{aero}	Aerodynamic drag force
F_x	Longitudinal traction force
F_{xf}	Longitudinal traction force on front wheel
F_{xr}	Longitudinal traction force on rear wheel
F_y	Tyre lateral force
F_z	Normal force on wheel
H_u	Fuel energy constant
I_e	Effective inertia of engine and torque converter's pump parts
I_w	Wheel inertia
J	Cost function index
J_e	Effective vehicle inertia
K	Control input constant for sinusoidal input

K_D	Derivative gain
K_I	Integral gain
K_P	Proportional gain
K_u	Proportional gain
L	Desired distance between the two vehicles
L_{th}	Stoichiometric air/fuel mass ratio of gasoline
MAX	Maximum intake flow rate
N_C	Length of control horizon
N_P	Length of prediction horizon
P_{atm}	Atmospheric pressure
P_u	Oscillation period
PRI	Pressure ratio influence
R	Range between the two vehicles
R	MPC control input cost weighting function
R	Gas constant of air
R_d	Final gear reduction in the differential
R_g	Gear ration in the transmission (g = 1,2,3,4,5)
R_s	Vector which contains the desired set point information
R_x	Rolling resistance on wheel
R_{xf}	Rolling resistance in front wheel
R_{xr}	Rolling resistance in rear wheel
S	Sliding mode surface
S_1	Sliding surface for throttle control
S_2	Sliding surface for brake control
T	Sampling time for MPC
T_a	Accessory torque
T_{bf}	Brake torque on front wheel
T_{br}	Brake torque on rear wheel
T_{bc}	Commanded brake torque
T_{bd}	Desired brake torque
TC	Throttle characteristics
T_f	Engine friction torque
T_i	Engine combustion torque
T_{load}	Load torque (represents the pump torque)

T_{man}	Intake manifold temperature
T_{net}	Engine net torque after losses
T_{net_des}	Desired engine net torque after losses
T_p	Pump torque
T_t	Turbine torque
T_w	Wheel torque
V_d	Displacement volume/Engine displacement
V_{man}	Intake manifold volume
V_{wind}	Wind velocity
V_x	Longitudinal speed of the vehicle
$\mathbf{Y}$	Vector of predicted output

σ_x	Slip ratio
σ_{xf}	Slip ratio of the front tyre
σ_{xr}	Slip ratio of the rear tyre
α	Throttle input
$\mathbf{\Phi}$	Prediction model state space outputs matrix
$\mathbf{\Delta U}$	Vector of predicted control input
Δu	Future control input in MPC control algorithm
η_{vol}	Volumetric efficiency
η	Sliding mode constant
η_i	Thermal efficiency
η_1	Sliding mode constant for throttle control
η_2	Sliding mode constant for brake control
θ	Gradient of the road
ρ	Air density
τ	Time delay
τ_b	Time constant for brake
λ_{CTG}	Weighting factor between $\dot{R}$ and δ
λ	Air/fuel equivalence ratio
δ	Inter-vehicle distance error

sgn(.)	Signum, sign function
(.)^T	Vector transpose

List of abbreviations:

ABS	Anti-lock brake system
ACC	Adaptive cruise control
AHS	Automated highway system
CACC	Cooperative adaptive cruise control
CTG	Constant-time-gap
CW/CA	Collision warning/collision avoidance
DOT	Department of Transportation
EGR	Exhaust gas recirculation
GPS	Global positioning system
HEV	Hybrid electric vehicle
IC	Internal combustion
MPC	Model predictive control
NVH	Noise, vibration, harshness
PID	Proportional-Integral-Derivative
PRI	Pressure ratio influence
PVC	Polyvinyl chloride
R	Range
SAACC	Semi-automatic adaptive cruise control
SIVD	Safe inter-vehicle distance
SISO	Single input single output
TC	Throttle characteristics
TCS	Traction control system
TM	Transitional manoeuvre
VGT	Variable time gap
VSC	Variable structure control

Chapter 1.   Introduction

1.1 Motivation

A large majority of the world's vehicles operate on roads, rather than on rails, on the air, or/in water. Highway congestion has become a serious problem in many urban areas. The main cause of the congestion is the travel demand which has exceeded the present highway capacity. The present highway capacity is not capable of smooth traffic flow which results in traffic congestion, unnecessary delays and accidents.

It was estimated by Fenton (1994) that in 2010 the travelling demand will be more than double as compared to 1992 travelling demand. It was also estimated that the average speed of vehicles during peak hours would drop to 11 mph in 2005 from 35 mph in 1995, which has a corresponding significant effect on productivity. Traffic congestion costs around $100 billion each year in the United States because of delays in productivity. The intensive vehicles emission, due to traffic congestion, affects the environmental issues up to the critical level and poses an ever-increasing damage to the public health. Each year around 2 billion gallons of fuel is wasted due to traffic congestion. The intensive vehicles emission affects the environment up to a critical level and poses an increasing damage to the public health. Along with the health and environmental issues, safety and comfort levels for the drivers and other passengers are significantly important (Terzano, 2001) in order to provide secure journeys. It has been analysed in a study that the traffic congestion is a big reason for personal frustration which in turn is the main cause of human errors and accidents (Fenton, 1994).

A statistical report (Report., 1992) has shown that over 90% of accidents are caused by human errors. Only a small percentage of the accidents is caused by vehicle component errors or due to weather conditions e.g. raining, slippery roads.

Table 1-1 shows the accident statistics on Great Britain roads, the figures shows that car users account for most of the accidents (Unknown, 2009). Therefore, it is vital to improve the present vehicle's control to ensure the safety measures in order to reduce the number of accidents or reduce the impact of the accidents. A reliable highway infrastructure is required which can significantly reduce the causes of these affects and ensure the safety and provide a comfortable less-stress driving. The core problems or issues are the significant number of fatalities from car accidents all over the world, especially in Great Britain, safety and control, traffic congestion, vehicle emission, and environmental effects. Among these issues, car accidents, safety and control of a passenger car have been focused in this study.

As the travelling demand increased over the years, the highway networks were also expanded to meet the requirements. At some point it was not feasible to extend them because, if the existing highway networks are further increased then this will increase the economical burden coupled with high construction costs and the difficulties faced in expanding the current highway infrastructure. Expanding the existing highways is no more useful in most of the urban areas because of the increasing travelling demands (Terzano, 2001). These social and economical challenges have triggered interest in alternate methods to increase the highway capacity.

In order to overcome these problems an efficient infrastructure for the highway network is required. The concept of Automated Highway System (AHS) is one of the approaches which are under considerable research to overcome the problems. In the last few years the research work has been focused to investigate how safety measures and comfort level in urban areas and highway transportation networks can be improved by means of on-board intelligent driver assistance systems.

1.2 The Concept of Automated Highway Systems

Significant research effort has been dedicated within the last 20 years to the development of AHS (Huang and Chen, 2001; Shladover, 2005), most noteworthy research group is the California PATH program at the University of California, Berkeley (Hedrick *et al.*, 1993; Hedrick *et al.*, 1997; Swaroop, 1997). Its main objectives are making the driving safer and more comfortable, and to develop the means to reduce the undesirable traffic congestion on highways. These objectives are achieved by making vehicles travel together in tightly spaced platoons. An AHS system requires that only instrumented fully-automated vehicles are allowed on this special highway while the other manually operated vehicles cannot operate on these highways. Recent advances in the technology have facilitated the development of the necessary components of an AHS. Over the last two decades, the technology developments in control systems, computer technology, sensor technologies, communication systems and data processing capabilities have provided constructive support to automate the decision-making process and execution of driving manoeuvres with greater accuracy.

An important aspect of AHS is the automatic vehicle itself which is intended to improve the driver's control and relieve the driver of some or all of the driving tasks. An automated vehicle is equipped with different intelligent systems e.g. anti-lock brake system (ABS), traction control system (TCS), adaptive cruise control (ACC) system, and automatic collision avoidance systems. The automated systems reduce the traffic congestion by enabling vehicles to travel in the form of platoon by keeping a safe distance and provide driver assistance and help to reduce the driver burden which certainly leads to reduced accidents (Rajamani, 2006). There are number of approaches designed in the literature to increase the safety on the AHS. ACC is one of the approaches which have attracted the attention of the vehicle manufacturers and users in order to serve as a mean of providing comfort and safety for the drivers. An ACC is an autonomous system which requires further modifications and can significantly help to overcome the causes of the problems stated in Section 1.1. This study focuses on the vehicles equipped with an ACC system, and the problems associated with these vehicles have been reviewed in detail in Chapter 2.

3

1.3 Adaptive Cruise Control Systems

Standard cruise control is a familiar example of a longitudinal controller that controls the speed of a vehicle. The control system operates on the throttle to maintain the desired speed specified by the driver (Girard *et al.*, 2005; Rajamani, 2006). The cruise control system can become a source of irritation for the driver if he/she has to set the speed or disengage the cruise control in a heavy traffic. With traffic continually increasing, the basic cruise control is becoming less useful. The performance of cruise control can be improved by adding a distance sensor, radar sensor, and equip the vehicle with a limited authority braking system which controls the distance and relative velocities between a vehicle and a preceding vehicle (Haney and Richardson, 2000). This modified cruise control system is termed as Adaptive Cruise Control (ACC) and the vehicles equipped with an ACC system are also termed as 'thinking' cars. ACC technology is widely regarded as a key component of any future generations of intelligent cars (Ioannou, 2003).

There are number of upscale vehicles which are equipped with the ACC system. Mitsubishi were the first to introduce a laser-based ACC system in 1995, although their early system did not use the brake actuators and the speed could only be controlled by throttle control and transmission down-shifting (Naranjo *et al.*, 2003). The other manufacturers who also offer an ACC system in their vehicles are; Audi, BMW, Jaguar, Mercedes-Benz (Naranjo *et al.*, 2003; Girard *et al.*, 2005).

Ioannou (2003) stated that ACC vehicle is the first step for collision avoidance systems and can be beneficial for future vehicle automation. A survey accomplished by the Foundation for Traffic Safety (Unknown, 2008) has revealed that 76 % of the ACC vehicle users are happy to use ACC technology in their vehicles. The other key finding of this survey are that 38% of ACC users think that using ACC made them a safer driver than using standard cruise control system and only 7% had the opposite opinion. More than half of the ACC users have agreed that they tend to change lane less frequently and using ACC system relieves them from stress while driving. It has been noticed that most of the ACC users do not know about the ACC system limitations and they have a false assumption that an ACC system would help avoid a collision. This survey reveals that the old drivers prefer more ACC systems than young drivers, as an ACC system can assist elder drivers more safely with less

stress. Despite all this acceptance from the ACC system users, it was found that 30% of the ACC users have reported a need for improvement in the current ACC system. The areas suggested for the improvement are the occurrence of unsafe and uncomfortable reduction or increase in the speed and the sensitivity of the system.

Out of these areas this study is focused on the improvement in the unsafe and uncomfortable reduction in speed which also takes in account the physical limitations of the ACC system- equipped vehicles. Thus, an ACC vehicle is required to execute the higher deceleration manoeuvres to avoid the accidents or reduce the severity of the accidents. During these manoeuvres it is necessary to investigate the response of the ACC vehicle and its controllers. Because this sudden deceleration may affect the controllers response which will in turn affect the ACC vehicle response. Therefore, a detail understanding of an ACC vehicle is necessary under these critical manoeuvres. Furthermore, an ACC vehicle requires an optimal control strategy to execute these critical manoeuvres.

Road Users	All reported casualties				Reported killed or seriously injured casualties			
	2006	**2007**	**2008**	**2009**	**2006**	**2007**	**2008**	**2009**
Car Users	66.1	65.1	64.6	64.5	44	42.2	41.9	41.3
Motorcycle Users	9	9.5	9.3	9.3	20.3	22	21	21.6
Pedal Cycle Users	6.3	6.5	7	7.7	7.7	8.3	9	10
Others	18.6	18.9	19.1	18.5	28	27.5	28.1	27.1

Table 1-1   Accident statistics in Great Britain (road user's percentage), (Unknown, 2009).

Chapter 2. Literature Review

2.1 Introduction

The motivations discussed in Chapter 1 emphasize to improve the present vehicle's control to ensure the safety measures in order to reduce the number of accidents or reduce the impact of the accidents. The intelligent vehicle proposed in order to address these issues is equipped with the adaptive cruise control (ACC) system. The main objectives for an ACC vehicle to achieve are to reduce the number of accidents by executing the higher deceleration or transitional manoeuvres (TMs). A survey reported a need for improvement in the current ACC system especially during the unsafe/uncomfortable reduction in speed which should take in account the physical limitations of the ACC-system equipped vehicles in order to avoid the collision or severity of the collision. According to Ioannou (2003), an ACC system is the first step for collision avoidance systems and can be beneficial to reduce significantly the number of accidents or their severity. Before reviewing the relevant research work conducted in the field of ACC systems, it is necessary to understand the nature of the control model presented and the effects generated by difference sources on the performance of an ACC system.

As mentioned above that during the critical TMs an ACC vehicle has to perform high decelerations in order to avoid the collision from the vehicle in front of it or from any other stationary and moving obstacle. An ACC vehicle consists of different sub-models; the engine, transmission, and driveline (Connolly and Hedrick, 1999; Li *et al.*, 2010). In addition to that, an ACC vehicle comprises the upper-level and lower-level controller models (Rajamani, 2006). Thus, the combined models consist

of a large number of state variables which, during a TM, have a corresponding affect on the performance of the ACC vehicle. Therefore, it is important to understand from the previous studies that how these affects have been taken in account.

The dynamic response of an ACC vehicle is influenced by the desired control input computed by the upper-level controller (Connolly and Hedrick, 1999; Rajamani, 2006). The desired control input in turn is affected by the variation in the states variables of the ACC vehicle itself. There are number of forces which influence the dynamic response of the ACC vehicle. These forces can be traction force, aerodynamic force, force exerted due to rolling resistance in the tyre, gravitational force, forces due to transmission up-shifting and down-shifting, brake force, and come from a number of resources. The combined effect of these forces plays a vital role in the overall stability characteristics of the ACC vehicle. Among these forces, the brake force is the most influential force in order to perform a TM for the ACC vehicle to avoid a collision with the preceding vehicle.

The motivations discussed in Chapter 1 lead to the need of a complex ACC vehicle model for the longitudinal dynamic control which should reflect the physical features of the realistic model, the characteristics of the sub-models, and a stable coordination among these sub-models. It is also equally important to use an optimal control method which can compute the control laws for the ACC vehicle to track smoothly the desired acceleration commands and at the same time should respect the unavoidable physical constraints associated with the vehicles equipped with the ACC system. In this document the physical constraints have also referred as operational constraints.

Significant amount of research efforts have been conducted in the areas of engine dynamic control system, automatic transmission dynamic control system, and drivetrain dynamic control system. The combination of all these sub-systems forms a dynamic model of a complete vehicle which can be used to analyse and improve the response of the real vehicle. This vehicle dynamic control model is useful to improve the design characteristics of the sub-models, and can help to improve and support the manufacturing process; can considerably help to understand the physical characteristics of the entire system. Furthermore, this complex vehicle

longitudinal dynamic control model will be analysed in this study using the automotive vehicle following systems.

Automotive vehicle following systems are essential for the design of automated highway system. An ACC system is one of the important control systems used to provide safety and less-stress driving characteristics in the present upscale vehicles (Haney and Richardson, 2000). Different control algorithms for the longitudinal control of an ACC have been reviewed based on different spacing policies and communication link between the vehicles.

In this chapter significant research work will be reviewed in the area of vehicles equipped with adaptive cruise control (ACC) system. Section 2.2 outlines the basic vehicle models for the longitudinal dynamics control. The aim is to explore the vehicle powertrain models which can capture the essential dynamics of all the sub-systems and can guarantee a stable coordination among the sub-models. The focus here is to understand that how these models affect the vehicle overall performance and what are their roles towards the control of the vehicle longitudinal dynamics. In Section 2.3 various ACC vehicle models will be reviewed based on different vehicle longitudinal dynamic control models. The ACC vehicle models range from simple first-order models to complex vehicle models. These sections provide important background knowledge about the ACC vehicle models developed in the previous studies and help exploring the opportunities for a novel research work in the field of automated vehicle systems.

2.2 Vehicle Dynamics Models

Modelling of the vehicle's sub-models is difficult because the dynamic characteristics of these sub-models are non-linear and time-varying. Basically, two different types of model have been developed for the purpose of controller synthesis. The 1st type is based on the physical models which are derived from fundamental mathematical laws. The advantage of this type of model is that the governing equations for the system are expressed in terms of physical parameters and can be used to evaluate the controller performance for a range of different operating conditions. The disadvantage of the physical model is that the nature of

model is very complex and cannot practically calculate the actual parameters of the system (Ramli and Morris, 1991).

The 2nd type is based on the empirical models where the models are based on the measured data. The functional relationship between input and output is determined by mapping techniques to obtain the steady-state response or by statistical correlations to evaluate operation using measured engine data (Ramli and Morris, 1991).

2.2.1 Engine Models

Most of the engine models discussed in the previous studies are concerned with combustion dynamics control, pollution formation control, or engine dynamics control. There has also been a great deal of development in the area of automotive powertrain system dynamics for control during automotive transmission up-shifting and down-shifting of gear ratios.

Engine is a non-linear and time-varying system whose dynamic is mainly influenced by an induction-to-power delay (Feng *et al.*, 2005). One of the first engine models studied was developed by (Powell, 1979). His model is a combination of first-principle, physical laws, and identification techniques using empirically obtained data for the specific engine. Powell (1979) study is mainly focused on dynamic characteristics of throttle system, intake manifold dynamics, sonic EGR valve, fuel injection system, and engine power system.

The state equations for the intake manifold are obtained by considering the law of conservation of mass to the intake manifold (Cook and Powell, 1988; Cho and Hedrick, 1989). Rajamani, R, (2006) has used the manifold pressure as a state variable by considered the ideal gas equation to relate mass and pressure. The engine rotational dynamics is concerned with the indicated torque, friction torque, and load torque (Cho and Hedrick, 1989; Chaing *et al.*, 2007).

Cook and Powell (1988) have presented a nonlinear model of a spark ignition engine. Their engine model consists of a throttle body, intake manifold dynamics, engine pumping phenomena, induction process dynamics, fuel system, engine

9

torque generation, and rotating inertia. They have derived a linear model of the spark ignition engine from the nonlinear model and produced the simulation results using the static experimental data.

Cho and Hedrick (1989) have presented a concise mathematical model of automobile powertrain dynamics, which consists of a four-stroke spark-ignition engine with automatic transmission system. Their model captures the important dynamics even during the transmission gear shifting, also including the throttle input characteristics and dynamic constraints to remain in a certain gear ratio. All the necessary friction forces and resistances have also been taken in account during the simulation development process. Their work preserves the generic nature of the modelling and can be adapted for a vehicle longitudinal dynamics control analysis.

Rajamani (2006) has studied mean-value spark-ignition engine models based on previous studies. The engine models discussed are neither detailed cycle-by-cycle models nor empirical models but are intermediate between these two categories and can still predict the mean values of major engine variables, like crank shaft speed and manifold pressure in time domain. According to his study such models can be well utilized for longitudinal vehicle control applications. He has presented the parametric mean-value engine models and mean-value engine models based on engine maps, the steady-state engine maps have also been reviewed in his study. Engine maps have been widely utilized in longitudinal dynamic control applications. For a particular engine size, the engine maps can be generated with the help of dynamometer tests which is very time consuming and expensive process (Ganguli and Rajamani, 2004). Rajamani (2006) has presented the rotational dynamic of the engine in the form of mathematical equation in terms of indicated torque, pump torque, friction torque, and accessory torque. The mathematical expressions for each term have also been presented.

Ganguli and Rajamani (2004) have also presented a similar mean value spark ignition model as studied by Rajamani (Rajamani, 2006). They have further extended their study to identify certain parameters of vehicle dynamic model which can be derived directly by analytical methods and are not part of the standard sub-model specifications, e.g. maximum intake flow rate (MAX), the volumetric efficiency, and the constants associated with friction and pumping losses. The

algorithm they have used to identify these parameters is least-square algorithm and the parameter identification has been obtained directly from on-the-vehicle road tests. Chaing, *et al.* (2007) have also presented a mean value engine model for a 4-stroke single cylinder gasoline engine which uses an automatic throttle control for maintaining a fixed speed. In these kinds of engine models the throttle plate is not controlled mechanically using the accelerator but controlled electrically based on the current powertrain operating conditions. These types of engines are only suitable for the control of small cylinder gasoline engine such is mower where speed control is needed.

Puleston, *et al.* (2001) have presented the non-linear sliding-mode technique in order to control the speed on the automotive engine. The engine model presented in their study is an empirical model, where, the engine torque, load torque, air mass flow in and out are obtained through the experimental methods. A number of constants have also been obtained for these variables using the experimental data. The main objective of their study is to steer the engine speed to the desired engine speed when subjected to the uncertainties in the system and the load torque disturbance on the engine.

Ni and Henclewood (2008) have presented three different simple engine models in order to compare the engine power and engine torque against the engine speed with no dynamics included in these models. The three models they have presented are polynomial model, parabolic model, and Bernoulli model and are based on steady-state calculations. They have used these models for four engine's specifications in order to compare and obtain the best engine model. The four engines used are 2008 Mercedes CLS, 2006 Honda Civic, 2006 Pagani Zonda, and 1964 Chevrolet Corvair. The simulation results obtained from these engines are then compared with an empirical model in order to validate the three different approaches. The models presented in their study are not suitable for the study carried out in this thesis as these models doesn't consider the dynamic involved in the engine and transmission.

A hybrid electric vehicle (HEV) engine model (Feng *et al.*, 2005) has been reviewed where an IC engine is combined with an electrical motor in order to run the engine at its most efficient speed and to lower emissions and fuel consumption. The differential equation presented for rotational dynamics is similar to what reviewed

in Cho and Hedrick (Cho and Hedrick, 1989) and Ganguli and Rajamani (2004) models. It has been stated in this paper that the addition of an electrical motor lowers the emission and improves the fuel consumption but also increases the speed oscillation which is disadvantage of using an electrical motor. In order to damp out the oscillation they have used a Fuzzy-PID controlled governor which also improves the fuel consumption, drivability and noise, vibration, harshness (NVH). They have shown the engine profile for a transient operation, where, the engine speed has increased from 1500 rpm to 4000 rpm which is meeting the requirements of their controller. However, it doesn't show in their result that the engine dynamics considers the dynamics during the transmission gear shifting. It can be observed that their simulation shows the engine speed during idling. Yi and Chung (2001) and used a simplified engine model where the net engine torque is computed using the steady state engine map based on the engine speed and the throttle angle.

2.2.2 Transmission Systems

Transmission is mechanical device that transmits power from engine to the wheels. It provides different gear or drive ratios between the engine and drive wheels of an automotive vehicle. Its main function is to enable the vehicle to accelerate from rest through a wide speed range while the engine operates within its most effective speed range. There are mainly three types of transmission system used in automobile; manual transmission, automatic transmission, and dual clutch transmission. The main objective of these three transmission systems is the same but the objective is accomplished in an entirely different way.

A manual transmission is a geared system which reduces the road-load to a suitable amount before engaging to the engine. It mainly translates the engine revolution speed to an appropriate vehicle speed. In manual transmission system another mechanical device called clutch, which is manually operated, is used in order to engage or disengage the engine and transmission system. The clutch pedal is stepped down during gear shifting and released smoothly after a proper gear is engaged (Hong, 1996). A manual transmission is beyond the scope of this study but

its basic principal is covered for the fundamental understanding of a transmission system in comparison with the automatic and dual clutch transmission systems.

An automatic transmission performs the same purpose as the manual transmission but it uses a torque converter between engine and transmission system rather than using a manually operated clutch. The torque converter is a type of fluid coupling that connects the engine to the transmission. A torque converter consists of a pump (driving member), a turbine (driven or output member), and a stator (reaction member). The pump is attached to the engine and turns at engine speed, and the turbine is the input to the transmission (Cho and Hedrick, 1989). The main advantage of using the torque converter are its fluid coupling property, its damping characteristics and its torque multiplying characteristics (Cho and Hedrick, 1989; Zhang *et al.*, 2002). Usually an automatic transmission system consists of two interconnected planetary gears, final drive unit, associated clutches and bands and uses the clutch and band pressures information supplied by the transmission hydraulics model to determine the transmission torque. The output of the torque convertor is connected to the two interconnected planetary gears and the final drive output is connected directly to the driveshaft of the vehicle (Zhang *et al.*, 2002). The transmission hydraulics model uses the engine speed, manifold pressure and desired gear-ratio information to calculate the pressure build-up profiles in the clutch cavities (Runde, 1984; Zhang *et al.*, 2002). Vehicles equipped with automatic transmission provide advantages such as easy operation, smooth acceleration and safety. This transmission system selects gears automatically based on the power required in various driving situations and conditions.

The third type of transmission is the dual-clutch transmission system, sometime referred as twin-clutch or semi-automatic transmission system which works like a two manual gearboxes (Goetz *et al.*, 2005). In order to understand the working principal of a dual-clutch transmission system it's necessary to understand the conventional manual gearbox. In a manual transmission vehicle when driver wants to change from one gear to another, he first presses down the clutch pedal. This disconnects the engine from the gearbox and interrupts power flow to the transmission. The driver then uses a stick shift to select a new gear which moves a toothed collar from one gear to another gear wheel of different size. Once the new gear is engaged, the driver releases the clutch pedal, which reconnects the engine to

the gearbox and transmits power to the wheels. It can be observed from this discussion that there is no continuous power flow from the engine to the wheels. Instead, power supply changes from on to off to on during gear-shifting, this phenomenon is called 'shift shock' or 'torque interrupt' (Harris and Beckman, 2010). On the contrary, a dual-clutch gearbox uses two clutches and has no clutch pedal. Sophisticated electronics and hydraulics control the clutches in a similar way as in automatic transmission system. Both clutches operate as an independent unit, one clutch controls the odd gears, while the other controls the even gears. In this arrangement, the gear can be changed without interrupting the power flow from the engine to the transmission (Harris and Beckman, 2010). In this study an automatic transmission system will be used, therefore, the dual-clutch transmission system has not been reviewed in detail.

Cho and Hedrick (1989) has presented a two-state and four-speed automatic transmission model and have simulated the transition between first gear and second gear. The two states are the turbine speed and the reaction carrier speed. In their model they have used a combination of two planetary gears which is also called compound planetary gear set. The dynamic equations for the first and second gears and the conditions to stay in gear and to start the transition between these two have also been defined in their paper. The simulation results produced in their work has been used for the validation for this thesis work. Zhang, *et al.* (2002) have also presented a similar work which also describes the transient dynamics of a four-speed automatic transmission system in order to investigate the transient characteristics during the gear changes. A torque convertor model, hydraulic system module, geartrain module and modules of clutches and bands have also been developed in their paper. The transient characteristics are then used to determine the optimum pressure profiles for the shifting elements.

Han and Yi (2003) have presented an automatic transmission model in order to investigate the shift transient characteristics which is equipped with a Ravigneaux-type planetary gear set. In their study optimum clutch pressure trajectories are constructed and engine torque reduction characteristics are determined in order to improve the shift transient characteristics.

Short, *et al.* (2004) have presented a report on safety and reliability of distributed embedded systems. They have developed mathematical models for the sub-systems which comprise a complete vehicle model and can be used to analyse the longitudinal dynamic of the vehicle. In their work they have adopted a different approach to perform the transmission gear shifting. The shift maps for the automatic transmission up-shifting and down-shifting are constructed in order to perform the gear shifting, where the gear up or down shifting is performed as a function of throttle input and the wheel speed. In their study they have used a 5-speed automatic transmission system; however, they haven't shown the dynamic effects developed by the gear shifting in their simulation.

Wu, *et al.* (2008) have presented a fuzzy control strategy to perform the transmission up-shifting and down-shifting using the shift maps. The control parameter to operate the shifting is the vehicle acceleration. When the vehicle's acceleration is positive the system is controlled by up-shifting controller and when the vehicle's acceleration is negative the system is controlled by down-shifting controller. Runde (1984) has presented a detailed automatic transmission model which intend to control the dynamics during the transmission gear shifting. They have analysed the transient effect on the overall vehicle performance during the first to second gear shift. Rajamani (2006) have presented a simplified automatic transmission model and have not discussed the necessary conditions for the gear up-shifting and down-shifting. Their transmission model does not consider the planetary gear set and the other elements associated with it.

2.2.3 Drivetrain Dynamics

A drive-train serves as a simple power transfer device between the transmission and the vehicle. The angular velocity of the transmission output is the input to the drive shaft. Cho and Hedrick (1989) and Hedrick, *et al.* (1993) have presented a three-state drivetrain model where the three states are axle torque, front wheel speed and the vehicle longitudinal speed. However, the differential equation for the wheel speed in Cho and Hedrick model (1989) does not include the brake torque which means that they have simulated the powertrain model using the throttle control only. On

the contrary Rajamani (2006) has proposed a separate model for wheel dynamics and vehicle longitudinal dynamics. He has established a direct relation between the wheel angular speed and transmission speed. In his model the final gear reduction in the differential is included in the transmission gear ratio.

The traction force generated by the tyre model or brake force applied to tyre model is the function of longitudinal tyre slip ratio. The slip ratio can be defined as the difference between the actual longitudinal velocity at the axle of the wheel and the equivalent rotational velocity of the tyre (Chen and Shih, 2004; Rajamani, 2006).

Mathematically the longitudinal slip ratio is defined as (Fling and Fenton, 1981).

$$\sigma_x = \frac{r_{eff}\omega_w - V_x}{V_x} \qquad \textbf{(During deceleration)} \qquad (2.1)$$

$$\sigma_x = \frac{r_{eff}\omega_w - V_x}{r_{eff}\omega_w} \qquad \text{(During acceleration)} \qquad (2.2)$$

where, V_x is the longitudinal speed of the vehicle, r_{eff} is the effective radius of the wheel, and ω_e is the angular speed of the wheel. One can conclude from the definition that when $\sigma_x = 0$ the wheel is in perfect rolling i.e. moving without slipping, on the contrary, when $\sigma_x = 1$ then the wheel is locked and pure sliding occurs and this happens during the hard braking manoeuvre (Wong, 2008). A tyre is subjected to different ground forces e.g. longitudinal force, normal force, and lateral force. The longitudinal force is generated during driving and braking, the normal force is due to the weight and load of the vehicle, and the lateral force helps the vehicle in turning and manoeuvring (Chen and Shih, 2004).

The wheel dynamic model presented by Yi and Chung (2001) is the function of the driving axle shaft torque, longitudinal forces, wheel rolling resistances, and wheel brake torque. The driving axle shaft torque has been defined in terms of turbine torque of the torque converter using the transmission gear ratio which includes the final drive gear ratio. The longitudinal force presented in their paper is based on empirical formula which is usually obtained through the experimental measurements. Rolling resistance is an opposing force to the motion of the vehicle

and is roughly proportional to the normal forces acting on each tyre. Brake torque is an opposing torque to reduce the speed the vehicle when ever desired (Wong, 2008).

Longitudinal dynamics of a passenger car is mainly influenced by longitudinal traction force on front and rear tyres, aerodynamic force, rolling resistance, brake torque, and gravitational force (Wong, 2001). Different differential equations of motion have been developed and used in order to simulate the longitudinal dynamic behaviour of a passenger car. Cho and Hedrick (1989), Rajamani (2006) , Short, *et al.* (2004), Yi and Chung (2001), and Hedrick, *et al.* (1993) have presented different state variables for the longitudinal motion of a vehicle. The simulation result by each study has been produced as expected.

2.2.4 Brake Systems

In the daily routine driving situations a human driver applies two different control inputs in order to control the speed of a vehicle; the accelerator/throttle input and brake input. The vehicle under these inputs is considered as an open loop system as the vehicle doesn't need to follow a desired variable. In the case of standard cruise control system the vehicle has to follow a desired user-set speed and the control system operates on the throttle input in order to maintain the desired speed, this system is called a closed loop system. Furthermore, the safety and comfort level can be improved if a vehicle is equipped with an ACC system. In the case of ACC system the control system operates on throttle and brake actuators in order to maintain a desired speed and a safe distance from a vehicle in front of it. As a requirement of this study both, an open loop and a closed loop brake models have been reviewed. In the case of closed loop brake model the desired brake torque is the function of desired acceleration.

In the simulation scenarios the ACC vehicle has to perform critical TMs to reduce the speed in order to avoid the collision with its preceding vehicle, only a throttle control input cannot bring the vehicle in rest position within a short stopping distance, a brake control system is also required to stop the vehicle and avoid the collision with a preceding vehicle. Various brake control model have also been

reviewed so a suitable brake system could be developed to perform the braking manoeuvres.
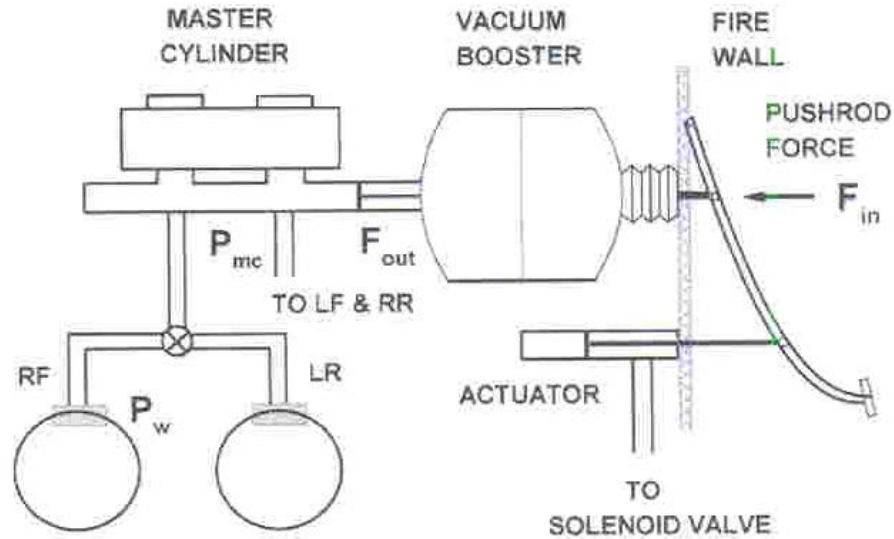
Figure 2-1   Brake system (Liang *et al.*, 2003)

Figure 2-1 shows different components of one of the brake system used in modern cars (Liang *et al.*, 2003). A brake system usually consists of brake pedal, vacuum booster, master cylinder, slave cylinders, actuator, solenoid valve, etc. With their combination a higher multiple of the force applied on the brake pedal is obtained on the wheels to reduce the speed of vehicle. The description and modelling details of these components is not the part of this study. The brake actuator is controlled by a solenoid valve; the hydraulic system which consists of a master cylinder and slave cylinders generates pressure on the wheels. The brake torque obtained on the wheel is proportional to this wheel pressure through a gain (Yi and Chung, 2001).

There are several factors which significantly influence the brake model behaviour. Some considerable discussed are frictional coefficient, the effective radius of the wheel at which the brake is applied and the servo effect (in the case of drum brake). It should be noted that the friction coefficient is a non-linear function of wheel speed and brake pad temperature (Hedrick *et al.*, 1997).

The initial automatic brake control model was presented by Maciuca, *et al.* (1994) which achieved very good speed following in the experimental phase. Gerdes and Hedrick (1996) have argued that the brake system for platooning control should bypass the vacuum booster to avoid the delays in the time response. Maciuca and Hedrick (1995) have developed a non-linear brake system for a vehicle-platoon control. Based on the shortcomings in the previous models they have developed a second generation brake controller which designed in a way to bypass the vacuum booster in the automatic vehicle following mode while in the manual driving mode the driver can still take advantage of the vacuum booster. They have identified that the vacuum booster has a very low actuation bandwidth caused by the air flow dynamics. This results in a weak control on the pressure in the vacuum booster. In this way the bandwidth of the system has been increased by eliminating the air flow dynamics in the vacuum booster. On the contrary, Liang, *et al.*(2003) have used a variable parameter sliding mode control approach to reduce the errors generated in the vacuum booster.

Yi and Chung (2001) have presented a solenoid-valve-controlled hydraulic brake actuator model for vehicle collision warning/collision avoidance (CW/CA) systems. They have used a non-linear vehicle model to investigate the effects of brake control on the vehicle's response with CW/CA systems. They have developed an approximated linear second-order system for the brake hydraulic dynamics where the dynamic equations are defined in terms of brake pressure at the wheel. The input to the system is given through the solenoid valve and the system works as an open loop system. The brake pressure is related to the brake torque through a non-linear function and does not consider the time constant of the brake line. They have also developed a closed-loop brake model for a vehicle-platoon where the control input to the brake system is the function of desired acceleration required to maintain a safe distance from a preceding vehicle. They have used the sliding mode control method for the brake model in order to achieve the desired objectives.

2.3 Adaptive Cruise Control System

Control problems arising in automatic vehicle-following systems have been receiving increasing attention, due to requirements for high safety and traffic capacity. Decreasing inter-vehicular spacing is the major way to increase highways capacity. There are several approaches that can be used to increase the traffic flow. Automated vehicle is one of the approaches which are getting the attention from manufacturers and the academia in order to provide safety and comfort to the drivers and other road users. Other important aspects of the automated vehicles are to improve the traffic flow, reduce the number of accidents, reduce the vehicle emission and traffic congestions by maintaining a continuous traffic flow (Shladover, 2005).

Two different approaches of an automated vehicle are reviewed here. One of them requires the communication among the vehicles, and the road infrastructure through navigation devices. These vehicles require a modified automated highway system which should be equipped with computerised and navigation devices in order to set the communication among automated vehicles. Important issue here is that these automated vehicles cannot operate with the conventional vehicles. On the other hand the vehicle equipped with an adaptive cruise control (ACC) system can operate on its own and can travel with other conventional vehicles. An ACC is an autonomous system which does not require modified road infrastructure to communicate with other vehicles. An ACC vehicle (Liang and Peng, 1999; Swaroop *et al.*, 2001; Rajamani and Zhu, 2002; Sun *et al.*, 2004; Girard *et al.*, 2005; Martinez and Canudas de Wit, 2007) is equipped with radar or a similar sensor to measure the distance from a preceding vehicle.

In both approaches the vehicles travel in the form of a platoon. A platoon (automatic vehicle following system) can be defined as group of vehicles travelling together with relatively small spacing to improve capacity and to minimize the relative velocity of the vehicles in case of emergency (Huang and Chen, 2001). The stable behaviour of a platoon can be achieved if the individual vehicle stability and string stability of the platoon are ensured (Rajamani, 2006). String stability of a string of vehicles refers to a property in which spacing errors are guaranteed not to amplify as they propagate towards the tail of the string (Swaroop *et al.*, 2001; Rajamani and

Zhu, 2002; Sun *et al.*, 2004; Rajamani, 2006). In some studies a two-vehicle system (Bageshwar *et al.*, 2004; Bleek, 2007; Li *et al.*, 2010) which consists of a preceding vehicle and an ACC vehicle has been considered where a detailed analysis of the ACC vehicle has been carried out. Noteworthy analysis have been carried out during the critical driving situations using a simple ACC vehicle model (Bageshwar *et al.*, 2004) which requires further investigations when a lower level controller and a complex vehicle model is used under the same critical driving situations.

ACC vehicle has two modes of steady state operation: speed control and vehicle following control (Rajamani, 2006). In the speed control mode, much like a cruise control system, ACC vehicle travels at user set speed. In the vehicle following mode, ACC vehicle maintains a desired spacing from the preceding vehicle. ACC control the throttle and brake to maintain that desired distance. The longitudinal control model of an ACC vehicle is usually composed of two separate controllers, the upper level controller and lower level controller (Connolly and Hedrick, 1999; Rajamani *et al.*, 2000). The upper level controller uses the range (spacing difference) and range-rate (velocity difference) between the ACC vehicle and its preceding vehicle and the ACC vehicle's velocity and acceleration to determine the acceleration commands to perform the manoeuvres required in the spacing-control law of the ACC vehicle. The lower-level controller uses this acceleration signal to generate the throttle and braking commands to track the spacing-control law computed by the upper-level controller.

There are mainly two types of controllers for an ACC vehicle; *longitudinal control*, which deals with the spacing regulation without considering the steering, and the *lateral control,* which controls the steering of the vehicle to keep it in lane. This study focuses only on longitudinal control of the vehicles equipped with ACC system, i.e. the vehicles are moving in a straight line.

2.3.1 Vehicle Models for ACC Analysis

A number of vehicle models equipped with an ACC system have been reviewed in the literature.

2.3.1.1 Simple ACC Vehicle Models

Simple ACC vehicle models have been presented in the previous studies to analyse the performance of the upper level controller. Some authors have used a longitudinal vehicle model (Sheikholeslam and Desoer, 1993; Swaroop and Hedrick, 1999; Huang and Chen, 2001; Swaroop *et al.*, 2001; Sun *et al.*, 2004; Ferrara and Vecchio, 2007) where input to the vehicle is the desired acceleration obtained from the upper-level controller algorithm. While some authors have simulated the desired acceleration computed from the upper-level controller (Peppard, 1974; Rajamani and Zhu, 2002; Bageshwar *et al.*, 2004; Yi and Chong, 2005; Rajamani, 2006) and have simulated the ACC vehicle's acceleration by considering a first-order lag due to finite bandwidth of the lower level controller. It has been argued by Rajamani, R., (2006) and Li *et al.*, (2010) that the desired acceleration cannot be obtained instantaneously, therefore, a first-order lag due to the finite bandwidth of the lower-level controller must be taken in account.

2.3.1.2 Complex ACC Vehicle Models

The desired acceleration obtained from the upper-level controller is then given to a complex vehicle model which also incorporates the lower-level controller model (Connolly and Hedrick, 1999; Li *et al.*, 2010). The desired acceleration commands are first received by the lower-level controller which computes the required throttle and brake commands for the complex vehicle model to track the desired acceleration.

2.3.2 Control Algorithms

In literature, a number of control algorithms have been developed for the upper level controller task. The control algorithm computes the desired acceleration using the states information of the preceding and the ACC vehicle itself. Previous studies reviewed have used a proportional-integral-derivative (PID) control (Peppard, 1974; Murdocco *et al.*, 2000), sliding mode control (Gerdes and Hedrick, 1997; Connolly and Hedrick, 1999; Rajamani *et al.*, 2000; Sun *et al.*, 2004; Girard *et al.*, 2005; Ferrara and Vecchio, 2007), constant-time-gap (CTG) (Bageshwar *et al.*, 2004; Rajamani, 2006), and model predictive control (MPC) (Bageshwar *et al.*, 2004; Corona and

Schutter, 2008; Li *et al.*, 2010; Li *et al.*, 2010; Zlocki and Themann, 2010). The relevant studies in which these control strategies have been used will be reviewed in detail in Section 2.3.6.

2.3.3 Spacing Control Strategies

2.3.3.1 Constant spacing

Different approaches to control the spacing between the vehicles have been discussed in the literature. Swaroop and Hedrick (Swaroop and Hedrick, 1999) have debated on the performances of a platoon based on different spacing strategies and the information available for the controlled vehicle. They have presented different control algorithms using the constant and variable spacing control strategies with the information of reference vehicle, lead vehicle and preceding vehicle to the controlled vehicle. They (Swaroop and Hedrick, 1999; Swaroop *et al.*, 2001) designed a decentralized controller which is based on a constant spacing policy where the desired inter-vehicle distance is independent of the velocity of the controlled vehicle. Swaroop and Hedrick (Swaroop and Hedrick, 1999) used the information of vehicles in front of the controlled vehicle for vehicle following control algorithm. They discussed the limitations and problems associated with other control strategies like autonomous control, semi-autonomous control, controller with the information of the reference vehicle only, controller with the information of lead vehicle and preceding vehicle, semi-autonomous control with vehicle ID knowledge, controller with information of only "r" immediately preceding vehicles, mini-platoon control strategy, mini-platoon control with lead vehicle information. They argued that the control algorithms which do not use the lead vehicle information result in the weak string stability. Also these controllers are not robust to signal processing/actuator lags.

2.3.3.2 Variable spacing

The ACC vehicle model presented by Bageshwar *et al.*, (2004), Liang and Peng (1999), Sun *et al.*, (2004), Ferrara and Vecchio (2007), Rajamani and Zhu (2002), Girard *et al.*, (2005), Martinez and Canudas de Wit (2007), Naranjo *et al.*, (2003) have

used a variable spacing control policy which is based on the headway time where the desired inter-vehicle distance is not constant but varies linearly with vehicle's velocity. The headway time can be defined as the time taken by the follower vehicle to reach the point where the preceding vehicle is at present speed (Naranjo *et al.*, 2003). As discussed above that the two important performance criteria, for vehicle following control, are the individual vehicle stability and the string stability of the platoon (Rajamani, 2006). For a constant spacing policy, ACC vehicle satisfies the individual vehicle stability condition but the string stability condition is not satisfied. Rajamani (2006) and Canudas de Wit and Brogliato (1999) have concluded that the constant spacing policy is unsuitable for autonomous control operations. Therefore, the headway spacing policy should be adopted for ACC systems.

Some studies (Yi and Horowitz, 2002; Wang and Rajamani, 2004) have focused on the ACC vehicle's impact on the traffic flow stability. Wang, J and Rajamani, R, (2004) have developed a new spacing policy called variable-time-gap (VTG) which results in a higher highway capacity and a stable traffic flow as compared to traditional headway spacing policy but at the cost of a decrease in safety. The inter-vehicle distance is a non-linear function of the vehicle velocity in the case of VTG.

2.3.4 Interaction with Preceding Vehicle or Lead Vehicle

Different types of communication network among the vehicles travelling in the form of a platoon have been presented. Global communication network, wirelessly linking the vehicles, uses the highway infrastructure to transmit the lead vehicle information to the following vehicles at the cost of introducing and maintaining continuous inter-vehicle communication (Shladover, 1991). On the contrary, local/decentralized communication network links the predecessor and follower vehicles, where the controlled vehicle uses the relative information of the preceding vehicle's position, velocity and acceleration (Liang and Peng, 1999; Swaroop *et al.*, 2001; Yi and Chong, 2005; Ferrara and Vecchio, 2007) based on feedback linearization. Global communication networks causes noise in the measurement and inaccuracies in the performance of the platoon and increases the cost of the operation (Sheikholeslam and Desoer, 1993). Global communication links, due to

setting the link between the lead vehicle and the following vehicle through the highway infrastructure, can be avoided by using the local communication network.

Sheikholeslam and Desoer (1993) presented a vehicle platoon model based on global communication. They designed a control law in the case if the communication between the lead vehicle and other vehicles is the platoon is lost or if there is no communication between the lead vehicle and other vehicles. In the case of full communication the deviation in vehicle spacing increases down the tail of the platoon, resulting, a higher acceleration command for each vehicle in the platoon downstream. They have analysed that with no communication these effects can be reduced.

2.3.5 Transitional Manoeuvres for Accident Avoidance

An ACC vehicle operates in the speed control mode when there is no vehicle in front of it (like a standard cruise control system). When a vehicle is encountered in front of the ACC vehicle at a certain distance (this distance is defined by the range of the radar sensor) then the mode of operation is switched to the vehicle following mode (Rajamani *et al.*, 2000; Rajamani, 2006; Li *et al.*, 2010). It is not always necessary that an ACC vehicle has to perform steady-state operations (Sheikholeslam and Desoer, 1993; Liang and Peng, 1999; Sun *et al.*, 2004; Zlocki and Themann, 2010) , it might need to execute the transient operations, e.g. it might encounter a slower or halt vehicle in front of it (Connolly and Hedrick, 1999; Bageshwar *et al.*, 2004) in the same lane or during a cut in (another vehicle comes in between ACC and preceding vehicles when ACC vehicle is in vehicle following mode) from another lane (Kato *et al.*, 2002), or sudden braking applied by the preceding vehicle (Li *et al.*, 2010; Li *et al.*, 2010) or stop & go scenario (Murdocco *et al.*, 2000; Bleek, 2007; Martinez and Canudas de Wit, 2007). In every situation the acceleration tracking capability of an ACC vehicle must be of high accuracy (Rajamani, 2006).

2.3.5.1   Acceleration limits and tracking capability during TMs

An ACC system provides safety and convenience and can be viewed as a first step toward collision avoidance and future vehicle automation (Ioannou, 2003). During the TMs, due to higher deceleration and unsafe/uncomfortable reduction in the speed, an ACC vehicle must take into account the comfort level of the passengers. This comfort level has been defined by applying the upper and lower limits to the acceleration of the ACC vehicle (Bageshwar *et al.*, 2004; Rajamani, 2006; Li *et al.*, 2010). The acceleration limits considered in Bageshwar *et al.*, (2004) model are 0.25g and -0.5g and in Li *et al.*, (2010) model the upper and lower limits are 0.5 m/s^2 and -1.5 m/s^2 respectively. The acceleration limits assumed by Bageshwar *et al.*, (2004) are much higher than Li *et al.*, (2010), therefore, the former acceleration limits have been assumed in this study during the TMs to avoid the collision with the vehicle infront of it.

It is equally essential for an ACC vehicle to accurately track the desired acceleration commands computed by the upper level controller. Due to the inertia of the ACC vehicle and the dynamic changes in the engine, torque converter, transmission system, and lower-level controller the tracking capability is seriously disturbed (Rajamani *et al.*, 2000; Li *et al.*, 2010; Zlocki and Themann, 2010). The critical TMs simulated (up to upper-level controller level) by Bageshwar *et al.*, (2004) have not been analysed using the lower-level controller and a complex vehicle model, where, the deceleration limits are higher than the previous studies.

2.3.5.2   Control objectives during critical TMs

Different approaches for an ACC vehicle model have been developed in previous studies. The control objectives vary from situation to situation and the nature of the model developed. For example, some researcher have investigated the string stability (the spacing error never amplify down the platoon) of the platoon of ACC vehicles (Liang and Peng, 1999; Rajamani *et al.*, 2000; Rajamani and Zhu, 2002), some researchers have analysed the lane merging and lane split operations (Huang and Chen, 2001; Kato *et al.*, 2002), others have focused on the ACC vehicle's fuel economy (Li *et al.*, 2010; Li *et al.*, 2010; Zlocki and Themann, 2010) and the driver's

response (Li *et al.*, 2010). In all studies the common control objective for an ACC vehicle is to track accurately the desired acceleration commands computed by the upper level controller. During a critical TM the acceleration tracking task is more challenging, because due to the deceleration limits an ACC vehicle is not allowed to apply the necessary brake torque to avoid a collision with any object in front of it, which causes the brake torque saturation. An important aspect that needs to be investigated is the acceleration tracking capability of a complex ACC vehicle model in the presence of internal complexities of the vehicle dynamics and within the predefined constrained boundaries.

2.3.5.3   ACC vehicle's operational constraints

There are mainly three types of operational constraints which are frequently encountered in control engineering applications. The first two types are applied on the control input variable and the third type of constraint is applied on the state variable or the output variable (Wang, 2009). In the previous studies (Bageshwar *et al.*, 2004; Li *et al.*, 2010; Li *et al.*, 2010), for an ACC system the upper and lower acceleration limits are translated as control input constraints. Collision avoidance has been included as state constraint. The condition ensuring the ACC vehicle has a nonnegative velocity has been also formulated as state constraints. All these constraints will be included in the control algorithm formulation to execute the required TMs.

2.3.6 ACC Systems Studies

In early studies, Peppard (1974) designed a PID feedback control algorithm for the string stability of relative motion for individual vehicle which uses the velocity error of that vehicle from a specified value and its distance error to the vehicle ahead and the vehicle behind while a constant spacing policy has been adopted. His model disregarded the actuation and sensing lags of the system operations. One drawback of the PID controller is that if the controlled model is nonlinear and the initial condition changes then it will be necessary to retune the controller gains in order to keep the desired performance. As the technology advanced in the platoon dynamics

control systems, PID controllers were modified and replaced by advanced controllers. The widely used controllers in the literature are adaptive controller, sliding mode controller, predictive controller, switching mode controller, transitional controller and so on.

One of the initial platoon models for the automated longitudinal control of the vehicles has been propoded by Shladover (1991) where the model is designed to maintain a very small distance of 1 meter among the vehicles. He has focused on the effects of severe manoeuvres, rapid changes in acceleration and jerks, measurement noise and different vehicle propulsion dynamics (due to less responsive power-train and dynamics of internal combustion engine which include both first-order and transport lags). In his work he has simulated a five vehicle platoon which is reaching the highest desired velocity of 2 m/s which is far less than the velocity considered in the present research work. Also, 1 m distance among the vehicles could possibly be critical if the dynamic of any of the vehicle is interrupted.

Canudas de Wit and Brogliato (1999) reviewed some stability issues regarding safe control of the platoon of the vehicles. Their analysis shows that the conditions for the string stability in the previous studies are not sufficient to avoid the collision. They have observed that there are some initial conditions which lead to the vehicles collision. They have referred the problem of designing the safe controllers for the internal dynamics of the platoon of ACC vehicles as the objective for the future work. Previous studies focused on the effects of parametric uncertainties on the performance of the platoon. Shladover (1991) and Swaroop *et al.*, (2001) have analysed the behaviour of platoon in the presence of uncertainties in mass, aerodynamic drag coefficient, and rolling resistance.

Sun *et al.*, (2004) presented a model of a platoon of ACC vehicles and used sliding model control method to compute the control laws for the following ACC vehicles. The ACC vehicle has been analysed under the steady-state operation, only the longitudinal dynamic model has been considered which does not include the internal dynamics of the complex vehicle sub-model e.g. engine model, torque converter model, transmission model with no brake input to the model as well. They have estimated the parameters for the vehicles which can improve the stability of the platoon under the parametric uncertainties due to varying road conditions

like weather changes or road gradients. Their controller achieves the platoon stability as the parameter estimates converge to their true values.

Rajamani and Zhu (2002) have developed a semi-autonomous ACC (SAACC) system, where the ACC vehicle is equipped with radio receiver on its front bumper and a radio transmitter on its rear bumper. The advantage of using these equipments is that if the preceding vehicle is also equipped with the SAACC system then the ACC vehicle can follow the preceding vehicle closer and if the preceding vehicle is not equipped with radio devices that it follows as a standard ACC equipped vehicle. They have only produced a design model of the upper level control which does not include the complex dynamics of the real vehicle.

Girard *et al.,* (2005) tested an Adaptive Cruise Control (ACC) and Cooperative Adaptive Cruise Control (CACC) system using real-time, embedded, hybrid control software while tracking the speed profile and vehicle following applications for passenger vehicles. They have developed a two-vehicle system for ACC vehicle analysis and have used the sliding mode control to obtain the control laws for the ACC vehicle. According to their study the sensor used in an ACC vehicle is subjected to the noise and requires heavy filtering and eventually cause a delay in the system performance. They have replaced the position sensor with the wireless communication link between the two vehicles where both vehicles can communicate the information with each other; this modified system is called as CACC system. It should be noted that this wireless communication system requires an advanced highway infrastructure and cannot perform the operation with the conventional vehicles. The ACC vehicle has been analysed under the steady-state operation and within the small range of vehicle speed which does not reach the acceleration/deceleration limits. Ferrara and Vecchio (2007) have presented the platoon model of ACC vehicles which is based on the sliding mode control method. They have developed the control strategies to avoid a collision with any obstacle in front of it. Their proposed model does not take in account the complex dynamics of the engine, transmission and brake models during the ACC vehicle analysis. Even the velocity profiles of the following vehicles are unstable and noisy during the transition operation and it takes longer time to achieve the steady state operation. A robust control algorithm is required for the stable response of the ACC vehicle's analysis.

Liang and Peng (1999) have also presented a platoon model which consists of ACC vehicles. Again the control law is based on the sliding mode control method and the ACC vehicle's analysis is carried out for a steady state operation where the vehicles are travelling within the comfort level. Here, comfort level means that the ACC vehicles are travelling within the acceleration and deceleration limits. For the simulation scenario they have presented the ACC vehicles do not need to apply the brakes, therefore, no brake model is developed while a disturbance caused by the lane changes have been included in the simulation program. A servo-level control has been designed which ensures the string stability and the desired acceleration commands are closely followed. With the growing popularity and wide acceptance, it is necessary that a complex ACC vehicle should be analysed for critical driving situations.

Yi and Chong (2005) designed an impedance control system which uses serial chain of spring-damper to generate the link between the vehicles. The lead vehicle's information propagates to the following vehicles through the elasticity of the spring-damper. The spring-damper is a force control strategy to minimize the effects of forces exerted from uncertain environment. Although their model is stable in the presence of noise and parametric uncertainties, it suffers in the situation when high acceleration and deceleration are applied to any one of the platoon's vehicle. Martinez and Canudas de Wit (2007) proposed a non-linear model with simple feedback loop to compensate for the un-modelled dynamics and external disturbances and the control algorithm uses the acceleration signal of the lead vehicle to maintain the safe distance among vehicles.

Huang and Chen (2001) introduced a control theorem for merging and splitting of the vehicle platoon with other platoons based on a safe velocity profile which is outside the scope of this study. Kato *et al.,* (2002) proposed a model which uses the current speed of the preceding vehicle as control input for the following vehicle; tracking the maximum acceleration and deceleration coupled with road geometry and adopted the real-time data transmission characteristics for the inter-vehicle communication control. They have used the global positioning system (GPS) and other communication devices in order to read the information of the preceding vehicle or any other obstacle in front of it.

Naranjo *et al.*, (2003) has presented a fuzzy logic basic ACC controller where only the throttle input is applied to the ACC vehicle model. They have used an electronic interface to generate the electrical signal to the accelerator pedal using the onboard computer. They used different reference velocity profile for the ACC vehicle analysis which does not required any brake input for the ACC vehicle, also the complex dynamics of the vehicle's sub-models have not been covered in their study.

Rajamani *et al.*, (2000) presented an ACC-vehicle-platoon model for the longitudinal dynamic control analysis. Each vehicle model consists of the upper level and lower level controller, the control algorithm in the upper and lower level controller is based on the sliding mode control method. The platoon is analysed only for low speed operation which only requires the throttle control and no brake control. The vehicles have a communication link between each other and are based on a constant spacing policy where the average spacing between the vehicles is 6.5 m. It should be noted here that constant spacing could be critical in severe driving situations.

Hedrick *et al.*, (1993) and Swaroop (1997) have presented a vehicle-platoon model for longitudinal dynamic control for automated highway systems. They have developed a detail model of the vehicle dynamics, upper-level and lower-level control model. The control algorithm of the upper and lower level controller is based on the sliding mode control based. The simulation results show the throttle control for the following vehicles for the steady state operation and do not show the brake control for the platoon. Their models do not cover the dynamic effects generated by engine model, transmission model, and brake model. However, they have shown the brake model for the lower-level controller and a switching logic between the throttle and brake control. It can be seen in their results that the platoon is manoeuvring within acceleration/deceleration limits and do not require brake inputs to reduce the speed of the vehicles. Gerdes and Hedrick (1997) have presented the engine and brake controllers, based on sliding mode control, for automated highway system and a swtiching logic between these two controllers. However, the velocity profile used for the vehicles changes within 3 m/s and the acceleration response changes between 0.7 to -1 m/s^2 which does not require brake control in order to control the speed of the vehicle. Also, the complex dynamics of the engine and transmission modes have not been taken into the account.

Connolly and Hedrick (1999) have presented a model to design the control laws for the upper level controller of an ACC vehicle under TMs in an automated highway system. The control algorithm in the upper-level controller is synthesized based on the sliding mode control theory. The TMs they have considered are within the 2 m/s velocity difference and do not reach the acceleration or deceleration limits and does not require brake actuator input to control the speed of the ACC vehicle. Their model doesn't consider the complex dynamics of the vehicle sub-models. Bageshwar *et al.*, (2004) have presented a two-vehicle system to analyse the ACC vehicle response against the critical transitional manoeuvres where the ACC vehicle reaches the acceleration/deceleration limits and requires the throttle and brake inputs in order to track the desired acceleration and to avoid a collision with the preceding vehicle. The control laws synthesized are based on the model predictive control (MPC) theory which can incorporate the acceleration/deceleration constraints within its control algorithm. They have design only the upper level controller and have used a first-order ACC vehicle for their analysis without the lower level controller model. Their analysis does not take in account the necessary dynamic effects generated by the engine model, transmission model during gear shifting, and brake model during the braking manoeuvres. Corona and Schutter (2008) have developed an ACC vehicle model for a SMART car and have addressed the piecewise affine (PWA) systems which are mainly based on MPC method. They have used different strategies for PI and MPC control methods in order to compare the features, advantages and disadvantages of each strategy. They have finally constructed a comparison (in the form of table) Benchmark for the different vehicle parameters and variables.

Zlocki and Themann (2010) have presented the unconstrained MPC based ACC vehicle model which also uses a digital map which contains the information about the surrounding environment such as lane inclination or maximum speed limitations. The main idea of using this digital map is to develop an energy efficient system as the fuel consumption and CO_2 emissions are the major issues for ACC vehicle design after the desired acceleration tracking issue. They have used a hybrid vehicle for the testing which operates under the throttle control. Li *et al.*, (2010) have addressed different issues related to an ACC vehicle in addition to the desired acceleration tracking. The other issues discussed are the low fuel consumption and

driver desired response characteristics. The control algorithm in the upper level controller is based on the MPC theory where they have also incorporated the constraints related to acceleration tracking, fuel consumption, and driver response characteristics, however, the ACC is only decelerated up to -2.5 m/s². Their simulation results show that the ACC vehicle is unable to track the desired acceleration precisely during the transition operation even in the presence of a first-order lag in the lower-level controller formulation.

In critical driving situations a human reaction capability is not reliable in order to avoid the accident because of the driver error during these emergency manoeuvres. The major reasons of the human errors are the frustration caused by the traffic congestion (Fenton, 1994) and the impact of shock in an emergency situation. On the contrary, a control system can react significantly faster than a human reacting in the same situation (Murdocco *et al.*, 2000). In previous studies, an upper-level control laws, using a simple ACC vehicle model, have been developed (Bageshwar *et al.*, 2004) for performing the longitudinal TMs where the deceleration limit is -4.9 m/s². The ACC vehicle model developed by Li *et al.*, (2010) shows a poor acceleration traction capability during a TM where the deceleration limit is only -2.5 m/s². The ACC model developed by Bleek, (2007) also tracks poorly the desired deceleration of -3 m/s², his model doesn't consider the affects of the transmission system on the controller performance.

In Section 2.3 various ACC vehicle models have been reviewed, the areas where these models require improvement have been discussed. The review of previous studies indicates that the complex ACC vehicle model has not been analysed for critical driving manoeuvres where the vehicle reaches the acceleration limits and the brake saturation occurs. It has also been observed that the dynamics effects generated by engine model, transmission model and brake actuator during the critical TMs have not been fully addressed in the previous studies.

The key features of a TM are to establish a zero-range-rate (relative velocity) at the point where the ACC vehicle maintains the safe inter-vehicle distance (SIVD) and avoid a collision with the preceding vehicle while performing the TM (Bageshwar *et al.*, 2004). During this TM the complex ACC vehicle should also take in account the physical constraints discussed in Bageshwar *et al.*, (2004). It is important to mention

here that due to these deceleration limits an ACC vehicle is not allowed to apply the necessary brake torque to avoid a collision with any object in front of it which causes the brake torque saturation. Therefore, a robust control method is required in order to cope with the nonlinearities of the complex vehicle model which can also compute the control laws in the presence of physical constraints. It is also vital to investigate the ACC vehicle response (using a complex vehicle model) when the physical constraints are only applied within the upper-level controller algorithm and the ACC vehicle has to obey it. These problems have been analysed in this study using a detail longitudinal dynamic control model of a vehicle in the presence of physical constraints.

2.4 Knowledge Gaps

The literature review shows that a significant amount of research work has been developed in the area of ACC vehicles. A number of ACC vehicle models and controller approaches have been developed which cover a wide range of ACC vehicle applications. Although an ACC vehicle has been analysed for a variety of situations in previous studies, its response needs to be investigated for the critical/emergency driving situations and under the influence of internal complexities of vehicle dynamics. Most of the work has been done, so far, for the unconstrained response of an ACC vehicle which provides new leads to investigate the constrained ACC vehicle response. The gaps in the reported research area are as follows:

- The analysis of a complex ACC vehicle model with lower-level controller under high deceleration manoeuvres and within the deceleration limit of up to -0.5g. It is yet to be investigated how the complex vehicle model and lower-level controller will respond under these emergency TMs in the presence of internal complexities of vehicle dynamics and operational constraints.
- The existing ACC vehicle models and control algorithms used for these models are not capable of tracking the desired acceleration commands during the TMs. Therefore, a deeper understanding of the entire system is required.

- Analysis and comparison of different control strategies for the upper-level controller under the same critical driving manoeuvres is needed.
- Analysis of throttle and brake actuators response of the complex vehicle model within the constrained boundaries is needed.
- Analysis of the dynamical effects of the vehicle's sub-models on the controller's and vehicle itself is necessary.

2.5 Research Aims and Objectives

The aims of the research are to obtain deeper understanding of the ACC system and to model and simulate the interaction between vehicle and the vehicle controllers. The measureable objectives are to develop generic mathematical models and to implement computer simulations in order to prevent pitfalls in practical design. This research is targeted at improved ACC system along with better road safety for reducing collision, casualties and deaths. After close examination of literature presented in this thesis and to fill the gaps in the knowledge this study proposes to meet the following study objectives:

- To adopt and extend existing vehicle models and implement detailed models containing all essential dynamic effects and nonlinearities in the considered vehicle systems.
- To design and compare vehicle controllers for longitudinal vehicle dynamics and for a generic set of critical/emergency manoeuvres by splitting the control task in to appropriate levels of control.
- To perform validation of models and verification of different control strategies and safety properties.
- To design a study methodology that can systematically analyse the ACC vehicle response.
- To conduct parameter studies with the aim to assess the performance of control system(s).
- Numerical testing of the complex ACC vehicle under the different situations.
  a. For different ACC vehicle masses
  b. For a different set of gear ratios
  c. For a cut-in manoeuvre

    d. For different values of headway time

    e. On a road gradient

The contribution of this thesis is towards the enhancement of the existing ACC systems. An entirely simulation-based approach is used in this thesis, with initial experimental data adopted from the existing literature. The vehicle and controller models are analysed by developing a software code in the environment of Matlab. The development of the overall system model includes the following stages of activity: vehicle modelling, controllers modelling, and their interaction. This analysis will help to improve the vehicle model and controller design parameters and provide direction for further research to improve the ACC vehicle performance.

2.6 Thesis Outline

An overview of the thesis structure is shown in Figure 2-2. The contribution of each chapter to fill the knowledge gaps is as follows:

Chapter 2: Chapter 2 presents the extensive literature review of the relevant studies and the identification of improvements which can enhance the performance of the ACC vehicle

Chapter 3: In Chapter 3, the following two types of the vehicle models will be developed which will be used for the ACC vehicle analysis.

1. Complex vehicle model

2. Simple first-order vehicle model.

The complex vehicle model consists of engine model, torque convertor model, transmission model, and drivetrain model. This vehicle model captures the important dynamic even during the transmission gear shifting. The simple first-order vehicle model is developed to analyse the upper-level controller using different control strategies. Simple vehicle model is also used as a first-order lag after the upper-level controller which corresponds to the lower-level controller performance.

The steady state engine maps are also constructed in this chapter in order to perform the calculations for the lower-level controller. Usually the data for the engine maps are provided by the manufacturers, but in this study the steady-state engine maps are constructed offline by computation using the Matlab software. The methodology of the research work carried out in this thesis is also presented in Chapter 3.

Chapter 4 and Chapter 5: In Chapter 4 and 5, four well-known control methods; PID, sliding mode, CTG and MPC method will be used to design the control-laws for the upper-level controller. In these chapters, the ACC vehicle is based on the simple first-order model. The idea of using a simple first-order ACC vehicle model is to compare the performance of these control methods at the upper-level controller level. After the comparison, the most appropriate, out of these four control methods will be applied to the lower-level controller and the complex vehicle model for longitudinal dynamics control of an ACC vehicle.

Chapter 6: In Chapter 6, the lower-level controller will be developed and the complex vehicle model will be used for the ACC vehicle analysis under the high deceleration manoeuvres. Robustness of the most suitable control method (among four mentioned above) and the response of the ACC vehicle and its actuators (throttle and brake actuators) in the presence of internal complexities of the vehicle dynamics and within the constraint boundaries will be analysed. The testing and sensitivity analysis of the ACC vehicle against some internal and external parameters is also carried out in Chapter 6.

Chapter 7: Chapter 7 presents the conclusion of this study and highlights the contribution of this study towards this research area. Further possible steps for the future work have also been suggested.
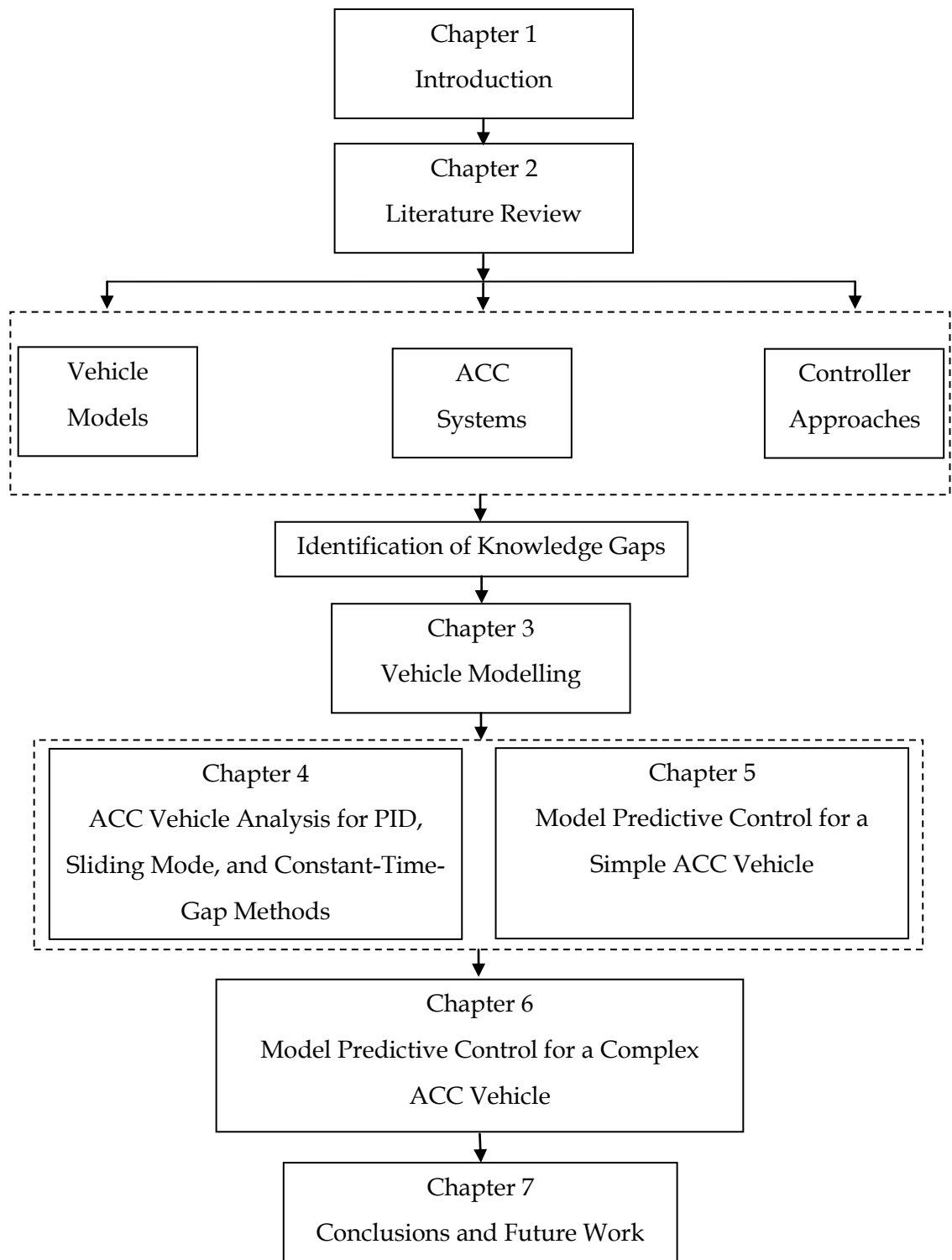
Figure 2-2   An Overview of the Thesis

Chapter 3.   Vehicle Modelling

3.1   Introduction

Vehicle dynamic models, adaptive cruise control (ACC) system, and platoon longitudinal dynamic control models have been reviewed in Chapter 2. Various ACC vehicle models (complex and simple vehicle models) for the longitudinal dynamic control have been developed in previous studies based on different control algorithms, different control strategies, medium of communication between ACC and other vehicles in the same lane. In the literature, the ACC vehicle has been analysed under various situations ranging from steady-state to transitional operations. Knowledge gaps have been drawn and to fill these gaps the study aims and objectives have been proposed in Chapter 2. The most important study objective is to develop a complex vehicle model to control the longitudinal dynamics which will be used to analyse the ACC vehicle response under high deceleration manoeuvres of up to -0.5g. A complex vehicle model is developed in this chapter. One of the important objectives of this study is to develop, analyse, and compare four control algorithms (Section 2.6) used for the upper-level controller under transitional manoeuvres (TMs) on a simple ACC vehicle model. In this chapter the simple ACC vehicle model has also been developed which will be used in Chapter 4 and Chapter 5 for the control algorithms analysis and comparison. After comparison the most appropriate control algorithm will be used for the complex ACC vehicle model in Chapter 6.

The research work available in the literature for the ACC vehicle is based on the vehicle dynamic model, while the effects associated with the internal complexities of the vehicle dynamics have not been addressed in detail. Here the internal complexities of the vehicle dynamics can be defined as the dynamic effects generated due to the automatic transmission up-shifting and down-shifting, sudden throttle input variations, at uphill, especially during the sudden braking manoeuvres while respecting the acceleration/deceleration limits and when the brake force saturates. It is necessary to analyse and understand the response of the vehicle following control law under these dynamic effects.

In this study a two-vehicle system is developed which consists of a preceding vehicle and an ACC vehicle. In order to analyse the longitudinal dynamics of an ACC vehicle a longitudinal vehicle dynamic model is required. The longitudinal vehicle model presented in this chapter is useful in the development of control systems for cruise control, adaptive cruise control and other longitudinal vehicle control applications. It is assumed that the same longitudinal vehicle model will be used for both vehicles. The complex vehicle model presented in this chapter will be analysed under different throttle inputs, and road gradient in order to investigate the behaviour of the vehicle during up-shifting and down-shifting. It should be noted that the developed vehicle model operates as an open loop system when it is used separately or for the preceding vehicle, while when it is used for the ACC vehicle it will operate as close loop system because the throttle and brake commands are determined by the feedback control laws obtained from the upper-level controller.

The two major components of the longitudinal vehicle model are the powertrain dynamics and the vehicle longitudinal dynamics. The automotive powertrain is divided into the following sub-models: an engine model, a torque converter model, an automatic transmission model, and a drivetrain model. The vehicle longitudinal dynamics are mainly influenced by the longitudinal tyre forces, aerodynamic drag forces, rolling resistance forces and the gravitational forces.

There has been a great deal of development in the area of automotive powertrain system dynamics for control during automotive transmission up-shifting and down-shifting. A complex automotive powertrain model based on the combination of Cho

and Hedrick (1989) and Rajamani (2006) models is developed based on the physical principles and captures the powertrain dynamics in the continuous-time domain which consists of four states. Several physical assumptions are made to simplify the mathematical modelling. To further simplify the model the gear up-shifting and down-shifting in the transmission model is controlled by transmission look-up tables (Kulkarni *et al.*, 2006; Rajamani, 2006) rather than a complex planetary gear system model. The look-up tables contain the gear up-shifting and down-shifting schedules and the gear transmission takes place using the information from these look-up tables. This approach has significantly saved the modelling and computation time. The simulation results, using these look-up tables, will be compared with the other automatic transmission models for the validation purpose.

Steady-state engine maps are constructed in this chapter. Usually the data for the engine maps is provided by the manufacturers, but in this study the steady-state engine maps have been constructed off-line by computation using the Matlab software.

Figure 3-1 shows a vehicle model which comprises of the sub-models developed in this study. The block diagram shows the inputs and outputs to each sub-model. The power generated in the engine by combustion of fuel travels from engine to the wheel through the crankshaft, torque convertor, transmission system, and driveline. Finally, the vehicle longitudinal motion is captured in continuous time domain using a set of differential equations.

Throttle
angle (α)

Engine
model

Engine speed
(ω_e)

Pump torque
(T_p)

Aerodynamic drag
force (F_{aero})

Torque
converter
model

Turbine angular
speed (ω_t)

Drivetrain

Turbine torque
(T_t)

Wheel angular speed (ω_w)

$x, \dot{x}, \ddot{x}$

Transmission
model

Wheel
model

Vehicle
longitudinal
dynamic
model

Wheel torque (T_w)

Traction force
(F_x)

Rolling
resistance
(R_x)
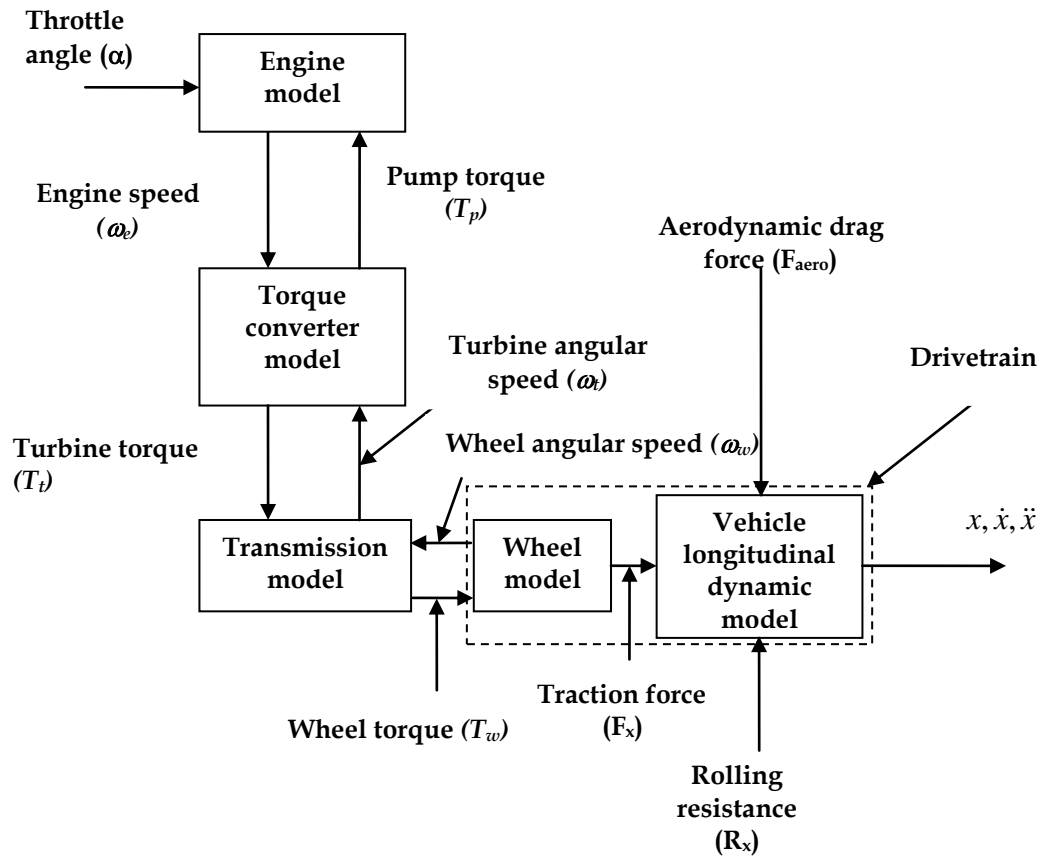
Figure 3-1   Block diagram for a single vehicle

This chapter outline is as follows. In Section 3.2 a mean-value engine model is developed. In Section 3.3 a torque converter model is presented. Section 3.4 presents 5-speed automatic transmission model which is based on look-up tables. Section 3.5 presents a two-state drivetrain model. The complex vehicle model developed is analysed against throttle and road gradient in Section 3.6. Section 3.7 presents 2nd order and 1st order engine map models. Simple vehicle model for the controller's analysis is developed in Section 3.8. The methodology to achieve the objectives of this study is laid out in Section 3.9. Finally, Section 3.10 presents the conclusions of this chapter.

The subsequent sections present the modelling of an engine model, an automatic transmission model, a drivetrain model, engine map models, and engine map construction. These models have also been validated at the end of each section.

3.2 Engine Dynamics

Most of the engine models are concerned with combustion dynamics, pollution formation, or engine dynamics control. The engine model required in this study is a dynamic engine control model. The type of engine model developed is called a mean value model (Cho and Hedrick, 1989; Rajamani, 2006). A mean value model is a mathematical engine model which is intermediate between large cyclic simulation models and simplistic transfer function models. It predicts the mean values of the engine states e.g. engine speed and the intake manifold pressure. The engine model is developed as torque-producing device with one inertia where the engine torque is the function of the throttle angle (α), mass flow rate of fuel ($\dot{m}_f$), and the engine speed (ω_e).

In this chapter a 3.8L spark-ignition engine model with six cylinders and a five-speed automatic transmission for a typical front-wheel-drive passenger car is developed where the input to the engine model is the throttle angle (α). The proposed mathematical engine model is used to control the longitudinal dynamics of the vehicle and can be divided into different subsystems namely throttle body, intake manifold, fuel injection, combustion chamber and torque production, and crank shaft rotation. The block diagram for all these subsystems is shown in Figure 3-2. The inputs and outputs for each block are also shown in Figure 3-2. The input to the throttle body is the throttle angle which can be controlled instantly and contains no dynamic elements; on the contrary, the modelling of the intake manifold is quite complicated. The input to the intake manifold is the air-fuel mixture. The combustion model of the engine calculates the indicated torque developed in the cylinders together with manifold pressure. The inputs to the combustion model are the throttle angle, and air-fuel ratio. The accelerating torque produced at the vehicle crankshaft is the difference between the indicated torque and the torque absorbed by friction torque, pump torque, and the load torque. The output from the engine dynamic is engine speed which is an input to the torque converter. The engine speed is fed back to the combustion model in order to compute the volumetric efficiency.

A continuous time domain, 2 state engine model based on the combination of Cho and Hedrick (1989) and Rajamani (2006) models is developed, where the two states

are intake manifold pressure (p_{man}) and the engine angular speed (ω_e). The intake manifold can be defined as the volume between the throttle plate and the intake valves of the cylinder. The mass of the intake manifold (m_{man}) can be related to the intake manifold pressure (p_{man}) using the ideal gas equation.

$$p_{man}V_{man} = m_{man}RT_{man} \qquad (3.1)$$

where, T_{man} is the manifold temperature which assumed as constant, R is the gas constant of air, and V_{man} is the intake manifold volume.
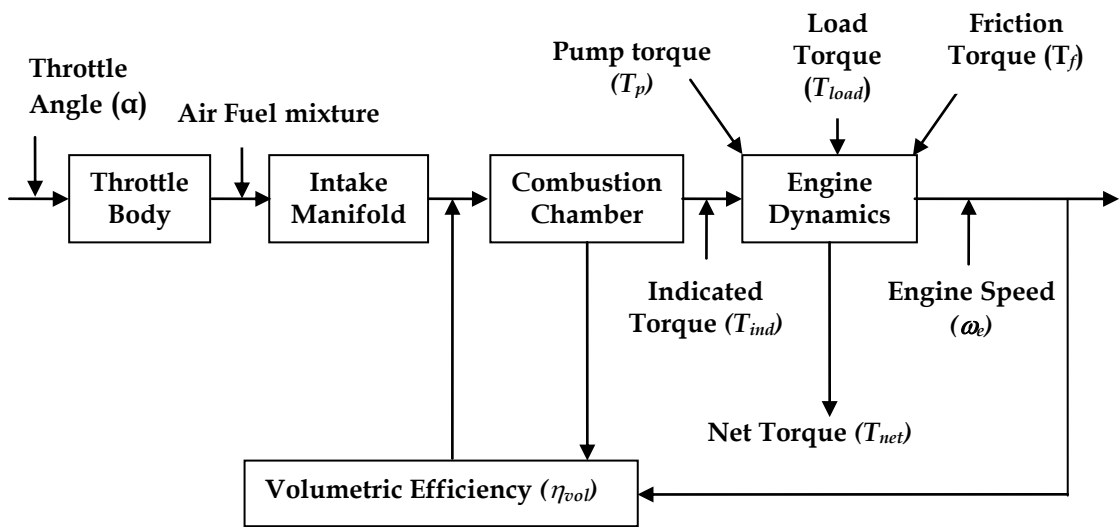
Figure 3-2   Block diagram for the engine model.

Taking derivative of Equation (3.1) gives the state equation for the intake manifold pressure.

$$\dot{p}_{man} = \frac{RT_{man}}{V_{man}}(\dot{m}_{man}) \qquad (3.2)$$

where, $\dot{m}_{man}$ is the mass flow rate in the intake manifold. When the law of conservation of mass is applied to the intake manifold then we get

$$\dot{m}_{man} = \dot{m}_{ai} - \dot{m}_{ao} \qquad (3.3)$$

where, $\dot{m}_{ai}$ and $\dot{m}_{ao}$ represent mass flow rate in and out of the intake manifold i.e. through the valve and into the cylinder respectively. Then Equation (3.2) becomes

$$\dot{p}_{man} = \frac{RT_{man}}{V_{man}}(\dot{m}_{ai} - \dot{m}_{ao}) \qquad (3.4)$$

The throttle body describes the transformation of throttle angle inputs to mass rates of air entering the intake manifold $\dot{m}_{ai}$, and is expressed by

$$\dot{m}_{ai} = MAX \cdot TC(\alpha) \cdot PRI \qquad (3.5)$$

where, MAX is the maximum flow rate of air through the throttle body. TC is the normalized throttle characteristics and is a function of throttle angle α (Cho and Hedrick, 1989).

$$TC = \begin{cases} 1 - \cos(1.14459 \times \alpha - 1.0600) & for \alpha \leq 79.46^0 \\ 1 & for \alpha > 79.46^0 \end{cases} \qquad (3.6)$$

PRI is the normalised pressure ratio influence and is a function of manifold to atmospheric pressure ratio. PRI can be defined as (Cho and Hedrick, 1989)

$$PRI = 1 - \exp\left[9\left(\frac{p_{man}}{P_{atm}} - 1\right)\right] \qquad (3.7)$$

$\dot{m}_{ao}$, the mass rate of air leaving the manifold (and thus, entering the combustion chamber), is dependent upon engine characteristics, e.g. displacement volume V_d, volumetric efficiency η_{vol}, intake manifold pressure p_{man}, and the engine speed ω_e and is described by (Rajamani, 2006)

$$\dot{m}_{ao} = \eta_{vol} \frac{\omega_e}{4\pi} V_d \frac{p_{man}}{RT_{man}} \qquad (3.8)$$

Volumetric efficiency η_{vol} is a complex function of the engine state ω_e. As discussed above the engine model from Cho and Hedrick (1989) and Rajamani (2006) models has been adopted in this study, the dynamics involved in the volumetric efficiency is not clear. It is very essential to incorporate the volumetric efficiency dynamics in this simulation model. Therefore, the η_{vol} as a function of engine speed given in

Heywood (1988) has been chosen to make the model more realistic and a similar curve for η_{vol} has been plotted and used for this model as shown in Figure 3-3.
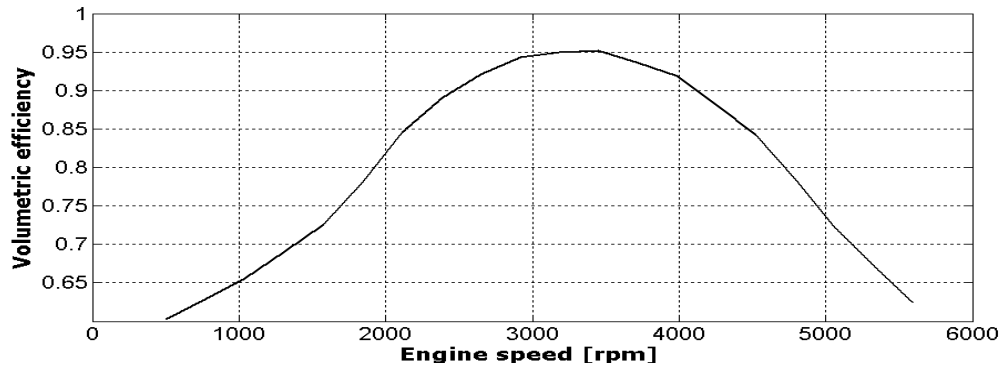
Figure 3-3   Volumetric efficiency as a function of engine speed

The second state concerns with the rotational dynamics of an engine. The crank shaft follows the conservation of moment about a rigid shaft.

$$I_e \dot{\omega}_e = T_i - T_f - T_a - T_p \qquad (3.9)$$

where, T_i is the engine combustion torque which is dependent on the ignition of a cylinder charge of air, fuel and residual gas (Cook and Powell, 1988), T_f is the engine friction torque, T_a is the accessory torque and T_p is the pump torque and represents the external load on the engine. I_e is the effective inertia of engine.

Equation (3.9) can be written as (Rajamani, 2006)

$$I_e \dot{\omega}_e = T_{net} - T_{load} \qquad (3.10)$$

where, $T_{net} = T_i - T_f - T_a$, is the net engine torque after losses and depends on the dynamics in the intake and exhaust manifolds of the engine and on the accelerator input from the driver. T_{load} is the load on the engine which represents the pump torque T_p. T_{load} is provided by the torque converter which couples the engine to the transmission.

The indicated torque T_i is generated by combustion and can be represented by (Rajamani, 2006)

$$T_i = \frac{H_u \eta_i \dot{m}_f}{\omega_e} \tag{3.11}$$

where, H_u is the fuel energy constant, η_i is the thermal efficiency multiplier, and accounts for the cooling and the exhaust system losses, and $\dot{m}_f$ represents the fuel mass flow rate into the cylinder. The fuel mass flow rate $\dot{m}_f$ is typically determined by a fuel injection control system which attempts to maintain a stoichiometric air to fuel ratio in the cylinder. It is assumed that the stoichiometric air fuel ratio is successfully maintained in the cylinder and the fuel mass flow rate $\dot{m}_f$ is related to the outflow from the intake manifold into the cylinder of the engine as follows (Rajamani, 2006):

$$\dot{m}_f = \frac{\dot{m}_{ao}}{\lambda \cdot L_{th}} \tag{3.12}$$

where, L_{th} is the stoichiometric air/fuel mass ratio for gasoline (fuel) and λ is the air/fuel equivalence ratio. The torque due to friction (T_f), is curve-fitted from experimental data and is the function of engine speed ω_e (Cho and Hedrick, 1989).

$$T_f = 0.1056\,\omega_e + 15.10 \tag{3.13}$$

3.3 Torque Converter

The output from the engine dynamic model is engine speed which is in turn an input to the torque converter. A torque converter consists of a pump (driving member), a turbine (driven or output member), and a stator (reaction member). The pump is attached to the engine and turns at engine speed, and the turbine is the input to the transmission (Cho and Hedrick, 1989). The torque converter uses the engine speed and transmission speed to compute the pump and turbine torques. The turbine torque is used to accelerate the mechanical elements of the transmission. The torque converter is a type of fluid coupling that connects the engine to the transmission. The torque converter is used in automatic transmissions for several reasons. First, its fluid coupling prevents an engine from stalling under high load conditions (e.g., idling while in gear with no vehicle motion). Second, its damping

characteristics isolate the drive-train from the engine firing pulses. Third, its torque multiplying characteristics are desirable for vehicle accelerations.

The schematic of a torque converter in Figure 3-4 shows the input, output and load associated with a torque converter. Engine speed is the input from engine model to torque converter model and the turbine torque is the output from torque converter model to the transmission model. The load from the transmission model is the transmission shaft speed which is transmitted to engine model through torque converter model in the form of pump torque.

Engine speed (ω_e) $\longrightarrow$ | **Torque converter Model** | $\longleftarrow$ *Transmission shaft speed (ω_t)*

Pump Torque (T_p) $\longleftarrow$ | | $\longrightarrow$ *Turbine Torque (T_t)*

Figure 3-4   Block diagram for torque converter model.

The equations for the pump torque T_p and turbine torque T_t can be found in (Cho and Hedrick, 1989)

For converter mode (ω_t / ω_p < 0.9), the pump and turbine torques are given by:

$$T_p = 3.4325es - 3\omega_p{}^2 + 2.2210x10^{-3}\omega_p\omega_t - 4.60141x10^{-3}\omega_t{}^2 \qquad (3.14)$$

$$T_t = 5.7656x10^{-3}\omega_p{}^2 + 0.3107x10^{-3}\omega_p\omega_t - 5.4323x10^{-3}\omega_t{}^2 \qquad (3.15)$$

For fluid coupling mode (ω_t / ω_p ≥ 0.9), the pump and turbine torques are given by:

$$T_p = T_t = -6.7644x10^{-3}\omega_p{}^2 + 32.0024x10^{-3}\omega_p\omega_t - 25.2441x10^{-3}\omega_t{}^2 \qquad (3.16)$$

The output from the torque converter i.e. turbine torque is the input to the transmission model. When the torque converter is locked then the pump torque is equal to the turbine torque and in term of load the pump torque is the load on the engine from the wheels and the transmission systems. On the contrary the torque converter is unlocked when the driver removes his foot from accelerator pedal and applies the brakes. This allows the engine to keep running even if the driver brakes to slow the wheels down.

3.4 Transmission Model

The output from the torque converter model is the turbine torque which is in turn the input to the transmission model. The transmission output torque is used to accelerate the vehicle against the aerodynamic drag load, the road friction, and road gradient loads. The transmission model considered is a five-speed automatic transmission model and also includes the final drive reduction in the differential; therefore, the operating gear ratio also includes the final gear reduction in the differential. Usually an automatic transmission system consists of several planetary gears and associated clutches and bands (Cho and Hedrick, 1989) and uses the clutch and band pressures information supplied by the transmission hydraulics model to determine the transmission torque. The transmission hydraulics model uses the engine speed, manifold pressure and desired gear-ratio information to calculate the pressure build-up profiles in the clutch cavities. While in this study instead of the complex mathematical automatic transmission model look-tables (explained below) have been used for gear up shift and down shift operation.

Turbine Torque → **Transmission Model** → Wheel Torque

Transmission shaft speed ← **Transmission Model** ← Wheel speed (ω_w)

Figure 3-5 Block diagram for the transmission model.

The schematic of a transmission model in Figure 3-5 shows the input and output associated with a transmission system. Turbine torque is the input from torque converter to transmission model and the wheel torque is the output from transmission model to the wheel model. The load from the wheel model is the wheel speed which is transmitted to torque converter model through transmission model in the form of transmission shaft speed.

If the torque transmitted to the wheels is T_w then for the steady-state operation under the first, second or higher gears of the transmission, the torque transmitted to the wheel is (Rajamani, 2006).

$$T_w = \frac{1}{R_g R_d} T_t \tag{3.17}$$

Similarly, the relation between the transmission and wheel speeds is

$$\omega_t = \frac{1}{R_g R_d} \omega_w \tag{3.18}$$

where, R_g is the gear ratio on the transmission (g = 1, 2, 3, 4, 5) and R_d is the final gear reduction in the differential. The value of R_g depends on the operating gear and increases as the gear shifts upwards.

Different automatic transmission models have been reviewed in Chapter 2 for various performance objectives. To avoid the complexities and to save the modelling and computation time mathematical model of a transmission system has been replaced by look-up tables. The look-up tables (Kulkarni *et al.*, 2006; Rajamani, 2006) have been used for a 5-speed automatic transmission up-shifting and down-shifting as shown in Figure 3-6, Figure 3-7, and Figure 3-8. The operating gear is determined by a gear shift schedule that depends on both the transmission shaft speed and the throttle opening in case of Rajamani (2006) look-up tables in Figure 3-6 and Figure 3-7, while the operating gear is obtained by a gear shift schedule in Kulkarni et al. (2006) look-up table in Figure 3-8 which is the function of the throttle angle and the longitudinal vehicle speed. The control strategy to decide and select the up-shifting or down-shifting control is the function of the acceleration of the vehicle (Wu *et al.*, 2008). When the acceleration is positive, the system is controlled by the up-shift controller and when the acceleration is negative the system is

controlled by the down-shift controller. The simulation results have been produced using both look-up tables and have been validated with the other models available in the literature. Note that the up-shift for each gear change occurs at higher speeds in comparison with the down-shift for each gear as the throttle input from the driver is higher.

Figure 3-6   Gear up-shift schedules for an automatic transmission, (Rajamani, 2006).
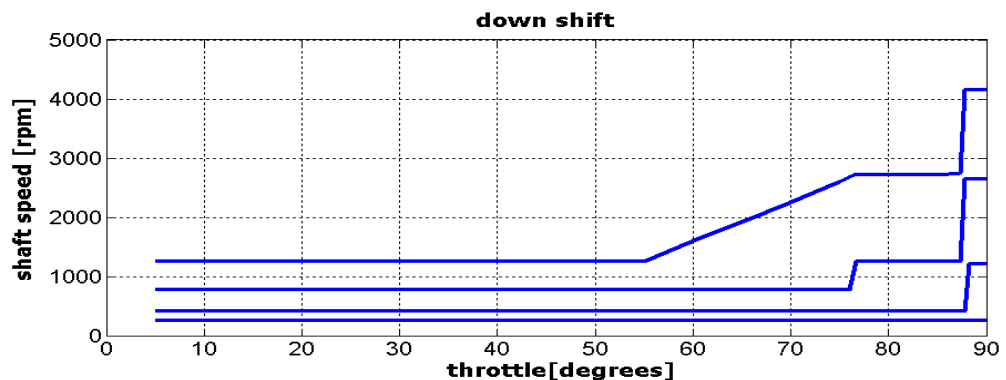

Figure 3-7   Gear down-shift schedules for an automatic transmission, (Rajamani, 2006).

Figure 3-6 shows the look-up table from Rajamani (2006) for gear up-shifting where the gear shift schedule is based on the throttle input and the transmission shaft speed. The transmission from 1st to 2nd gear takes place at highest transmission shaft

speed; the transmission shaft speed reduces as the gear up-shift takes place for higher gears and is lowest for the up-shift from 4th to 5th up-shift as shown in Figure 3-6. Similarly the gear down-shift from 5th to 4th gear takes place at lowest transmission shaft speed and the transmission from 2nd to 1st takes place at the highest transmission shaft speed as shown in Figure 3-7. The difference between the gear up-shift and gear down-shift can be observed by comparing Figure 3-6 and Figure 3-7, as one can see that for each gear there is higher transmission shaft speed for up-shifting than the transmission shaft speed for down-shifting, for e.g. at full throttle for 1st to 2nd up-shifting the required transmission shaft speed is 5050 rpm and for 2nd to 1st down-shifting the required transmission shaft speed is 4150 rpm.

Figure 3-8 shows the gear shift schedule for up-shifting and down-shifting from Kulkarni, et al (2006) model, here the gear shift schedule is the function of throttle input and the vehicle longitudinal speed. Initially at 0 MPH speed and at constant full throttle (90 degrees), 1-2 gear up-shift takes place at 33.2 MPH, as the speed of the vehicle increases the 2-3 gear up-shift takes place at 52.5 MPH, 3-4 gear up-shift takes place at 80 MPH, and 4-5 gear up-shift takes place at 95 MPH. Similarly, assuming the full throttle, the gear down-shifting from 5-4 down-shift takes place at 89 MPH, the 4-3 down-shift takes place at 70 MPH, 3-2 down-shift takes place at 47.5 MPH, and 2-1 down-shift takes place at 30 MPH.
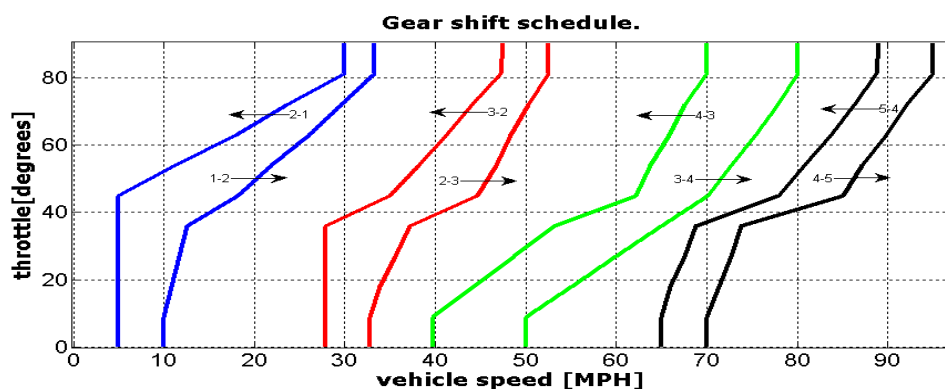

Figure 3-8   Gear up-shift and down-shift schedules for an automatic transmission, (Kulkarni *et al.*, 2006)

3.5 Drivetrain Model

A drive-train serves as a simple power transfer device between the transmission system and the vehicle. A two state drive train model has been presented (Rajamani, 2006) where the two states are front wheel angular speed (ω_{wf}) and the longitudinal vehicle speed ($\dot{x}$) of the vehicle.

3.5.1 Wheel Dynamics

The output from the transmission model, as described in Equation (3.17), is the wheel torque which is in turn the input to the wheel model. When the vehicle is moving, the wheel is subjected to the ground forces as shown in Figure 3-9. The ground forces on a wheel are normal force F_z which is due to the weight and load of the vehicle, the longitudinal traction/braking force F_x which is generated during driving and braking, and the lateral force F_y which helps the vehicle in turning and manoeuvring, or in the case of minimizing the disturbing effect of wind or other side forces. The lateral force is not the part of this study, therefore, only the longitudinal force F_x is considered in the modelling.
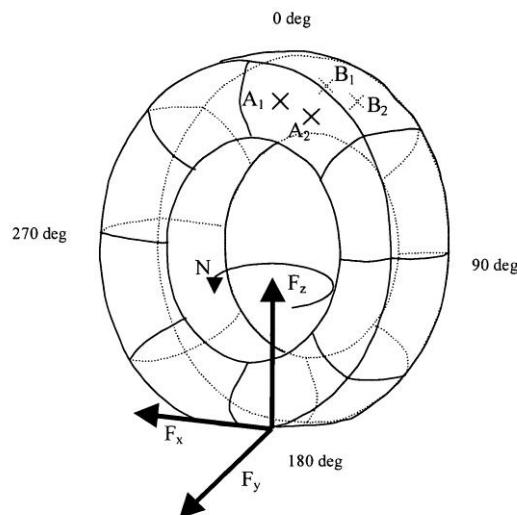

Figure 3-9   Free body diagram of a wheel (Bertrand, 2006)

During acceleration or braking manoeuvre, the contact patch (explained in next section) between tyre and ground begins to slip. The longitudinal slip can be defined as the difference between the actual longitudinal velocity at the axle of the wheel V_x and the equivalent rotational velocity $r_{eff}\omega_w$ of the tyre. The readers who are interested to know how the longitudinal forces depend on the slip ratio are referred to Solyom et al (2004). The longitudinal slip ratio is defined as (Fling and Fenton, 1981).

$$\sigma_x = \frac{r\omega_w - V_x}{V_x} \text{ (during braking)} \tag{3.19}$$

$$\sigma_x = \frac{r\omega_w - V_x}{r\omega_w} \text{ (during acceleration)} \tag{3.20}$$

where, V_x is the longitudinal speed of the vehicle, r is the rolling radius of the free-rolling tire, and ω_e is the angular speed of the wheel. One can conclude from the definition that when $\sigma_x = 0$ the wheel is in perfect rolling i.e. moving without slipping, on the contrary, when $\sigma_x = 1$ then the wheel is locked and pure sliding occurs and this happens during some braking manoeuvre.

A front wheel drive vehicle is considered in this study and the differential equation relating the wheel angular speed ω_{wf}, wheel torque T_w, and the longitudinal tyre force F_{xf} is

$$I_w \dot{\omega}_{wf} = T_w - r_{eff} F_{xf} - R_{xf} - T_{bf} \tag{3.21}$$

where, r_{eff} is the effective radius of the wheel which is the ratio of the longitudinal speed of the tire centre to the angular speed of the tire, R_{xf} is the rolling resistance in the front wheel and T_{bf} is the front brake torque. R_{xf} is explained in the next section as this vehicle is front wheel drive; therefore, the rear wheel is the non-driven wheel.

The differential equation relating the rear wheel angular speed ω_{wr} and the longitudinal tyre force F_{xr} at the rear wheel is

$$I_w \dot{\omega}_{wr} = -r_{eff} F_{xr} - R_{xr} - T_{br} \tag{3.22}$$

where, I_w is the wheel inertia and is taken as 2.8 Kg m² and R_{xr} is the rolling resistance in the rear wheel and T_{br} is the rear brake torque.

The block diagram in Figure 3-10 shows the schematic of the wheel dynamics. When the wheel torque is applied, a friction torque due to the friction force between road and tyre and rolling resistance is generated. The wheel rotational dynamic is controlled by this torques as defined by Equation (3.21).

Wheel angular speed (ω_w) ← **Wheel Model** ← $r_{eff} F_x$
Wheel Torque (T_w) → **Wheel Model** ← T_{bf}
← R_x
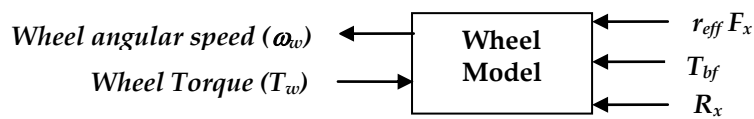
Figure 3-10   Block diagram for wheel model.

Rolling resistance is an opposing force to the motion of the vehicle and is roughly proportional to the normal forces acting on each tyre. This is the amount of energy spent in deforming the tyre material in the contact patch. The contact patch is the area where the tyre and road are in contact with each other as shown in Figure 3-11. Energy is absorbed in deforming the tyre material due to the internal damping of the tyre material and that amount of energy is not recovered even once the tyre material leaves the contact patch and returns back to its original shape. This loss of energy on the tyre is termed as rolling resistance. Wong (2008) has stated that the rolling resistance is mainly caused by the hysteresis in tyre materials due to the deflection of the carcass while rolling. The experimental results from the same source present that 90-95% of the rolling resistance losses are due to internal hysteresis in the tyre, 2-10% due to friction between the tyre and the ground, and 1.5-3.5% due to air circulating inside the tyre.
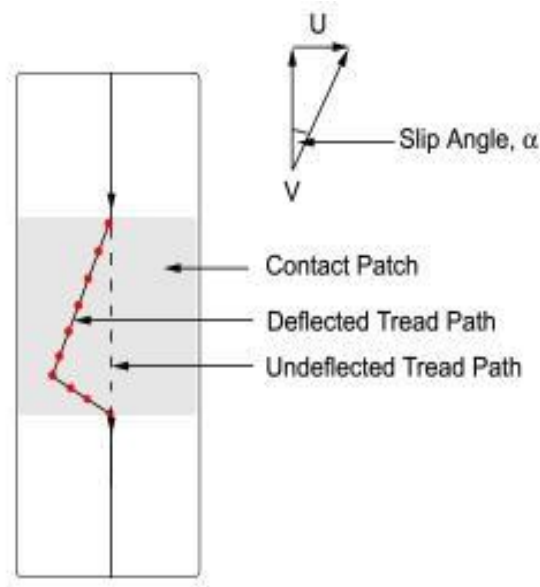
Figure 3-11   Contact patch (Gorski, 2008)

A simple model for rolling resistance has been developed in Cho and Hedrick (1989) powertrain model and has been chosen for this study.

$$R_{xf} = R_{xr} = 0.001546 \times m \times g[N.m] \tag{3.23}$$

3.5.2 Longitudinal Vehicle Dynamics

The external longitudinal forces acting on the vehicle include aerodynamic drag forces, gravitational forces, longitudinal tyre forces and rolling resistances. If the state equation for the rear wheel angular velocity in Equation (3.22) can be eliminated for simplicity then a force balance along the vehicle longitudinal axis yields (Cho and Hedrick, 1989).

$$m\ddot{x} = F_{xf} - F_{aero} - \frac{R_{xf}}{r_{eff}} - mg\sin\theta \tag{3.24}$$

where,

m = mass of the vehicle

x = vehicle displacement [m]

F_{xf} = longitudinal tyre force at the front tyre

F_{aero} = longitudinal aerodynamic drag force

g = gravitational acceleration

θ = gradient of the road

There are two main sources which can generate the aerodynamic resistance: one is the air flow over the exterior of the vehicle body, and the other is flow through the engine radiator system and the interior of the vehicle for the purposes of cooling, heating, and ventilating. The former has more significant effect and accounts for more than 90% of the total aerodynamic resistance of a passenger car (Wong, 2008). The aerodynamic drag force on a vehicle can be represented as (Rajamani, 2006)

$$F_{aero} = \frac{1}{2}\rho C_d A_F (V_x + V_{wind})^2 \qquad (3.25)$$

where, ρ = air density , C_d = aerodynamic drag coefficient, A_F = frontal area, V_x= vehicle longitudinal velocity, and V_{wind} = wind velocity.

The term A_F can be defined as the area calculated from the vehicle width and height for passenger cars (Wong, 2008) which is roughly in the range of 79-84 % of the total frontal area of a passenger car. Wong (2008) has used the following relationship between the frontal area and the vehicle mass as:

$$A_F = 1.6 + 0.00056(m - 765) \qquad (3.26)$$

where, the vehicle mass (m) is in the range of 800-2000 kg.

When a driving torque is applied to a pneumatic tyre, a longitudinal force is developed at the tyre-ground contact patch. This longitudinal tyre force on the wheels is the force which moves the vehicle forward. Experimental results have shown that the longitudinal tyre forces depends on (Solyom *et al.*, 2004).

a) the slip ratio (σ_x)

b) the normal load on the tyre

c) the friction coefficient of the tyre-road interface

Longitudinal traction forces at the front and rear tyre as the function of slip ratio are:

$$F_{xf} = C_{\sigma f} \sigma_{xf} \tag{3.27}$$

$$F_{xr} = C_{\sigma r} \sigma_{xr} \tag{3.28}$$

where,

$C_{\sigma f}$ = longitudinal tyre stiffness of the front tyre = 80000 N

$C_{\sigma r}$ = longitudinal tyre stiffness of the rear tyre = 80000 N

In this study, the friction coefficient of the tire-road interface is assumed as 1 and the normal force is assumed to be a constant. Figure 3-12 shows the longitudinal tyre force as a function of the slip ratio. It is assumed that the longitudinal force is generated instantaneously and has been considered within the proportional range with the slip ratio.
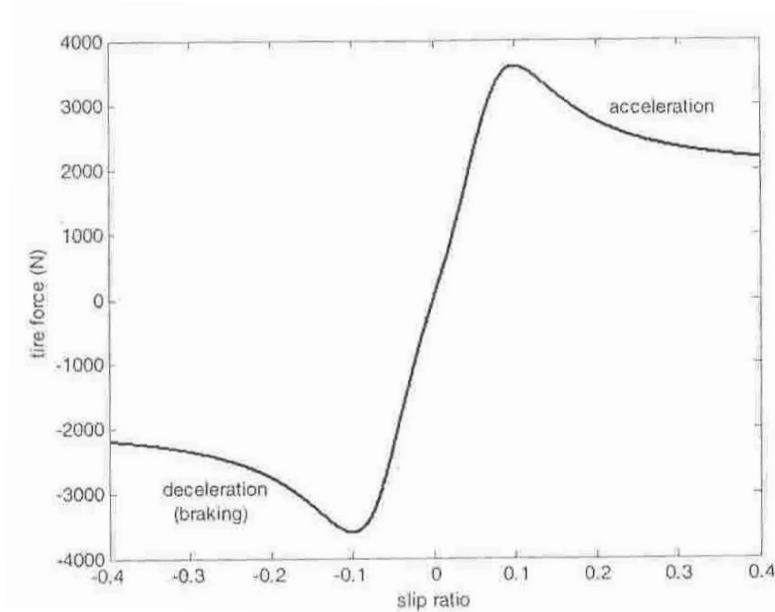
Figure 3-12   Longitudinal tyre force as a function of slip ratio (Rajamani, 2006)

For the purpose of detailed analysis, the longitudinal vehicle model will be subjected to gear up-shifting and down-shifting using the throttle control and on a gradient of the road. Simulations will be run to analyse the transient and steady-state behaviour of the powertrain dynamic model based on the above control input signals.

Table 3-1 shows all the powertrain parameters used in the entire vehicle model. Most of the parameters are taken from Cho and Hedrick (1989) model. There are two different types of gear ratios shown in Table 3-1; one is used for Rajamani (2006) look-up tables and the other is for Kulkarni, et al (2006) look-up table.

Powertrain Parameters		
Engine displacement	V_d	0.0038 m³
Intake manifold volume	V_{man}	0.0027 m³
Universal gas constant	R	287
Manifold temperature	T_{man}	293 K
Max. Flow rate of air in the intake manifold	MAX	0.1843 kg/s
Air/fuel equivalence ratio	λ	1
Stoichiometric air/fuel mass ratio for gasoline(fuel)	L_{th}	14.67
Fuel energy constant [J/kg]	H_u	4.3e7 J/kg
Thermal efficiency	η_i	0.32
Moment of inertia of engine	I_e	0.1454 kg.m²
1st gear speed reduction ratio (Cho and Hedrick, 1989)	R_1	0.3424
2nd gear speed reduction ratio (Cho and Hedrick, 1989)	R_2	0.6379
Final drive speed reduction ratio (Cho and Hedrick, 1989)	R_d	0.3521
1st gear speed reduction ratio (Kulkarni et al., 2006)	R_1	0.3184
2nd gear speed reduction ratio (Kulkarni et al., 2006)	R_2	0.505
3rd gear speed reduction ratio (Kulkarni et al., 2006)	R_3	0.73
4th gear speed reduction ratio (Kulkarni et al., 2006)	R_4	1
5th gear speed reduction ratio (Kulkarni et al., 2006)	R_5	1.3157
Final drive speed reduction ratio (Kulkarni et al., 2006)	R_d	0.3257
Moment of inertia of wheel	I_w	2.8 kg.m²
Effective radius	r_{eff}	0.3 m
Longitudinal tyre stiffness (for both tyres)	C_{of}	80000 N
Air density	ρ	1.225 kg/m³
Aerodynamic drag coefficient	C_d	0.4
Wind velocity	V_{wind}	10 m/s
Mass of the vehicle	m	1644 kg

Table 3-1   Powertrain Parameters

The simulation results have been carried out in Figure 3-13 for a particular scenario using a combined Cho and Hedrick (1989) and Rajamani (2006) model under the same initial conditions, throttle input, speed reduction ratios in transmission and in final drive and when an automatic transmission takes place from 1st gear to the 2nd

gear (Cho and Hedrick, 1989). The throttle input is ramped up from 0 to 100 percent in 250 ms, since physically; the throttle cannot be changed instantaneously. In addition, 25 Nm (T_a), as an accessory torque is added to account for the driver's load.

The simulation result for engine speed from Cho and Hedrick (1989) model has been reproduced in Figure 3-13 in order to confirm that the proposed vehicle model in this study is producing satisfactory results so that this can be used for the ACC vehicle analysis. The corresponding longitudinal speed is shown in Figure 3-14.
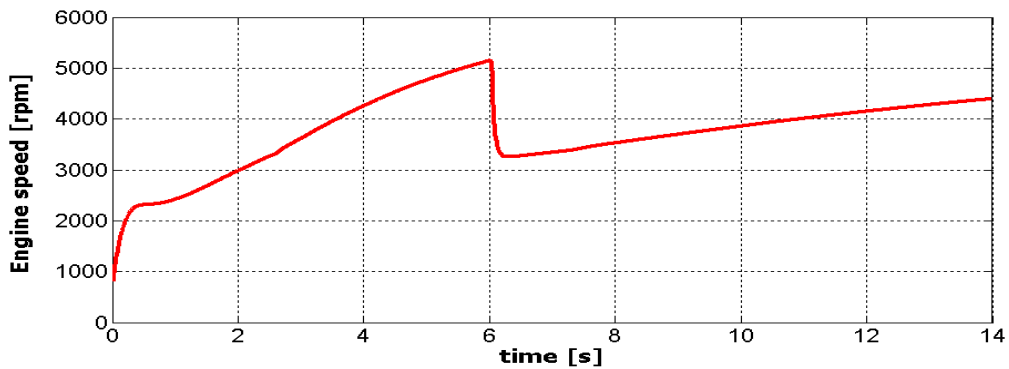
Figure 3-13   Engine Speed during 1-2 gear up-shift
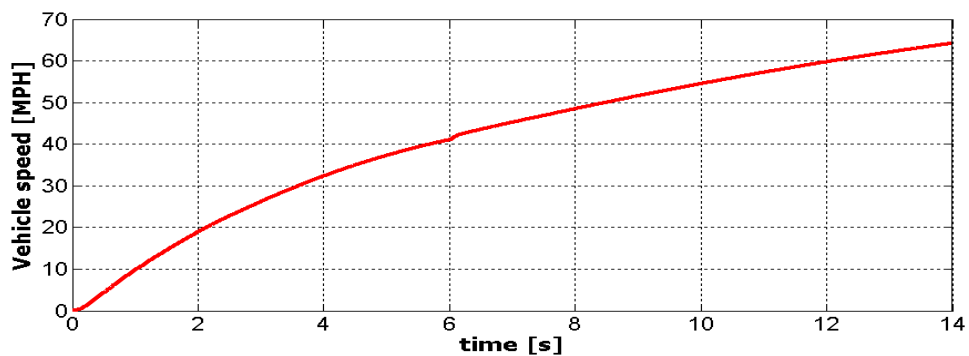
Figure 3-14   Vehicle Speed during 1-2 gear up-shift

Figure 3-13 shows the engine speed for the 1-2 gear up-shift. The transmission from 1st to 2nd gear is based on the Rajamani (2006) look-up table for the gear schedule where the gear schedule is the function of throttle angle and the transmission shaft

speed. The above result has been confirmed against the Cho and Hedrick (1989) model. The simulation results show that the shift started at t = 6.03 s and ended at t = 6.35 s. The corresponding engine speeds at that time were 5155 rpm and 3254 rpm. These results show a close agreement with the Cho and Hedrick (1989) model and ensure that the longitudinal vehicle model can be used for the two-vehicle system. The longitudinal speed in Figure 3-14 has been validated with Cho and Hedrick (1989) model. The simulation results for their model reaches up to 64 MPH where the simulation result shown in Figure 3-14 shows the similar result and agrees well with their model with the same initial conditions and at full throttle.

During the process of mathematical modelling many attempts have been made to use the transmission down-shift pattern (Rajamani, 2006) shown in Figure 3-7 by decreasing the throttle input or moving on the uphill. But due to inadequate information given in Figure 3-7 for the transmission down-shifting the required simulation results for engine speed and vehicle speed were not possible. Therefore, a gear shift schedule (Kulkarni *et al.*, 2006) shown in Figure 3-8 has been adopted for the transmission up-shifting and transmission down-shifting where the gear schedule is the function of throttle angle and the vehicle longitudinal speed. Furthermore the simulations have been carried out using the Kulkarni et al. (2006) look-up table. Figure 3-15 shows engine speed and transmission shaft speed for 5-speed automatic transmission at full throttle using the Kulkarni, et al. (2006) gear shift schedule as shown in Figure 3-8. The gear ratios used in Figure 3-15 are the same as in the Kulkarni, et al. (2006) model as the gear shift schedule is from the same model.
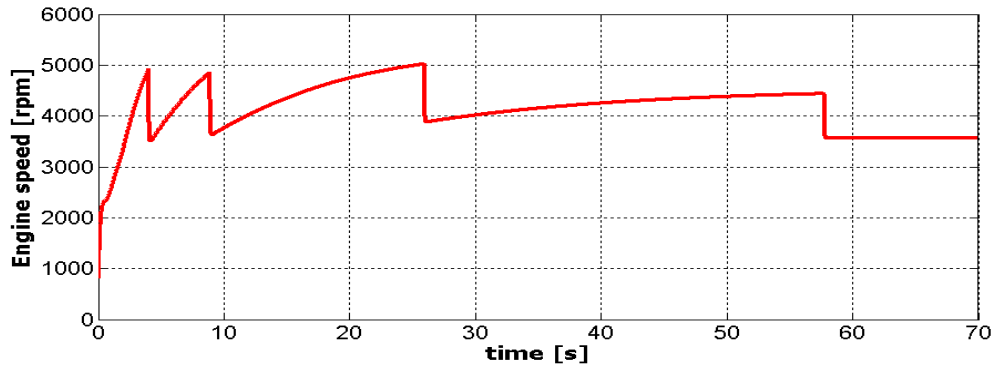
Figure 3-15   Engine speed during 1-2-3-4-5 gear up-shift

Figure 3-16 shows the corresponding vehicle longitudinal speeds for the engine speed shown in Figure 3-15. The simulation result in Figure 3-16 has also been validated with Kulkarni, et al. (2006) model. The gear shift schedule is controlled by the throttle angle and vehicle longitudinal speed as shown in Figure 3-8. The throttle input to the engine model is 100 % and the gear up-shifts take place at the velocities shown in Figure 3-8. The simulations for down-shifting are produced in the later part of this chapter for different throttle inputs and on a slope. The down-shifting are also based on the same gear schedule pattern (Figure 3-8).
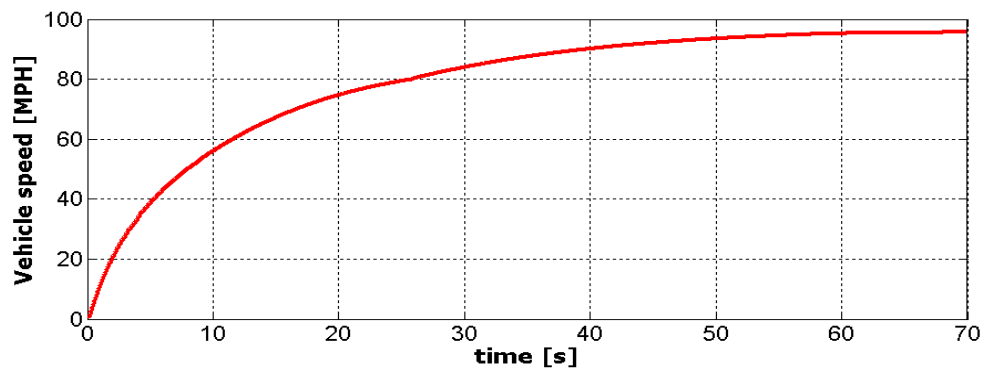

Figure 3-16   Vehicle Speed during 1-2-3-4-5 gear up-shift

Since the proposed powertrain model has been reproduced and validated against the experimental results (Cho and Hedrick, 1989; Kulkarni *et al.*, 2006) and the look-

up table approach for the automatic transmission has also been justified, therefore, this model is useful in the development of a longitudinal dynamic control system for the vehicles equipped with ACC system.

3.6 Complex Vehicle Model Analysis for Longitudinal Dynamic Control

In the previous sections the longitudinal vehicle model was analysed under a constant throttle input (full throttle) right from the start of the simulations. This section presents the longitudinal vehicle model analysis for a transient operation under the throttle change and on a gradient of road to analyse the performance of the proposed vehicle model. It is necessary to analyse the vehicle response when the vehicle is undergoing through transmission down-shifting.

3.6.1 Throttle Change

Figure 3-17 and Figure 3-18 show the engine speed and the vehicle longitudinal speed respectively of the vehicle under the throttle change. Figure 3-19 shows the throttle input for this simulation. The vehicle initially reaches the steady state condition in the 5th gear operation and then at t = 70 s the throttle input is ramped down to 10 degrees within 10 s (Figure 3-19), and after t = 80 s the throttle input remains at 10 degrees for the rest of the simulation. The drop of throttle input from 90 degrees to 10 degrees brings the vehicle down to 1st gear as shown in Figure 3-17.

The main purpose of this throttle drop is to simulate and analyse the behaviour of the vehicle during the down-shifting. It is clear from Figure 3-17 that as the throttle input drops down to 10 degrees the engine speed drops down and finally the vehicle longitudinal speed reduces as well. This makes the transmission to move to the lower gear ratios. Figure 3-18 shows the corresponding vehicle speeds at 10 degrees throttle input where the each down-shift takes place which is similar to the gear schedule shown in Figure 3-8 (Kulkarni *et al.*, 2006).
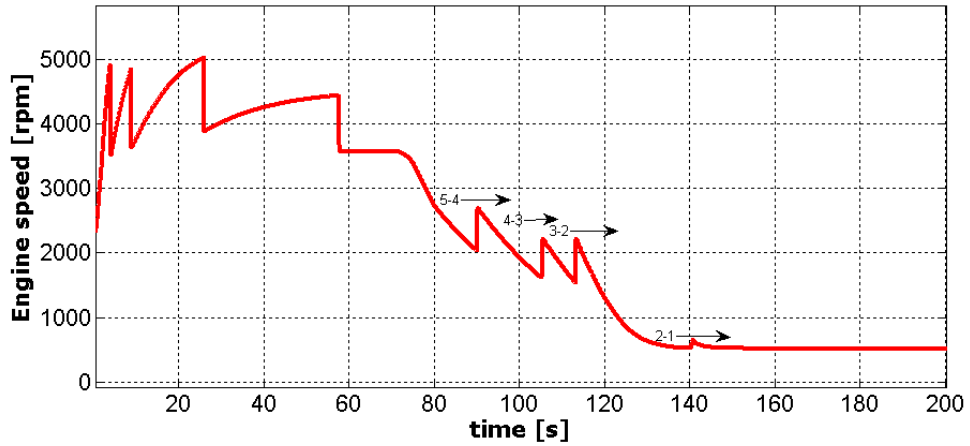
Figure 3-17   Engine Speed during 1-2-3-4-5 gear up-shift and 5-4-3-2-1 down shift using throttle input (throttle, ramped down from 90 degrees to 10 degrees)
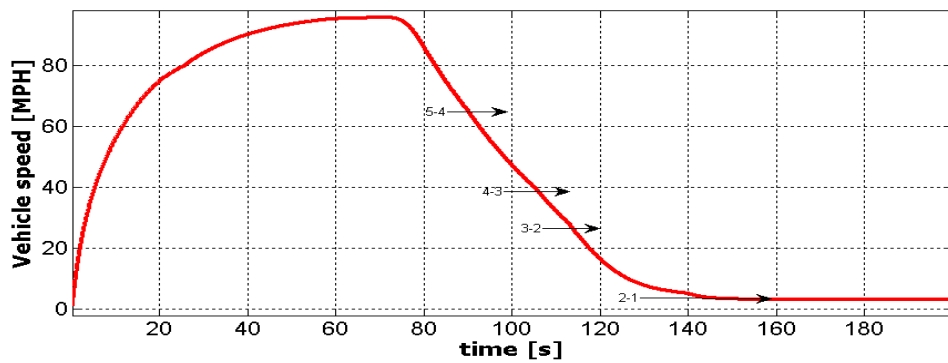

Figure 3-18   Vehicle Speed during 1-2-3-4-5 gear up-shift and 5-4-3-2-1 down-shift using throttle input (throttle, ramped down from 90 degrees to 10 degrees)
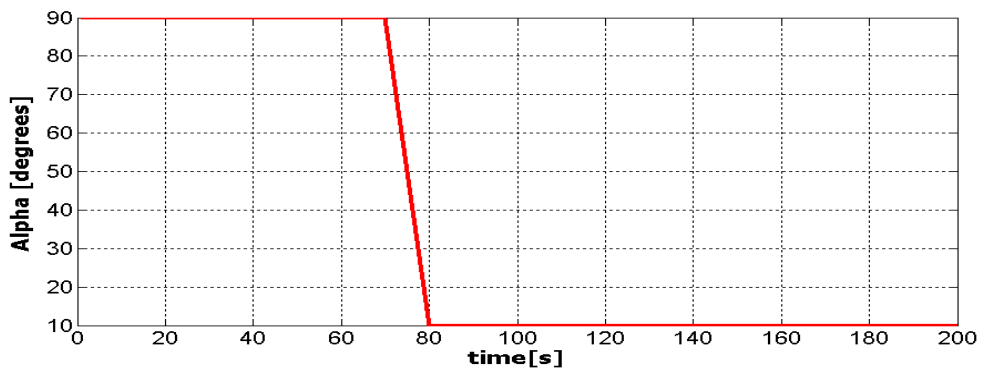

Figure 3-19   Throttle input for Figure 3-17 and Figure 3-18, (α ramped down from 90 degrees to 10 degrees

3.6.2 Gradient of Road

The proposed vehicle model has been simulated on a 15 degrees gradient of the road to observe the down-shift transmission pattern. During this manoeuvre the throttle input was maintained at 90 degrees, i.e. full throttle. Initially the vehicle is in the 5th gear and under a steady state operation then at t = 70 s the vehicle is subjected a slope of 15 degrees uphill. The vehicle speed decreases, when subjected to the slope, till the point where 5-4 down shift takes place and decreases further till the transmission comes back in the 1st gear as shown in Figure 3-20. The engine speed in the first gear is high enough, this is because the driver is demanding the high torque from the engine and using the full throttle input. The corresponding vehicle speed is also shown in Figure 3-21 the down-shift for each gear takes place according to the gear shift schedule shown in Figure 3-8.
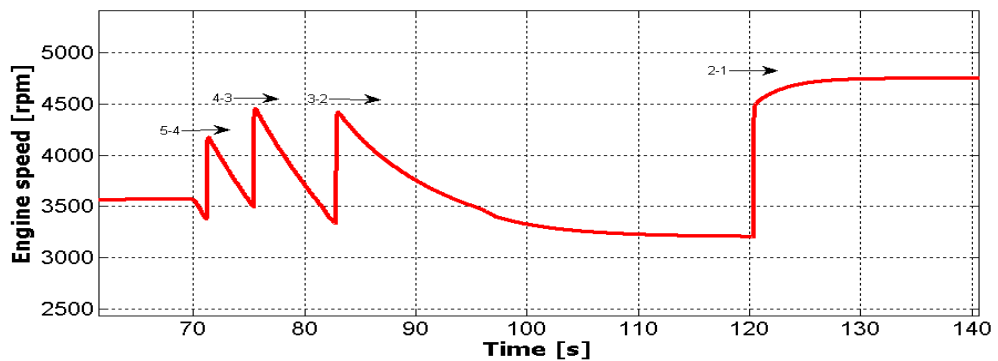

Figure 3-20   Engine Speed during 5-4-3-2-1 down shift on a 15 degrees road slope at full throttle
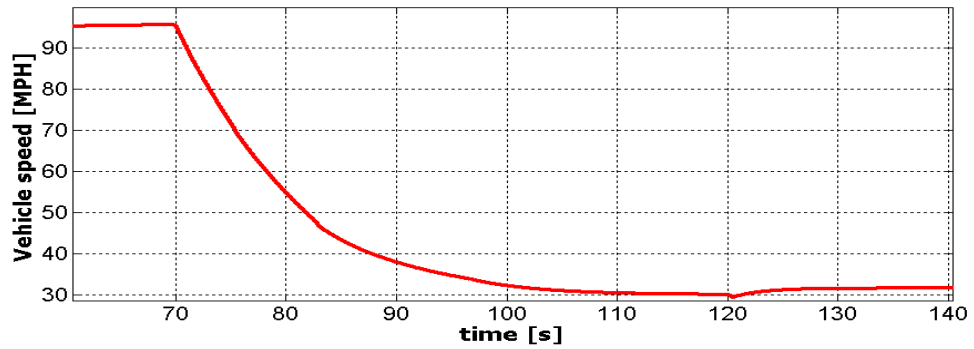
Figure 3-21   Vehicle Speed during 5-4-3-2-1 down shift on a 15 degrees gradient road slope at full throttle.

3.7   Development and Comparison of Mathematical / Parametric Engine Models and Engine Map Models

As discussed in Chapter 2, the lower-level controller requires steady state engine maps for the calculation of desired throttle angle for the following ACC vehicle. Therefore, engine map models have been developed and compared with the mathematical model in this section. In Section 3.2 a two-state mathematical/parametric model for the engine dynamics was presented and the simulation result were been produced during the 1-2 gear transmission under full throttle in Figure 3-13. The two states are the intake manifold pressure (p_{man}) and the engine speed (ω_e). The simulation results for p_{man} and ω_e have been produced using different throttle inputs.

An alternate to the parametric model is the engine map (look-up map) which is based on steady-state experimental data and is usually available from the manufacturers. In this study an attempt has been made to construct the engine maps for a second order engine model and a first order engine model respectively using the parametric model. The engine dynamic model presented in Section 3.2 is used to compute the intake manifold pressure (p_{man}) and the engine speed (ω_e) and then the engine maps have been constructed using the steady state intake manifold pressure (p_{man}) and the engine speed (ω_e) for the net combustion torque (T_{net}).

In the literature, the engine-map based models are mostly second order consisting of two states, the intake manifold pressure (p_{man}) and the engine speed (ω_e), or first

order consisting of only one state, the engine speed (ω_e). The second order system is analogous to the parametric model described in Section 3.2.

Figure 3-22 shows the block diagram for the three similar engine models with the same throttle input and the engine states as outputs. The difference between the three models is that the parametric model obtains the parametric function, e.g. T_{net}, from the set of parametric equations explained in Section 3.2, while the engine map models obtain the T_{net} and $\dot{m}_{ao}$ from the engine.
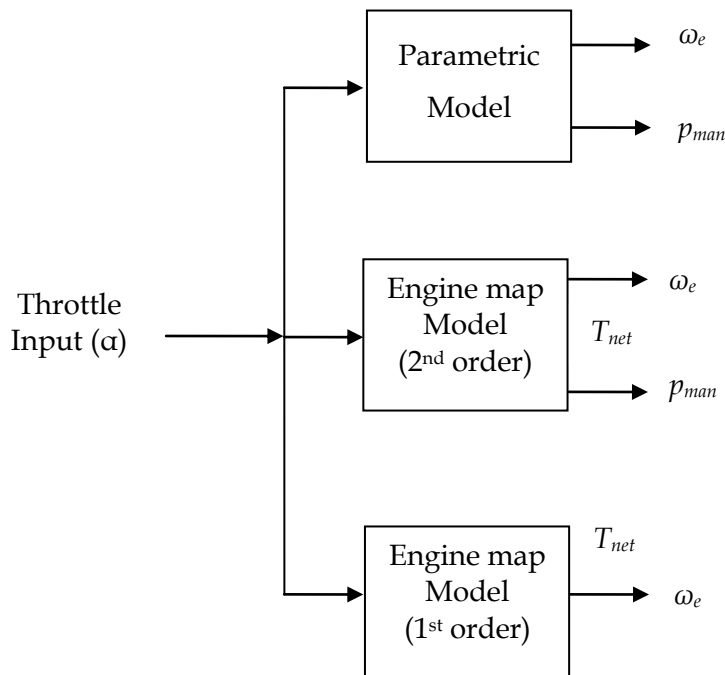

Figure 3-22   Block diagram for three models for the same input and output

The purpose of the comparison of the parametric model and engine map model is to confirm that the engine model is producing the similar results for the engine speed under the same throttle input. The first order engine map model has also been developed and compared with the parametric model to ensure that for the same throttle input, as in parametric model, the engine speed is the same as for the parametric model.

3.7.1 Second Order Engine Model Based on Engine Maps

The two equations of the second order engine model are described as follows:

The state equation for the intake manifold pressure is as follows:

$$\dot{p}_{man} = \frac{RT_{man}}{V_{man}}(\dot{m}_{ai} - \dot{m}_{ao})$$
(3.29)

All the parametric functions in Equation (3.29), except $\dot{m}_{ao}(\omega_e, p_{man})$, have been computed using the parametric equations described in Section 3.2. T_{net} (ω_e, p_{man}) and $\dot{m}_{ao}(\omega_e, p_{man})$ are obtained from the engine map. The state equation for the engine rotational dynamics is as follows:

$$I_e \dot{\omega}_e = T_{net} - T_{load}$$
(3.30)

where, T_{net} (ω_e, p_{man}) is obtained after the losses from the engine map constructed in Figure 3-24. T_{load} is the load torque from the torque converter and represents the external load on the vehicle.

To draw the engine map for T_{net} (ω_e, p_{man}) the tabular data is required for a pair of engine speed and manifold pressure. The data has been computed using the computer simulation as shown in Table 3-2 which shows the partial data for p_{man} (10kPa – 13.91kPa). For each pair of (ω_e, p_{man}) there is a corresponding value for T_{net} (ω_e, p_{man}). For constructing an engine map such tabular data is essential for the specific type of engine. Every engine has its own engine map based on the (ω_e, p_{man}) pair. Based on Table 3-2, the engine map has been constructed in Figure 3-24 for the manifold pressure ranging from 10 kPa to 100 kPa. The engine map drawn in Figure 3-24 shows the $T_{net}(\omega_e, p_{man})$ as the function of engine speed and the manifold pressure.

S.No	Angular speed(ω_e)rad/s	Manifold Pressure, p_{man}(kPa)			
		10	11.30	12.61	13.91
1	52.0000	-0.3534	2.2863	4.9261	7.5658
2	80.1053	-2.4261	0.3304	3.0869	5.8434
3	108.2105	-4.4988	-1.6255	1.2477	4.1210
4	136.3158	-6.3119	-3.2880	-0.2642	2.7597
5	164.4211	-8.0732	-4.8920	-1.7107	1.4705
6	192.5263	-9.2114	-5.7915	-2.3716	1.0484
7	220.6316	-10.0386	-6.3394	-2.6403	1.0589
8	248.7368	-11.4113	-7.5041	-3.5969	0.3103
9	276.8421	-13.3283	-9.2841	-5.2398	-1.1955
10	304.9474	-15.5185	-11.3727	-7.2270	-3.0813
11	333.0526	-18.2529	-14.0767	-9.9005	-5.7243
12	361.1579	-21.1178	-16.9282	-12.7385	-8.5489
13	389.2632	-24.6306	-20.5121	-16.3935	-12.2750
14	417.3684	-28.1444	-24.0970	-20.0497	-16.0023
15	445.4737	-32.4097	-28.5316	-24.6534	-20.7753
16	473.5789	-36.6750	-32.9661	-29.2571	-25.5482
17	501.6842	-41.5902	-38.1353	-34.6804	-31.2255
18	529.7895	-46.6341	-43.4500	-40.2659	-37.0817
19	557.8947	-51.3657	-48.4117	-45.4576	-42.5035
20	586.0000	-55.9424	-53.1982	-50.4539	-47.7097

Table 3-2   Tabular data for an engine map for T_{net} (ω_e, p_{man})
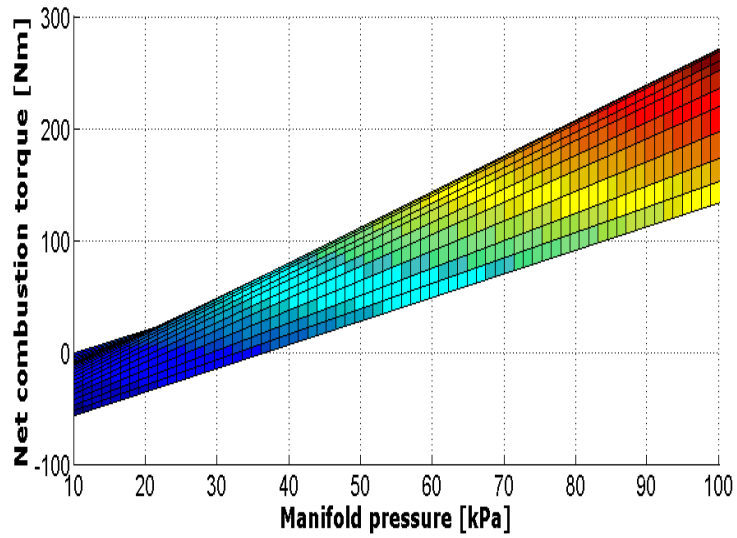
Figure 3-23   Engine map for T_{net} as a function of p_{man} for various fixed values of ω_e
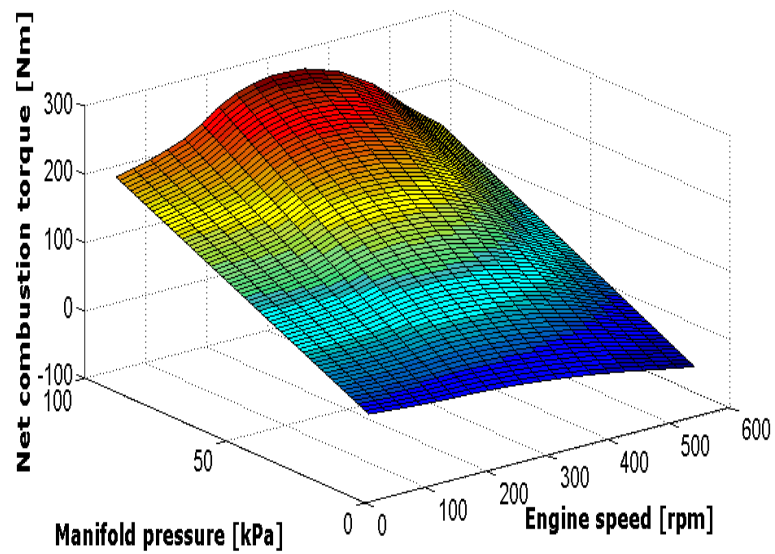
Figure 3-24   Engine map for T_{net} as a function of p_{man} for various fixed values of ω_e
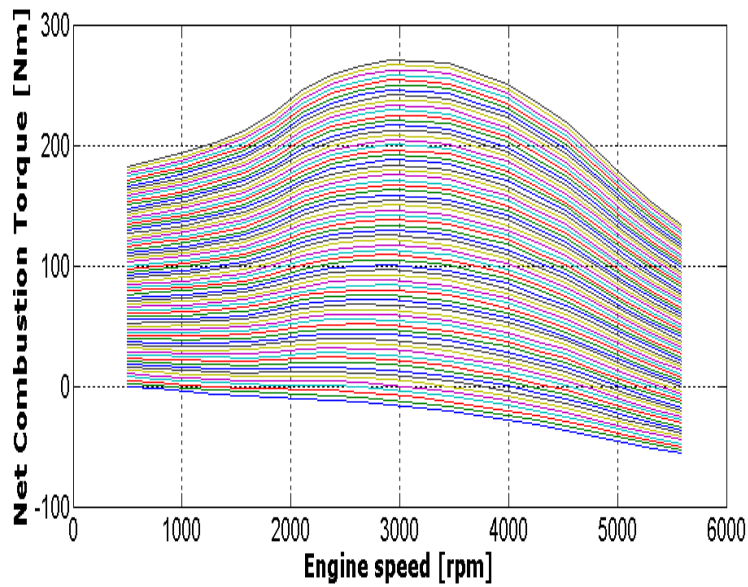
Figure 3-25 T_{net} as a function of ω_e for different fixed manifold pressure p_{man}
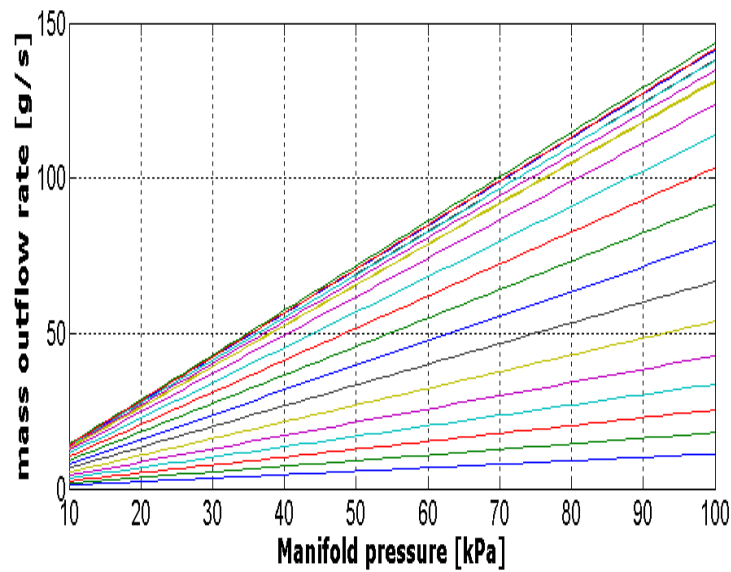

Figure 3-26 $\dot{m}_{ao}\ (\omega_e, p_{man})$ as a function of p_{man} for different fixed engine speeds ω_e

Another analysis, shown in Figure 3-25, reveals that for every fixed manifold-pressure p_{man} the magnitude of T_{net} initially increases as a function of engine speed and reaches to a maximum and drops down for higher values of engine speed. The

result shown in Figure 3-25 has been compared with Fig. 9-4 (Rajamani, 2006) for the same variables and shows a good agreement with it. Figure 3-26 shows the mass outflow rate from the manifold $\dot{m}_{ao}$ (ω_e, p_{man}) as a function of manifold pressure p_{man} for various fixed engine speed ω_e which can be compared with Fig. 9-5 (Rajamani, 2006). At lower ω_e $\dot{m}_{ao}$ is not increasing significantly, while at higher ω_e $\dot{m}_{ao}$ is increasing as a function of p_{man}.

Figure 3-27 shows the structure for the second order engine map model. The input to the engine map model is the throttle input and the outputs are the engine speed ω_e and the intake manifold pressure p_{man}. At each time step the states are fed back to the engine map to compute the T_{net} for the next step.
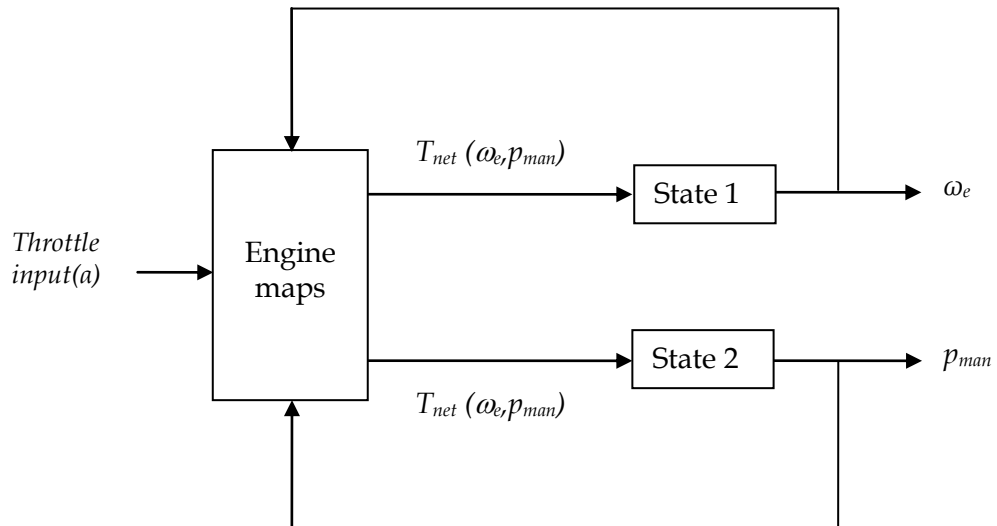

Figure 3-27   Engine map structure for the second order engine model

3.7.2 First Order Engine Model Based on Engine Maps

If the intake manifold filling dynamics are ignored then the second order engine model in Section 3.7.1 can be reduced to the first order engine model where the engine dynamics has only one state, the engine speed ω_e (Rajamani, 2006). These engine models based on engine maps are essential for the lower-level controller of the ACC vehicle to compute the desired throttle angle to track the desired acceleration.

The state equation of the engine dynamics is as follows:

$$I_e \dot{\omega}_e = T_{net} - T_{load} \tag{3.31}$$

where, T_{net} (a, ω_e) is obtained after the losses from the engine map constructed in Figure 3-28. T_{load} is the load torque from the torque converter and represents the external load on the vehicle. T_{net} (a, ω_e) is determined as a steady state function of the throttle angle a and engine speed ω_e.
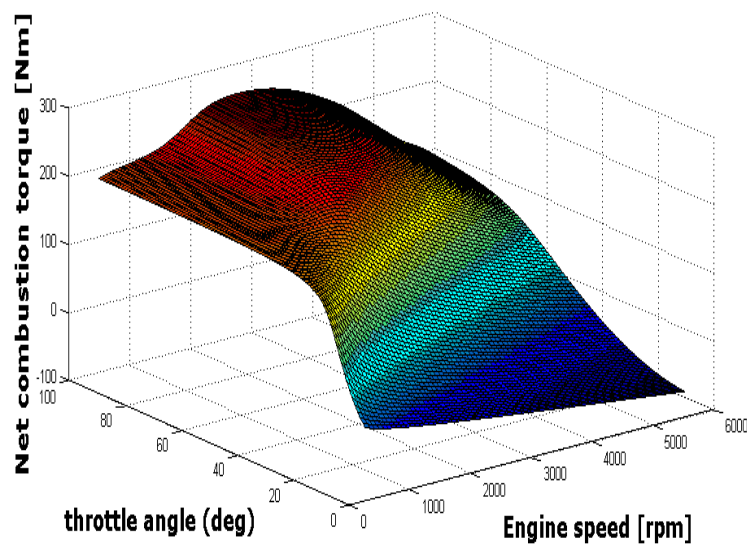

Figure 3-28   Engine map for T_{net} as a function of a for various fixed values of ω_e
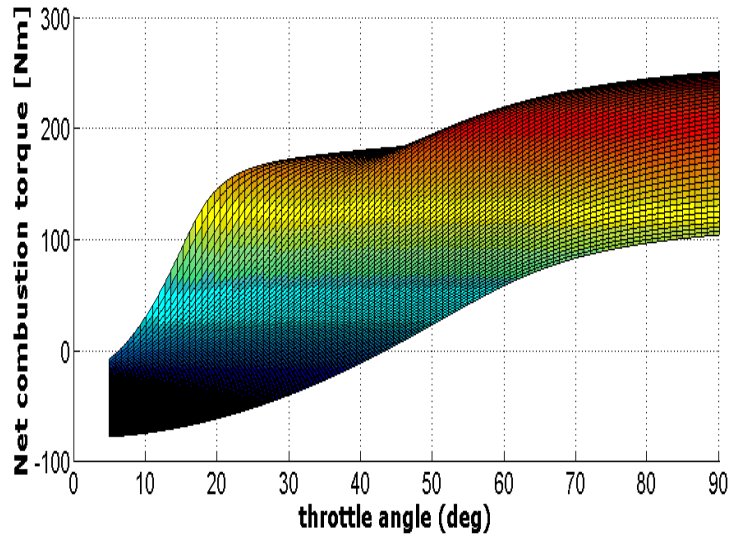
Figure 3-29   Engine map for T_{net} as a function of a for various fixed values of ω_e
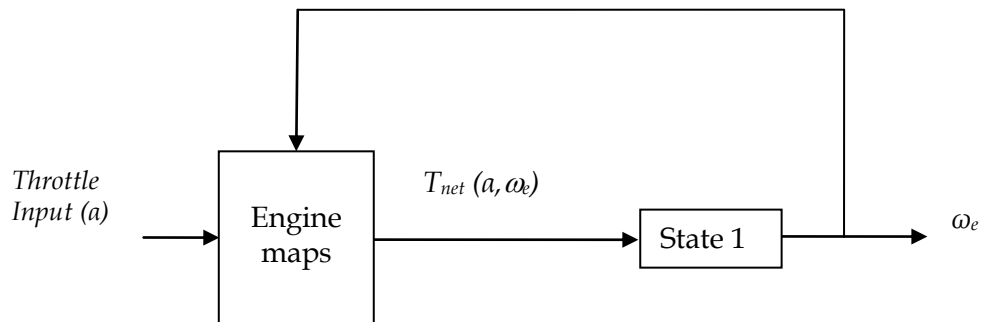
Figure 3-30   Engine map control structure for first order engine model

Figure 3-30 shows the control structure for the first order engine map model. The input to the engine map model is the throttle angle and the output is the engine speed ω_e. At each time step the state variable is fed back to the engine map to compute the T_{net} for the next step.

The simulation results in Figure 3-31, Figure 3-32, and Figure 3-33 for engine speed, vehicle longitudinal speed and the vehicle displacement respectively show the comparison of parametric engine model and the two engine models based on engine

maps for 1-2 gear up-shifts. The comparison show that all the three models agree well (overlapping) with each other and that verifies that the engine maps constructed in Figure 3-24 and Figure 3-28 are producing the satisfactory results.
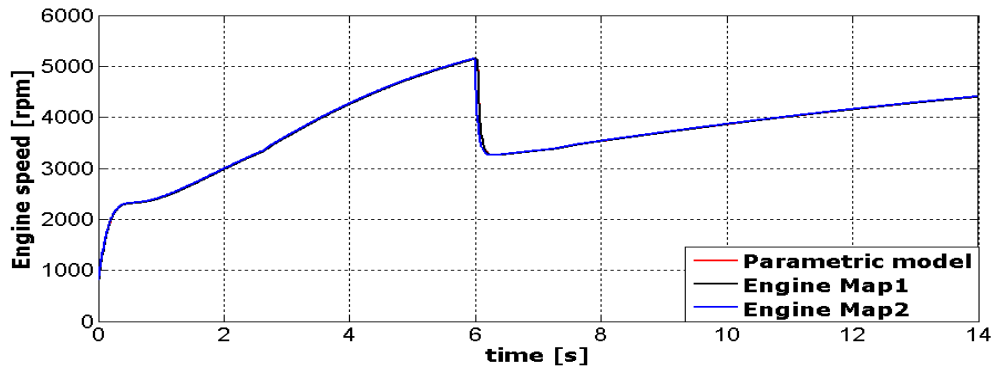
Figure 3-31   Engine Speed during 1-2 gear up-shift for three models
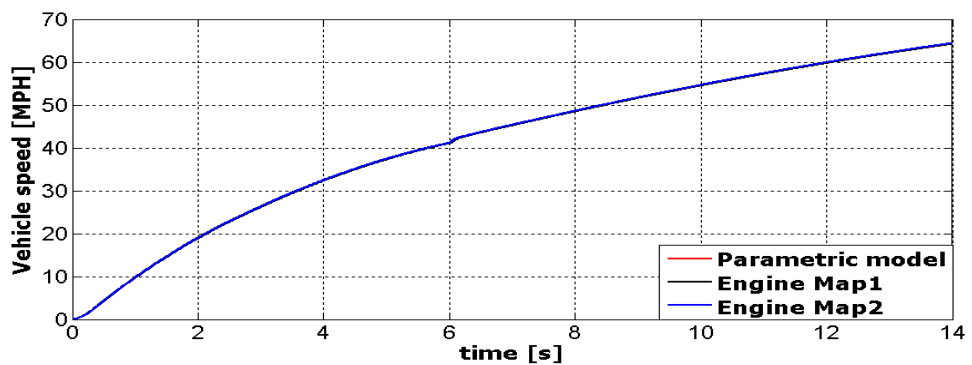
Figure 3-32   Vehicle speed during 1-2 gear up-shift for three models

The engine map model has been validated with the parametric engine model. The reason for the validation is to ensure that the results from the engine map models match well with the parametric model because these engine maps will be used for the lower-level controller of the ACC vehicle in Chapter 6. The control input to all models is the same throttle input. The validation has been performed for different throttle inputs and the transient and the steady-state behaviours have been compared.
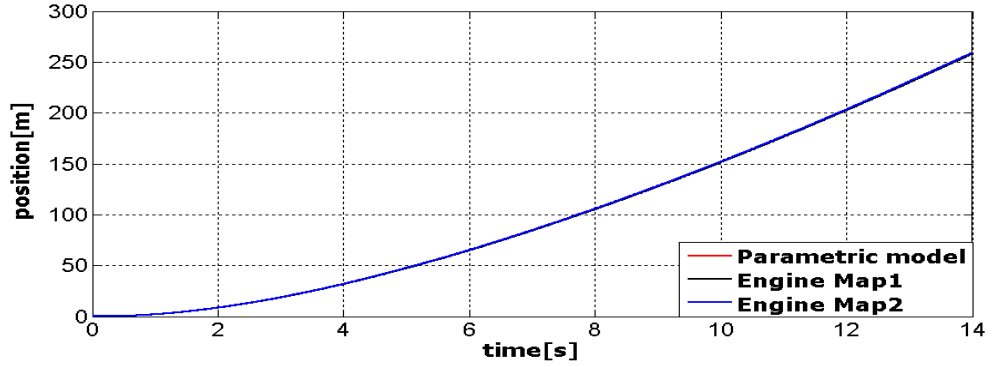
Figure 3-33   Vehicle displacements during 1-2 gear up-shift for three models

3.8   Simple ACC Vehicle Model

A simple ACC vehicle model used in the previous studies is based on a first-order lag (Rajamani, 2006; Li *et al.*, 2010). This lag is considered in the control input command computed by the upper-level controller. In this thesis, it is referred as first-order vehicle model. This lag corresponds to the lower-level performance and comes from brake or engine actuation lags and sensor signal processing lags. This first-order model is used between upper-level and lower-level controller (Figure 3-34) can be defined as (Rajamani, 2006; Li *et al.*, 2010).

$$\tau\dddot{x}(t) + \ddot{x}(t) = u(t) \tag{3.32}$$

where, x, $\dot{x}$ and $\ddot{x}$ are the absolute position, velocity, and the acceleration of the ACC vehicle. u refers to the control input commands computed by the upper-level controller. τ is the time lag corresponding to the lag in the lower-level controller performance. Analytical and experimental studies show that τ has a value of 0.5 s (Rajamani and Zhu, 2002; Rajamani, 2006) and the same value is used in this study. It should be noted that the first-order model does not consider the dynamics of the vehicle sub-models.

The first-order model is used for two following important reasons:

1. It is used for the analysis of the upper-level controller using four control methods: proportional-integral-derivative (PID), sliding mode, constant-time-gap (CTG), and model predictive control (MPC). The upper-level

77

control can be designed because the vehicle dynamics and nonlinearities from engine, transmission, are aerodynamic drag are not considered in the first-order model.

2. The simulation results obtained from the first-order model will be used for the validation of the complex ACC vehicle analysis.

3.9 Methodology

Different control laws for a vehicle equipped with ACC system have been designed in the literature and in most of the studies the ACC vehicles are travelling in a form of platoon (Rajamani and Zhu, 2002; Sun *et al.*, 2004; Ferrara and Vecchio, 2007). A platoon (automatic vehicle following system) can be defined as a group of vehicles travelling together with relatively small spacing to improve the road capacity and to minimize the relative velocity of the vehicles in case of emergency (Huang and Chen, 2001). In the literature different control algorithms for the longitudinal dynamic control of a platoon have been discussed based on different spacing control policies and the communication link among the vehicles of a platoon. In many cases the research work has been devoted to the upper-level controller for different spacing control policies and different communication media and then the control law is applied to a first-order ACC vehicle model (Bageshwar *et al.*, 2004; Rajamani, 2006).

Some researchers have presented an ACC vehicle dynamic model where the desired acceleration commands computed from the upper-level controller are given to the lower-level controller of the ACC vehicle which determines the desired throttle input for the ACC vehicle to track the desired acceleration (Hedrick *et al.*, 1993; Swaroop, 1997). In previous studies, the ACC vehicle dynamic models have been analysed within the comfort level of the driving, i.e. the ACC vehicle does not reach the acceleration/deceleration limits. These vehicle models do not consider the important dynamics of the vehicle's sub-models. The comfort level of an ACC vehicle is disturbed when subjected to abrupt and sudden brake forces.

In the literature, ACC vehicle's control laws have been designed for a steady-state vehicle-following mode (Hedrick *et al.*, 1993; Sun *et al.*, 2004). It is not always

necessary that an ACC vehicle should operate in the steady-state vehicle following mode, it might have to respond to sudden variations occurring in the preceding vehicle dynamics which could be due to throttle input change or brake input. Another possible scenario is when an ACC vehicle encounters a slow or halt preceding vehicle and has to switch from speed-control mode to vehicle-following mode. The effect of noise on the ACC vehicle's sensors can also lead to the disturbance in the computation of the specified inter-vehicle distance (SIVD) which in turn can disturb the behaviour of the ACC vehicle and generate a transitional manoeuvre. Under these transient operations an ACC vehicle must perform a transitional manoeuvre and then restore to the steady-state operation.

There are mainly two types of controllers designed in previous studies for an ACC vehicle analysis: *longitudinal controller*, which deals with the spacing regulation without considering the steering; and, *lateral controller,* which controls the steering of the vehicle to keep it in lane. This study focuses only on longitudinal control of a two-vehicle system, i.e. the vehicles are moving in a straight line.

In this study a two-vehicle system, which consists of a preceding vehicle and an ACC vehicle, is developed which is represented by the block diagram as shown in Figure 3-34. Each vehicle's longitudinal motion is captured in continuous time domain using a set of differential equations. The longitudinal motion of the preceding vehicle and the ACC vehicle is measured by the upper-level controller in order to compute the desired acceleration commands. Since the desired acceleration is not a true input, a lower-level controller is required to determine either a throttle input or brake input in order to track the desired acceleration (Connolly and Hedrick, 1999). The lower-level controller then determines the required throttle and brake input commands for the ACC vehicle in order to track the desired acceleration computed by the upper-level controller. The information of the longitudinal motion of ACC vehicle is fed back to the upper-level controller to establish a feedback closed loop system (Figure 3-34). A first-order is considered in the control input command computed by the upper-level controller (as discussed in Section 3.8).
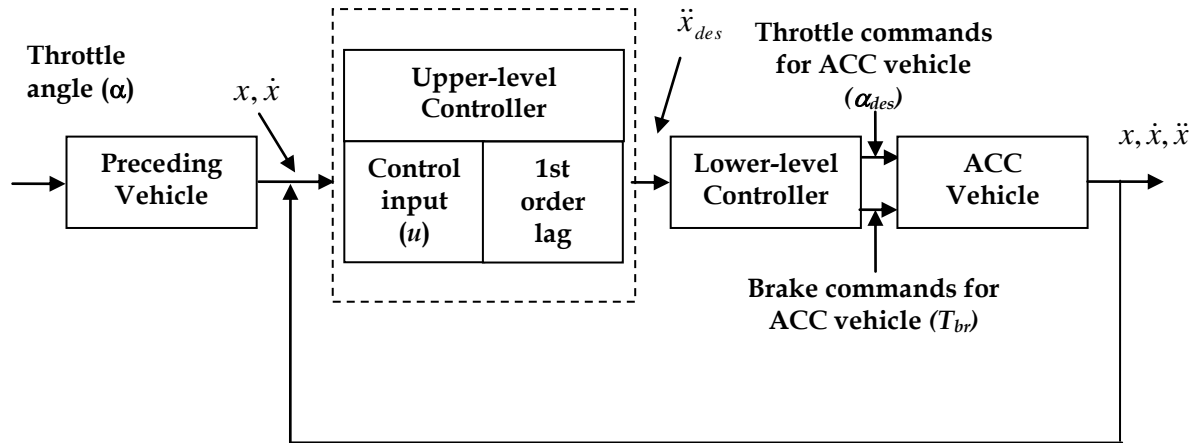
Figure 3-34   Block diagram for a two-vehicle system consisting of a preceding and an ACC vehicle.

The preceding vehicle, usually referred to as lead vehicle, is independent of the ACC vehicle, travels on its own and there is no any communication between the two vehicles. The onboard radar sensors of the following ACC vehicle measure the longitudinal motion of the preceding vehicle and this information is used by the upper-level controller to calculate the instantaneous desired acceleration commands for the ACC vehicle to perform the manoeuvre.

A detailed analysis of the complex vehicle longitudinal dynamic control has been carried out in Section 3.6. Before analysing the lower-level controller and the complex ACC vehicle model, it is important to understand the design of the upper-level controller and investigate the control strategy used for the upper-level controller. A first-order lag is also considered after the upper-level controller which corresponds to the performance of the lower-level controller (explained in Section 3.8). An important aspect of this study is to investigate the response of the upper-level controller using different control strategies employed in previous studies. Four well-known control methods: PID, sliding mode, CTG, and MPC methods will be used to design the control laws for the upper-level controller. The simulation results obtained from these control methods will be compared and the most appropriate among them will be used for the lower-level controller and the complex ACC vehicle analysis. For the purpose of upper-level controller analysis, the simple first-order ACC vehicle model (Section 3.8) will be used in order to investigate the upper-level controller response exclusively. It is important to mention here that in

all the simulation analysis the preceding vehicle is based on the complex vehicle model. As the last objective, the complex vehicle will be tested under different situations and for different parameters as discussed in Section 2.4.

3.10 Conclusions

In this chapter a 5-speed automatic transmission powertrain model has been developed for the longitudinal dynamic control of a vehicle. The proposed model captures the powertrain dynamics in the continuous-time domain. A simplified approach for gear up-shifting and down-shifting using the gear schedule maps (Figure 3-8) has been proposed where the transmission gear up-shifting and down-shifting is triggered using the look-up maps based on the throttle input and vehicle's longitudinal speed information (Kulkarni *et al.*, 2006). The simulation results obtained from the proposed model have been validated against previous studies (Cho and Hedrick, 1989). Different throttle inputs and a road gradient have been applied to the vehicle in order to analyse the response of the complex vehicle model. It has been observed that the vehicle longitudinal dynamics is precisely controlled using these input commands.

This complex vehicle model can be used for the ACC vehicle analysis for longitudinal dynamic control. Due to the lower-level controller computing the throttle and brake input commands for the ACC vehicle, the proposed complex model is also controlled using these two control inputs. This complex vehicle model will be used for both vehicles in the two-vehicle system (Figure 3-34) which consists of a preceding vehicle and an ACC vehicle (following vehicle).

Two engine models, a second order and a first order engine model, based on engine maps have also been developed in this chapter. The simulation results obtained from engine map models have been compared with parametric engine model. This comparison ensures that the engine maps are producing the required satisfactory results. The validation of engine maps is necessary because these engine maps will be adopted in the lower-level controller in order to compute the required throttle commands for the complex ACC vehicle model.

This chapter also presents a simple ACC vehicle model which will be adopted for the upper-level controller analysis and the complex vehicle validation. A first-order lag has also been incorporated in this simple vehicle model which corresponds to the performance of the lower-level controller.

The methodology to accomplish the research study objectives has also been discussed in this chapter. In Chapter 4 and Chapter 5, the first-order ACC vehicle model will be employed in order to compare four control strategies, namely, proportional-integral-derivative (PID) control, sliding mode control, constant-time-gap (CTG), and Model Predictive Control (MPC) method. Based on their analyses and comparison the most suitable control algorithm will be adopted for the lower-level controller and the complex ACC vehicle analysis in Chapter 6.

Chapter 4. ACC Vehicle Analysis for PID, Sliding Mode, and Constant-Time-Gap Methods

4.1 Introduction

A 5-speed automatic transmission powertrain model to control the longitudinal dynamics of a vehicle has been developed in Chapter 3. The powertrain model has been simulated for different input command, mainly from throttle input and a positive road gradient. The simulation results obtained from the powertrain model have been validated against previous studies and show a good agreement with them. The developed vehicle longitudinal dynamic model will be used for a two-vehicle system developed in this study which consists of a preceding vehicle and an adaptive cruise control (ACC) vehicle. The main focus is to investigate the complex ACC vehicle response during critical transitional manoeuvres (TMs) under the influence of vehicle internal complex dynamics and within constraint operational boundaries.

The longitudinal control model of an ACC vehicle is usually composed of two separate controllers, the upper-level controller and lower-level controller (Connolly and Hedrick, 1999; Rajamani *et al.*, 2000). Before using the lower-level controller and complex ACC vehicle model for the ACC vehicle analysis, it is important to understand and synthesize the upper-level controller model and the control strategies used for it.

A control system can be defined as a system which consists of interconnected components, designed to achieve a desired objective. The main purpose of a feedback system is to control the behaviour of a system in order to benefit the society, provided that the nature of the controlled system is well understood and modelled. Typically, a controller can be viewed as a function of state variables, or as a dynamical system driven by certain system outputs. There are many different types of controllers being used in industrial processes, chemical process systems, mechanical systems, electrical systems, and economical processes. These controllers could be anything ranging from a simple classical proportional-integral-derivative (PID) controller to the most sophisticated non-linear controllers. The challenging task for a controller is to perform well in spite of uncertainties present in a system (Dorf and Bishop, 2001).

The system to be controlled in this study is a two-vehicle model, Figure 4-1, which consists of a preceding vehicle and an ACC vehicle. The objectives for the ACC vehicle are to establish and maintain a specified inter-vehicle distance (SIVD) with zero range-rate behind the preceding vehicle under steady-state and TMs. A TM can be defined as a manoeuvre performed by the ACC vehicle to establish the SIVD using measurements of range, range-rate, and the ACC vehicle velocity and acceleration. There are two requirements for a successful TM: (1) the ACC vehicle must establish a zero range-rate when at the SIVD; and, (2) the ACC vehicle must avoid a collision with the preceding vehicle (Bageshwar *et al.*, 2004).
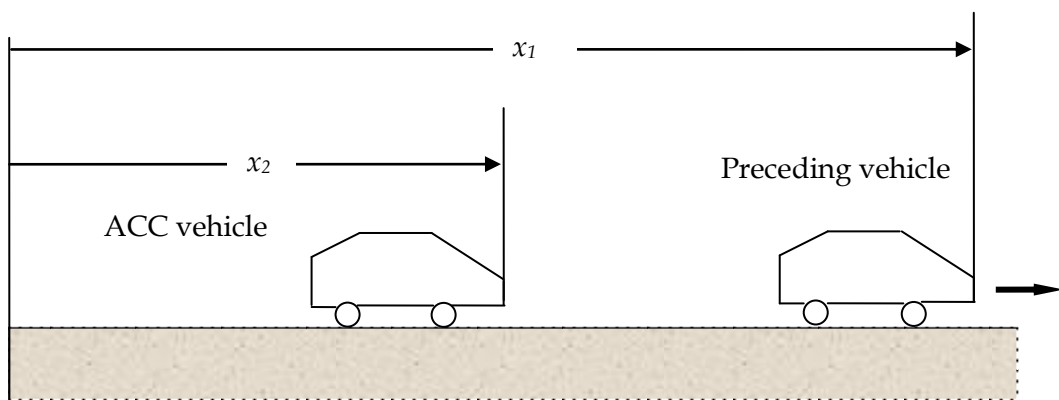

Figure 4-1   A two-vehicle system

This chapter focuses on the study of Adaptive Cruise Control (ACC) System for a passenger vehicle, ACC system components, ACC system limitations, and the important features of the ACC system which play a significant role to control the longitudinal dynamics of an ACC vehicle. Two modes of operation of an ACC vehicle, namely speed control mode and vehicle following, and the switching between these two modes, the effects of transitional manoeuvres on the ACC vehicle's longitudinal dynamics when it is operating in the vehicle following mode are covered here.

One of the important objectives of this study is to develop and analyse the upper-level controller using four well-known control strategies under steady-state and transitional operations. The four control strategies used for the upper-level controller analysis are:

(1) Proportional-Integral-Derivative (PID) Control

(2) Sliding Mode Control

(3) Constant-Time-Gap (CTG) Control

(4) Model Predictive Control (MPC).

The first three control strategies will be developed and analysed in this chapter and the fourth control method will be developed in Chapter 5. In these controllers analysis, the preceding vehicle is based on the complex vehicle model which includes engine, torque converter, transmission, and drivetrain models (Section 3.2 to Section 3.5) and the ACC vehicle model is based on the first-order vehicle model (Section 3.8). A simple first-order ACC vehicle model is used to compare the performance of these control methods at the upper-level controller level under the same critical encounter scenarios between the two vehicles. After the comparison, the most appropriate out of these four control methods will be applied to the lower-level controller and the complex vehicle model for longitudinal dynamics control of an ACC vehicle in Chapter 6. It should be noted that due to the finite bandwidth of the lower-level controller the ACC vehicle will be unable to track the desired acceleration commands. Therefore, the ACC vehicle model must consider the finite bandwidth of the lower-level controller (Rajamani, 2006). Based on this

consideration the upper-level controller is designed and then the first-order ACC vehicle model is used.

The simulation scenarios considered for all controllers analysis range from steady-state to transitional operations. In the first scenario, the same initial conditions have been considered for both vehicles, i.e. same initial velocities. The only initial condition that differs is the initial position of both vehicles. Once the controllers are analysed for this simple scenario, then more complexities are added in the simulation scenarios to analyse the stability and robustness of each controller. In the second and third scenario, a high speed ACC vehicle encounters an accelerating or a halt preceding vehicle in the same lane. Under these scenarios the ACC vehicle exceeds the deceleration limit of -0.5g. The results obtained from each control algorithm are compared and discussed in detail.

The main tasks for the control methods to perform on the ACC system are:

1   Track smoothly desired acceleration commands

2   Reach and maintain a SIVD in a comfortable manner and at the same time react quickly in the case of dangerous scenarios.

3   System performance optimization.

4   Optimize the system performance within defined constrained operational boundaries.

There are many benefits of the entire system from a control point of view, e.g. in case of emergency manoeuvres the control system can react significantly faster than a human reacting in the same situation.

This chapter outline is as follows. In Section 4.2 the ACC system with its fundamental features, its components, and its limitations are explained. In Section 4.3, the PID control method and its application to the two-vehicle system are presented. In Section 4.4, sliding mode formulation is presented and its application to the two-vehicle system is analysed. In Section 4.5, CTG algorithm is applied to the two-vehicle system. Finally, Section 4.6 presents the conclusions of this chapter.

4.2 Adaptive Cruise Control System

A standard cruise control system enables a ground vehicle to control its longitudinal speed. A desired speed is selected by the driver, and a control system operates on the throttle to maintain this desired speed (Girard *et al.*, 2005; Rajamani, 2006; Ferrara and Vecchio, 2007). ACC systems have been developed as an enhancement to the standard cruise control systems. In addition to the speed control mode, an ACC-system equipped vehicle can also regulate the set speed to maintain a SIVD from a preceding vehicle (Liang and Peng, 1999; Haney and Richardson, 2000; Girard *et al.*, 2005). This additional feature is termed as vehicle following mode. The control law for the vehicle following mode is computed using onboard radar sensors that measure the range (relative distance) and the range-rate (relative velocity) between the ACC vehicle and the preceding vehicle (Liang and Peng, 1999; Bageshwar *et al.*, 2004; Rajamani, 2006). Therefore, both throttle input and brake input are required to control the distance and the relative velocity between an ACC vehicle and a preceding vehicle. In the vehicle following mode the SIVD is a function of the preceding vehicle's velocity (Bageshwar *et al.*, 2004). SIVD is the spacing control policy between the two consecutive vehicles, and in this study it varies with the speed of the preceding vehicle. In the literature (Ferrara and Vecchio, 2007) it is termed as headway spacing control policy.

The headway control can be viewed as a composition of two separate operations: transitional operation and steady-state operation. At the point of contact with the preceding vehicle, an ACC vehicle tends to establish the SIVD with the preceding vehicle by tracking a transition trajectory which is called the transitional operation and then maintains the required SIVD with the preceding vehicle, which is known as steady-state operation. During the transitional operation, the ACC vehicle has to decide when to switch from speed control mode to vehicle following mode and use a control strategy to manoeuvre the vehicle to establish the SIVD.

4.2.1 Vehicle Controllers

The longitudinal controller system of an ACC vehicle is usually composed of two
separate controllers, the upper-level and lower-level controllers (Rajamani and Zhu,
2002), Figure 4-2.

Information from
preceding vehicle

Upper-level controller

Desired
acceleration

Error signal

Lower-level controller

Desired
throttle/brake input
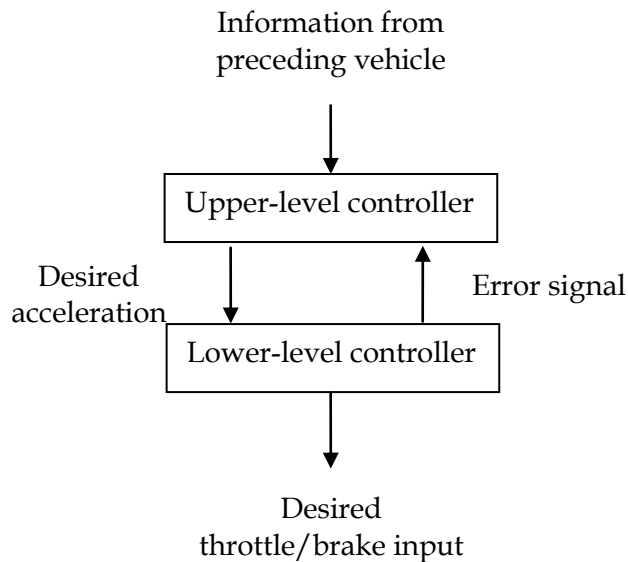
Figure 4-2   ACC vehicle longitudinal control system (Rajamani, 2006)

The spacing control law is designed within the upper-level controller model of an
ACC vehicle where the kinematic relation between the range (R) and range-rate ($\dot{R}$)
between the two vehicles and the ACC vehicle velocity and acceleration are used to
compute the desired acceleration for the lower-level controller (Bageshwar *et al.*,
2004). The lower-level controller uses this desired acceleration command to generate
the required throttle and braking commands for the ACC vehicle to track the
spacing-control laws computed by the upper-level controller (Girard *et al.*, 2005).
The error signal generated due to differences in the longitudinal motion of the
preceding vehicle and the ACC vehicle is sent back to the upper-level control where
the desired acceleration for the next time step is calculated.

4.2.2 Range vs. Range-Rate Diagram

The terms range, range-rate and switching between different modes of operation of an ACC vehicle can be exemplified well by constructing a range versus range-rate diagram using the kinematic relationship between range and range-rate (Bageshwar *et al.*, 2004; Rajamani, 2006) to illustrate the requirements of transitional operation, as shown in Figure 4-3. A negative range means that the ACC vehicle has collided with the preceding vehicle. Figure 4-3 shows the regions and conditions for the switching between the different control modes of an ACC vehicle. Based on the measurement of range and range-rate, an ACC vehicle selects the control mode and decides when to switch between these modes. The region above the dashed line is for speed-control mode (cruise control) and the region between the dashed and solid line is for vehicle-following mode. The region below the solid line shows that the deceleration by the ACC vehicle is not enough and the driver should take control of the vehicle to avoid the collision by applying emergency braking or by lane changing (Rajamani, 2006). This study is focused on the transitional manoeuvres when an ACC vehicle is operating on vehicle-following mode, and on the switching from speed-control mode to the vehicle-following mode. The range vs. range-rate diagram plays a vital role in computing the desired acceleration in order to follow a preceding vehicle at a safe distance. Different properties of the relation between range and range-rate can be discussed. For example, the relation between range and range-rate shows different trends of motion for an ACC vehicle and how the switching between speed-control mode and vehicle-following mode is initiated. The details of these properties will be discussed.

For a more in depth understanding of the range vs. range-rate diagram one can study Figure 4-3 by developing a relation between range and range-rate. The range between the two consecutive vehicles depends upon the range-rate of the two vehicles (Rajamani, 2006). For example, when the range-rate is positive i.e. when in the right half of the range vs. range-rate diagram, the range will always increase, while the range-rate is negative i.e. in the left half of the range vs. range-rate diagram, the range will always decrease. In other words, in the right-half plane an ACC vehicle always encounters a faster preceding vehicle and travels under throttle control, while in the left-half plane an ACC vehicle always detects a slower or halt preceding vehicle and operates under brake control in the same lane on a highway.
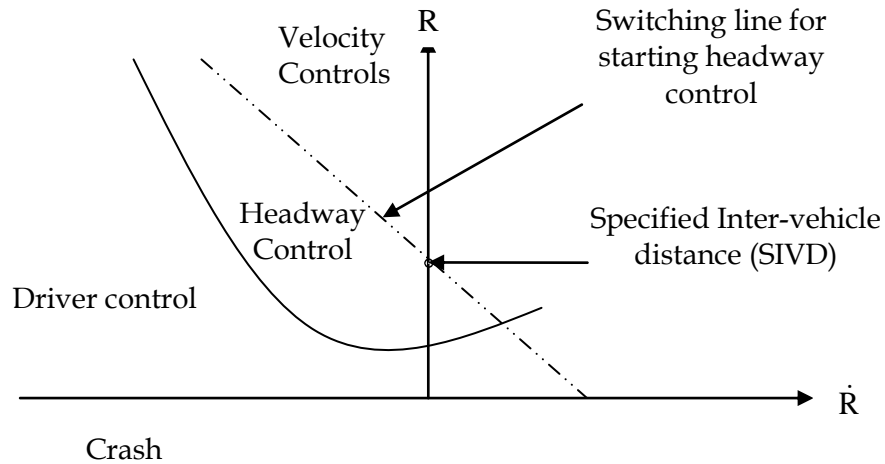
Figure 4-3   Range vs. range-rate diagram (Rajamani, 2006)

4.2.3 System Components

An ACC system is an autonomous system because it does not depend on the
wireless communication with the other vehicles on the highway. An ACC system
makes its control decision based on information captured from its preceding vehicle
through its sensors and the corresponding action is performed by using some
advanced actuators. The important components of an ACC vehicle are sensors,
throttle system, and brake system.

4.2.3.1   Range sensor

The most important component in an ACC system is a sensor which measures the
distance, the relative speed, and the relative position of the preceding vehicle. This
sensor is usually called range sensor and different types of a range sensor, e.g.
optical, laser, and radar, have been discussed in the literature. Among these three
types of range sensor, the radar sensor has been used in the previous studies due to
the following reasons: (1) a measurement up to 150m is achievable; (2) a range
sensor can be packed behind plastic surfaces; and, (3) the most important is its

performance which is less sensitive to weather conditions. The radar sensor used in ACC vehicles operates at a frequency of 77 GHz (Haney and Richardson, 2000).

4.2.3.2 Throttle system

In the speed-control mode like, as in cruise control system, the driver sets the desired speed of the ACC vehicle and the control system operates on the throttle to maintain a desired speed. In the vehicle-following mode, the throttle angle is controlled by the signal received from the lower-level controller. The lower-level controller determines the desired throttle angle based on the desired acceleration commands computed by the upper-level controller. It is assumed that the driver has the control of the steering of the vehicle at all time when ACC vehicle is in vehicle-following mode unless a critical situation arises when the driver interaction is required to control the ACC vehicle in order to avoid collision.

4.2.3.3 Braking system and traction/braking force saturation

An ACC system is designed to provide comfort to the driver and other passengers and to help improve the safety in an uneven or critical driving situation. An ACC system equipped vehicle uses the throttle actuator and brake actuator to accomplish these objectives. It is the requirement of the braking system to apply the brake smoothly without exceeding the comfort level which can be defined by the maximum deceleration level when brake torque is applied i.e. -0.5g (Bageshwar *et al.*, 2004). The brake system of an ACC system is controlled by the control signal received from the lower-level controller. The lower-level control computes the desired brake torque based on the desired acceleration commands computed by the upper-level controller. In this study a number of critical driving manoeuvres have been simulated when the brake torque reaches the saturation level, i.e. no further brake torque can be applied once maximum value is reached.

4.2.4 System Limitations

An ACC system attractive for the automobile manufacturers and most of luxurious vehicles, Mercedes, Sedans, Lexus LS340, etc, are equipped with an ACC system. Due to its advanced features, it relieves the driver of stress associated with tiresome driving tasks such as maintaining speeds on long journeys, driving behind other vehicles in congested traffic, safety assurance. Despite its advanced functions an ACC system also contains some operational and physical constraints. Two physical constraints for an ACC vehicle have to be incorporated in the formulation of the upper-level controller, used for the vehicle-following control law. Firstly, the ACC vehicle is not permitted to have a negative velocity during a transitional manoeuvre, and secondly, the ACC vehicle is assumed to have limited accelerations: a lower limit equal to -0.5g and an upper limit equal to 0.25g (Bageshwar *et al.*, 2004). Equation (4.1) and Equation (4.2) show the two physical constraints applied on this ACC vehicle model during the high deceleration (transitional) manoeuvres.

$$\dot{x}_2(t) \geq 0 \tag{4.1}$$

$$u_{\min} \leq u(t) \leq u_{\max} \tag{4.2}$$

It should be noted that the lower acceleration limit implies that the ACC vehicle cannot apply the necessary brakes to avoid the collision with the preceding vehicle. Even while providing a support for the driver, he/she still remains responsible for the vehicle handling while performing lateral manoeuvres and in a complex decision making. According to a study (Troppmann and Hoger, 2006), an ACC vehicle is activated in highways or motorways, and when the long journeys are required. An ACC vehicle still cannot allow the control operation in congested city environment.

Initial conditions for the transitional manoeuvres are based on the range, range-rate, and the ACC vehicle velocity and acceleration when the preceding vehicle is first encountered. The possible initial conditions are those for which the ACC vehicle

avoids the collision with the preceding vehicle, while reducing its speed from its
initial velocity to the velocity of the preceding vehicle. The minimum range required
for the ACC vehicle can be computed using the maximum available deceleration for
the ACC vehicle for the transitional manoeuvres (Bageshwar *et al.*, 2004). The same
initial conditions determined by Bageshwar (2004) model have been adopted in this
study which corresponds to the possible deceleration level to reduce the speed of
the ACC vehicle in order to avoid the collision with the preceding vehicle.

4.3   PID Control Architecture

The PID control approach is simple and easy to implement. It is widely applied in
industry to solve various control problems. It has been estimated that 98% of all
control systems in the pulp and paper industries are controlled by PI controllers,
and in process control applications, more than 95% of the controllers are based on
PID controllers (O'Dwyer, 2009). The ability to keep the controlled variable response
close to the desired closed-loop response has gained a considerable acceptance in
the chemical process industries because of its simplicity, robustness and successful
practical applications (Lee *et al.*, 1998). The PID controller has been a convenient
method of compensation in wide range of applications where a simple control
system is used or where a lengthy modelling and design process is unacceptable
(O'Dwyer, 2009). In this section, the basic PID control architecture is presented and
then it is applied to the two-vehicle system.
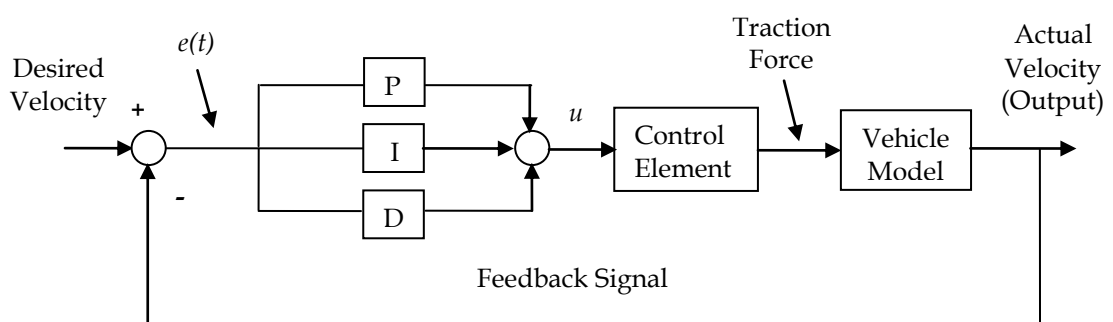
Figure 4-4   Block diagram for the PID feedback control system

Figure 4-4 shows the schematic diagram of a classical PID controller for the two-vehicle systems. Before analysing the two-vehicle system using the PID control approach, it is necessary to understand the PID control algorithm. Basically, the PID controller operates as a closed-loop system where an error signal $e(t)$ which is the difference between the desired input (desired velocity) and the actual output (actual velocity) is applied to the PID controller. The PID controller then determines both the derivative and the integral of this error signal $e(t)$. The control signal (u) generated by the PID controller is merely equal to the proportional gain (K_P) times the magnitude of the error signal $e(t)$ plus the integral gain (K_I) times the integral of the error signal $e(t)$ plus the derivative gain (K_D) times the derivative of the error signal $e(t)$,Equation (4.3). The control element then produces the correspondent traction force for the ACC vehicle to follow the preceding vehicle at a safe desired distance.

$$u = K_P e(t) + K_I \int e \, dt + K_D \frac{de}{dt} \tag{4.3}$$

With the initial error signal $e(0)$, the control signal (u) is computed and sent to the vehicle model which produces a new output (actual velocity), this new output signal is fed back to be compared with the desired input (desired velocity) which generates a new error $e(t)$, the new error $e(t)$ is sent again to the controller which also computes the integral and derivative of this new signal. The new output signal is sent back as a negative feedback signal such as the objective is to steer the $e(t)$ toward zero.

The error signal to the PID controller is the difference between the velocities of the two vehicles. The three components of the PID controller: proportional, integral, and derivative, play their corresponding role in order to improve the performance of the PID controller, e.g. the proportional controller can influence the rise time but it is unable to eliminate the steady-state error. The task of eliminating the steady-state error is monitored by the integral controller. Eliminating the steady-state error may result in worse transient response. To avoid that and to improve the stability of the system the derivative action is used. It should be noted that these three controllers are co-related to each other, if one of the controller gain change then it has a corresponding effect on the other two. One by one, all three control gains are

selected and the best combination of the three is selected which improves the stability of the system. In the tuning process, each control gain is varied while keeping the other two fixed such as a further improvement in the control output can be achieved (Visioli, 2006).

4.3.1 PID Control for Two-Vehicle System with Headway Spacing Policy

In the early stage of this study a PID control strategy was used for the upper-level controller of the ACC vehicle and the analysis was carried out for different transitional manoeuvres. The PID control algorithm is applied on the upper-level controller of the ACC vehicle to analyse the performance of the ACC vehicle. The PID control law for the follower ACC vehicle can be expressed as:

$$u = K_P (\dot{x}_1 - \dot{x}_2) + K_I (x_1 - x_2 - h\dot{x}_2) + K_D (\ddot{x}_1 - \ddot{x}_2) \qquad (4.4)$$

where K_P, K_I, and K_D are the controller gains, x_1 and x_2 are the actual positions of the preceding vehicle and the follower ACC vehicle respectively. The longitudinal states of the preceding vehicle are obtained from Equation (3.24) and the longitudinal states of the ACC vehicle are obtained from Equation (3.32). The term $h\dot{x}_2$ is called headway spacing policy where the spacing (SIVD) between the two vehicles varies linearly with the vehicle's speed such that the headway time (h) between the two vehicles remains constant. The headway time (h) can be defined as the time taken by the follower vehicle to reach the point where the preceding vehicle is at present speed (Naranjo et al., 2003). In this study, h is assumed as 1 s (Bageshwar et al., 2004; Rajamani, 2006). The control input (u) is the desired acceleration command applied to Equation (3.32) to determine the response of the first-order ACC vehicle model.

Rajamani (2006) has used the PID controller for the speed control of a cruise control system. Peppard (1974) designed a model for the string stability of relative-motion between the vehicles based on the PID feedback control algorithm for individual vehicle which uses the velocity error of the controlled vehicle from a specified value and its distance error to the vehicle ahead and the vehicle behind it. A constant

spacing policy has been adapted in this model. Peppard (1974) did not consider the measurement of error propagation towards the tail of the platoon, instead, Peppard (1974) investigated the relative-motion stability of the vehicles and his model disregarded the actuation and sensing lags of the system operations. In this study an attempt has been made to use the PID controller for an ACC vehicle when it is operating in the vehicle-following mode. The PID control algorithm has been used in order to compare the performance of the ACC vehicle when the MPC method is used for the same two-vehicle system (Chapter 5) under the same operating conditions. Different situations which consist of different encounter scenarios of the preceding vehicle and the ACC vehicle have been considered as follows.

4.3.1.1 Preceding vehicle with throttle input of 50 degrees and same initial conditions for both vehicles

There are different scenarios which have been considered for the two vehicle system as discussed in Section 4.1. In the first scenario, the same initial conditions, i.e. same initial speeds and same initial accelerations accept the vehicle positions for both vehicles are considered, the throttle input for the preceding vehicle is set to 50 degrees for the entire simulation time of 30 s. The upper-level controller is based on a PID control algorithm and the ACC vehicle model used is a first-order model (Section 3.8). The PID controller gains in all scenario are obtained using the famous Ziegler-Nichols method as shown in the Table 4-1.

| Control Type	K_P	K_I	K_D
PID	$0.6K_u$	$2\,K_P\,/\,P_u$	$K_P P_u\,/\,8$

Table 4-1   Ziegler-Nichols method

where K_u is the proportional gain at the point when the output of the system starts to oscillate while setting the integral and derivative gain to zero, and P_u is the total oscillation period. For the ACC vehicle model, K_u = 2.2 and P_u = 5 s (Franklin *et al.*, 2006).

In this scenario as shown in Figure 4-5, both vehicles are starting from rest and the initial positions of the preceding vehicle and the ACC vehicle are 10 m and 0 m respectively. Figure 4-5(a) shows that the first-order ACC vehicle model maintains the same speed as the preceding vehicle. The acceleration of the ACC vehicle is matching well with the preceding vehicle acceleration, Figure 4-5(c). The positions of both vehicles are shown in Figure 4-5(c). The ACC vehicle, starting 10 m behind the preceding vehicle, follows the preceding vehicle using the headway spacing policy, which can be seen in Figure 4-5(d). During this simple manoeuvre, the ACC vehicle has successfully established and maintained the desired SIVD between the two vehicles, Figure 4-5(d). It should be noted here that Figure 5-4(c) also shows the acceleration profile of the preceding vehicle. This profile shows the dynamic effects during the gear shifts at t = 2.4 s (1-2 gear shifting) and at t = 11.6 s (2-3 gear shifting). The gear transmission takes place automatically based on the information of the throttle input and the longitudinal velocity as discussed in Section 3.4. The ACC vehicle's doesn't show these dynamic effects because the vehicle's sub-models are not considered in the simple vehicle model.

Since the ACC vehicle has smoothly performed in this simple scenario, therefore, the ACC vehicle will be analysed now for the complex situations using the PID control algorithm.
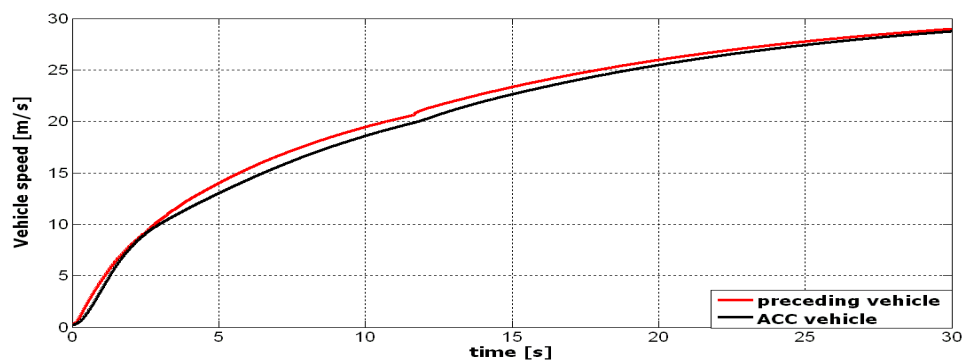

(a)
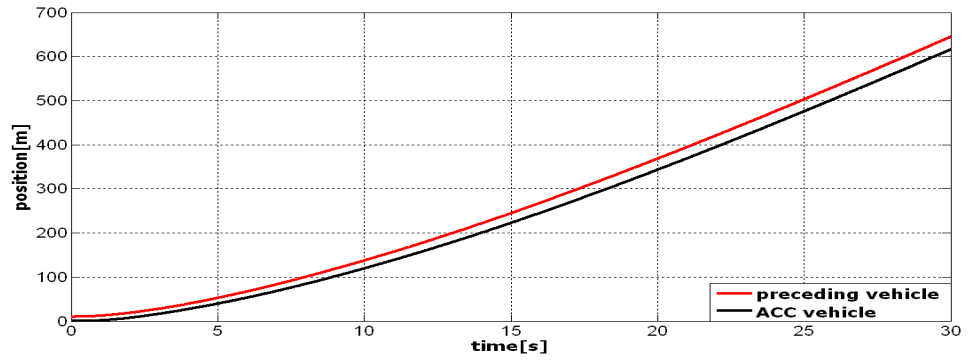
(b)
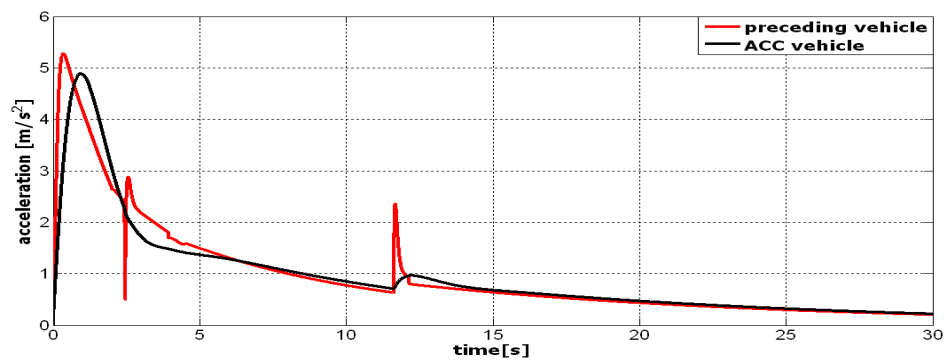
(c)
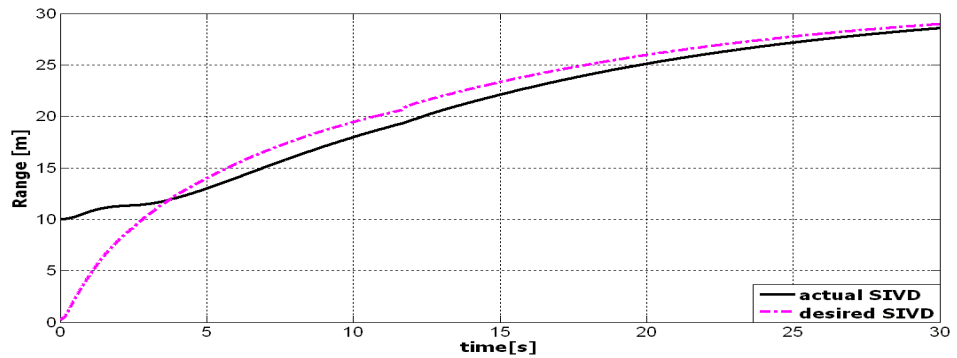
(d)

Figure 4-5   (a) Velocities of the vehicles, (b) Positions of the vehicles, (c)
Accelerations of vehicles, (d) Range between both vehicles

4.3.1.2 Preceding vehicle with throttle input of 50 degrees and different initial conditions for both vehicles

In the second scenario as shown in Figure 4-6, both vehicles start with the different initial speeds and different initial positions while the throttle angle for the preceding vehicle is kept constant at 50 for the entire simulation time of 20 s. The baseline scenario is that an ACC vehicle travelling at 30 m/s (67 MPH) in the speed control mode detects a preceding vehicle which is accelerating from 10 m/s (22.34 MPH), the ACC vehicle is 60 m behind the preceding vehicle when it detects the preceding vehicle. The ACC vehicle response, using the PID control method, has been analysed for two different situations: (1) the ACC vehicle has no acceleration limits and (2) the ACC vehicle is restricted to the acceleration limits. In situation (2), if the acceleration command computed by Equation (4.4) is less than the deceleration limit, then the acceleration command is set equal to the deceleration limit.

The velocity of the ACC vehicle for both conditions is shown in Figure 4-6(a), the velocity profile, with limited acceleration, establishes first the SIVD and then maintains the zero-range-rate behind the preceding vehicle; this manoeuvre can be well understood by observing acceleration graph in Figure 4-6(c). The ACC vehicle without the acceleration limits, only concerns with establishing a SIVD with zero-range-rate and is unable to meet the other requirements of the transitional manoeuvre.

Figure 4-6(b) shows the corresponding positions of the two vehicles for this scenario. The initial relative distance between the two vehicles is 60 m. In response to the initial deceleration commands computed using by the PID control method; the ACC vehicle decelerates and successfully establishes a SIVD with a zero range-rate behind the preceding vehicle based on the headway spacing control policy for both limited and unlimited acceleration conditions. Once the SIVD is established, the ACC vehicle maintains the steady-state operation with a SIVD, which is the function of the vehicle speed. Figure 4-6(d) shows the range (relative distance) between the two vehicles. It can be seen that the ACC vehicle is smoothly establishing the desired SIVD after the transitional operation. It has been observed from this analysis that the ACC vehicle, using the PID control algorithm, has performed all the control tasks discussed in Section 4.1.
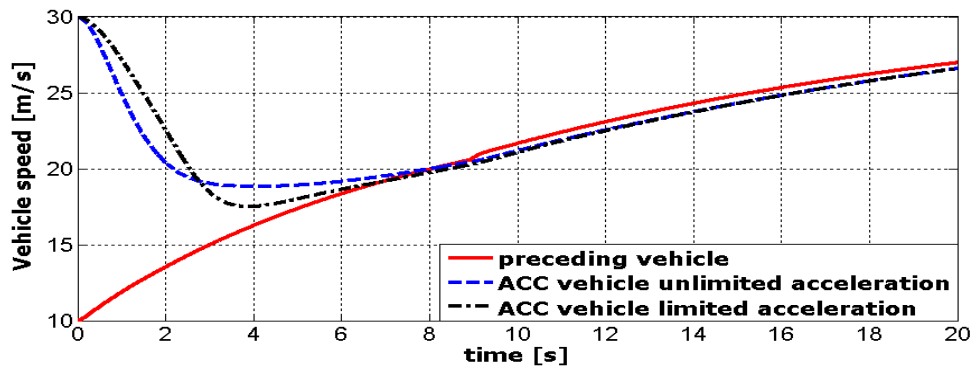
(a)
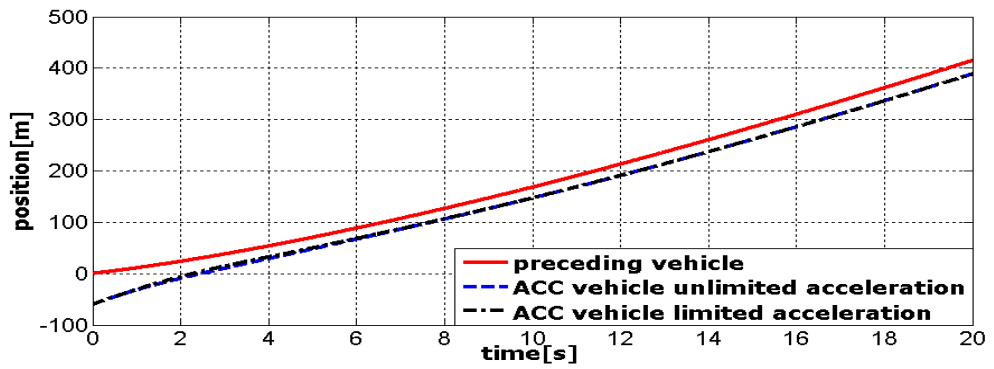
(b)
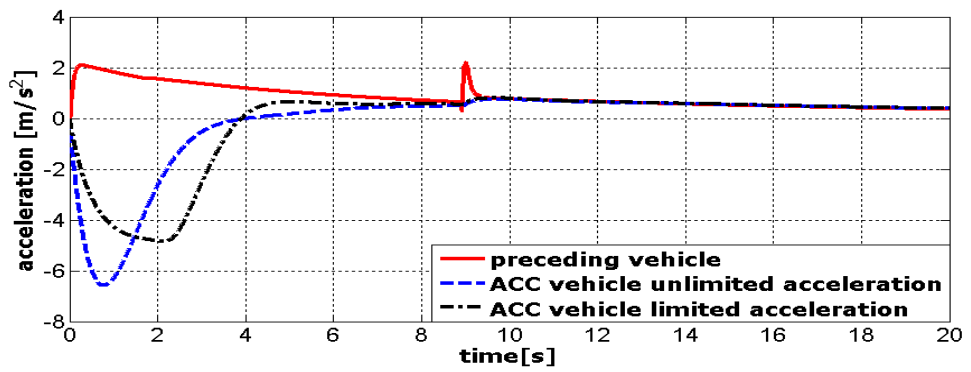
(c)
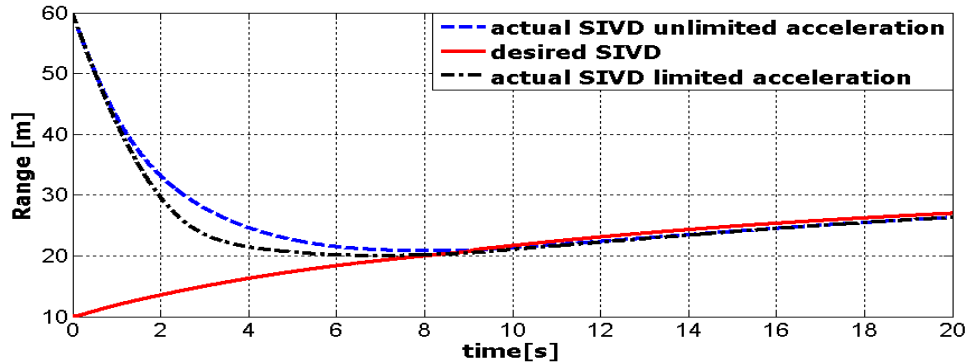
(d)

Figure 4-6   (a) Velocities of the vehicles, (b) Positions of the vehicles, (c)
Accelerations of vehicles, (d) Range between both vehicles

### 4.3.1.3   ACC vehicle response against a halt preceding vehicle

In the third scenario considered below, an ACC vehicle detects a halt vehicle in
front of it. The initial speed of the ACC vehicle is 30 m/s, and it is 110 m behind the
preceding vehicle. This encounter scenario has also been analysed for two different
situations; (1) ACC vehicle with unlimited acceleration, (2) ACC vehicle with
limited acceleration. In situation (2), if the acceleration command computed by
Equation (4.4) is less than the deceleration limit, then the acceleration command is
set equal to the deceleration limit.

The simulation results for both conditions are shown in Figure 4-7. It can be seen
with unlimited acceleration, the ACC vehicle successfully performs the TM (dashed
line). In the case of acceleration limits (dashed-dotted line), the ACC vehicle cannot
meet the required control objectives of establishing the desired SIVD with zero
range-rate and collides with the preceding vehicle as shown in Figure 4-7(b)
(dashed-dotted black-line). During this TM, the ACC vehicle is executing a negative
velocity, Figure 4-7(a) (dashed-dotted black-line), which does not satisfy Equation
(4.1) constraint. The initial commands computed by the PID control law for the ACC
vehicle is to accelerate rather than to decelerate, Figure 4-7(c). If the initial
commands are to accelerate then the deceleration limits would not allow using the
necessary brakes to avoid a collision with the preceding vehicle. It is essential that
ACC vehicle must decelerate to avoid the collision. After analysing this scenario, it
can be concluded that the PID control law is not feasible for these kinds of

transitional manoeuvres of the ACC vehicle, because, the PID control algorithm
does not include either the state constraints or the control constraints in its
formulation.
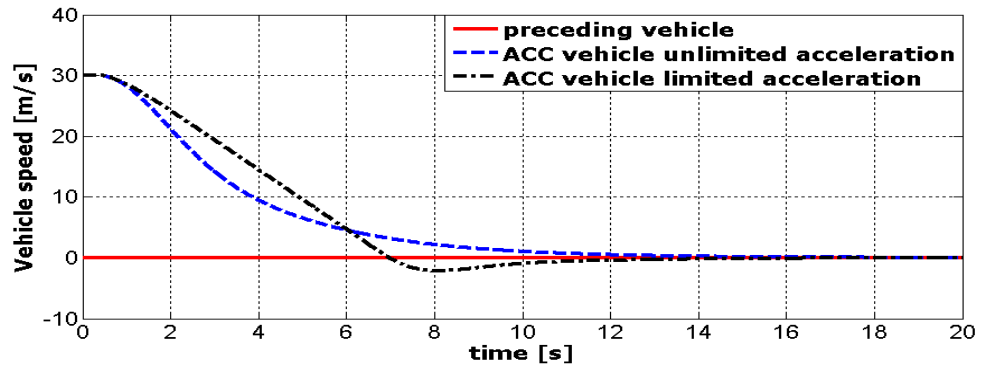
(a)
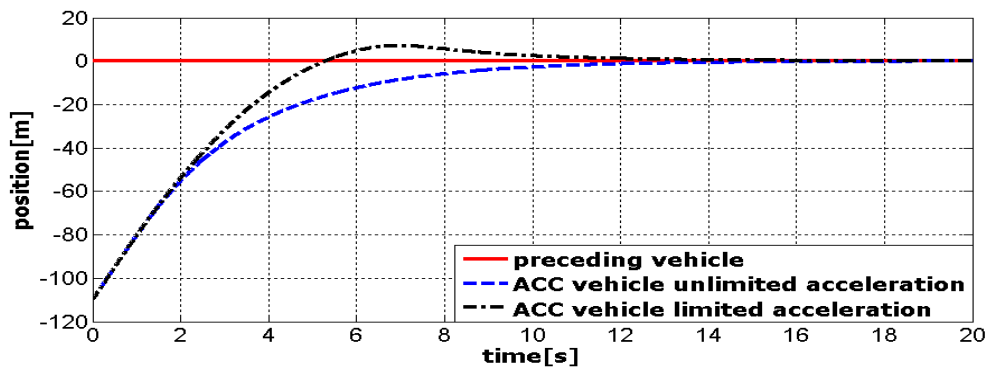
(b)
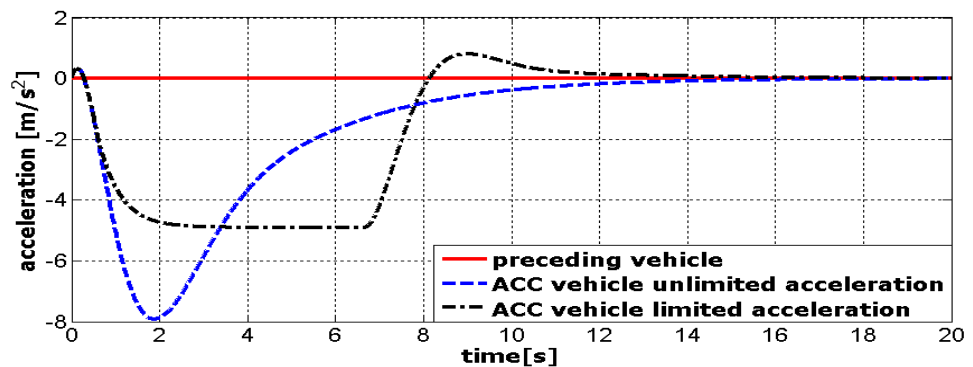
(c)

Figure 4-7   (a) Velocities of the vehicles, (b) Positions of the vehicles, (c)
Accelerations of vehicles

102

Basic ordinary PID controllers are used for the distance control of an ACC vehicle. These controllers are easy to set up and allow high performance on the micro-controller due to low demands of calculating power. Problems arise, if several variables have to be controlled within the constrained boundaries, e.g. states and control constraints as we have seen in the above simulation results. It has been observed that the functionality of the PID controller is limited and approaches for stability determination of more than one variable are complicated.

4.4   Sliding Mode Control Method

Sliding mode is an advanced type of variable structure system. Sliding mode control is an efficient tool to control complex high-order dynamic plants operating under uncertainty conditions. Sliding mode control can be conveniently used for both non-linear systems and systems with parameter uncertainties due to its discontinuous controller term. That discontinuous control is used to negate the effects of nonlinearities and/or parameter uncertainties (Utkin *et al.*, 1999). The sliding mode approach is used in this study for the longitudinal dynamic control of an ACC vehicle in order to minimize the effects generated due to the nonlinearities in a vehicle dynamic model. Before using sliding mode method for an ACC vehicle system it is necessary to understand the structure and algorithm of the sliding mode method. The subsequent section describes the sliding mode method and its properties, and an example is given illustrate and understand how the sliding mode method controls the system dynamics.

The sliding mode control approach is used in a dynamic system which is governed by ordinary differential equations with discontinuous right-hand sides. The term sliding mode was first used in the context of relay systems. It may happen that the control as a function of the system state switches at high (theoretical infinite) frequency; this motion is called sliding mode (Bhatti *et al.*, 1999). The sliding mode approach is method which transforms a higher-order system into first-order system. In that way, simple control algorithm can be applied, which is very straightforward and robust (Utkin *et al.*, 1999). The two main properties of an ideal sliding motion are the disturbance reduction and order reduction. These are the key properties that

have motivated the study of controllers which induce sliding motions (Edwards and
Spurgeon, 1998).

The major advantage of sliding mode is low sensitivity to plant parameter
variations and disturbances which eliminates the necessity of exact modelling.
Sliding mode control enables the decoupling of the overall systems motion into
independent partial components of lower dimension and, as a result, reduces the
complexity of feedback design (Utkin, 2008).

4.4.1 The Sliding Surface

Variable structure control (VSC) systems, as the name suggests, are a class of
systems where the control law is changed during the control process according to
some defined rules which depends on the state of the system (Edwards and
Spurgeon, 1998). Due to nonlinearities and uncertainties in a system the control
objectives cannot be achieved with a strict pairing (gains) on one
sensor/controller/valve. One needs the flexibility to change the pairing
automatically, as part of the control systems. This section provides understanding of
a VSC system as a high-speed switched feedback control resulting in sliding mode.
For example, the gains in each feedback path switch between two values according
to a rule that depends on the value of the state at each instant. The purpose of the
switching control law is to drive the nonlinear plant's state trajectory onto a pre-
specified (user-chosen) surface in the state space and to maintain the plant's state
trajectory on this surface for subsequent time. The surface is called a switching
surface. When the plant state trajectory is above the surface, a feedback path has one
gain and a different gain if the trajectory drops below the surface. This surface
defines the rule for proper switching. This surface is also called a sliding surface
(sliding manifold). Once intercepted, the switched control maintains the plant's
state trajectory on the surface for all time steps and the plant's state trajectory slides
along this surface (Edwards and Spurgeon, 1998; Bhatti *et al.*, 1999; Utkin *et al.*,
1999).

The most important task is to design a switched control that will drive the plant
state to the switching surface and maintain it on the surface upon interception. For

the purpose of illustration, a simple example has been demonstrated below to understand the structure of sliding mode control technique.

Consider the double integrator given by (Edwards and Spurgeon, 1998)

$$\ddot{y}(t) = u(t) \tag{4.5}$$

Then the feedback control law for variable structure is given by

$$u(t) = \begin{cases} -1 & if \quad s(\mathrm{y}, \dot{\mathrm{y}}) > 0 \\ 1 & if \quad s(\mathrm{y}, \dot{\mathrm{y}}) < 0 \end{cases} \tag{4.6}$$

The switching function is given by

$$s(\mathrm{y}, \dot{\mathrm{y}}) = \mathbf{m}\mathrm{y} + \dot{\mathrm{y}} \tag{4.7}$$

where, s is the sliding surface which defines the switching of the control input given in Equation (4.6) and is used to decide which control structure is in use at any point $(\mathrm{y}, \dot{\mathrm{y}})$ in the phase plane, $\mathbf{m}$ is a positive design scalar. Equation (4.6) is usually written in the form:

$$u(t) = -\mathrm{sgn}(s(t)) \tag{4.8}$$

where sgn($\circ$) is the signum, the sign function. The signum function can be expressed by the property such that

$$s\,\mathrm{sgn}(s) = |s| \tag{4.9}$$

A high frequency switching between the two different control structures takes place as the system trajectories repeatedly cross the line s. This high frequency motion is also called as chattering (Utkin *et al.*, 1999). This motion when restrained to the line satisfies the differential equation obtained from rearranging $s(\mathrm{y}, \dot{\mathrm{y}}) = 0$

$$\dot{y}(t) = -\mathbf{m}y(t) \tag{4.10}$$

This represents first-order decay and the trajectories will slide along the line to the
origin as shown in Figure 4-8.
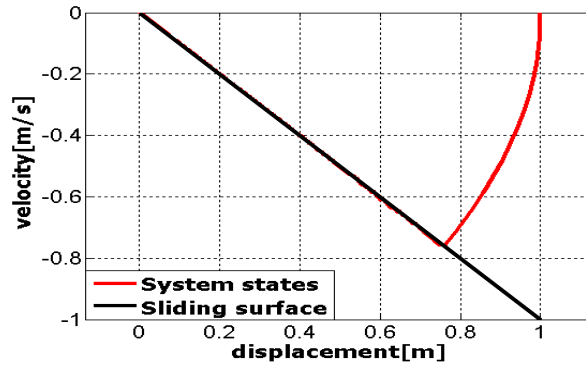
Figure 4-8   Phase portrait of a sliding motion

Such dynamical behaviour is described as an ideal sliding mode or an ideal sliding
motion and the line is termed as sliding surface. During sliding motion, the system
behaves as a reduced-order system which is apparently independent of the control
(Utkin *et al.*, 1999). It is necessary for the control input to maintain $s(y, \dot{y}) = 0$ and
the condition which guarantees that $s(y, \dot{y}) = 0$ is

$$s\dot{s} < 0 \tag{4.11}$$

Which is referred as the reachability condition (Edwards and Spurgeon, 1998; Bhatti
et al., 1999). Figure 4-8 shows a phase portrait of the sliding motion which is a plot of
velocity against position and it shows the state trajectory (red line) starting from an
arbitrary initial condition moves toward the sliding surface (black line).

4.4.2 Sliding Mode Control Technique for a Two-Vehicle System

The above discussion gives a brief understanding of the sliding mode control technique and this technique has been applied on a simple example and the simulation result has been shown and discussed. The sliding mode control technique is now applied to a two-vehicle system which consists of a preceding vehicle and an ACC vehicle. Ferrara and Vecchio (2007) longitudinal dynamic model for a follower vehicle has been considered using sliding mode controller which is based on headway spacing policy.

The longitudinal states of the preceding vehicle are obtained from Equation (3.24) and the longitudinal states of the ACC vehicle are obtained from Equation (3.32). A variable $d = x_1 - x_2$ is introduced which is the relative distance between the preceding and ACC vehicle measured by ACC vehicle. The control objective is to make the relative distance d be equal to

$$L(\dot{x}_2) = h\dot{x}_2 \tag{4.12}$$

where, h is the 'headway time'. With reference to the ACC vehicle, the separation error is

$$e = L(\dot{x}_2) - d = h\dot{x}_2 - x_1 + x_2 \tag{4.13}$$

The control objective can be redefined as to manoeuvre this error (e) to zero, by using the sliding mode control approach (Edwards and Spurgeon, 1998; Utkin $et\ al.$, 1999), one can select this error as a sliding variable

$$S = e = h\dot{x}_2 - x_1 + x_2 \tag{4.14}$$

According to Edwards and Spurgeon (1998) and Utkin (1999), the control law (u) has to satisfy the so-called 'reaching condition'.

$$\dot{S}S \le -\eta|S| \tag{4.15}$$

With η positive constant. Equation (4.15) shows that a suitable choice of the control signal has to guarantee

$$\dot{S} = -\eta \operatorname{sgn}(S) \tag{4.16}$$

where η is chosen sufficiently high to satisfy Equation (4.15), which automatically proves that the sliding manifold $S = 0$ is reached in finite time (Edwards and Spurgeon, 1998). By differentiating Equation (4.14) with respect to time, one has

$$\dot{S} = hu - \dot{x}_1 + \dot{x}_2 \tag{4.17}$$

By substituting Equation (4.16) in Equation (4.17), it is possible to determine the acceleration which the ith vehicle should exhibit to satisfy condition Equation (4.15), i.e.

$$u = \frac{1}{h}(-\eta \operatorname{sgn}(S) - \dot{x}_2 + \dot{x}_1) \tag{4.18}$$

The control input (u) is applied to Equation (3.32) to determine the response of the first-order ACC vehicle model. After several attempts, the η is selected as 2, which gives the satisfactory results.

4.4.2.1 Preceding vehicle with throttle input of 50 degrees and same initial conditions for both vehicles

In the first scenario, same initial speeds and same initial accelerations accept the vehicle positions for both vehicles are considered, the throttle input for the preceding vehicle is set to 50 degrees for the entire simulation time of 30 s. The upper-level controller is based on the sliding mode control method and the ACC vehicle model used is a first-order model (Section 3.8). In this scenario, both vehicles are starting from rest and the initial positions of the preceding vehicle and the ACC vehicle are 10 m and 0 m respectively.

In the case of sliding mode method, both the control input (u) and the acceleration of the first-order ACC vehicle (which is actually a first-order lag in the control input (u) command) model have been plotted in Figure 4-9(a). The control input (u) is computed using the sliding surface, Equation (4.14). Using a suitable value of η (η = 2), the control input (u) satisfies the condition in Equation (4.15) and makes the system state to move towards the sliding surface and reach it in finite time Figure 4-9(e). A high frequency switching takes place as the system trajectories repeatedly cross the sliding surface and this high frequency motion is called chattering. The parameter η decides the rate of convergence of system states towards the sliding surface and the magnitude of chattering in the sliding mode.

The effect of the chattering is not significant during the u computation. It has been noticed that when u is applied to the first-order ACC vehicle model, the lag (τ = 0.5 s) in control input (u) results in the higher magnitude of chattering. This is due to the discontinuous reaching condition Equation (4.16). The effect of this chattering can be seen in Figure 4-9(a). Using the smaller values of lag (τ) reduce the magnitude of chattering. The lag is considered due to lag in actuators, the bandwidth of the lower-level controller that tracks the desired acceleration and filtering of the radar sensor. The chattering can be avoided by keeping into account the dynamics of the actuators in the model and by improving the bandwidth of the lower-level controller or by using a linear reachability condition.

Figure 4-9(b) shows the velocities of both vehicles, Figure 4-9(c) shows the positions of both vehicles, Figure 4-9(d) shows the range between the two vehicles, and Figure 4-9(e) shows the phase portrait for the ACC vehicle. These results seem promising during the steady-state operation. The velocity of the ACC vehicle is matching well with the preceding vehicle velocity Figure 4-9(b), the ACC vehicle is obeying the headway spacing law and tracking the desired SIVD Figure 4-9(d), and the most importantly, the ACC vehicle is switching to the sliding surface (phase portrait) and follows it for the rest of the simulation time Figure 4-9(e).

In has been observed from this simple scenario, due to the chattering effect the sliding mode control method is not suitable for the two-vehicle system considered in this study. As this study is focusing on the critical TMs, therefore, the chattering effects will be higher under these manoeuvres.
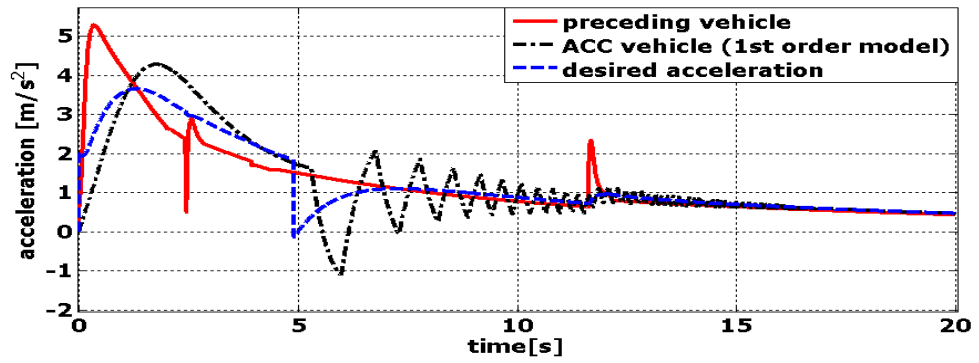
(a)
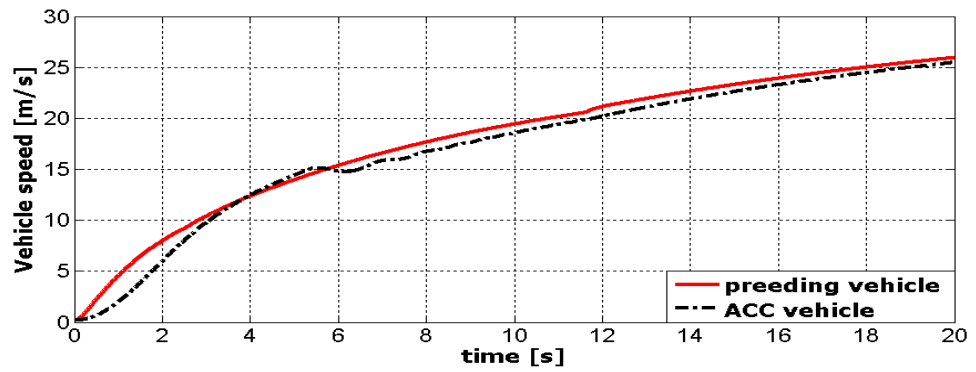
(b)
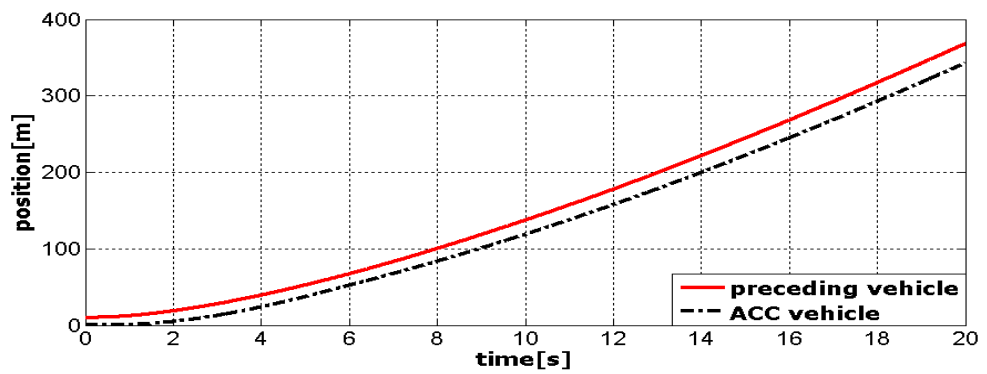
(c)
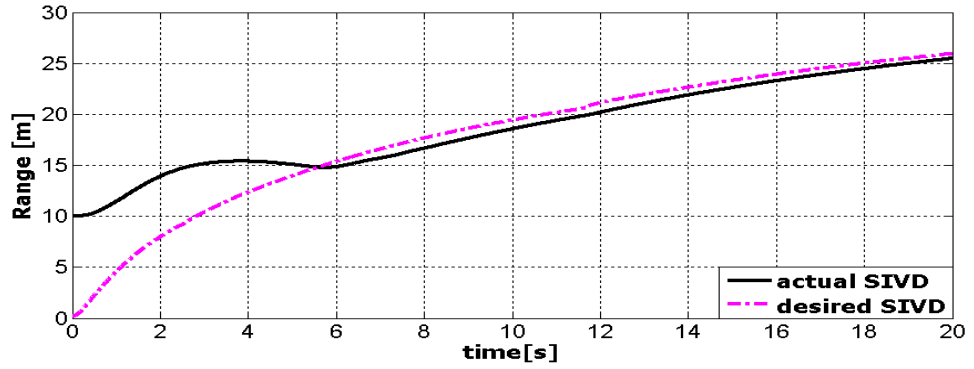
(d)
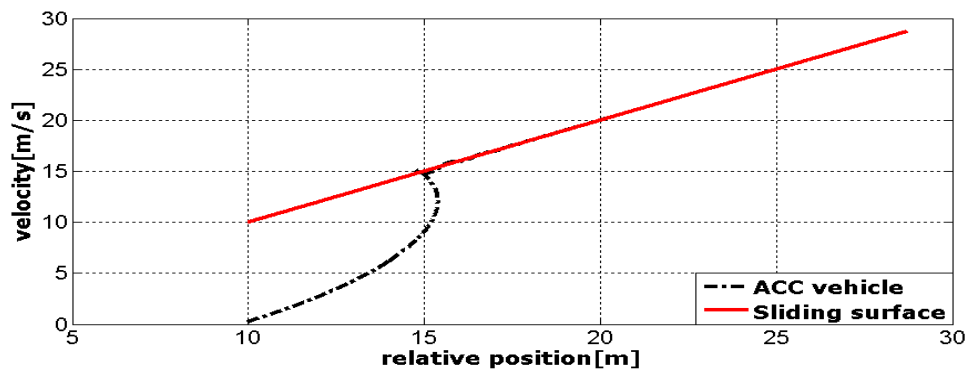
(e)

Figure 4-9   (a) Accelerations of vehicles, (b) Velocities of vehicles, (c) Positions of vehicles, (d) Range between both vehicles, (e) phase portrait

4.5   Constant-Time-Gap Law

In the above discussion PID and sliding control methods have been used for an ACC vehicle analysis under steady-state and transitional manoeuvres as defined in Section 4.1. The results from each method have been produced and their short comings have been discussed. The next step is to use a more suitable control method for an ACC vehicle analysis when it is going through the TMs. A control method which is now used for the ACC vehicle analysis is the constant-time-gap (CTG) law, which can be used for the autonomous control of the ACC vehicle (Rajamani, 2006). The upper-level control algorithm is based on the CTG control method and the ACC vehicle model used is a first-order model (Section 3.8).

The control law for CTG policy can be defined as:

$$u(t) = -\frac{1}{h}(\dot{R}(t) + \lambda_{CTG}\delta(t)) \qquad (4.19)$$

where,

$$\dot{R}(t) = \dot{x}_2(t) - \dot{x}_1(t) \qquad (4.20)$$

$$\delta(t) = x_2(t) - x_1(t) + h\dot{x}_2(t) \qquad (4.21)$$

The control input (u) is the desired acceleration command applied to Equation (3.32) to determine the response of the first-order ACC vehicle model. R is the range between the two vehicles, x_1 and x_2 are the actual positions of the preceding vehicle and the follower ACC vehicle respectively. The longitudinal states of the preceding vehicle are obtained from Equation (3.24) and the longitudinal states of the ACC vehicle are obtained from Equation (3.32). δ Refers to the inter-vehicle error, λ_{CTG} is a constant weighting factor between $\dot{R}$ and δ. The constant h and λ_{CTG} are selected to provide the vehicle with individual vehicle stability and string stability of the platoon of vehicles (Swaroop and Hedrick, 1999; Rajamani and Zhu, 2002; Bageshwar *et al.*, 2004). The requirement for a following vehicle to be individually stable can be defined as that the spacing error between itself and the immediately preceding vehicle should converge to zero when the preceding vehicle is not accelerating. For a following vehicle to be individually stable λ_{CTG} should be greater than zero. For the above model h and λ_{CTG} have been assumed to be 1 s and 0.4 respectively (Bageshwar *et al.*, 2004; Rajamani, 2006). The CTG control algorithm will be analysed under the same situations discussed in Section 4.1, and the simulation results obtained will be compared with the other control methods.

4.5.1 Preceding Vehicle with Throttle Input of 50 Degrees and Same Initial Conditions for Both Vehicles

In the first scenario as shown in Figure 4-10 both vehicles are starting from the rest position. The initial positions of the preceding vehicle and the ACC vehicle are 10 m

and 0 m respectively, and the throttle input for the preceding vehicle is 50 degrees
for the entire simulation time. The desired inter-vehicle distance between the two
vehicles is based on the headway spacing policy, where the inter-vehicle distance is
the function of the preceding vehicle velocity.

The ACC vehicle recieves the desired acceleration commands computed by CTG
spacing policy and then maintains a steady-state operation for the rest of the
simulation. It can be seen in Figure 4-10, the ACC vehicle is smoothly tracking the
desired acceleration commands and following the preceding vehicle with the zero-
range-rate and maintaining a safe distance from the preceding vehicle. Figure
4-10(a) shows that the ACC vehicle speed is matching closely with the preceding
vehicle speed.

Figure 4-10(b) shows the positions of both vehicles, the CTG spacing control law
manoeuvres the ACC vehicle to establish and maintain desired SIVD, Figure
4-10(d), according to the headway policy behind the preceding vehicle. Figure
4-10(c) shows the accelerations of both vehicles, the acceleration of the ACC vehicle
matches well with the preceding vehicle acceleration. This analysis shows that the
CTG spacing control policy can be used for the ACC vehicle analysis under the
similar steady-state operations.
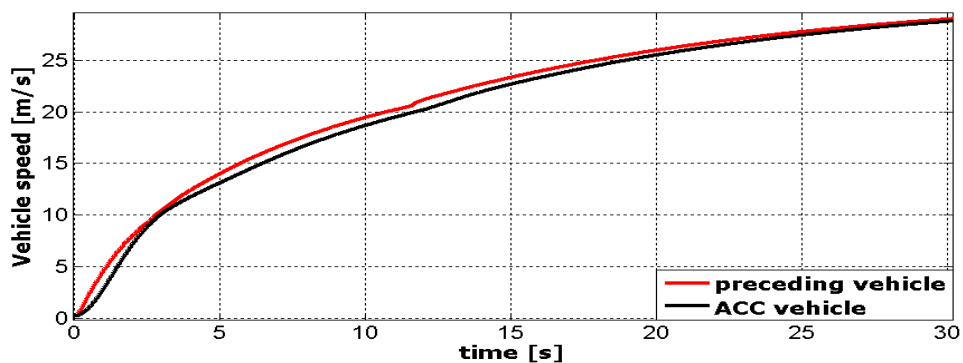
(a)
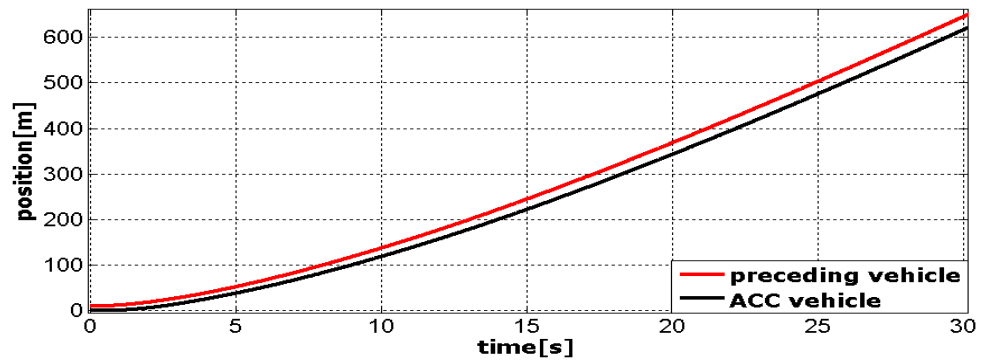
(b)
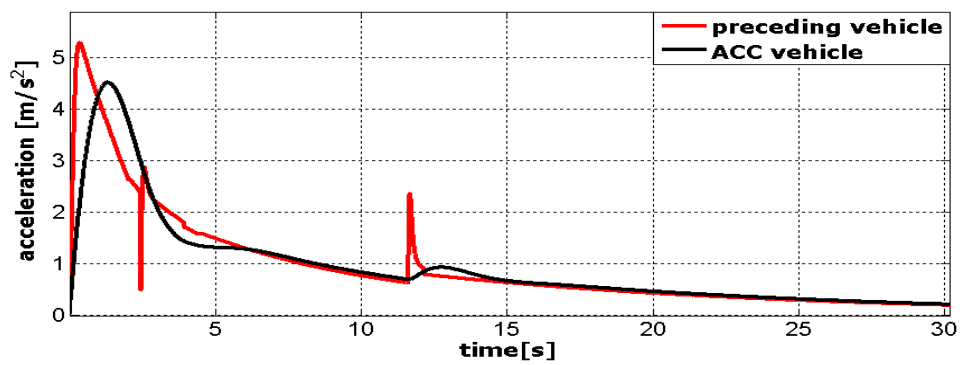
(c)
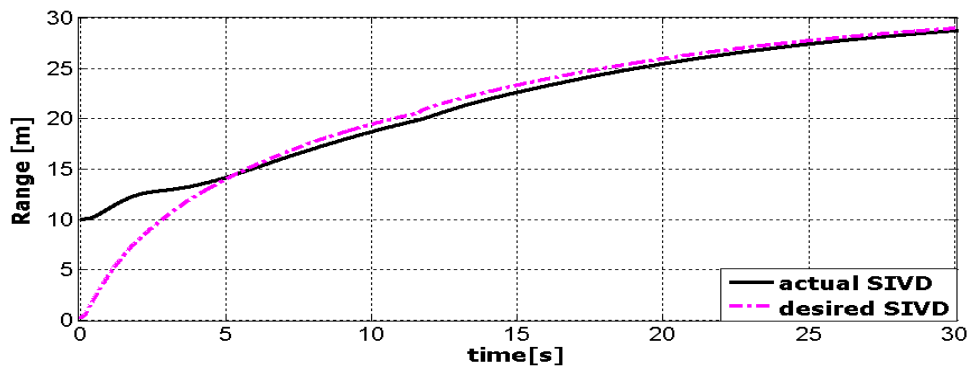
(d)

Figure 4-10   (a) Velocities of the vehicles, (b) Positions of the vehicles, (c)
Accelerations of vehicles, (d) Range between both vehicles

114

4.5.2 Preceding Vehicle with Throttle Input of 50 Degrees and Different Initial Conditions for Both Vehicles

In the second scenario, both vehicles start with the different initial speeds and different initial positions, the throttle input for the preceding vehicle is set to 50 degrees for the entire simulation time of 20 s. The baseline scenario is that an ACC vehicle travelling at 30 m/s in the speed control mode detects a preceding vehicle which is accelerating from 10 m/s, the ACC vehicle is 60 m behind the preceding vehicle when it detects a preceding vehicle.

The ACC vehicle response has been analysed for two different situations: (1) the ACC vehicle has no acceleration limits and (2) the ACC vehicle is restricted to the acceleration limits. In situation (2), if the acceleration command computed by Equation (4.19) is less than the deceleration limit, then the acceleration command is set equal to the deceleration limit.

Figure 4-11(a) shows the ACC vehicle velocity, situation (2), manoeuvres quickly to reach the preceding vehicle's velocity than the ACC vehicle velocity profile without acceleration limits. Figure 4-11(b) shows the positions of both vehicles and the ACC vehicle distance, relative to preceding vehicle, can be seen in Figure 4-11(d). During the TM, the ACC vehicle establishes and then maintains the desired SIVD, Figure 4-11(d). ACC vehicle accelerations for both situations are shown in Figure 4-11(c). The ACC vehicle, without the acceleration limits, only concerns with establishing a SIVD with zero-range-rate and is unable to meet the other requirements of the TM. It has been observed that with acceleration limits included, the ACC vehicle, using the CTG control algorithm, has performed all the control tasks discussed in Section 4.1.
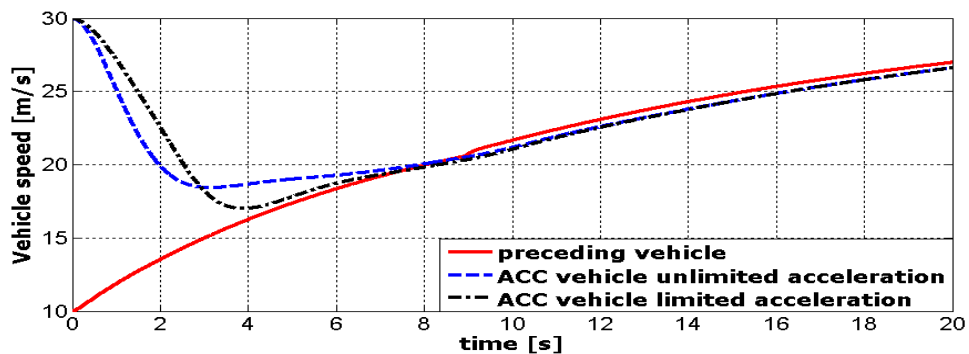

(a)
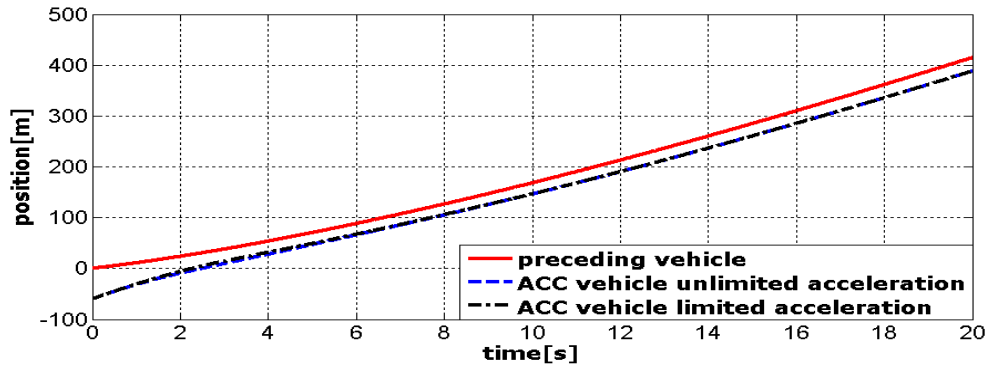
(b)
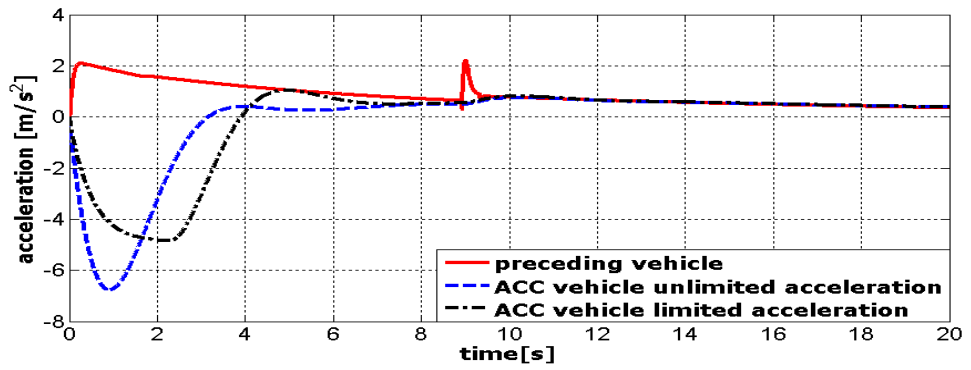
(c)
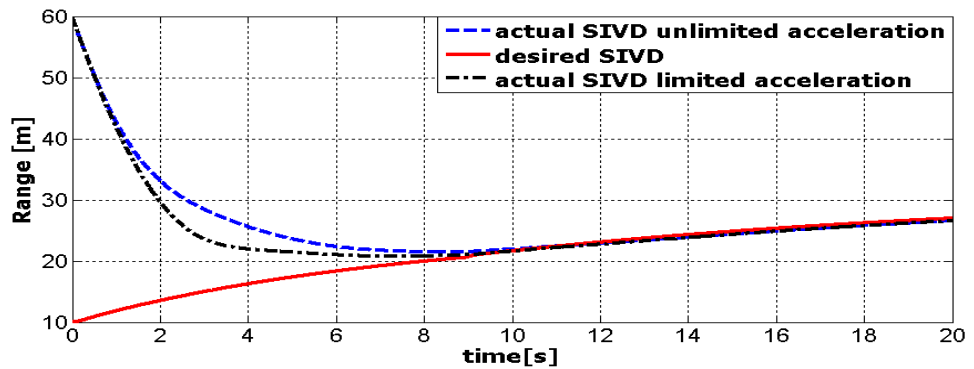
(d)

Figure 4-11   (a) Velocities of the vehicles, (b) Positions of the vehicles, (c)
Accelerations of vehicles, (d) Range between both vehicles

4.5.3 ACC Vehicle Response against a Halt Preceding Vehicle

In the third scenario, an ACC vehicle detects a halt vehicle in front of it. The initial speed of the ACC vehicle is 30 m/s and it is 110 m behind the preceding vehicle. This encounter scenario has been analysed for two different situations; (1) ACC vehicle with unlimited acceleration, (2) ACC vehicle with limited acceleration. In situation (2), if the acceleration command computed by Equation (4.19) is less than the deceleration limit, then the acceleration command is set equal to the deceleration limit.

The simulation results for both conditions are shown in Figure 4-12. It can be seen that with unlimited acceleration, the ACC vehicle successfully performs the TM (dashed line). In the case of acceleration limits (solid line), the ACC vehicle cannot meet the required objectives of establishing the desired SIVD with zero range-rate and collides with the preceding vehicle as shown in Figure 4-12(b) (solid line). During this TM, the ACC vehicle is executing a negative velocity, Figure 4-12(a) (solid line), which does not satisfy Equation (4.1) constraint. Also the initial commands computed by the CTG control law for the ACC vehicle is to accelerate rather than to decelerate, Figure 4-12(c). If the initial commands are to accelerate then the deceleration limits would not allow using the necessary brakes to avoid a collision with the preceding vehicle. It is essential that ACC vehicle must decelerate to avoid the collision. After analysing this scenario, it can be concluded that the CTG control law is not feasible for these kinds of transitional manoeuvres of the ACC vehicle, because, the CTG control algorithm does not include either the state constraints or the control constraints in its formulation.
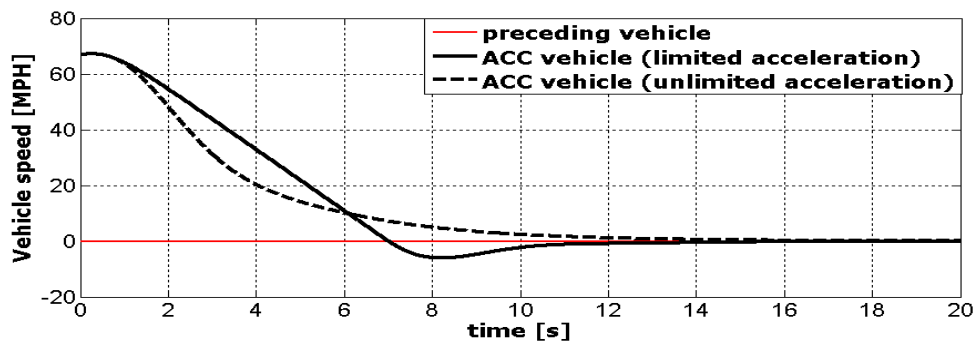

(a)
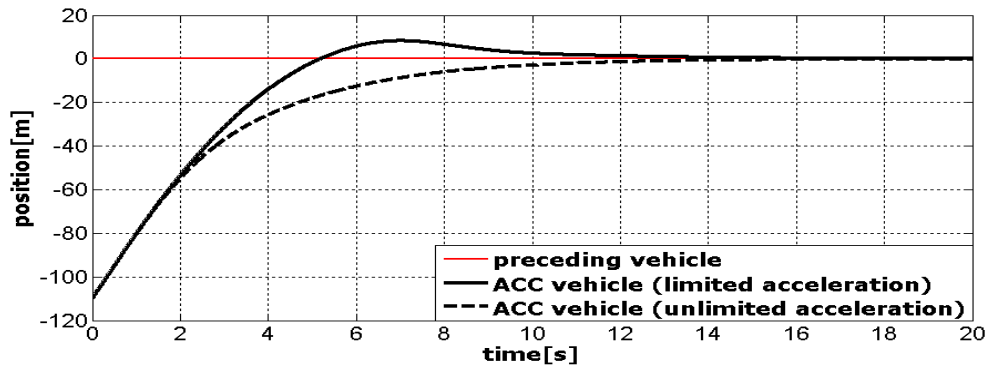
(b)
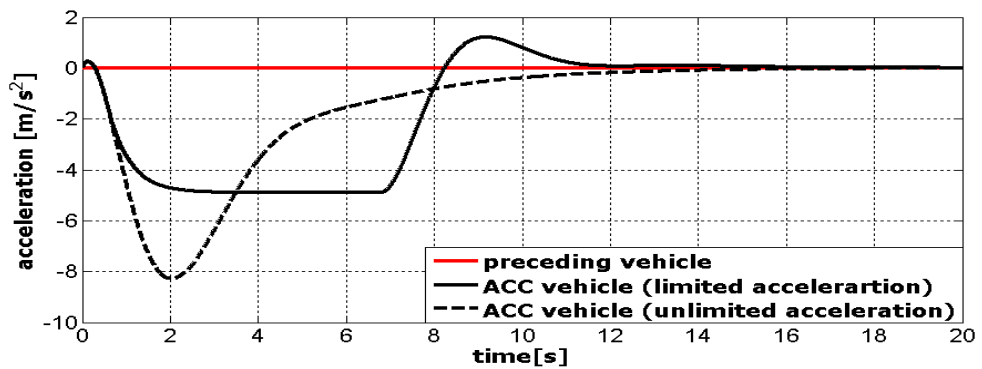
(c)

Figure 4-12   (a) Velocities of the vehicles, (b) Position of the vehicles, (c) Absolute
acceleration of both vehicles

## 4.5.4 CTG Law Sensitivity to Parameter Changes

In this section a parametric study for the CTG law has been carried out. The CTG
spacing control law has been analysed for different values of weighing factor (λ_{CTG})
and the headway time *(h)*. It is necessary to understand that how these parameters
affect the performance of an ACC vehicle especially when the ACC vehicle is
executing a TM. The situation in Section 4.5.2 is considered for the parameter study
as the ACC vehicle smoothly performs the TM for the selected parameters. Since the
variation in headway time *(h)* will have a similar effect on the ACC vehicle
performance, whether it's PID, sliding mode control method or CTG spacing control
method, therefore, its variation is only considered for CTG law.

### 4.5.4.1   ACC vehicle response to weighing factor variation

Figure 4-13 shows the ACC vehicle performance for different values of weighing factor (λ_{CTG}), and by definition λ_{CTG} is the weighing factor between range-rate ($\dot{R}$) and inter-vehicle spacing error *(δ)*. The actual value of λ_{CTG} considered for the CTG spacing control law is 0.4 which has been compared against λ_{CTG} = *0.2* and λ_{CTG} = *0.6*. The comparison shows that there is a small effect due to the changes is λ_{CTG} on the ACC vehicle performance during the transition behaviour. It is clear that λ_{CTG} variation has no effect during the steady state operation of the ACC vehicle. After this analysis it can be concluded that the spacing error converges to zero within the range of λ_{CTG} considered in this analysis and the individual closed-loop performance of the following vehicle is retained.
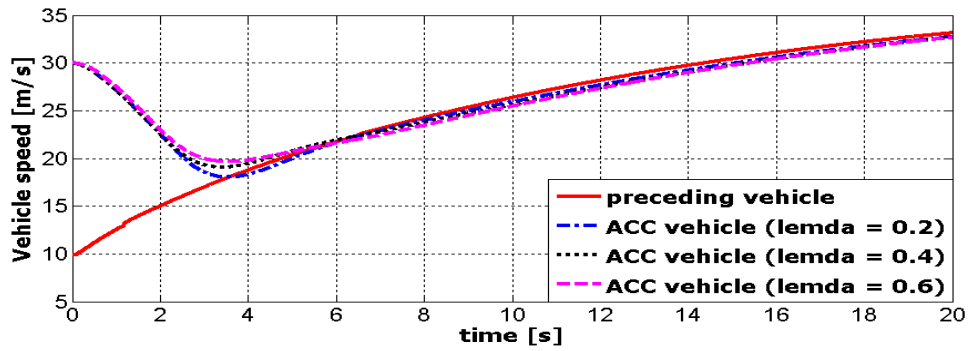

(a)
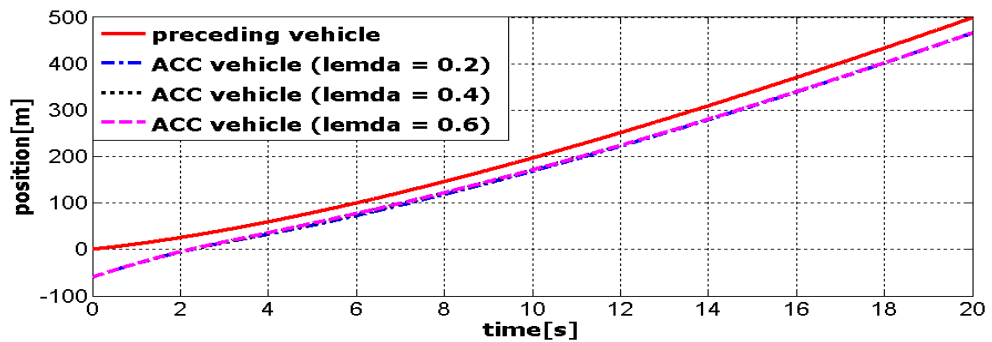
(b)
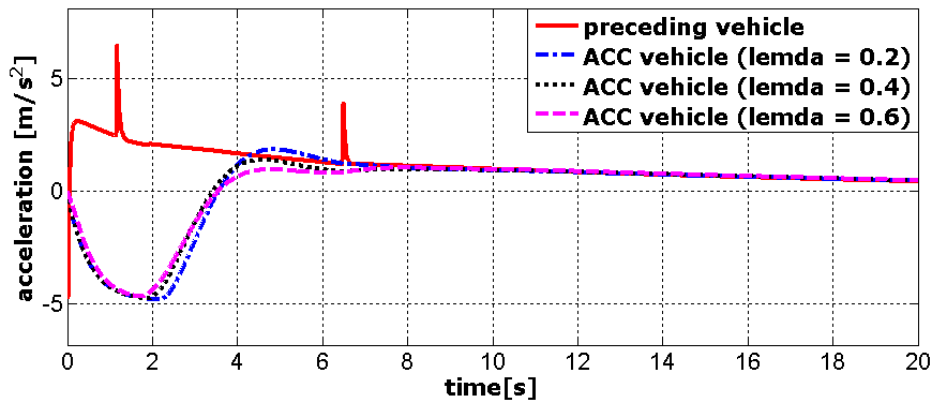
(c)

Figure 4-13   (a) Velocities of vehicles, (b) Position of vehicles, (c) Acceleration of vehicles, for different values of weighing factor λ_{CTG}

### 4.5.4.2   ACC vehicle response to headway time *(h)* variation

Figure 4-14 shows the ACC vehicle performance for different values of headway time *(h)*. The actual value of *h* considered for the CTG spacing control law is 1 s which has been compared against *h = 0.5 s* and *h = 1.5 s*. This comparison shows a very interesting behaviour of ACC vehicle because the variation in *h* shows a significant effect on the performance of the ACC vehicle not only during the transitional operation but also during the steady-state operation. For the lower value of *h = 0.5*, it takes longer to steer to the zero range-rate. Also during the steady state operation and at high speed the SIVD between the two vehicles becomes smaller. For example, at t = 15 s the vehicle speed is 30 m/s and the SIVD between the two vehicles is 15.08 m. It is, therefore, dangerous to follow the preceding vehicle at such a small distance (in the case of emergency situation). For a higher value of *h = 1.5*, the deceleration process and catching up the zero range-rate take longer than the other two *h* values. Due to the higher value of *h* the corresponding SIVD is higher, e.g. at t = 15 s the SIVD between the two vehicles is 44 m which will cause an increase in the average journey times or other vehicles might cut-in between the two vehicles.
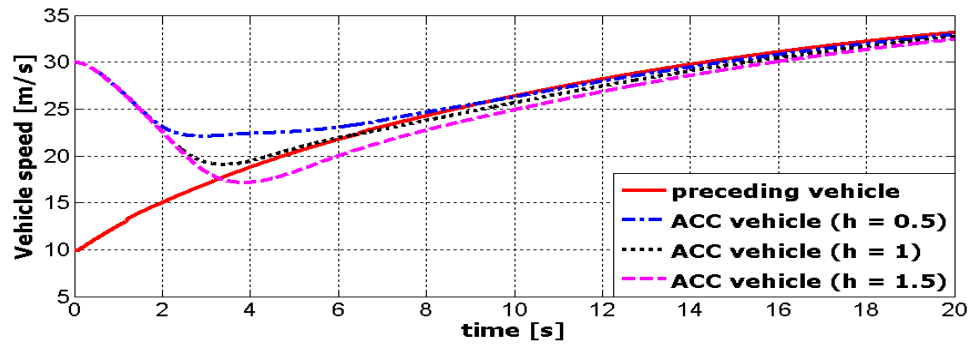
(a)
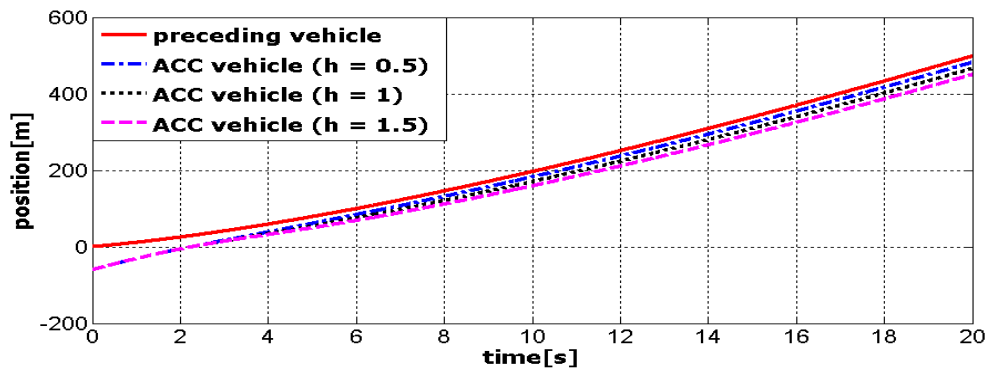
(b)
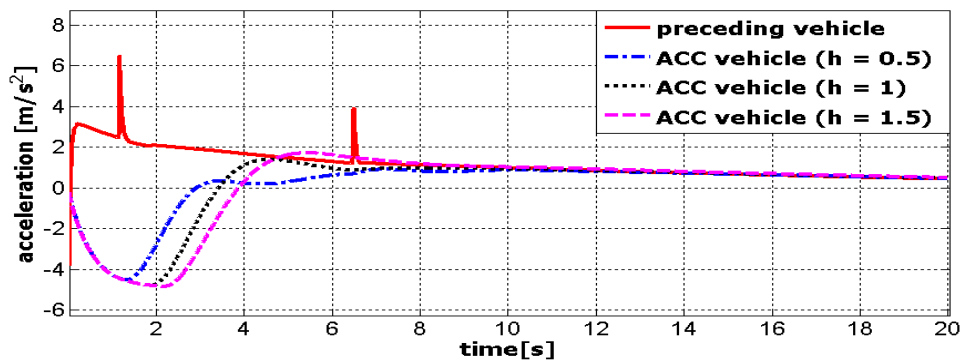
(c)

Figure 4-14   (a) Velocities of the vehicles, (b) Position of the vehicles, (c) Absolute
acceleration of vehicles, for different values of headway time *(h)*

4.6   Conclusions

This chapter is an attempt to study and understand the ACC system and together
with controller strategies used for the upper-level controller. The two-vehicle

system which consists of a preceding vehicle and an ACC vehicle has been presented for an ACC vehicle analysis under steady-state and transitional manoeuvres. The ACC vehicle model considered in this chapter was a first-order vehicle model. The importance and function of the key components of an ACC system have been covered and two basic modes of operation, speed control and vehicle following mode, of an ACC vehicle have also been discussed. The two most important controllers of an ACC vehicle, upper-level controller and lower-level controller, have also been discussed and their respective tasks have been studied. The lower-level controller model will be developed in Chapter 6.

Three control methods, PID, sliding mode, and CTG spacing control, have been used for the upper-level controller to analyse the first-order ACC vehicle response under simple and complex situations. The simulation results obtained from PID and CTG methods for the first situation and second situation are satisfactory (even with the acceleration limits applied in the second situation). In has been observed that using these two control methods, the ACC vehicle is establishing the desired SIVD based on the headway-spacing policy, performing the control tasks discussed in Section 4.1 and executing smoothly the required TMs (Section 4.1).

The analysis carried out in the third situation shows that these two control methods (PID and CTG) can establish the required SIVD with the zero range-rate when no acceleration limit is applied on the control input (u), and the ACC vehicle exceeds the acceleration limits (-0.5g). When the acceleration limit is applied to the control input (u), the ACC vehicle is unable to achieve the required control objectives described in Section 4.1. The ACC vehicle is initially accelerating whereas it should decelerate straight away for the given initial range between the two vehicles. Also, the ACC vehicle is executing negative velocity, which does not satisfy the constraint in Equation (4.1), and finally, it cannot avoid the collision with the halt preceding vehicle.

The parametric analysis for the CTG control law has also been carried out by changing its two parameters: weighing factor and headway time. The analysis shows that the CTG is more sensitive to headway time than to the weighting factor.

In this chapter, the first-order ACC vehicle model has also been analysed using the sliding mode control method. After presenting the basic structure of a sliding mode technique using a simple example it has been applied to the two-vehicle system. In the first analysis the control input (u), computed using the sliding mode control approach, tracks well the acceleration of the preceding vehicle. But, when u was applied to the first-order ACC vehicle it results in high amplitude chattering. It has been observed that this chattering is due to the lag in the first-order vehicle model. Due to this chattering characteristic, sliding mode control method is not suitable for the two-vehicle system developed in this study. Because, the simple ACC vehicle is based on the first-order lag which corresponds to the lag in the lower-level controller performance.

After analysing the PID, sliding mode, and CTG control methods for the ACC vehicle analysis, it has been found that none of the three methods is suitable for the ACC vehicle analysis under the critical TMs. Because these control methods cannot take into account the operational constraints in their formulation. Therefore, it is essential to use a more robust control technique which can incorporate the constraints in its formulation and is able to compute the desired acceleration commands for the ACC vehicle under the TMs. In the next chapter (Chapter 5) a model predictive control (MPC) algorithm will be used for the two-vehicle system. Simulation results, under the same situations, obtained from MPC control method will be compared with the control methods presented in this chapter.

Chapter 5.   Model Predictive Control for a Simple ACC Vehicle

5.1   Introduction

In recent years, the technology developments in control systems, sensor technologies, communication systems and data processing have provided constructive support to automate the decision-making process and execution of driving manoeuvres with greater accuracy. With the current advancement in control systems, the dangerous driving task performed by a driver can be replaced by modern control techniques. There are a number of control algorithms available in the control engineering world which can safely cope with the nonlinearities and uncertainties within the constraints boundaries of complex systems.

A two-vehicle model has been developed in Chapter 4 which consists of a preceding vehicle and an adaptive cruise control (ACC) vehicle. The preceding vehicle was based on the complex vehicle model which has been developed in Chapter 3 (Section 3.2 to Section 3.5), and the ACC vehicle was based on a first-order model (Section 3.8). The ACC vehicle was analysed for different encounter scenarios with the preceding vehicle. Three well-known control strategies, proportional-integral-derivative (PID), sliding mode and constant-time-gap (CTG) control methods, have been used to control the response of the first-order ACC vehicle under steady-state and transitional operations. Simulation results have been produced and discussed and it has been observed that none of the above control methods are suitable for the ACC vehicle analysis when it is going through critical transitional manoeuvres (TMs).

The reason found is that these control algorithms are unable to take into account operational constraints. As this study considers the TMs, corresponding to critical driving situations, during these TMs an ACC vehicle needs to use sudden brake input to avoid a collision, within the operational constraints boundaries, with the preceding vehicle. Therefore, a robust controller technique is needed in order to achieve the required control objectives. The operational constraints referred to the control input, states and collision avoidance constraints as discussed in Chapter 4 will be later explained in this chapter.

In this chapter, the model predictive control (MPC) control algorithm is presented. The basic structure of a prediction model used in the MPC algorithm is discussed with the fundamental requirements for the MPC control system. This MPC control structure is then applied to a two-vehicle system. The MPC control approach is used to control the longitudinal dynamics of the ACC vehicle when the ACC vehicle is executing critical TMs under operational constraints.

The two-vehicle model developed in Chapter 4 will be used in this chapter in order to analyse the upper-level controller response of the ACC vehicle. The preceding vehicle is based on the complex vehicle model which include engine, torque converter, transmission, and drivetrain models (Section 3.2 to Section 3.5), and the ACC vehicle model is based on the first-order vehicle model (Section 3.8).

A simple first-order ACC vehicle model is adopted to analyse the performance of the MPC control method at the upper-level controller level under the same critical encounter scenarios between the two vehicles as used for the three control methods in Chapter 4. After the analysis, the desired acceleration commands, computed by the upper-level controller, will be applied to the lower-level controller and the complex vehicle model for longitudinal dynamics control of an ACC vehicle in Chapter 6. It should be noted that due to the time lag in the performance of the lower-level controller the ACC vehicle will be unable to track the desired acceleration commands. Therefore, a lag is considered in the form of first-order ACC vehicle model which corresponds to the lags from brake or engine actuation lags and sensor signal processing lags.

A discrete-time state-space prediction model is developed in this chapter which will be used to predict the future control inputs for the ACC vehicle. Using the MPC

based upper-level controller, the first-order ACC vehicle is analysed under the critical TMs and in the presence of operational constraints. In the scenarios considered, a high speed ACC vehicle encounters an accelerating or a halt preceding vehicle in the same lane. Under these scenarios, the ACC vehicle has to apply the sudden brake input in order to avoid a collision from the preceding vehicle. This causes the ACC vehicle to exceed the deceleration limit of -0.5g, where, the control objective for the ACC vehicle is to execute these manoeuvres under this limit.

The main tasks for the MPC control method to perform on the ACC system are:

1   Track smoothly desired acceleration commands

2   Reach and maintain a safe inter-vehicle distance (SIVD) in a comfortable manner and at the same time react quickly in the case of dangerous scenarios.

3   System performance optimization.

4   Optimize the system performance within defined constrained operational boundaries.

There are many benefits of the entire system from a control point of view, e.g. in case of emergency manoeuvres the control system can react significantly faster than a human reacting in the same situation.

The chapter outline is as follows. In Section 5.2, a general MPC approach is explained and the formulation of a discrete-time state-space prediction model is presented. In Section 5.3, the MPC control algorithm is applied on the two-vehicle system in order to analyse the first-order ACC vehicle model. In Section 5.4, simulation results are presented and discussed in detail. In Section 5.5, a parametric analysis of the ACC vehicle is carried out for different controller's parameters. Section 5.6 presents the conclusions of this chapter.

5.2   Model Predictive Control Systems

Over the last decade noteworthy progress has been achieved in the field of MPC (Mayne *et al.*, 1999; Camacho and Bordons, 2004; Wang, 2009), which is also known as receding horizon or moving horizon control. MPC method is receiving a significant acceptance from researchers in both industrial and academic circles because of its design methodology. Important issues such as plant optimization and constrained control which are critical to industrial engineers are naturally embedded in the design of MPC method. MPC is one of the few control techniques which is capable to deal with constrained system simultaneously providing an optimal control for a certain performance index (Richard and How, 2005; Magni *et al.*, 2009).

There are three important features of MPC method which make it attractive to process industries and academics: (1) the MPC design formulation uses a completely multivariable system framework where the performance parameters of the multivariable control system are related to the engineering aspect of the system, however, they can be understood and tuned by engineers; (2) the ability of the design methodology to handle both soft and hard constraints in a multivariable control framework. This is useful to industry where tight profit margins and limits on the process operation are inevitably present; and, (3) the capability to perform on-line optimization of the process (Wang, 2009).

There are numerous applications of MPC controller ranging from process industries, e.g. chemical industries, cement industries to the control of other processes and system e.g. robots, clinical anaesthesia, drying towers, PVC plants, steam generators, and servos (Camacho and Bordons, 2004). The efficient performance of these applications shows that the MPC technique has the capacity to achieve highly efficient control systems which are able to operate during long periods of time with hardly any intervention. The various MPC algorithms only differ amongst themselves in the type of model used which represent the control system and the cost function to be minimized (Camacho and Bordons, 2004). For example, in the case of a satellite, the optimization is for jet thrust needed to bring it to a desired trajectory that consumes the least amount of fuel.

For a more comprehensive approach, the MPC can be defined as a control technique in which a system's behaviour is predicted in order to generate an optimised control input. The characteristics of the system's dynamic behaviour and a set of future control inputs are used to predict the system behaviour. The predicted future system states can then be compared against a set of future target states, while at each time step the set of future control inputs continuously computed in order to ensure that the predicted future states agree with the target future states (Rowell, 2007).

From a control strategy point of view, the MPC control strategy can be well understood by comparing with the control strategy used by a car driver. The driver knows, in advance, the desired reference trajectory to follow for a finite control horizon. He then uses the car characteristics (mental model of the car) to decide which control action, e.g. accelerator, brakes, steering, to take in order to follow the desired reference trajectory. Only the first control action is used at each instant and the procedure is repeated to the next control decision in a receding horizon manner. It should be noted that using a classical control scheme, such as PID, the control actions are taken (in case of driving a car) are based on the past errors, i.e. the driver looking through the rear view mirror to observe what is happening behind as he is moving forward, while MPC control method uses more information (the reference trajectory) in order to perform the same task and provides improved closed-loop stability and can comfortably cope with nonlinear systems.

The desired inter-vehicle distance between the two vehicles is directly proportional to the velocity of the preceding vehicle (Bageshwar *et al.*, 2004). It should be noted that the human eye cannot capture precisely the required safe inter-vehicle distance (SIVD) behind the preceding vehicle. Even with the driving experience, the driver, due to his incapability to respond quickly and accurately to the dynamic changes of the preceding vehicle, cannot establish the zero range-rate with the preceding vehicle.

5.2.1 MPC Control Algorithm

There are some fundamental features of a MPC control algorithm which differentiate it from other control methods: its capability to develop explicitly a prediction model to predict the process output at future time instants (horizon), the ability to design a reference path that the controller attempts to follow, calculation of a control sequence minimizing an objective function, and receding strategy; which means that at each instant the horizon moves forward to the future by applying the first control signal of the sequence calculated at each step (Camacho and Bordons, 2004). MPC forms a prediction model to predict the future response of the system by using a known set of future control input, and by making use of the known system response to controlling inputs (Rowell, 2007). Before developing the MPC control algorithm it is necessary to understand the fundamental driving features of the MPC approach.

5.2.1.1   Moving horizon window

The moving horizon window also referred as time-dependent window which can start from any arbitrary time t_i to the prediction horizon $t_i + N_P$ for $i = 1, \ldots, N_P$. The prediction horizon (N_P) defines how far ahead in time the future output states are predicted and its length remains constant. However, t_i which actually starts the optimization window, increases based on sampling instant (Wang, 2009).

5.2.1.2   Receding horizon control

Different approaches are available in the literature (Mayne *et al.*, 1999; Magni *et al.*, 2009; Wang, 2009) to understand the concept of receding horizon control. The methodology of the MPC controller is characterized by the following strategy as shown in Figure 5-1. A discrete-time setting is assumed, and the current time is labelled as time step *t*. A set-point trajectory shown is the absolute target for the system to follow. It is unlikely that the system will follow exactly the set-point trajectory. The reference path is therefore a newly defined path which starts from the current output at time *t* and defines an ideal path along which the plant should return to the set-point trajectory. The reference path defines an important aspect of

the closed-loop behaviour of the controlled system. The reference path can be chosen as an exponential function to reach the set-point trajectory within a finite time, or it could be a linear path, quadratic or any other chosen path which meets the set-point trajectory after a specified time (Rowell, 2007). It is therefore the new reference which the system aims to follow, Figure 5-1.

A MPC controller has an internal model which is used to predict the behaviour of the plant, starting at the current time t, over a future prediction horizon (N_P), Figure 5-1. Using the current output state information $y(t)$ of the system and with defined future control inputs $u(t + m \mid t)$ for m = 0,..., N_C, the system's predicted outputs $y(t + m \mid t)$ for m = 1,..., N_P are obtained up to a limited prediction horizon (N_P) (Maciejowski, 2002; Camacho and Bordons, 2004).

The set of future control inputs $u(t + m \mid t)$ for m = 0,..., N_C is determined up to the control horizon (N_C), Figure 5-1, by optimizing determined criterion in order to keep the process as close as possible to the reference path (Rowell *et al.*, 2008). This criterion usually takes the form of a quadratic function of the errors between the predicted output signal and the predicted reference trajectory, also taking into account the control effort input. The length of N_C defines that after a certain interval there should be no variation in the future control signal (Camacho and Bordons, 2004). Changes in the control input are weighted and accumulated in the quadratic function. During this process an online calculation is used to explore the state trajectories which are actually based on the current state and then a cost minimizing control strategy is determined until time $t + N_C$.

Once the future control inputs are determined then only the first element of the set of future control inputs is applied as the input signal to the plant. Then the whole process of output measurement, prediction and set of future control determination is repeated. One time instant later: a new output measurement is obtained; a new reference trajectory is defined; predictions are made over the horizon; a new set of future control inputs is determined; and finally the next input is applied to the plant. During this process the length of the prediction horizon remains the same as before, but slides along by one sampling interval at each step, this way of controlling a system plant is often called a receding horizon strategy (Maciejowski, 2002; Wang, 2009).

Figure 5-2 shows the basic structure of the MPC control method and is used to implement the receding horizon strategy. A prediction model is used to predict the future plant outputs, based on past and current values and on the optimal future control actions. The actions are computed by the optimizer which takes into account the cost function as well the constraints (Camacho and Bordons, 2004).
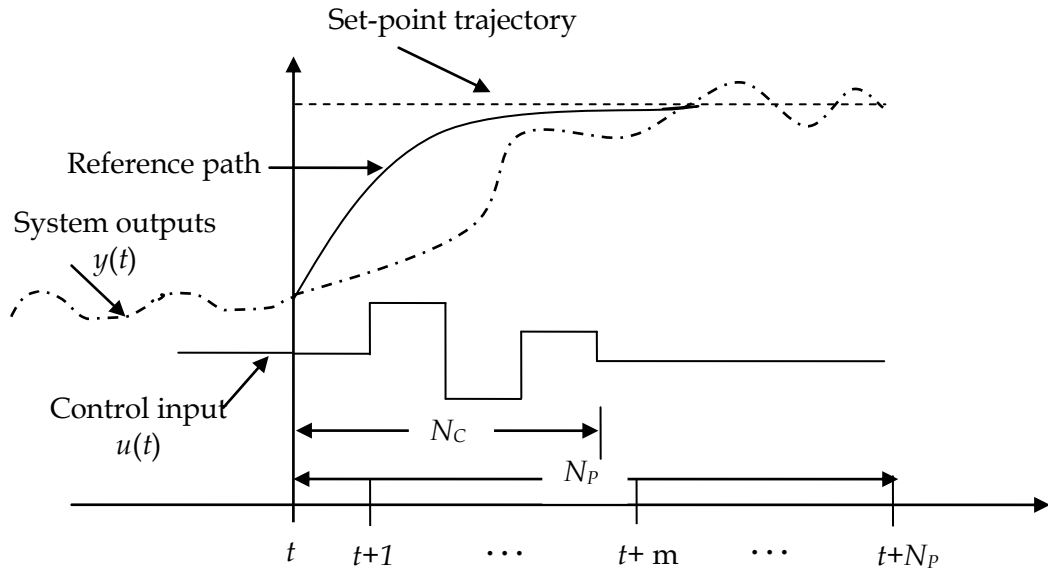

Figure 5-1   MPC strategy: basic idea (Maciejowski, 2002)
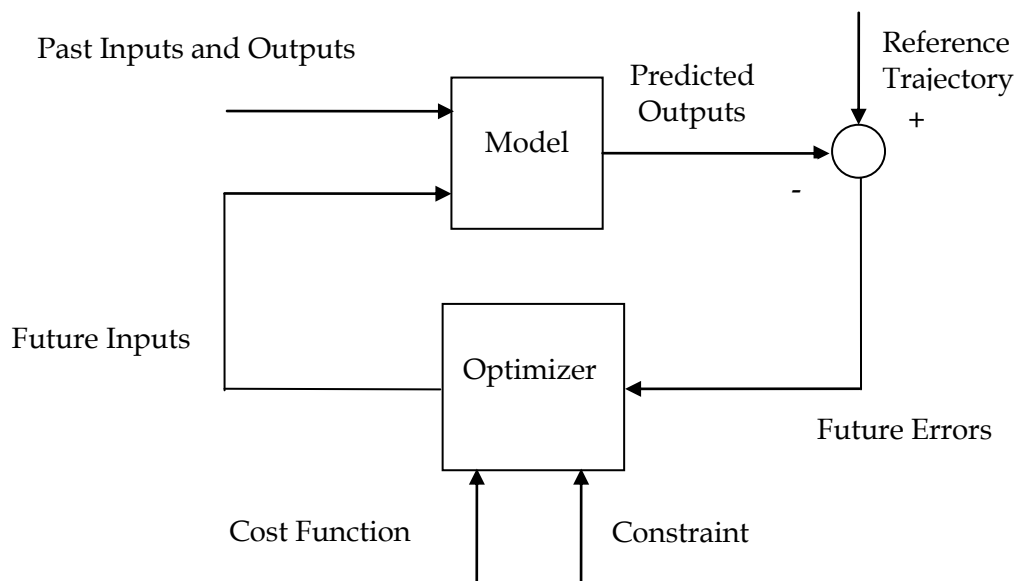
Figure 5-2   Basic Structure of MPC (Camacho and Bordons, 2004)

131

5.2.1.3 Control objective

At each time t, the state information is sampled in order to predict the future control strategy. The state information denoted by $y(t)$ is a vector which consists of relevant information of the states of the plant. The vector $y(t)$ is usually measured directly using sensors or in some cases where the precise measurement is not possible it can be estimated. Once the sampling process is completed this information is then compared with the desired value (reference path), this comparison then generates an error function which is based on the difference of these two values. This error function is formulated as a cost function, 'J', which consists of elements relating to the system's output accuracy and control effort input. The cost function also incorporates the weighting which penalizes the control input $u(t)$ for the desired closed-loop performance. The control objective is to minimize this cost function within the optimization window and by doing so the optimized control action is determined (Wang, 2009).

5.2.2 Formulation of Prediction Model

For the purpose of illustration of the MPC control algorithm a linearized, continuous-time, single-input and single-output (SISO) system is considered and is described by:

$$\dot{\mathrm{x}} = \mathbf{A}\mathrm{x} + \mathbf{B}u \qquad (5.1)$$

$$y = \mathbf{C}\mathrm{x} + \mathbf{D}u \qquad (5.2)$$

where, x is the state variable, u denotes the control input, y is the system output, and **A, B, C, D** are the discrete-time state-space matrices. It is implicitly assumed, due to the principle of receding horizon control, that the control input u cannot affect the output y at the same time, therefore, the system matrix **D** = 0 in the system model (Wang, 2009).

In the MPC literature the system to be controlled is usually modelled by a discrete-time state-space model (Mayne *et al.*, 1999; Li *et al.*, 2010). Therefore, the continuous-

time state-space model (Equation (5.1) and Equation (5.2)) is transformed into a discrete-time state-space model as:

$$x(k+1) = \mathbf{A}x(k) + \mathbf{B}u(k) \tag{5.3}$$

$$y(k) = \mathbf{C}x(k) \tag{5.4}$$

where, k represents the kth sampling point. MPC control algorithm is based on a prediction model and the main objective to develop a prediction model is to predict the future response of the plant based on a set of future control inputs. This prediction is performed within an optimization window, the length of this optimization window is assumed as N_P which is the number of samples and each sample is denoted by the time k_i, $k_i > 0$. At each sampling instant k_i, the state information vector $x(k_i)$ is measured which provides the current plant information. Having the current plant information $x(k_i)$, the future state variables are then predicted for N_P number of samples, the future state variables can be defined as:

$$x(k_i + 1 \mid k_i), x(k_i + 2 \mid k_i), \ldots, x(k_i + m \mid k_i), \ldots, x(k_i + N_P \mid k_i) \tag{5.5}$$

where, $x(k_i + m \mid k_i)$ is the predicted state variable at $k_i + m$ with the given current plant information $x(k_i)$. Similarly given the current plant information $x(k_i)$, the set of future control input, which minimizes the cost function J, are denoted by:

$$\Delta u(k_i), \Delta u(k_i + 1), \ldots, \Delta u(k_i + N_C - 1) \tag{5.6}$$

where $\Delta u(k) = u(k) - u(k-1)$ is the control increment., N_C is called the length of control horizon and it is defined as the number of parameters used to capture the future control trajectory (Maciejowski, 2002). It is important to note that the length of N_C is chosen less than or equal to the length of prediction horizon N_P.

Using the discrete-time state-space model, the future state variable in Equation (5.5) can be calculated sequentially using the current state vector and the set of future control parameters.

$$x(k_i + 1 \mid k_i) = \mathbf{A}x(k_i) + \mathbf{B}\Delta u(k_i)$$

$$x(k_i + 2 \mid k_i) = \mathbf{A}x(k_i + 1) + \mathbf{B}\Delta u(k_i + 1) = \mathbf{A}^2 x(k_i) + \mathbf{A}\mathbf{B}\Delta u(k_i) + \mathbf{B}\Delta u(k_i + 1)$$

$$\vdots$$

$$x(k_i + N_P \mid k_i) = \mathbf{A}^{N_P} x(k_i) + \mathbf{A}^{N_P - 1}\mathbf{B}\Delta u(k_i) + \mathbf{A}^{N_P - 2}\mathbf{B}\Delta u(k_i + 1)$$

$$+ , \dots , + \mathbf{A}^{N_P - N_C}\mathbf{B}\Delta u(k_i + N_C - 1) \tag{5.7}$$

Similarly, using these predicted state variables, the predicted output variables can be determined as:

$$y(k_i + 1 \mid k_i) = \mathbf{C}\mathbf{A}x(k_i) + \mathbf{C}\mathbf{B}\Delta u(k_i)$$

$$y(k_i + 2 \mid k_i) = \mathbf{C}\mathbf{A}x(k_i + 1) + \mathbf{B}\Delta u(k_i + 1) = \mathbf{C}\mathbf{A}^2 x(k_i) + \mathbf{C}\mathbf{A}\mathbf{B}\Delta u(k_i) + \mathbf{C}\mathbf{B}\Delta u(k_i + 1)$$

$$y(k_i + 3 \mid k_i) = \mathbf{C}\mathbf{A}^3 x(k_i) + \mathbf{C}\mathbf{A}^2 B\Delta u(k_i) + \mathbf{C}\mathbf{A}\mathbf{B}\Delta u(k_i + 1) + \mathbf{C}\mathbf{B}\Delta u(k_i + 2)$$

$$\vdots$$

$$y(k_i + N_P \mid k_i) = \mathbf{C}\mathbf{A}^{N_P} x(k_i) + \mathbf{C}\mathbf{A}^{N_P - 1}\mathbf{B}\Delta u(k_i) + \mathbf{C}\mathbf{A}^{N_P - 2}\mathbf{B}\Delta u(k_i + 1)$$

$$+ \dots + \mathbf{C}\mathbf{A}^{N_P - N_C}\mathbf{B}\Delta u(k_i + N_C - 1)$$

$$\tag{5.8}$$

It should be noted that all the predicted variable are expressed in terms of current state variable information $x(k_i)$ and the future control input $\Delta u\ (k_i + j)$, where $j = 0,1,2,..,N_c - 1$.

The above equations can be written in the vector form as

$$\mathbf{Y} = \begin{bmatrix} y(k_i + 1 \mid k_i) & y(k_i + 2 \mid k_i) & y(k_i + 3 \mid k_i) & \dots & y(k_i + N_P \mid k_i) \end{bmatrix}^T \tag{5.9}$$

$$\mathbf{\Delta U} = \begin{bmatrix} \Delta u(k_i) & \Delta u(k_i + 1) & \Delta u(k_i + 2) & \dots & \Delta u(k_i + N_C - 1) \end{bmatrix}^T \tag{5.10}$$

where, the dimension of $\mathbf{Y}$ is N_P and the dimension of $\mathbf{\Delta U}$ is N_C. Equation (5.9) and Equation (5.10) can be re-written into a state space expression, calculating all system outputs using the initial states $x(k_i)$ and vector of predicted control inputs $\mathbf{\Delta U}$ as:

$$\mathbf{Y} = \mathbf{F}x(k_i) + \mathbf{\Phi}\mathbf{\Delta U} \tag{5.11}$$

where,

$$\mathbf{F} = \begin{bmatrix} \mathbf{CA} \\ \mathbf{CA}^2 \\ \mathbf{CA}^3 \\ \vdots \\ \mathbf{CA}^{N_P} \end{bmatrix} \tag{5.12}$$

and

$$\boldsymbol{\Phi} = \begin{bmatrix} \mathbf{CB} & 0 & 0 & \cdots & 0 \\ \mathbf{CAB} & \mathbf{CB} & 0 & \cdots & 0 \\ \mathbf{CA}^2\mathbf{B} & \mathbf{CAB} & \mathbf{CB} & \cdots & 0 \\ \vdots & & & & \\ \mathbf{CA}^{N_P-1}\mathbf{B} & \mathbf{CA}^{N_P-2}\mathbf{B} & \mathbf{CA}^{N_P-3}\mathbf{B} & \cdots & \mathbf{CA}^{N_P-N_C}\mathbf{B} \end{bmatrix} \tag{5.13}$$

For the detailed understanding of discrete-time state-space model (Equation (5.3)) and its transformation into the state-space model (Equation (5.11)), the reader is referred to the book written by Wang, L, (2009).

5.2.3 Control Input Optimization

In general, the MPC control algorithm, within its control structure, develops a cost function J which reflects the control objective. Within a prediction horizon the objective of the predictive control system is to bring the predicted output as close as possible to a given set-point trajectory. It is assumed that the set-point trajectory remains constant within an optimization window and is updated depending upon the desired state of the controlled system (Wang, 2009).

The cost function J, that describes the control objective, can be defined as

$$J = (\mathbf{R}_s - \mathbf{Y})^T (\mathbf{R}_s - \mathbf{Y}) + \Delta\mathbf{U}^T \overline{\mathbf{R}}\Delta\mathbf{U} \tag{5.14}$$

The cost function J consists of two separate terms, the first terms is meant to minimize the error between desired output and the predicted output while the second term deals with the size of $\Delta\mathbf{U}$ when the cost function J is made as small as possible.

$\overline{\mathbf{R}} = \mathbf{R}\mathbf{I}_{N_C \times N_C}$ $(\mathbf{R} \geq 0)$ where $\mathbf{R}$ is used as a tuning operator for the desired closed-loop performance (Wang, 2009) which penalizes the control input vector ($\mathbf{\Delta U}$). $\mathbf{R}_s$ is the vector that contains the desired state information and can be defined as:

$$\mathbf{R}_s^T = \overbrace{\begin{bmatrix} 1 & 1 & \dots & 1 \end{bmatrix}}^{N_P} r(k_i) \tag{5.15}$$

where, $r(k_i)$ is the given set-point signal at sample time k_i. The control objective can briefly be defined as to find the best control parameter vector $\mathbf{\Delta U}$ such that an error function between the set-point and the predicted output is minimized (Camacho and Bordons, 2004).

The next step is to find the control parameter vector $\mathbf{\Delta U}$ which can be obtained by substituting $\mathbf{Y}$ in Equation (5.14) and re-arranging as:

$$J = (\mathbf{R}_s - \mathbf{F}\mathbf{x}(k_i))^T (\mathbf{R}_s - \mathbf{F}\mathbf{x}(k_i)) - 2\mathbf{\Delta U}^T \mathbf{\Phi}^T (\mathbf{R}_s - \mathbf{F}\mathbf{x}(k_i)) + \mathbf{\Delta U}^T (\mathbf{\Phi}^T \mathbf{\Phi} + \overline{\mathbf{R}})\mathbf{\Delta U} \tag{5.16}$$

Taking the first derivative of the cost function J:

$$\frac{\partial J}{\partial \mathbf{\Delta U}} = -2\mathbf{\Phi}^T (\mathbf{R}_s - \mathbf{F}\mathbf{x}(k_i)) + 2(\mathbf{\Phi}^T \mathbf{\Phi} + \overline{\mathbf{R}})\mathbf{\Delta U}, \tag{5.17}$$

And the necessary condition of the minimum J is obtained as

$$\frac{\partial J}{\partial \mathbf{\Delta U}} = 0, \tag{5.18}$$

From which the optimal solution for the control signal can be found as

$$\mathbf{\Delta U} = (\mathbf{\Phi}^T \mathbf{\Phi} + \overline{\mathbf{R}})^{-1} \mathbf{\Phi}^T (\mathbf{R}_s - \mathbf{F}\mathbf{x}(k_i)) \tag{5.19}$$

Once the control parameter vector is calculated then only the first element is applied to the controlled system.

5.3 MPC Prediction Model for the Two-Vehicle System

A general MPC control algorithm has been explained in Section 5.2 explaining a state-space representation of the predicted future states and future outputs of the controlled model while using the different control and prediction horizons. In this section the MPC control algorithm is applied to the two-vehicle system which consists of a preceding vehicle and a following ACC vehicle (developed in Chapter 4). The preceding vehicle is based on the complex vehicle model which includes engine, torque converter, transmission, and drivetrain models (Section 3.2 to Section 3.5). The ACC vehicle is based on the first-order vehicle model (Section 3.8).

The first-order ACC vehicle model used to analyse the upper-level control laws can be defined as (Equation (3.32))

$$\tau \dddot{x}_2(t) + \ddot{x}_2(t) = u(t) \tag{5.20}$$

where, x_2 is the position of the ACC vehicle and $u(t)$ is the control input. Equation (5.20) is used as an assumption for designing the upper-level controller(Li *et al.*, 2010), where, τ refers to the time lag in the performance of the lower-level controller. For the MPC control algorithm a discrete-time state-space model is required. The above continuous-time model can be re-written in a discrete-time state-space model as:

$$\begin{pmatrix} x_2(t+T) \\ \dot{x}_2(t+T) \\ \ddot{x}_2(t+T) \end{pmatrix} = \begin{pmatrix} 1 & T & 0 \\ 0 & 1 & T \\ 0 & 0 & 1-\dfrac{T}{\tau} \end{pmatrix} \begin{pmatrix} x_2(t) \\ \dot{x}_2(t) \\ \ddot{x}_2(t) \end{pmatrix} + \begin{pmatrix} 0 \\ 0 \\ \dfrac{T}{\tau} \end{pmatrix} u(t) \tag{5.21}$$

where, T is the discrete sampling time of the ACC system and assumed as 0.1 s and τ is assumed as 0.5 s and comes from different sources, e.g. brake or engine actuation lags and sensor signal processing lags (Rajamani *et al.*, 2000; Bageshwar *et al.*, 2004).

The information of the longitudinal states of both, preceding and ACC, vehicles is used by the upper-level controller to determine the control input $u(t)$ for the first-order ACC vehicle model. The longitudinal states of the ACC vehicle are obtained

from Equation (5.21) and the longitudinal states information of the preceding vehicle is obtained from Equation (3.24). The desired acceleration command ($\ddot{x}_{des}$) is then obtained for the lower-level and the complex ACC vehicle models which will be used in Chapter 6. This desired acceleration command ($\ddot{x}_{des}$) is used as an input for the lower-level controller model because within the lower-level controller formulation the desired net torque (T_{net}) is expressed as a function of this desired acceleration command. The desired net torque (T_{net}) is then used to compute the desired throttle or brake commands for the complex ACC vehicle model which is presented in Chapter 6.

5.3.1 Coordinate Frame for Transitional Manoeuvres

It is of paramount importance to develop and understand the mathematical relation between the state variables of the first-order ACC vehicle and the preceding vehicle. The control objectives for the ACC vehicle are to establish a safe inter-vehicle distance (SIVD) with the zero range-rate and within the operational constraints boundaries. The operational constraints are referred to the control input, states and collision avoidance constraints. The desired SIVD between the two vehicles varies linearly with the preceding vehicle's speed such that the headway time (h) between the two vehicles remains constant (SIVD = $hv_{preceding}$). The headway time (h) can be defined as the time taken by the follower vehicle to reach the point where the preceding vehicle is at present speed (Naranjo *et al.*, 2003). It should be noted that the measurement of range, range-rate, and ACC vehicle velocity can be used to obtain the velocity of the preceding vehicle.

A coordinate frame (Bageshwar *et al.*, 2004) as shown in Figure 5-3 travels with a velocity equal to the preceding vehicle velocity. This frame is used to determine the ACC vehicle motion relative to the preceding vehicle. The origin of this frame is situated at the desired SIVD and the objective of the TM is to steer the ACC vehicle to the origin of this frame in order to set up the zero range-rate with the preceding vehicle, where, R is the range (relative distance) between the two vehicles.
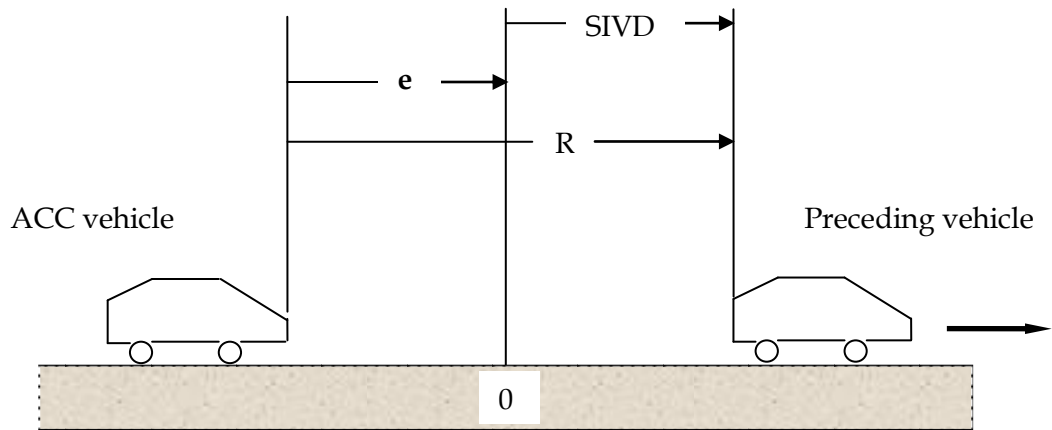
Figure 5-3   Coordinate frame for transitional manoeuvre.

Using this coordinate frame (Figure 5-3) for TM, the discrete-time state-space model of the error vector between the two vehicles can be defined as:

$$\mathbf{e}_{k+1} = \mathbf{A}\mathbf{e}_k + \mathbf{B}u_k \tag{5.22}$$

$$y_k = \mathbf{C}\mathbf{e}_k \tag{5.23}$$

where,

$$\mathbf{e}_k = \begin{pmatrix} err_k \\ \dot{err}_k \\ \ddot{err}_k \end{pmatrix} = \begin{pmatrix} -(\text{R-SIVD}) \\ \dot{R} \\ \ddot{x}_k \end{pmatrix} \tag{5.24}$$

where, err_k is spacing error, $\dot{err}_k$ is range-rate (relative velocity between the two vehicles), and $\ddot{err}_k$ is the absolute acceleration of the ACC vehicle. Each element of the error vector ($\mathbf{e}_k$) is the quantity which is measured by the ACC system and the control objective is to steer these quantities to zero (Bageshwar *et al.*, 2004). u_k is the control input, and y_k is the system output at time step k. The system matrices **A** and **B** can be obtained from the comparison of Equation (5.21) and Equation (5.22).

$$\mathbf{A} = \begin{pmatrix} 1 & T & 0 \\ 0 & 1 & T \\ 0 & 0 & 1-\dfrac{T}{\tau} \end{pmatrix}, \qquad \mathbf{B} = \begin{pmatrix} 0 \\ 0 \\ \dfrac{T}{\tau} \end{pmatrix} \tag{5.25}$$

And the system matrix C is defined as (Bageshwar *et al.*, 2004):

$$\mathbf{C} = \begin{pmatrix} 1 & 0 & 0 \\ 0 & -1 & 0 \end{pmatrix} \tag{5.26}$$

Using the MPC control approach, at each sampling instant k_i, the error vector ($\mathbf{e}_k$) is measured which provides the current error between the two vehicles. Having the current error information ($\mathbf{e}_k$), the future errors are then predicted for N_p number of samples (N_P is the length of optimization window), the future error can be defined as:

$$\mathbf{e}(k_i+1\,|\,k_i), \mathbf{e}(k_i+2\,|\,k_i), \ldots, \mathbf{e}(k_i+m\,|\,k_i), \ldots, \mathbf{e}(k_i+N_P\,|\,k_i) \tag{5.27}$$

where $\mathbf{e}(k_i+m\,|\,k_i)$ is the predicted error variable at k_i+m with the given current error information $\mathbf{e}(k_i)$. Similarly given the current error information $\mathbf{e}(k_i)$, the set of future control input, which minimizes the cost function J, are denoted by:

$$\Delta u(k_i), \Delta u(k_i+1), \ldots, \Delta u(k_i+N_C-1) \tag{5.28}$$

where $\Delta u(k) = u(k) - u(k\text{-}1)$ is the control increment, N_C is called the length of control horizon and it is defined as the number of parameters used to capture the future control trajectory (Maciejowski, 2002). It is important to note that the length of N_C is chosen less than or equal to the length of prediction horizon N_P.

The MPC controller forms a cost function (Equation (5.14)) which consists of these errors ($\mathbf{e}_k$) and the control input which determines the best set of future control inputs to balance the output error minimisation against control input effort.

Repeating the derivation steps from Equation (5.7) to Equation (5.19) one can find the optimal solution for the control input which is the function of current error information $\mathbf{e}(k_i)$.

$$\Delta\mathbf{U} = (\mathbf{\Phi}^T\mathbf{\Phi} + \overline{\mathbf{R}})^{-1}\mathbf{\Phi}^T(\mathbf{R}_s - \mathbf{F}\mathbf{e}_{k_i}) \tag{5.29}$$

where, $\mathbf{R}_s$ is the set-point vector ($\mathbf{R}_s^T = \overbrace{\begin{bmatrix} 1 & 1 & \dots & 1 \end{bmatrix}}^{N_P} r(k_i)$) and $r(k_i)$ is the given set-point signal at sample time k_i. For this study, $r(k_i) = 0$. Because the control objectives are to steer the error vector ($\mathbf{e}_k$) to 0, i.e. the spacing error (err_k) should steer to zero so the desired SIVD could be achieved, range-rate ($\dot{err}_k$) should converge to zero so the ACC vehicle follow the ACC vehicle with the same velocity, and the absolute acceleration ($\ddot{err}_k$) should steer to zero so the ACC vehicle moves with the constant speed. $\overline{\mathbf{R}} = \mathbf{R}\mathbf{I}_{N_C \times N_C}$ ($\mathbf{R} \geq 0$) where $\mathbf{R}$ is used as a tuning operator (scalar value) for the desired closed-loop performance (Wang, 2009) which, in this condition, consists of a single element and weights the control input command. For the predictive model developed $\mathbf{R} = 1$. $\mathbf{F}$ and $\mathbf{\Phi}$ matrices are defined in Equation (5.12) and Equation (5.13) respectively.

At each time step k the MPC algorithm determines a sequence of control input $(\Delta U_0 \ldots \Delta U_{N_C-1})$ to minimize the cost function J (Equation (5.14)). The parameters which have been used in the MPC controller formulation are shown in Table 5-1.

Parameters	Symbol	Value
Discrete time sample	T	0.1 s
Time lag	τ	0.5 s
Tuning operator	**R**	1
Set point	r	0
Headway time	h	1 s
Prediction horizon	N_P	230 samples
Control Horizon	N_C	3 samples
Upper acceleration limit	u_{max}	0.25g
Lower acceleration limit	u_{min}	-0.5g

Table 5-1   Controller parameters

A comparison study carried out in Wang, (2009) shows that the length of N_P effects significantly the closed-loop stability and performance of the system. With short prediction horizon, the closed-loop predictive control system is not necessarily stable. Therefore, a long prediction control horizon should be considered to guarantee the closed-loop stability, and for this characteristic N_P is also called a tuning parameter.

Different lengths of the prediction horizon have been tried. Using a short prediction horizon (N_P), the closed-loop performance of the controller was not stable. The stable performance of the controller is obtained by using a higher length of prediction horizons. In the following simulations the prediction horizon N_P assumed is 230 samples and the control horizon N_C is assumed 3 samples.

5.4 Simulation Results and Discussion

The two-vehicle system is analysed under different encounter scenarios to perform the TMs. The simulation results are produced to evaluate the performance of MPC based upper-level spacing-control laws under these critical TMs. The main objectives of the analysis are to manoeuvre the first-order ACC vehicle to the required SIVD with a zero range-rate while avoiding a collision with the preceding vehicle and at the same time satisfying the operational constraints. It should be noted that the first-order ACC vehicle model does not consider the nonlinearities and complex internal dynamics of the vehicle sub-models. A parametric and sensitivity analysis of the first-order ACC vehicle is carried out against the MPC controller parameters.

During the control algorithm formulation, the operational constraints are incorporated in the MPC controller formulation. The constraints incorporated are control input constraint which corresponds to the acceleration limits of the ACC vehicle Equation (5.30), state constraint which means that the ACC vehicle cannot have a negative velocity Equation (4.1), the collision avoidance has also been formulated as state constraint Equation (5.32), and terminal constraint which refers that the ACC vehicle should establish a SIVD with the zero range-rate.

The control input constraint included in the MPC control formulation is:

$$u_{\min} \leq u_k \leq u_{\max} \tag{5.30}$$

As mentioned above in Section 5.2.2 that the dimension of $\mathbf{\Delta U}$ is N_C and N_C is 3 samples, therefore, the constraints are fully imposed on all the components in $\mathbf{\Delta U}$ and can be translated to the six linear inequalities as

$$\begin{bmatrix} 1 & 0 & 0 \\ 0 & 1 & 0 \\ 0 & 0 & 1 \\ -1 & 0 & 0 \\ 0 & -1 & 0 \\ 0 & 0 & -1 \end{bmatrix} \begin{bmatrix} \Delta u(k_i) \\ \Delta u(k_i+1) \\ \Delta u(k_i+2) \end{bmatrix} \leq \begin{bmatrix} u_{max} - u(k_i-1) \\ u_{max} - u(k_i-1) \\ u_{max} - u(k_i-1) \\ u_{min} + u(k_i-1) \\ u_{min} + u(k_i-1) \\ u_{min} + u(k_i-1) \end{bmatrix} \tag{5.31}$$

And the state and collision avoidance constraints incorporated in the MPC control formulation are:

$$y_k = \begin{pmatrix} err_k \\ -\dot{err}_k \end{pmatrix} \leq \begin{pmatrix} \text{SIVD} \\ v_{preceding} \end{pmatrix} \tag{5.32}$$

$$\text{SIVD} = h v_{preceding} \tag{5.33}$$

where, h is the headway time.

5.4.1 Preceding Vehicle with Throttle Input of 50 Degrees and Different Initial Conditions for Both Vehicles

In this scenario, both vehicles start with the different initial speeds and different initial positions, the throttle input for the preceding vehicle is set to 50 degrees for the entire simulation time of 20 s. The baseline scenario is that an ACC vehicle travelling at 30 m/s in the speed control mode detects a preceding vehicle which is accelerating from 10 m/s, the ACC vehicle is 60 m behind the preceding vehicle when it detects a preceding vehicle. The initial error vector (**e**) for this situation is:

$$\mathbf{e}(0) = \begin{pmatrix} err \\ \dot{err}_k \\ \ddot{err}_k \end{pmatrix} = \begin{pmatrix} -(\text{R-SIVD}) \\ \dot{\text{R}} \\ \ddot{x}_k \end{pmatrix} = \begin{pmatrix} -(60-10) \\ 20 \\ 0 \end{pmatrix} = \begin{pmatrix} -50\text{m} \\ 20\text{m}/s \\ 0 \end{pmatrix} \tag{5.34}$$

The ACC vehicle response has been analysed for two different situations: (1) the ACC vehicle without any constraint considered, and (2) the ACC vehicle with all constraints incorporated in the formulation of the MPC control algorithm.

The result shows for both situations (Figure 5-4) that the ACC vehicle performs the required TM successfully by initially manoeuvring to set up the desired SIVD and then maintaining it for the rest of the simulation with the zero range-rate. The comparison shows in Figure 5-4(a) that the ACC vehicle, situation (2), manoeuvres quickly to reach the preceding vehicle's velocity than the ACC vehicle velocity profile without acceleration limits. Figure 5-4(b) shows the positions of both vehicles. The ACC vehicle distance, relative to preceding vehicle, can be seen in Figure 5-4(d). ACC vehicle accelerations for both situations are shown in Figure 5-4(c). The ACC vehicle, without the control input constraint, only concerns with establishing a SIVD with zero-range-rate and is unable to meet the other requirements of the TM. It has been observed that with control input constraint included, the ACC vehicle, using the MPC control algorithm, has performed all the control tasks discussed in Section 5.1.

Figure 5-4(b) shows the positions of both vehicles. With the initial range of 60 m the simulation starts and then the ACC vehicle initially reduces the range, Figure 5-4(d), once the desired SIVD is achieved the ACC vehicle then continues to follow the preceding vehicle. It should be noted that after establishing the SIVD the preceding vehicle's velocity is continuously increasing so the desired SIVD and it can be seen in Figure 5-4(d) which shows the range between the two vehicles. Once the SIVD is established then the range between the two vehicles becomes equal to the SIVD.

One can conclude after analysing the ACC vehicle response under two different encounter scenarios that the MPC control algorithm can successfully manoeuvre the ACC vehicle, with the given initially conditions, to the desired SIVD and with the zero range-rate. Another advantage of using the MPC control algorithm is that the MPC can incorporate the constraint in its formulation which improves the system stability and robustness.

The validation of these results has been performed by comparing with the Bageshwar, *et al.*, (2004) results. The comparison shows a good agreement between the two results because the first-order ACC vehicle is achieving the required control objectives. It should be noted that the Bageshwar, *et al.*, (2004) results does not show any detail about the preceding vehicle, e.g. what is throttle input for the preceding vehicle, engine details, gear ratio, etc. Also the behaviour of the preceding vehicle is

not convincing enough to show the actual vehicle behaviour. On the contrary, in this study the preceding vehicle is also based on the complex vehicle model, which means a realistic reference target for the ACC to achieve.
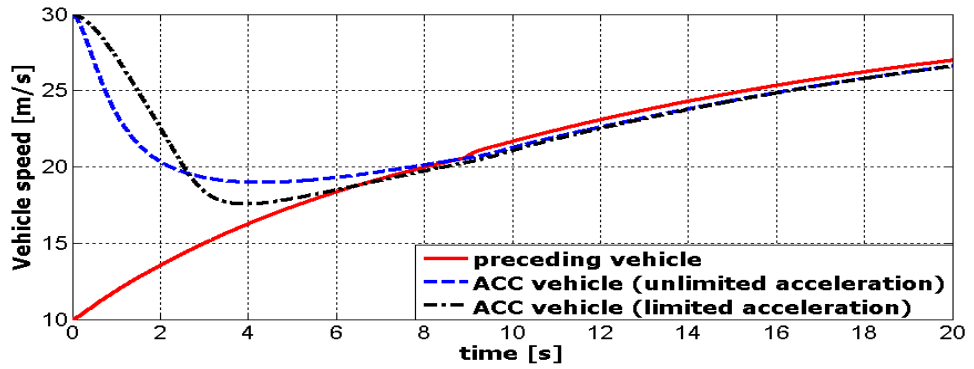

(a)
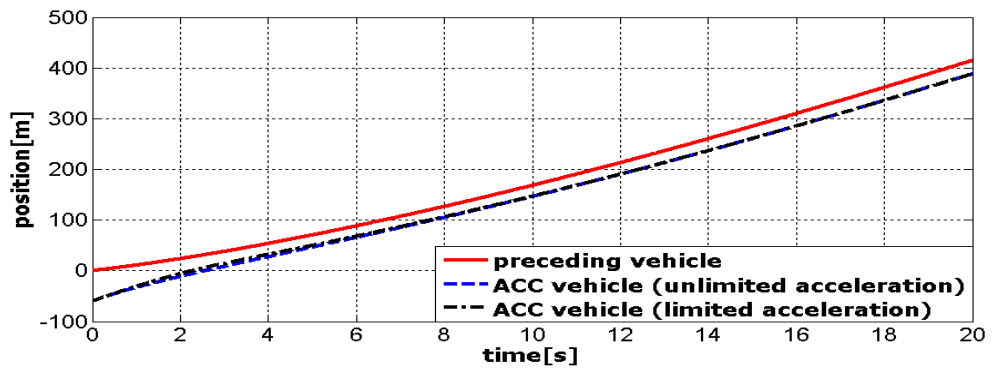
(b)
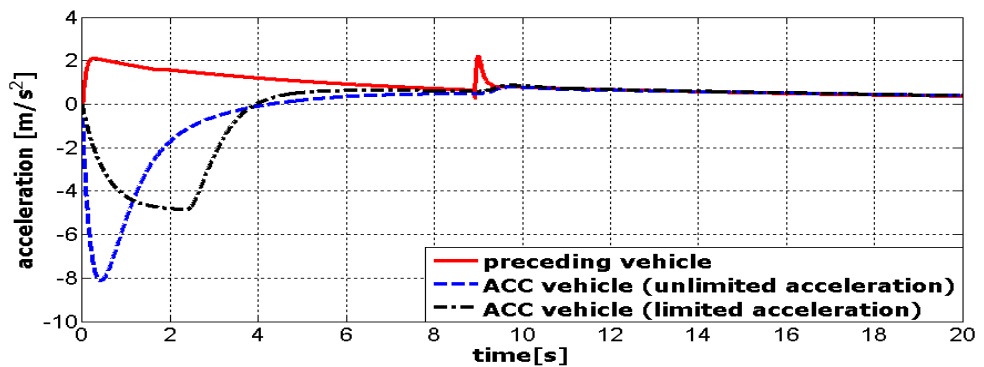
(c)
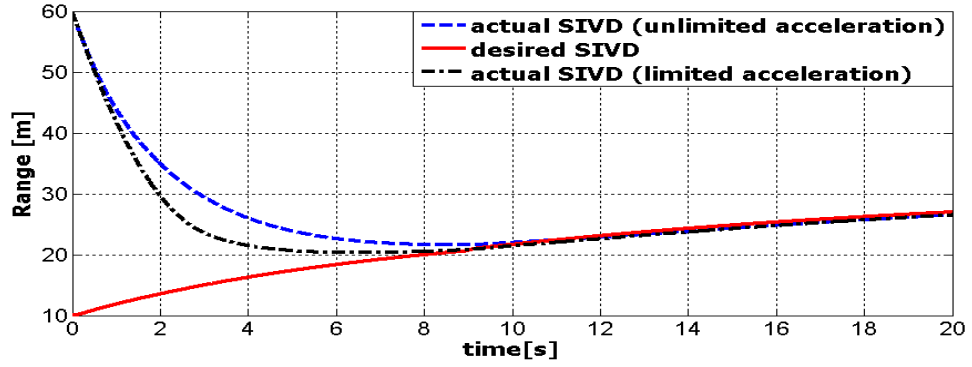
(d)

Figure 5-4   (a) Velocities of the vehicles, (b) Position of the vehicles, (c) Absolute acceleration of both vehicles, (d) Range

5.4.2 ACC Vehicle Response against a Halt Preceding Vehicle

In this encounter scenario, the ACC vehicle, in the speed control mode, with an initial velocity of 30 m/s detects a preceding vehicle which is at rest at a distance of 110m. In this scenario the ACC vehicle model has to decelerate from 30 m/s to the rest position. The spacing error between the two vehicles is -110 m and the initial range-rate between the two vehicles is 30 m/s as shown in Equation (5.35). According to Bageshwar (2004), this scenario is possible to avoid the collision as for the given range-rate of 30 m/s, the required minimum range is 106 m to decelerate to the velocity of the target vehicle. The required SIVD in this scenario is at the origin of the coordinate frame (Section 5.3.1) of the TM which remains constant throughout the length of the simulation as the preceding vehicle's velocity is equal to zero.

Based on this encounter scenario the initial error vector can be defined as:

$$\mathbf{e}(0) = \begin{pmatrix} err \\ \dot{err}_k \\ \ddot{err}_k \end{pmatrix} = \begin{pmatrix} -(\text{R-SIVD}) \\ \dot{R} \\ \ddot{x}_k \end{pmatrix} = \begin{pmatrix} -(110-0) \\ 30 \\ 0 \end{pmatrix} = \begin{pmatrix} -110\text{m} \\ 30\text{m}/s \\ 0 \end{pmatrix} \qquad (5.35)$$

where, -110 m is the initial spacing error, 30 m/s is the initial range-rate, and the 3rd element of the vector is the absolute acceleration of the ACC vehicle. It should be noted that the spacing error is equal to –(R – SIVD), here R is the initial range

(relative distance) which is 110 m and SIVD is the specified inter-vehicle distance which is 0 m in this case.

The simulation results in Figure 5-5 show the ACC vehicle response for two different situations. In the first situation, the ACC vehicle is analysed without using any constraint. In the second condition only the control input constraint is included in MPC formulation while the states and collision avoidance constraints are not included in the control algorithm. It can be seen in Figure 5-5(c) that without any constraints the ACC vehicle's acceleration is going below -0.5g m/s², the ACC vehicle successfully executed the TM and can establish a the SIVD with the zero range-rate with the preceding vehicle. However, an ACC vehicle should obey the constraints in any of its mode of operation and in any driving situation. With the control input constraint included only, the ACC vehicle cannot establish a safe SIVD and smashes with the preceding vehicle as shown in Figure 5-5(a). The control input commands for both situations are shown in Figure 5-5(d). It can also be observed from Figure 5-5(b) that the ACC vehicle is travelling with a negative velocity. This is due to the reason that the states constraints and collision avoidance are not included in the controller formulation. Therefore, it is necessary to include states constraints and collision avoidance in the formulation of the MPC control algorithm.
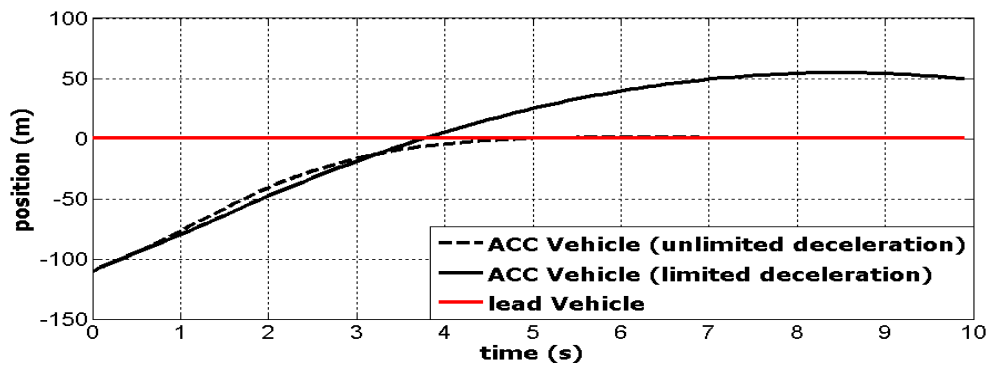
(a)
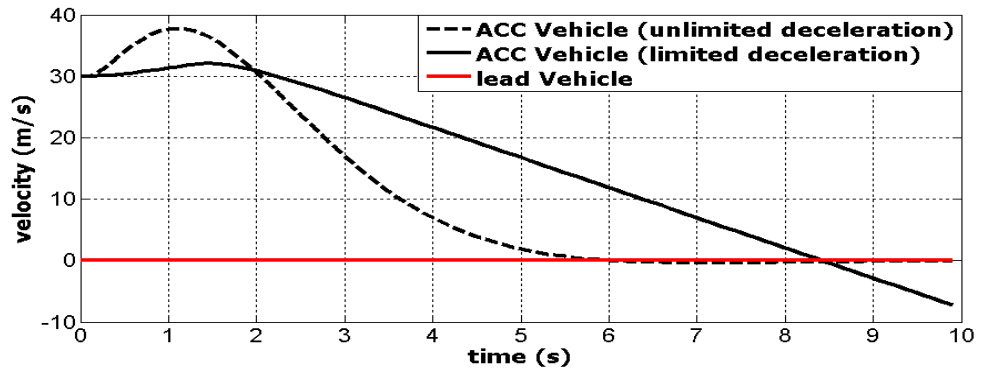
(b)
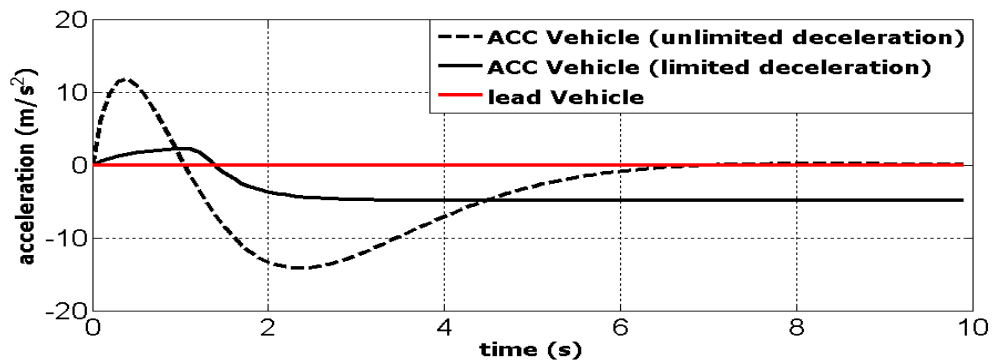
(c)
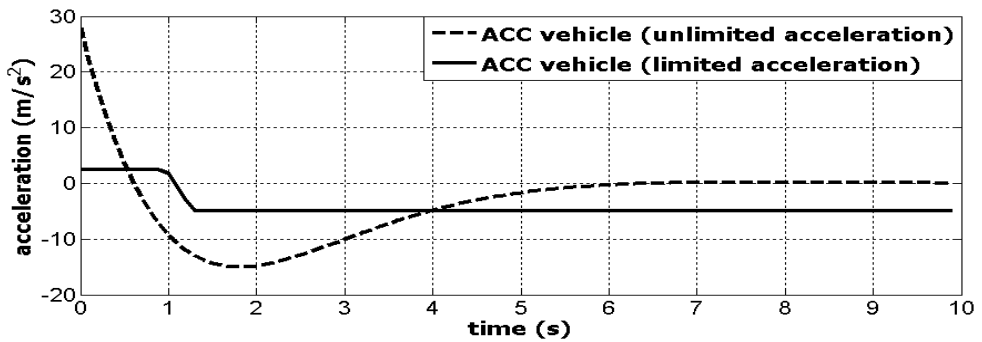
(d)

Figure 5-5   (a) Position of vehicle, (b) Velocity of   vehicle, (c) Absolute
acceleration of vehicle, (d) Commanded acceleration

Figure 5-6 shows the same simulation scenario as shown in Figure 5-5 but this time
the states and collision avoidance constraints are also included in MPC algorithm.
The MPC control law computes initially the deceleration commands for the ACC

vehicle, Figure 5-6(d). After reaching the deceleration limits the deceleration commands remains active till t = 5.93 s followed by the acceleration commands to bring the velocity of the ACC vehicle down in order to establish the SIVD with the zero range-rate. The velocity of the preceding vehicle is zero during the entire simulation time so the SIVD. It can be seen in Figure 5-6(a) that the ACC vehicle established the required SIVD and manoeuvres to the origin of the coordinate frame (Section 5.3.1) with the zero range-rate. Therefore, it is necessary to include control input, states and collision avoidance constraints in the controller formulation in order to execute the TM successfully and avoid the accident with the preceding vehicle.

These results have also been validated against the Bageshwar, *et al.*, (2004) model. The simulation produced in Figure 5-6 matches well with their results. It should be noted that in their results the simulation was stopped when the ACC vehicle came to a complete halt while its absolute acceleration still shows a negative sign. This does not show the complete response of the ACC vehicle. On the contrary, Figure 5-6 shows the ACC vehicle response for a longer time to emphasize that all the control objectives have been achieved.

(a)
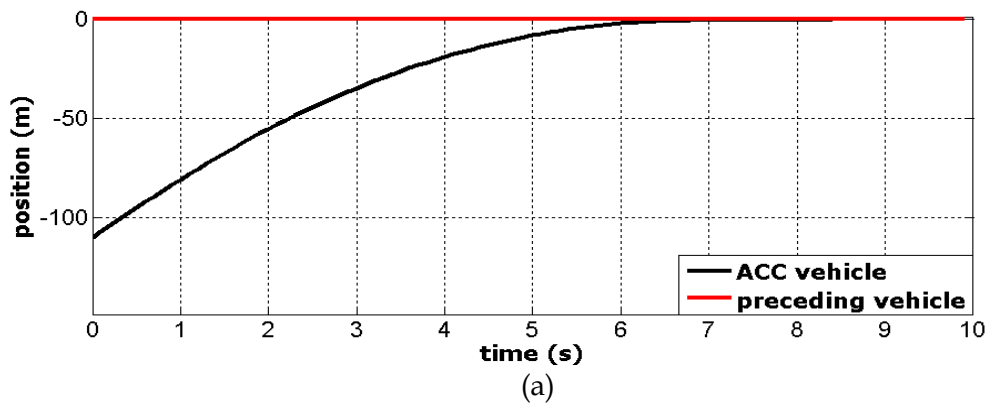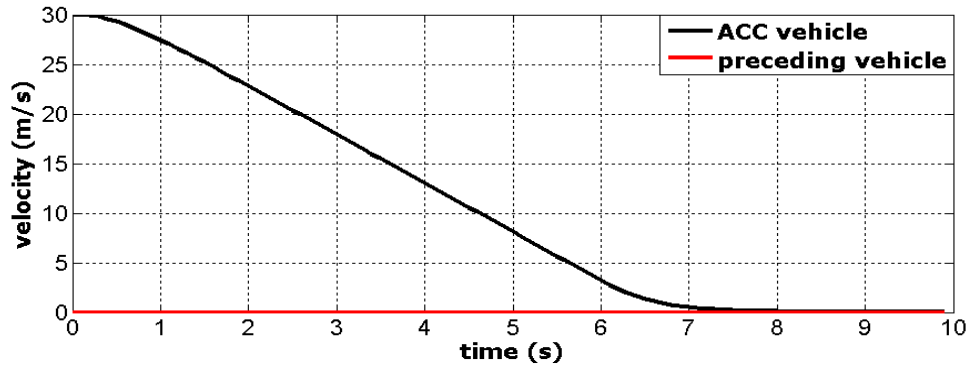
(b)
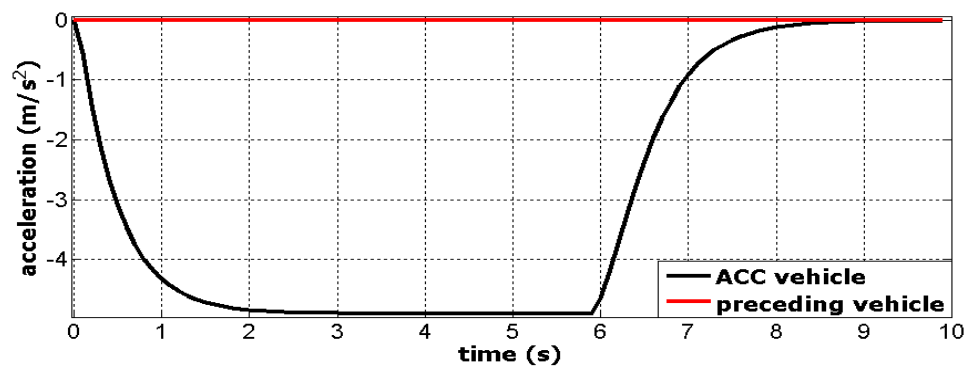
(c)
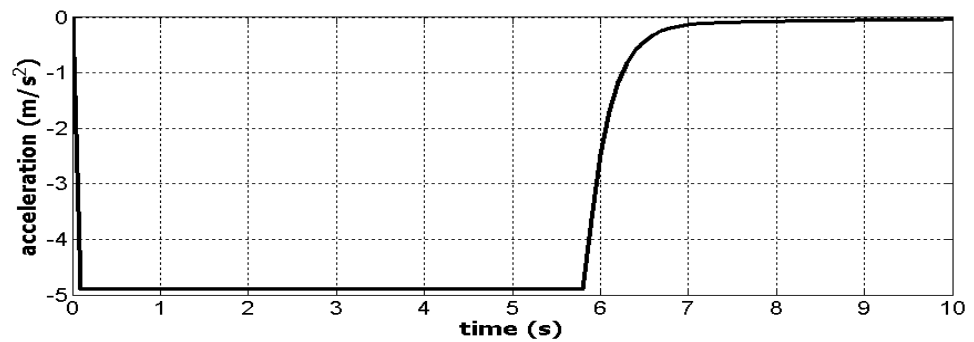
(d)

Figure 5-6 (a) Position of vehicle, (b) Velocity of the vehicle, (c) Absolute acceleration of ACC vehicle, (d) Commanded acceleration

5.5 Parametric and Sensitivity Analyses

In this section, the first order ACC vehicle model is analysed for different initial conditions, for different initial range while keeping the range-rate constant and

against different MPC controller parameters. The purpose of these analyses is to investigate the ACC vehicle behaviour against these different situations.

5.5.1 ACC vehicle Response against a Halt Preceding Vehicle with Different Initial Conditions for the ACC Vehicle

For the purpose of sensitivity analysis, the response of the ACC vehicle has been analysed for a scenario where the preceding vehicle is at rest but in this scenario the initial conditions are different. An ACC vehicle with its initial speed of 25 m/s detects a halt preceding vehicle at a distance of 80 m. The initial error vector for the considered encounter scenario is:

$$\mathbf{e}(0) = \begin{pmatrix} err \\ \dot{err}_k \\ \ddot{err}_k \end{pmatrix} = \begin{pmatrix} -(\text{R-SIVD}) \\ \dot{R} \\ \ddot{x}_k \end{pmatrix} = \begin{pmatrix} -80\text{m} \\ 25\text{m}/s \\ 0 \end{pmatrix} \tag{5.36}$$

It can be seen in Figure 5-7 that the ACC vehicle smoothly achieves the required objective (Section 5.1) in the presence of control input, states and collision avoidance constraints. Figure 5-7(a) shows the position and velocity of the ACC vehicle and Figure 5-7(b) shows the absolute acceleration (top) of the ACC vehicle and commanded acceleration (bottom) for the ACC vehicle. Again the initial acceleration commands computed by MPC control law are to decelerate to reduce the speed of the ACC vehicle to avoid the collision with the preceding vehicle.
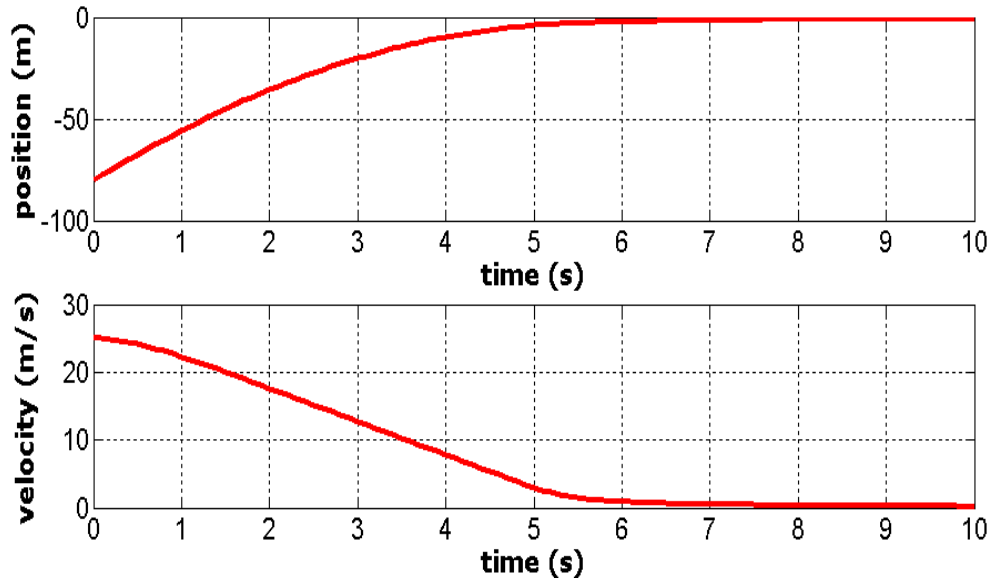
(a)
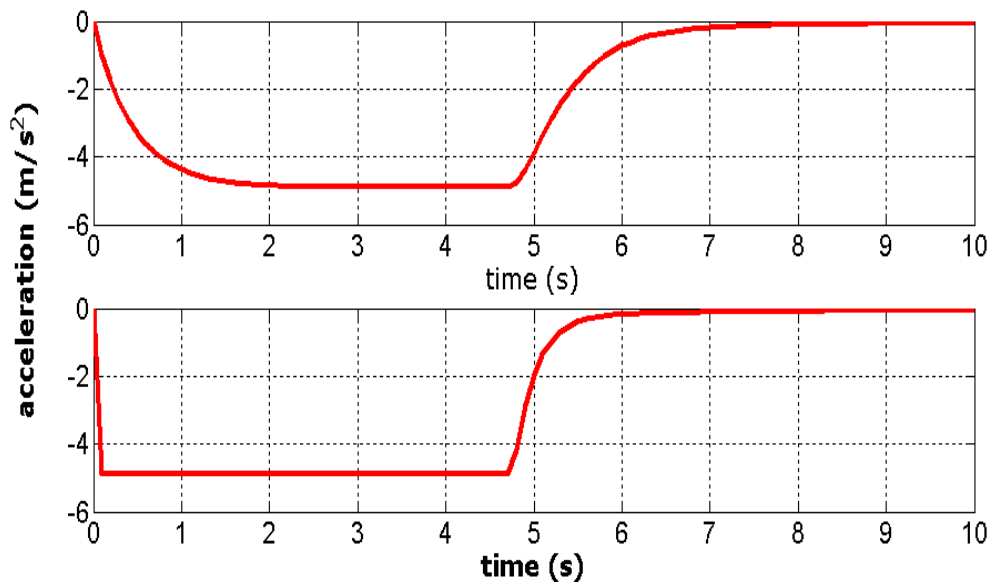
(b)

Figure 5-7   (a) Position and velocity of the ACC vehicle, (b) Absolute acceleration of ACC vehicle and commanded acceleration

5.5.2 ACC Response for Different Initial Range

The Figure 5-8 shows the response of the ACC vehicle for different initial ranges. The encounter scenario is same as shown in Figure 5-6. The initial range in Figure

153

5-6(a) is 110 m which is the minimum possible range between the two vehicles for given range-rate to avoid a collision with the preceding vehicle. If the range is below 106 m for same range-rate then according to Bageshwar, *et al* (2004) the ACC vehicle cannot avoid a collision with the preceding vehicle. In this section, the initial ranges of 105 m and 115 m have been used to analyse the behaviour of ACC vehicle while rest of the parameter are kept same. The aim of this simulation is to validate the ACC vehicle's performance against Bageshwar's, *et al* (2004) analysis and to examine the ACC vehicle's behaviour when the range is above and below 110 m. Figure 5-8(a) shows the position and velocity of the ACC vehicle and Figure 5-8(b) shows the absolute acceleration (top) of the ACC vehicle and commanded acceleration (bottom) for the ACC vehicle. For the initial range of 105 m Figure 5-8 (a) shows that ACC vehicle is unable to perform the TM and cannot avoid the collision with the preceding vehicle.

For the range of 115 m, which is higher than 110 m, the ACC smoothly performs the TM Because of the higher range the ACC vehicle has plenty of time to reduce its speed and stop behind the preceding vehicle. It is, therefore, can be concluded that the initial values computed by Bageshwar *et al* (2004) are appropriate and can be used for the two-vehicle encounter scenario in this study.


(a)

(b)
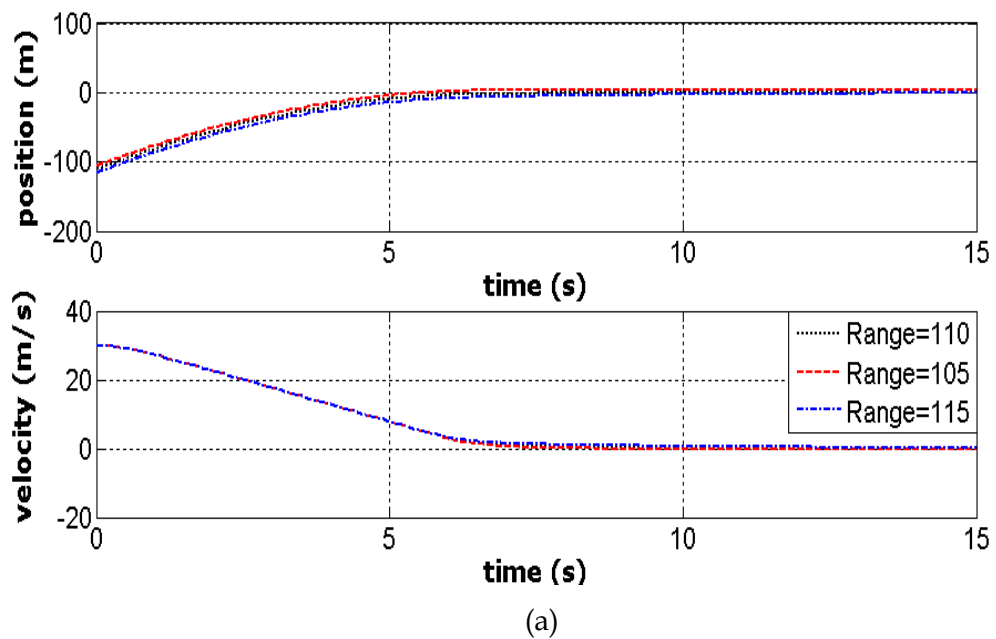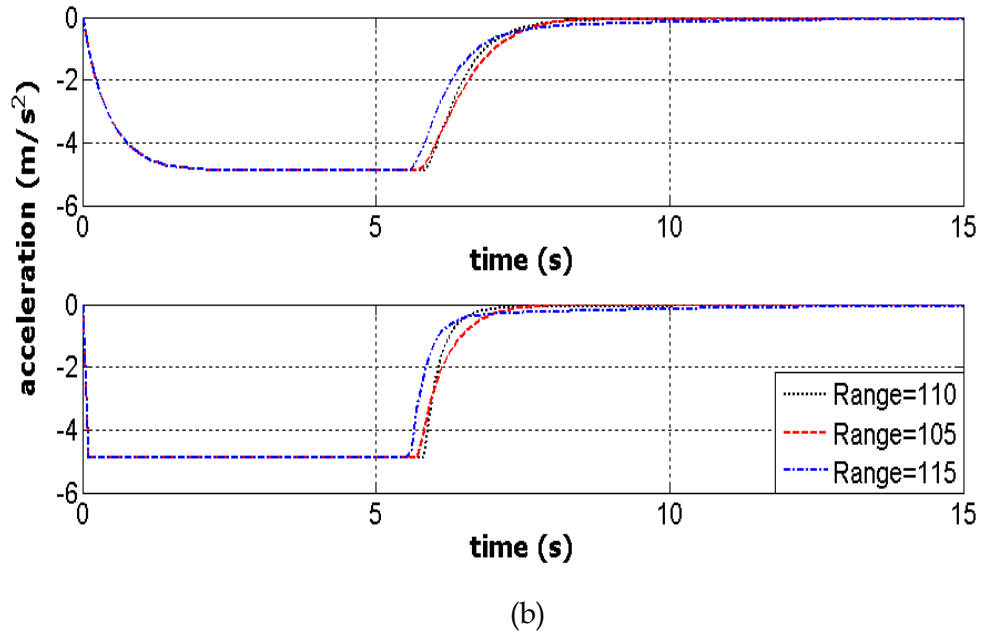
Figure 5-8 (a) Position and velocity of the ACC vehicle, (b) Absolute acceleration of ACC vehicle and commanded acceleration

5.5.3 ACC Response for Variable Control Input Cost Weighting (R)

In this section the sensitivity of the ACC vehicle has been analysed for different control input cost function weighting **R**. The actual value of **R** used in the above simulations is 1 and the other two values used for **R** are 10000 and 20000 which correspond to the two different levels of a tight control where a tight control means a higher optimized effort. Figure 5-9(a) shows the position and velocity of the ACC vehicle and Figure 5-9(b) shows the absolute acceleration (top) of the ACC vehicle and commanded acceleration (bottom) for the ACC vehicle. It can be seen in Figure 5-9 that due to the higher values of **R** the magnitude of the control input is significantly reduced and it takes longer for the state variables to reach the desired values. It should be noted that higher the value of **R** delayed the response of the ACC vehicle.
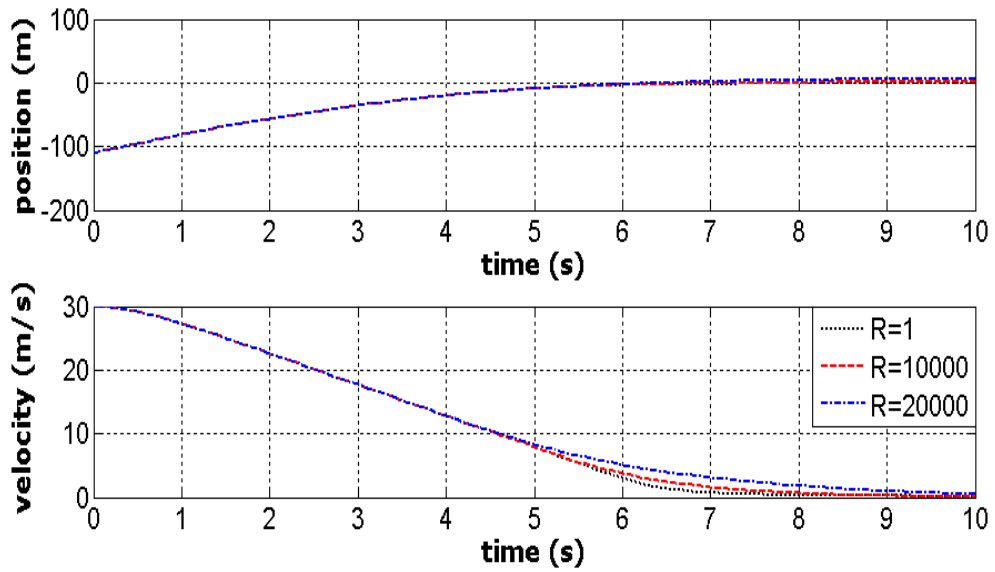
(a)
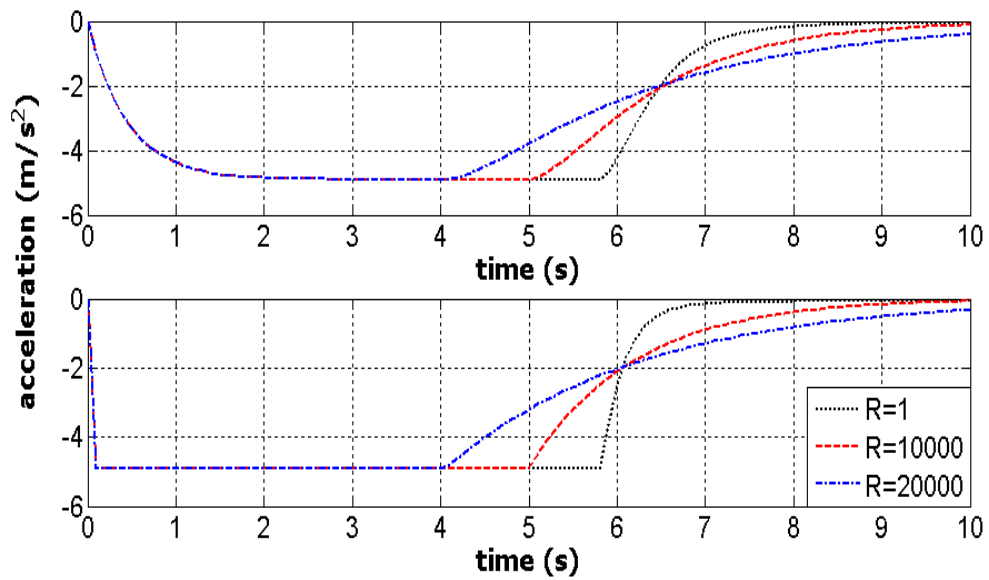
(b)

Figure 5-9   (a) Position and velocity of the ACC vehicle, (b) Absolute acceleration of ACC vehicle and commanded acceleration

## 5.5.4 Sensitivity Analysis against N_C Variation (Section 5.4.1 Scenario)

In Figure 5-10 the encounter scenario of Figure 5-4 has been considered where both vehicles are in motion. N_C chosen in Figure 5-4 was 3 samples and in Figure 5-10 N_C

= 5 samples is chosen. The effect of higher value of N_C has been analysed which shows that the control energy is distributed over a longer period of future times and this distribution causes a corresponding reduction in the control input magnitude, resulting error generation and causing a loss of control and this can also be termed as a 'loose' control because the initial acceleration commands are to accelerate rather than decelerate Figure 5-10(c).

It has been observed that this error in the ACC vehicle response can be reduced by increasing a higher value of **R** which is the control input cost weighting function. Using **R** = 5 the desired control objectives have been achieved i.e. the ACC vehicle establishes the SIVD with the zero range-rate. This analysis shows that higher the values of N_C higher the error generation and that error can be controlled by increasing the cost weighting function *(**R**)*. For N_C = 5 samples the value of **R** = 5 is suitable, if a N_C > 5 then a higher value of **R** is required to achieve the control objectives.
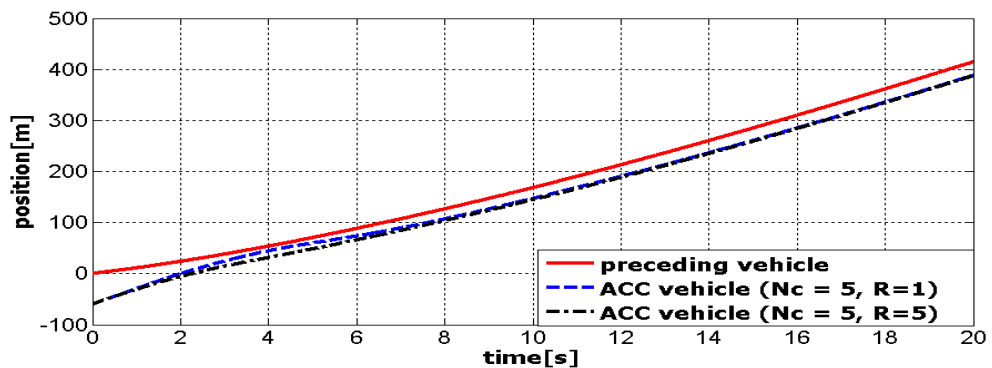

(a)
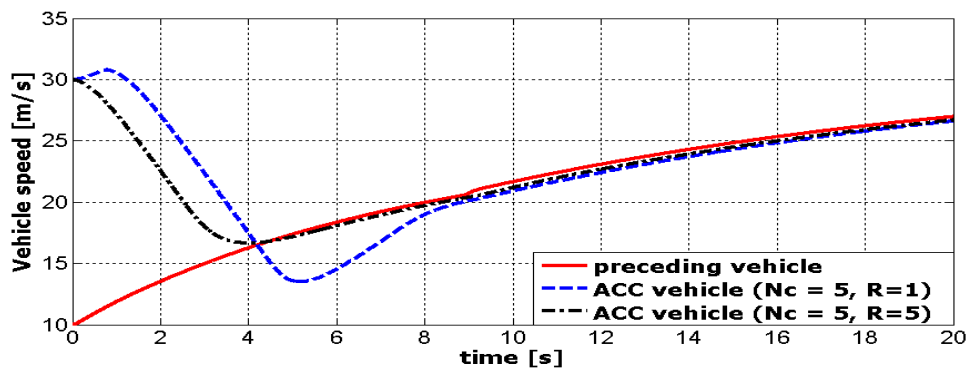
(b)
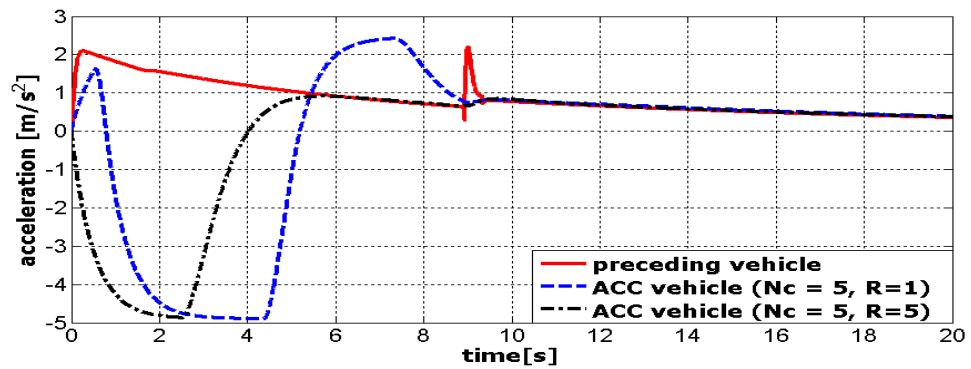
(c)
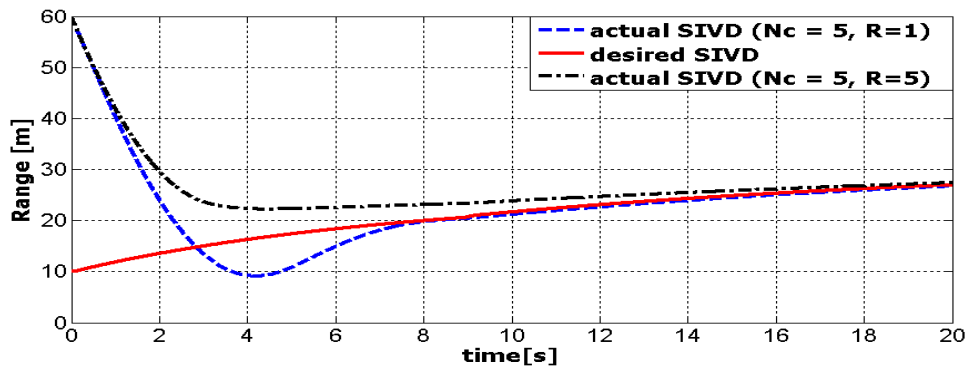
(d)

Figure 5-10   (a) Position of the vehicles, (b) Velocity of vehicles, (c) Acceleration of vehicles, (d) Range between two vehicles

5.5.5 Sensitivity Analysis against N_C Variation (Section 5.4.2 Scenario)

In Figure 5-11 the ACC vehicle analysis is carried out for a different value of N_C. Figure 5-11(a) shows the position and velocity of the ACC vehicle and Figure 5-11(b) shows the absolute acceleration (top) of the ACC vehicle and commanded acceleration (bottom) for the ACC vehicle. The encounter scenario considered is the same as in Figure 5-6 where N_C was chosen 3 samples. In this analysis $N_C = 5$ samples has been considered which means that the control energy is distributed over a longer period of future times. This distribution causes a corresponding reduction in the control input magnitude which is also clear from Figure 5-11(a) resulting in error generation and eventually the ACC vehicle cannot avoid the

collision with the halt preceding vehicle. This reduction in control input magnitude can also be termed as a 'loose' control because the initial acceleration commands are to accelerate rather than decelerate Figure 5-11(b).

It has been found that this error in the ACC vehicle response, due to higher value of N_C, can be reduced by using a higher value of **R** which is the control input cost weighting function. After several attempts using **R** = 5 the desired control objectives have been achieved i.e. the ACC vehicle establishes the SIVD with the zero range-rate and avoids the collision with the preceding vehicle. This analysis shows that higher the values of N_C higher the error generation and that error can be controlled by increasing the cost weighting function *(**R**)*. For N_C = 5 the value of **R** = 5 is suitable, if N_C > 5 then a higher value of **R** is required for the close-loop stable performance of the ACC vehicle.


(a)

(b)
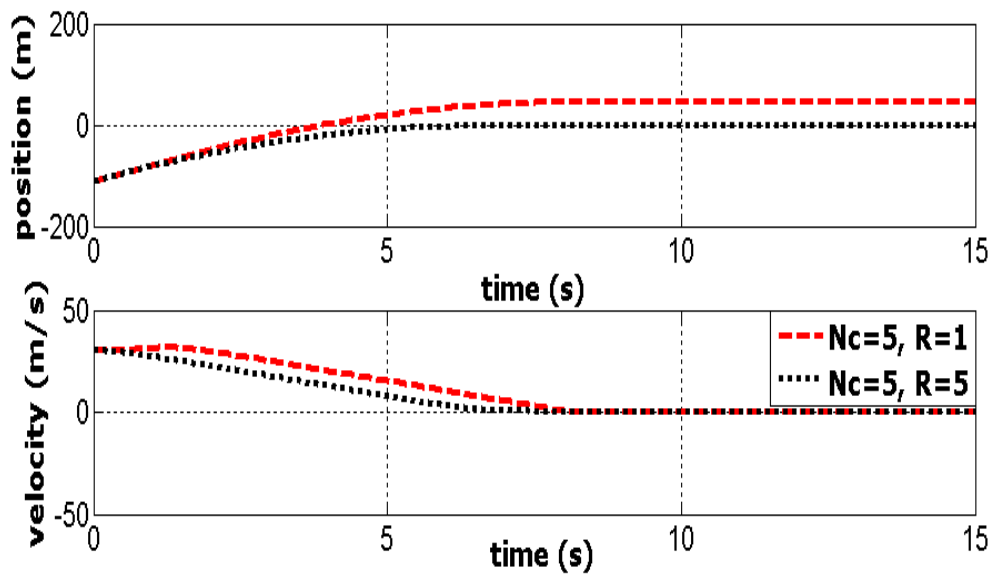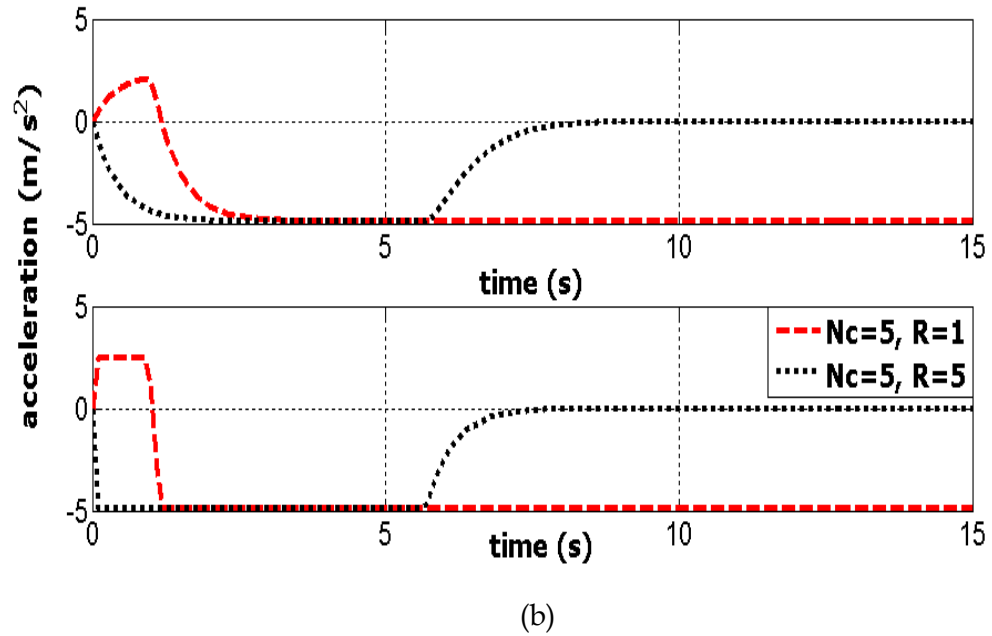
Figure 5-11   (a) Position and velocity of the ACC vehicle, (b) Absolute acceleration of ACC vehicle and commanded acceleration

5.6   Conclusions

As mentioned in the introduction of Chapter 4 (Section 4.1) throughout this thesis different control methods were used for the upper-level controller analysis. Three of them: PID, sliding mode, and CTG have been analysed in Chapter 4 and the fourth method (MPC) has been analysed in this chapter. The main advantages of using MPC method over the other control strategies are incorporating the operational constraints (control input, states and collision avoidance) in the control algorithm during the analysis process and an online optimization can be achieved. The control input constraints are fully applied on all the components of $\Delta\mathbf{U}_k$ and have been translated as six linear inequalities.

The MPC strategy is not a new control method of control design and is being used for different applications as discussed in Section 5.2. It mainly solves standard optimal control problems where the optimization is carried out in a finite horizon. The difference between the MPC and the other control methods used in Chapter 4 is that MPC solves the optimal control problem on-line for the current states of the system rather than solving it off-line using a feedback policy as in the case of other control methods.

The main difference between the MPC and PID control strategies is that the MPC control strategy uses the desired reference trajectory which is computed using the prediction model then, the MPC controller modifies the plant characteristics in order to follow the desired reference trajectory. Whereas, the control action taken by the PID control strategy is based on the past errors which can be viewed as if the driver is driving the vehicle using the rear-view mirror. Similarly in the sliding mode control method, the control objectives are designed as a sliding surface using the previous plant's states (off-line computation). The sliding mode control was found unsuitable due to the first-order lag considered in the upper-level controller formulation (discussed in detail in Chapter 4). The CTG control algorithm is also based on the previous plant's states which is not robust enough in comparison with the MPC control method. Also, the on-line optimization is not possible and the operational constraints cannot be included in the formulation of CTG control algorithm. After comparing all these control methods it can be concluded that the MPC control algorithm is the most appropriate for the ACC vehicle analysis.

In this chapter the fundamental features of the MPC control method have been discussed. The formulation of the prediction model used in the MPC control algorithm has been presented using a simple linear SISO system. The MPC algorithm was then applied to the two-vehicle system. The prediction model, used to compute the future control input for the first-order ACC vehicle, has been developed based on the error vector (Equation (5.27)) between the two vehicles.

The dynamic behaviour of the ACC vehicle, using the MPC controller technique, has been analysed for different TMs. The response of the first-order ACC vehicle model has been analysed with constraints and without constraints and results have been compared and discussed. The shortcoming occurring without using the constraints has also been highlighted. It has been observed that with a first-order model, the ACC vehicle successfully establishes the desired SIVD with the zero range-rate with all constraints included in the MPC controller formulation.

Parametric and sensitivity analyses of the ACC vehicle using MPC have also been carried out in this chapter for different initial conditions, different ranges, different control input cost weighting ($\mathbf{R}$) and different control horizon (N_C).

It has been noticed that the ACC using MPC can perform the TM successfully regardless of the initial conditions, provided the initial conditions are selected within the range of the Bageshwar *et al.,* (2004) model. A lower initial range for a given range-rate has been analysed and it has been found that the ACC vehicle cannot avoid the collision with the preceding vehicle. Also, higher values of initial range (more than for a given range-rate) provides ample time to the ACC vehicle to achieve the control objectives within the given constraints boundaries.

It has been observed that the higher values of control input cost weighting (**R***)* correspondingly penalize the control input magnitude which can also be termed as a 'tight' control. In this situation the control objectives are not violated but it results in a delayed response. Therefore, it should be noted that for the best performance of the system an appropriate value of **R** should be selected which neither relaxes the control input to have a 'loose' control nor affects excessively the control input to have a 'tight' control.

The effect of variable control horizon (N_C) has also been analysed in this chapter. For the stable response of the ACC vehicle, the value of N_C chosen is 3 samples. It has been observed in the analysis that using a higher value of N_C (N_C = 5) causes the control input to be distributed for a higher control horizon, resulting in an error for the desired objectives. This error, due to a higher value of N_C, has been reduced by increasing the cost weighting coefficient (**R**). It has been observed that for a higher value of N_C a higher corresponding value of **R** is required in order to achieve the required control objectives.

In this chapter the ACC vehicle analysed was based on a first-order model which does not consider the internal dynamics of the vehicle sub-models. In Chapter 6, the ACC vehicle will be based on a complex vehicle model that covers the effects of engine dynamics, transmission dynamics, and the brake model on the MPC control algorithm and the response of the ACC vehicle. Any changes in throttle input, engine dynamics, transmission dynamics, and brake input of the preceding vehicle and the ACC vehicle have the corresponding effect on the upper-level controller model; therefore, it would be interested to investigate how the MPC method will perform under these changes. Also, how the ACC vehicle (with internal dynamic complexities) will respond against these critical driving manoeuvres when the

operational constraints are applied on the vehicle controllers and the ACC vehicle has to obey them.

Chapter 6.   Model Predictive Control for a Complex ACC Vehicle

6.1   Introduction

A two-vehicle system which consisted of a preceding vehicle and an adaptive cruise control (ACC) vehicle was developed and analysed in Chapters 4 and 5. The preceding vehicle model was based on a complex vehicle model, developed in Chapter 3 (Section 3.2 to Section 3.5), and the ACC vehicle model was based on a simple first-order model (Section 3.8).   The purpose of the analysis was to investigate the response of the upper-level controller using the first-order ACC vehicle model under critical transitional manoeuvres (TMs) and within the constraints boundaries. During these TMs the first-order ACC vehicle model was performing higher deceleration manoeuvres of up to -13 m/s^2 (control input demand, see Figure 5-5 (c)) to avoid the collision with the preceding vehicle without any constraints applied to the ACC vehicle. Due to the ACC system limitation (Section 4.2.4) the first-order ACC vehicle was restricted to decelerate up to only -4.9 m/s^2 (-0.5g). With these deceleration limits the first-order ACC vehicle executed the required TMs successfully (Chapter 5) with model prediction control.

The upper-level controller was analysed using four well-known control algorithms. The control methods used were as follows:

(1) Proportional-Integral-Derivative (PID) Control

(2) Sliding Mode Control

(3) Constant-Time-Gap (CTG) Control

(4) Model Predictive Control (MPC)

The first three control methods were analysed in Chapter 4 and the fourth control method was analysed in-depth in Chapter 5. The comparison of the results obtained from the four control methods revealed that MPC is the most suitable control algorithm among them to be used for the ACC vehicle analysis. It was established that the first-order ACC vehicle model achieves the control objectives successfully during the TMs while accounting for the operational constraints by using MPC control method. The operational constraints are referred to as control input, states, and collision avoidance constraints. The operational constraints were discussed in detail in Section 5.4. A sensitivity analysis for the first-order ACC vehicle model using MPC control algorithm has also been carried out by changing the initial conditions, MPC parameters, and headway time. Important simulation results were produced and discussed in Chapter 5.

As discussed in Section 3.9, both vehicles (a two-vehicle system) are generally based on complex vehicle model. Therefore, in this chapter, two separate sets of differential equations developed in Chapter 3 (Section 3.2 to Section 3.5) will be used for both vehicles. Equation (3.24) is used to obtain the longitudinal states information of both vehicles. The traction force (F_{xf}) and longitudinal aerodynamic drag force (F_{aero}) are different for each vehicle, while the rolling resistance is assumed the same for both vehicles because it is a function of the mass of the vehicle (Equation (3.23)). It should be noted that the rolling resistance varies for both vehicles when the ACC vehicle is tested for different masses in the later parts of this chapter. The complex ACC vehicle model and lower-level controller model will be analysed in this chapter.

The first-order ACC vehicle model was used to analyse the upper-level controller response and to select the appropriate control algorithm under the critical TMs. The upper-level controller computes the desired acceleration commands for the lower-level controller from longitudinal motion information of the ACC vehicle and the vehicle in front of it. This first-order model will still remain part of the two-vehicle system as a first-order lag which corresponds to sensor signal processing lags and engine or brake actuation lags (Equation (3.32)). The desired acceleration commands

($\ddot{x}_{des}$) are then obtained and sent to the lower-level to compute the required throttle or brake input commands (see Figure 6-1) for the complex ACC vehicle model.

The nonlinear nature of the switching dynamics in the lower-level controller, as well as the presence of the operational constraints, make the task of designing an ACC system rather challenging, and the traditional control techniques may not be suitable for these applications. Moreover, the engine torque and the transmission gear shifting introduce nonlinearities, which force the use of a robust control algorithm. Therefore, the MPC algorithm will be used to compute the spacing-control laws for the complex ACC vehicle model which can, by nature, incorporate the operational constraints in its formulation. The robustness of the MPC method and the behaviour of the ACC vehicle in the presence of internal complexities of the vehicle dynamics will be analysed. The complex models include sub-models for the vehicle engine, transmission, wheels, brakes, upper-level controller, and lower-level controller.

The first-order ACC vehicle model (analysed in Chapter 5) did not consider any dynamic effects generated from engine, transmission, and brake models. It is an important requirement for the braking system to apply the brake smoothly without exceeding the comfort level which can be defined by the maximum deceleration level, for example -0.5g. The brake system of an ACC system is controlled by the control signal received from the lower-level controller. It should be noted that the deceleration limit implies that the ACC vehicle may not apply the necessary braking force to avoid the collision with the preceding vehicle, i.e. no further brake torque can be applied once the maximum brake signal value is reached. It is necessary to investigate how the complex vehicle model and the lower-level controller will respond under these emergency TMs in the presence of internal complexities of vehicle dynamics and operational constraints. Furthermore, it is important to analyse how the complex ACC vehicle model (sub-models) will respond when constraints are applied on the controller that the complex vehicle model has to obey.

It was observed in Chapters 4 and 5 that the gear transmission has its corresponding impact on the acceleration of the complex vehicle model (see Figure 4-5(c)). It should be noted that the error vector (**e**) between the two vehicles (Equation (5.24)) also takes into account the absolute acceleration of the ACC vehicle. In the case of a

complex vehicle model, during an entire critical TM, the ACC vehicle will perform transmission down-shifting and up-shifting which will affect its acceleration profile. This implies that the effects generated due to the gear transmission will affect the upper-level controller (because of the error vector) performance which will in turn affect the overall ACC vehicle's performance. Therefore, the effects of engine and transmission dynamics of both vehicles on the MPC controller and the ACC vehicle's performance are also to be investigated.

As the ACC vehicle can be also subjected to extreme decelerations to avoid a potential collision, a throttle control input alone cannot bring the vehicle to rest position within a short stopping distance. A brake control system is also required to stop the vehicle and avoid a collision with the preceding vehicle; therefore, a brake model is also developed in this chapter. The traction/brake control inputs for the lower-level controller are calculated using the engine maps. The control design for the brake model is based on the standard sliding model control technique where the actual brake torque tracks the desired brake torque (Hedrick *et al.*, 1993).

The objective of this chapter can be restated as: analysing the complex ACC vehicle model under critical TMs in order to establish and maintain a safe inter-vehicle distance (SIVD) with the zero range-rate behind a newly detected slower or halt vehicle. The TMs will be performed in the presence of acceleration, states and collision avoidance constraints when the brake and engine actuators have limited allowable forces and may saturate.

The baseline scenario is to evaluate the MPC technique with complex vehicle longitudinal dynamics model under these transitional manoeuvres to track smoothly the desired acceleration within the operational boundaries. Simulation results will be produced to analyse the stability and coordination of MPC method with complex vehicle sub-models.

Furthermore, a parametric and sensitivity analyses are carried out in this chapter to investigate the changes in the behaviour of the complex ACC vehicle by varying the throttle input to the preceding vehicle, by using different initial conditions, by varying the control horizon (N_C) in the MPC control algorithm, and by varying the control input cost weighting (**R**) in the MPC algorithm.

Finally, the complex ACC vehicle model will be tested numerically under the following situations:

    a. For different ACC vehicle masses;

    b. For a different set of gear ratios;

    c. For a cut-in manoeuvre;

    d. For different values of headway time;

    e. On a road gradient.

In each case, it is essential to examine how an ACC vehicle will respond to these variations, and if the dynamic behaviour of the ACC vehicle is disturbed how the control objectives can still be achieved. This parametric analysis will also help finding out the upper and lower limits for some of these parameters.

This chapter outline is as follows. Section 6.2 presents the lower-level controller model: engine torque and brake torque calculations to track the desired acceleration commands computed by the upper-level controller. Section 6.3 discusses briefly the system of equations for the two-vehicle system. Section 6.4 presents the simulation and discussion. Finally, Section 6.5 presents the conclusions from this chapter.

6.2 Lower-Level Controller

A block diagram of the ACC vehicle and its controllers is shown in Figure 6-1. The positions of the preceding and ACC vehicle are denoted by x_1 and x_2 respectively. The upper-level controller receives information from the preceding vehicle and the ACC vehicle itself and computes the desired acceleration commands ($\ddot{x}_{des}$) for the ACC vehicle. The control algorithm in the upper-level controller is based on the MPC method (Chapter 5) which uses prediction model of the error vector (**e**) (Equation (5.24)) between the two vehicles to compute the control law for the ACC vehicle. The lower-level controller computes the throttle (α) and/or brake (T_{br}) actuator commands using the desired acceleration commands ($\ddot{x}_{des}$) computed by the upper-level controller in order to track the desired acceleration, as shown in Figure 6-1. ACC vehicle's engine speed (ω_e) and manifold pressure (p_{man}) are fed back to the lower-level controller for the throttle and brake input calculations. The upper-level controller formulation is based on the MPC control algorithm which

also incorporates a first-order lag which corresponds to the finite band width of the lower-level controller. It is important to mention here that the lower-level control algorithm is based on the sliding model control algorithm which results in chattering effect. It has already been realised in this study (Section 4.4.2.1) that a lag results in higher magnitude of chattering. Therefore, the first-order lag is considered in the upper-level controller (before lower-level controller) which takes into account the desired acceleration lag, actuator lags, and lag in the filtering of the radar sensor. If the lag is considered after the lower-level controller then it will result in higher magnitude of chattering.
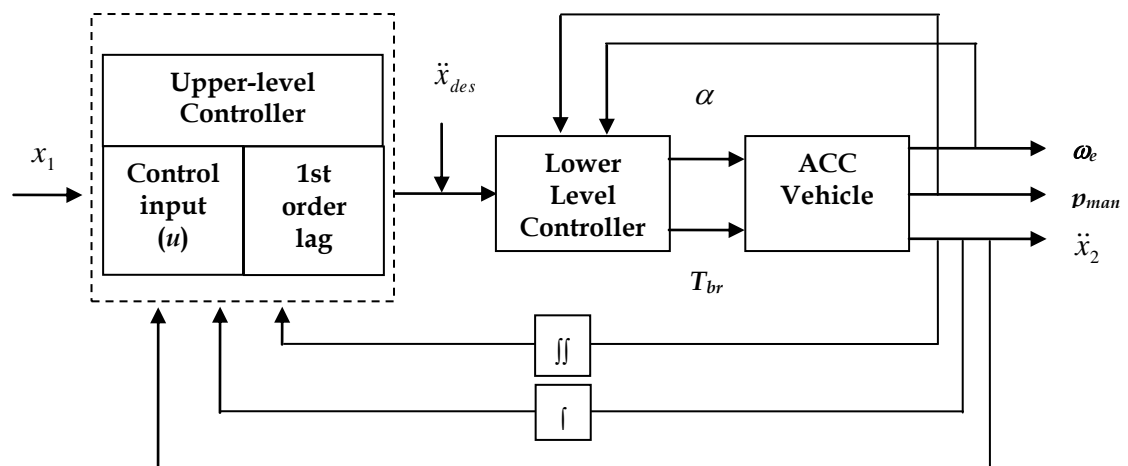
Figure 6-1   Block diagram for the ACC vehicle model

6.2.1 Engine Torque Calculations for Desired Acceleration

The main challenge faced during the development of the lower-level controller is the nonlinearities coming from engine, transmission, and aerodynamic drag. To compensate for them, a simplified vehicle dynamics model has been used which is based on the assumptions that the torque converter in the vehicle is locked, the drive axle is rigid, the temperature of the intake manifold is constant, and there is zero-slip between the tyres and the road (Swaroop, 1997; Rajamani *et al.*, 2000). Based on these assumptions one can develop a relation between the engine speed (ω_e) and the vehicle longitudinal speed ($\dot{x}$) as

$$\dot{x} = R_g R_d r_{eff} \omega_e \tag{6.1}$$

where, R_g is the gear ratio on the transmission (g = 1, 2, 3, 4, 5) and R_d is the final gear reduction in the differential, and r_{eff} is the effective tyre radius. Differentiating Equation (6.1), one obtains

$$\ddot{x} = R_g R_d r_{eff} \dot{\omega}_e \tag{6.2}$$

Under the above assumption the dynamics relating the engine speed (ω_e), net combustion torque (T_{net}), and brake torque (T_{br}) can be linked with the expression (Rajamani, 2006)

$$\dot{\omega}_e = \frac{T_{net} - C_d R_g{}^3 R_d{}^3 r_{eff}{}^3 \omega_e{}^2 - R_g R_d (r_{eff} R_x + T_{br})}{J_e} \tag{6.3}$$

where C_d is the aerodynamic drag coefficient, R_x is the rolling resistance, $J_e = I_e + (mr_{eff}^2 + I_w)R_g R_d$ is the effective vehicle inertia. Using Equation (6.2) and Equation (6.3) the desired net combustion torque (T_{net_des}) for the ACC vehicle can be determined by using the following relation.

$$T_{net\_des} = \frac{J_e}{R_{g_2} R_d r_{eff}} \ddot{x}_{des} + [C_d R_g{}^3 R_d{}^3 r_{eff}{}^3 \omega_{e_2}{}^2 + R_{g_2} R_d (r_{eff} R_x + T_{br_2})] \tag{6.4}$$

The transmission gear ratio (R_{g_2}) corresponds to the ACC vehicle's gear ratio, ω_{e_2} is the actual engine speed of the ACC vehicle. During throttle control the brake torque (T_{br_2}) is zero. The remaining parameters in Equation (6.4) are given in Table 3-1 and for both vehicles they are same. The lower-level controller uses the desired acceleration commands ($\ddot{x}_{des}$) to determine the desired net torque. Using the desired net torque, the desired intake manifold pressure (p_{man_des}) is obtained with the help of engine map. The steady-state engine map has been constructed offline in Chapter 3 (Section 3.7) for the engine model in use. The desired mass of air in the intake manifold (m_{man_des}) is then calculated using the ideal gas law.

$$p_{man\_des} V_{man} = m_{man\_des} R T_{man} \tag{6.5}$$

Where, T_{man} is the manifold temperature, assumed as constant, R is the gas constant of air, and V_{man} is the intake manifold volume.

A sliding surface control technique is designed to compute the throttle input (α) required to make the actual mass of air (m_{man_2}) of the ACC vehicle track the desired mass of air (m_{man_des}) in the intake manifold. The sliding variable can be defined as:

$$S_1 = m_{man_2} - m_{man\_des} \tag{6.6}$$

Differentiating Equation (6.6) one has

$$\dot{S}_1 = \dot{m}_{man_2} - \dot{m}_{man\_des} \tag{6.7}$$

According to Edwards and Spurgeon (1998) and Utkin (1999), the sliding mode control law has to satisfy the so-called 'reaching condition'.

$$\dot{S}_1 S_1 \leq -\eta_1 |S_1| \tag{6.8}$$

With η_1 positive constant. Equation (6.8) yields that a suitable choice of the control signal has to guarantee

$$\dot{S}_1 = -\eta \, \text{sgn}(S_1) \tag{6.9}$$

where η_1 is chosen to satisfy Equation (6.8), which automatically proves that the sliding manifold $S_1 = 0$ is reached in finite time (Edwards and Spurgeon, 1998). Then using Equation (6.7) and Equation (6.9) one can define the relation to determine the required throttle angle (α_2) for the ACC vehicle.

$$MAX \cdot TC(\alpha_2) \cdot PRI(man_2) = \dot{m}_{ao_2} + \dot{m}_{man\_des} - \eta_1 \, \text{sgn}(S_1) \tag{6.10}$$

In Equation (6.10) $\dot{m}_{man\_des}$ is obtained by numerical differencing. Once α_2 is computed, it is then applied to Equation (3.6) used for the ACC vehicle. If the desired torque computed by Equation (6.4) is negative then brake actuator is used to provide the necessary brake toque.

6.2.2 Brake Torque Calculations for Desired Acceleration

The desired brake torque (T_{bd}) used to track the desired acceleration can be obtained by re-arranging Equation (6.3), one has

$$T_{bd} = \frac{\left(T_{net} - \dfrac{J_e}{R_{g_2} R_d r_{eff}} \ddot{x}_{des} - C_d R_{g_2}^{\ 3} R_d^{\ 3} r_{eff}^{\ 3} \omega_{e_2}^{\ 2} - R_{g_2} R_d r_{eff} R_x\right)}{R_{g_2} R_d} \qquad (6.11)$$

Similar to the throttle control, the control design for the brake model is based on the standard sliding model control technique where the actual brake torque (T_{br_2}) is required to track the desired brake torque (T_{bd}) in order to place the ACC vehicle at correct position. The actual brake torque (T_{br_2}) is then applied to Equation (3.21) to reduce the speed of the ACC vehicle. T_{br_2} for the ACC vehicle can be expressed as:

$$\dot{T}_{br_2} = \frac{T_{bc} - T_{br_2}}{\tau_b} \qquad (6.12)$$

where, T_{bc} is the commanded brake toque, and τ_b is the time constant of the brake line and brake subsystem. Defining another sliding surface for the brake torque as:

$$S_2 = T_{br_2} - T_{bd} \qquad (6.13)$$

Differentiating Equation (6.13), one has

$$\dot{S}_2 = \dot{T}_{br_2} - \dot{T}_{bd} = \frac{T_{bc} - T_{br_2}}{\tau_b} - \dot{T}_{bd} \qquad (6.14)$$

According to Edwards and Spurgeon (1998) and Utkin , the sliding mode control law has to satisfy the so-called 'reaching condition'.

$$\dot{S}_2 S_2 \leq -\eta_2 |S_2| \qquad (6.15)$$

With η_2 positive constant. Equation (6.15) yields that a suitable choice of the control signal has to guarantee

$$\dot{S}_2 = -\eta_2 \operatorname{sgn}(S_2) \qquad (6.16)$$

According to Swaroop (1997) and Hedrick, *et al.* (1993) and using Equation (6.14) and Equation (6.16) for T_{bc}

$$T_{bc} = T_{br_2} + \tau_b(\dot{T}_{bd} - \eta_2(T_{br_2} - T_{bd})) \qquad (6.17)$$

In Equation (6.17), $\dot{T}_{bd}$ is obtained by numerical differentiation.

The necessary parameters of the vehicle model are listed in Table 6-1. The MPC controller parameters are the same as those in Table 5-1.

Engine displacement	V_d	0.0038 m³
Intake manifold volume	V_{man}	0.0027 m³
Manifold temperature	T_{man}	293 K
Engine moment of inertia	I_e	0.1454 kg.m²
Mass of the vehicle	m	1644 kg
Accessory torque	T_a	25 Nm
Effective tyre radius	r_{eff}	0.3 m
Wheel moment of inertia	I_w	2.8 kg.m²
Time delay	τ	0.5 s
Time constant of the brake line	τ_b	0.1 s
1st gear speed reduction ratio	R_1	0.3184
2nd gear speed reduction ratio	R_2	0.505
3rd gear speed reduction ratio	R_3	0.73
4th gear speed reduction ratio	R_4	1
5th gear speed reduction ratio	R_5	1.3157
Final drive speed reduction ratio	R_d	0.3257
Sliding mode constant for throttle input	η_1	0.05
Sliding mode constant for throttle input	η_2	0.025

Table 6-1   Vehicle and controller parameters

The simulations shown later in this chapter use a nonlinear longitudinal vehicle model that includes vehicle inertial and powertrain dynamics. The nonlinearities come from the engine and transmission models. The throttle and/or brake commands determined by the lower-level controller are sent to the vehicle longitudinal dynamics model to smoothly track the desired acceleration commands determined by the upper-level controller.

6.2.3 Lower-Level Controller Analysis

Before analysing the ACC vehicle response with respect to the preceding vehicle information, it is necessary to analyse the lower-level controller. In this analysis an arbitrary signal considered as desired control input ($\ddot{x}_{des}$) is applied to the lower-level controller. The lower-level control then computes the throttle and brake commands for the ACC vehicle model. The desired control input signal considered is a sinusoidal curve and can be defined by the expression.

$$\ddot{x}_{des} = K \sin(t) \tag{6.18}$$

where, K (K = 1) is the control input constant for sinusoidal curve and t is the time. Figure 6-2 shows the response of the ACC vehicle against sinusoidal input. It can be seen that the ACC vehicle closely follows the desired acceleration commands smoothly Figure 6-2(c). At t = 71 s the ACC vehicle has performed the gear transmission using the look-up table (Kulkarni *et al.*, 2006) explained in Chapter 3 (Section 3.4). This nonlinear behaviour of the transmission model can affect the upper-level controller performance, because the ACC vehicle acceleration is used in the error vector (**e**) (Equation (5.24)) between the two vehicles. These affects will be analysed in the later part of this chapter. The analysis in Figure 6-2 ensures that the lower-level control computes the required throttle and brake commands for the ACC vehicle and can be used for further detailed analysis of an ACC vehicle under critical TMs.
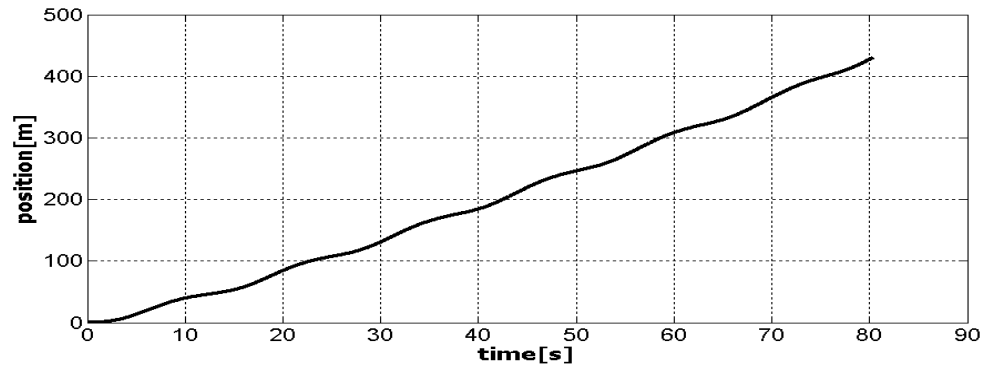
(a) Vehicle position
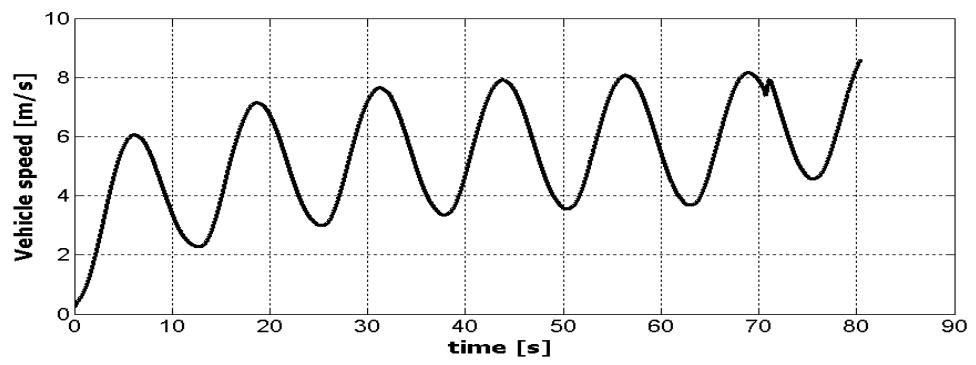
(b) Vehicle velocity
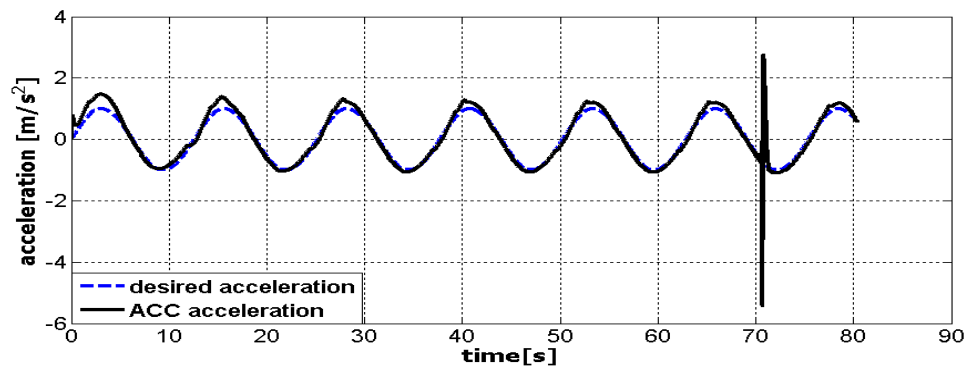
(c) Vehicle acceleration
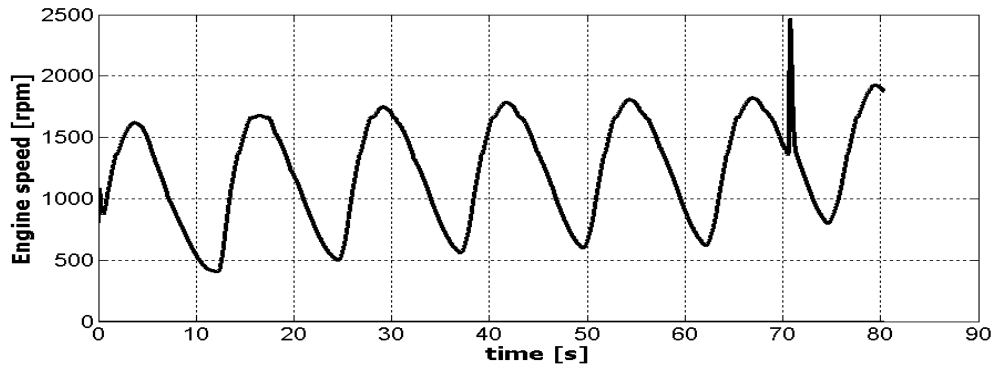
(d) Engine speed

Figure 6-2   ACC vehicle response for a sinusoidal input (desired acceleration)

6.3   Two-Vehicle System

Using Figure 5-3, the relative variables (range, safe inter-vehicle distance (SIVD)) between the two vehicles and longitudinal states of both vehicles are obtained by using Equation (3.24) (for both vehicles separately). The error vector (**e**) (Equation (5.24)) is then obtained which is used as the prediction model (Equation (5.27)) in the MPC control formulation. The optimal solution of the control input is computed using Equation (5.29), which is used to minimize the error vector (**e**) against the set-point trajectory which is set to zero value. The control input signal (Δu) is then applied to the first-order model (Equation (3.32)) and the output from this model is the desired acceleration commands ($\ddot{x}_{des}$). This entire process, receiving the preceding vehicle information and using the ACC vehicle information to compute the $\ddot{x}_{des}$, takes place in the upper-level controller. This desired acceleration commands ($\ddot{x}_{des}$) is applied to the lower-level controller which computes the desired throttle (α_2) and brake (T_{br_2}) commands for the ACC vehicle to track the desired acceleration ($\ddot{x}_{des}$). All details of the MPC controller formulation for the two-vehicle system are given in Section 5.3.1. It is important to mention here that some preliminary work based on this two-vehicle system was presented in Ali *et al.*, (2010). A similar encounter scenario (presented in Section 6.4.1) was used for the two-vehicle system (Ali *et al.*, 2010).

6.4   Simulation Results and Discussion

This section presents the simulation analyses of the complex ACC vehicle and its comparative discussion with the analyses carried out for the first-order ACC vehicle in Section 5.4. The complex ACC vehicle is analysed under the similar encounter scenarios as considered for the first-order ACC vehicle model in order to have a clear comparison between the two models. The control objectives for the complex ACC vehicle are same as for the first-order ACC vehicle i.e. to perform the critical TMs (under -0.5g deceleration limit) in order to establish and maintain the SIVD with the zero range-rate behind a newly detected slower or halt preceding vehicle. The TMs will be performed in the presence of acceleration (Equation (5.30)), states and collision avoidance constraints (Equation (5.32)) when the brake and engine actuators have limited allowable forces and may saturate. The aim of the comparison is to investigate the affects of complex vehicle's internal dynamics (engine, transmission, brake system) on performance of the MPC controller and the ACC vehicle itself. A wide range of situations have been considered which will be helpful to investigate an ACC vehicle's response and the MPC controller's robustness.

In this study, identical and non-identical ACC vehicle models with significant changes are considered. The term identical means during the analysis both vehicles are based on same parameters and the term non-identical means some parameters of the ACC vehicle are different from the preceding vehicle. For example, different set of gear ratios and different vehicle masses are considered for the ACC vehicle etc. It is also necessary to investigate how the MPC controller parameters influence the ACC vehicle response. The purpose and requirements for each analysis has been discussed in the beginning of each subsequent section.

6.4.1 Preceding Vehicle with Throttle Input of 70 Degrees

The following simulations have been carried out to evaluate the performance of the MPC controller and the complex vehicle model for a scenario where an ACC vehicle travelling at a speed of 30 m/s detects an accelerating preceding vehicle. In this scenario the complex ACC vehicle model has to decelerate from 30 m/s to the velocity of the preceding vehicle. The initial range between the two vehicles is 60 m.

The objective for the ACC vehicle is to establish the SIVD maintaining a zero-range-rate during the TM and avoiding the collision with the preceding vehicle under the presence of operational constraints i.e. obey the acceleration limits and avoid the collision with preceding vehicle . The initial velocity of the preceding vehicle is 10 m/s. In addition to the initial conditions for the position, velocity, and acceleration for the preceding vehicle and the ACC vehicle, the corresponding initial engine speed, throttle input, and gear ratio for the preceding vehicle are 1967 rpm, 70 degrees, 2nd gear, and for ACC vehicle are 4040 rpm, 70 degrees, and 5th gear, respectively.

The response of the ACC vehicle to the MPC controller is shown in Figure 6-3 where both vehicles are based on complex vehicle models. Vehicle positions (Figure 6-3(a)), velocities (Figure 6-3(b)), accelerations (Figure 6-3(c)), net torques (Figure 6-3(d)), mass of air in the intake manifold (Figure 6-3(e)), throttle inputs (Figure 6-3(f)), brake torque (Figure 6-3(g)), engine speeds (Figure 6-3(h)), range (Figure 6-3(i)), and gear shifting (Figure 6-3(j)) for the two vehicles have been plotted. The comparison between the preceding vehicle, desired input and the ACC vehicle responses shows the effects of throttle input, transmission gear shifting, and brake input and the switching between them in order to establish the desired SIVD and maintain the zero-range-rate between the preceding vehicle and the ACC vehicles.

The complex ACC vehicle has performed the higher deceleration manoeuvre under the deceleration limit of -4.9 m/s^2 as shown in Figure 6-3(c). Without the deceleration limits the ACC vehicle would have decelerated to -8.1 m/s^2 (Figure 5-4(c)). It should be noted that the deceleration limit is only applied within the MPC controller formulation and the vehicle actuators are strictly following it and controlling the inertia of the vehicle. This results show a very good coordination between the vehicle's sub-models and actuators.

The accelerating preceding vehicle starting from 10 m/s velocity and 2nd gear at 70 degree throttle input reaches up to 41 m/s (147.6 km/h) as shown in Figure 6-3(b). At this speed the operating gear ratio of the preceding vehicle is 4th gear (Figure 6-3(j)) and the throttle input is constant all the time. Figure 6-3 shows that the ACC vehicle has executed the TM successfully in the presence of acceleration limits and state constraints. At higher speed, the ACC vehicle detects an accelerating preceding

vehicle, and the control law gives the desired deceleration commands to the lower-level controller. In response to that, the lower-level controller generates a negative torque signal (Figure 6-3(d)) which implies a negative mass of air in the intake manifold (Figure 6-3(e)). The sliding-mode control based lower-level controller makes the actual mass of air in the intake manifold track the desired mass of air in the intake manifold with the physical limits applied on actual mass of air being a positive value which is in turn used to compute the throttle input (Figure 6-3(f)) for the ACC vehicle. The brake torque, corresponding to the desired deceleration, has also been simulated in Figure 6-3(g) to decelerate the ACC vehicle.

The brake torque is applied on the wheel model which reduces the speed of the ACC vehicle. At this speed, and due to lower throttle input, the transmission down-shifting takes place from 5th to 2nd gear (Figure 6-3(j)) and the ACC vehicle, with collision avoidance constraint, establishes the zero-range-rate with the preceding vehicle by performing the transmission up-shifting from 2nd to 3rd and from 3rd to 4th and maintains the steady-state operation for the rest of the 50 s simulation.

(a) Vehicle positions

(b) Vehicle velocities

179
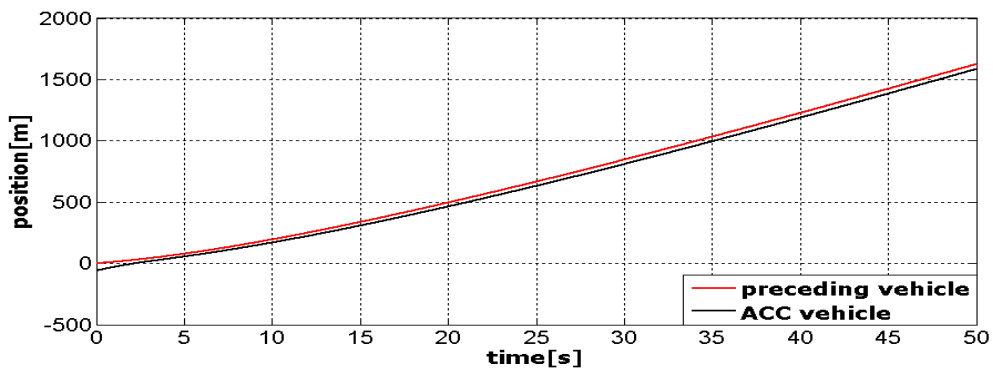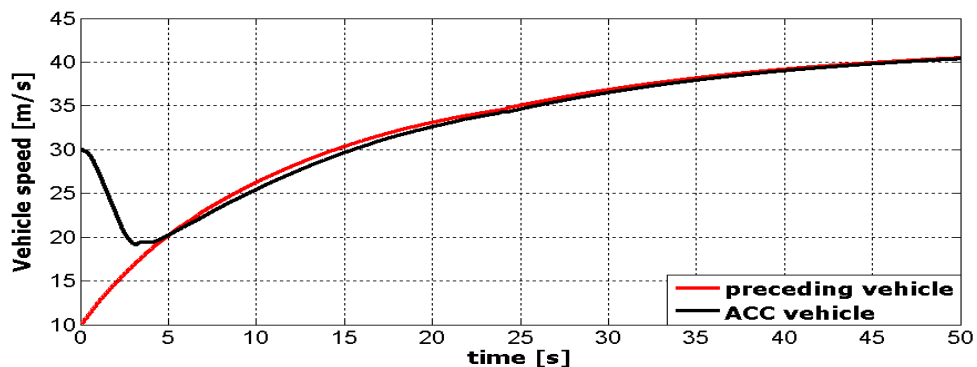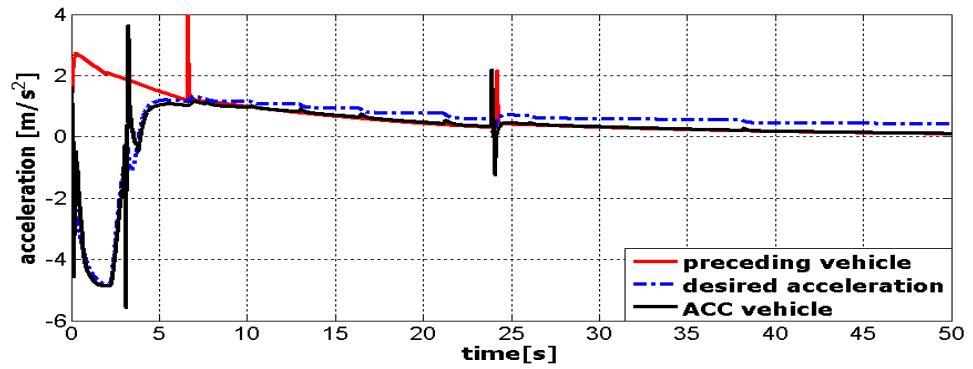
(c) Vehicle accelerations

(d) Net torque
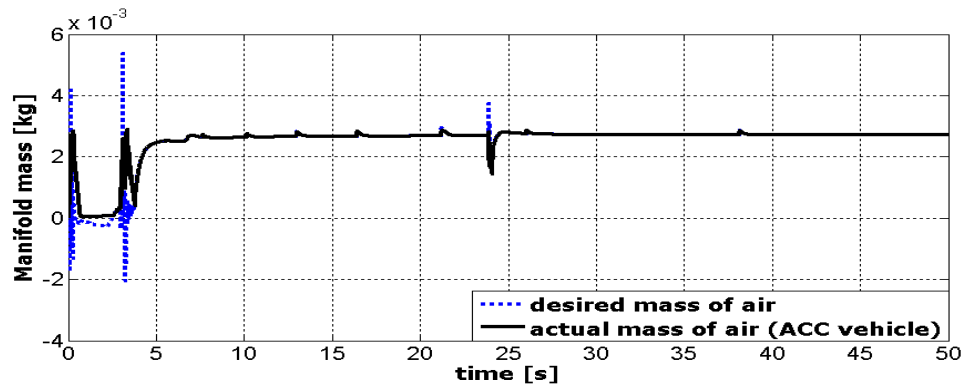
(e) Mass of air in the intake manifold
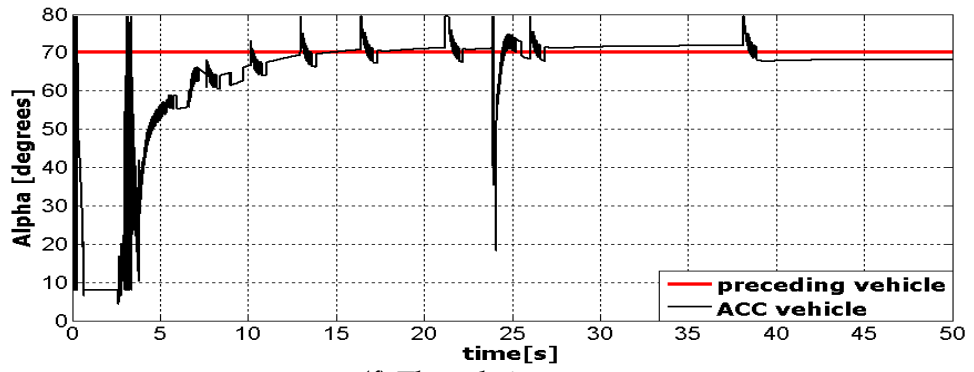
(f) Throttle input
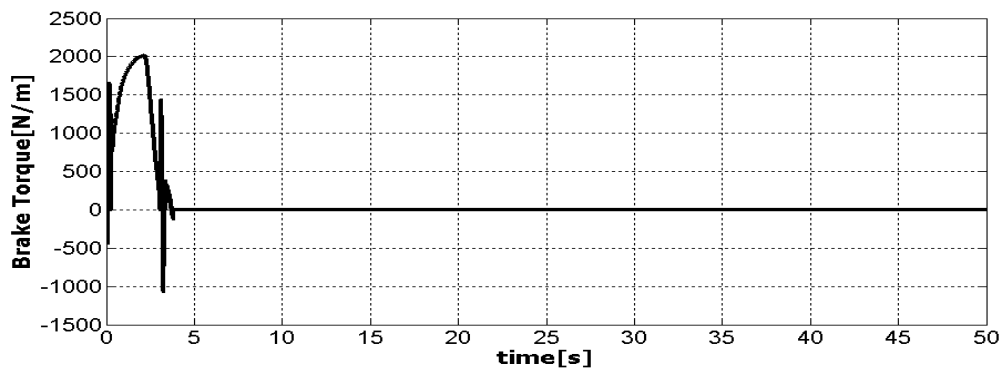
(g) Brake torque
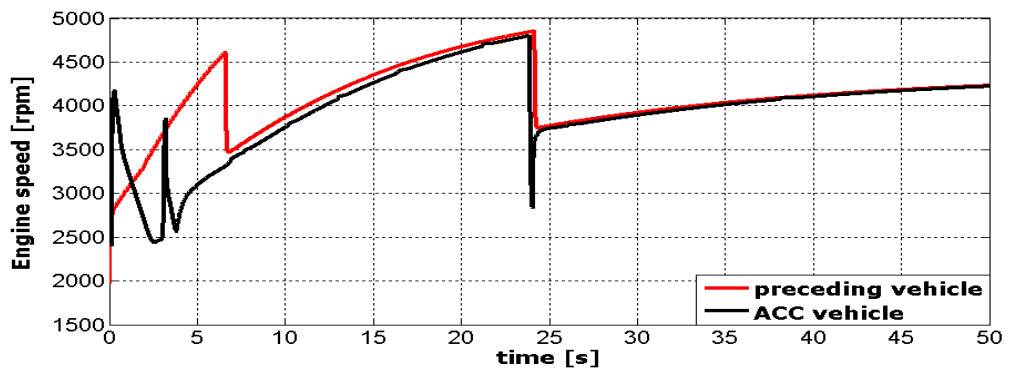
(h) Engine speed
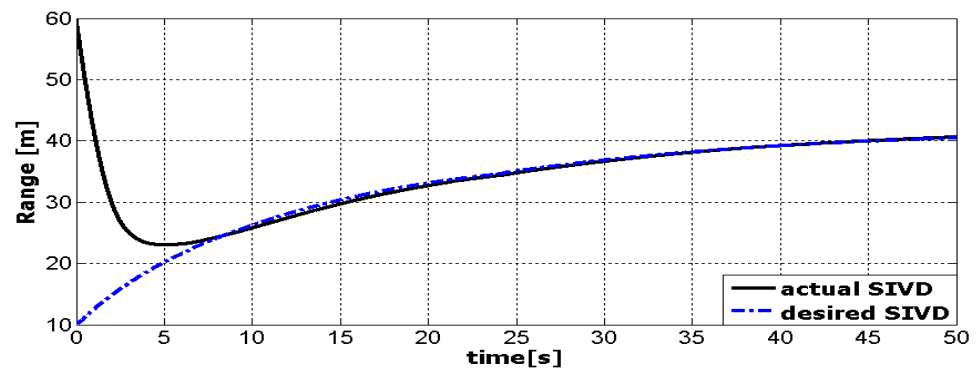
(i) Range
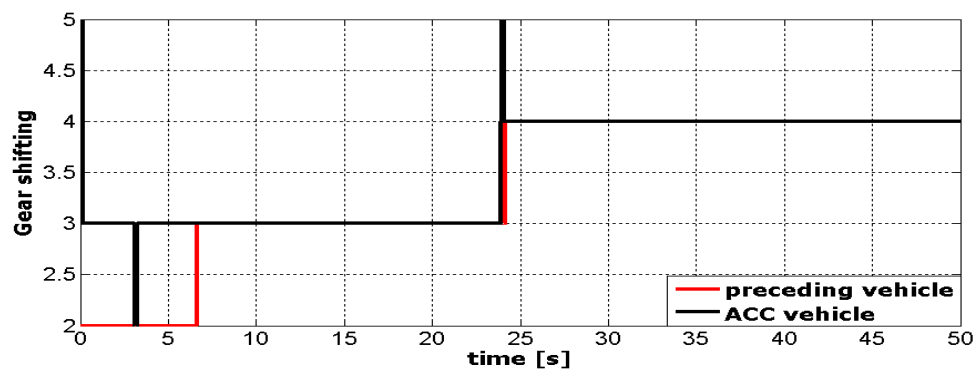
(j) Gear shifting

Figure 6-3   Response of ACC vehicle to the TM described in Section 6.4.1

Once in the vehicle following mode, the ACC vehicle also accelerates following the preceding vehicle with a desired SIVD (Figure 6-3(i)) and maintains the throttle input to 70 degrees (Figure 6-3(f)) and travels in the 4th gear to maintain the same velocity. At the maximum deceleration i.e. -4.9 m/s² the corresponding brake torque is 2000 Nm. Once the TM is completed, the acceleration tends to become zero (Figure 6-3(c)) which results in the net torque of the ACC vehicle following the net torque of preceding vehicle (Figure 6-3(d)). The brake torque (Figure 6-3(g)) becomes zero as no braking is required; the mass of the air in the intake manifold tracks the desired mass of air (Figure 6-3(e)). The effect of the transmission gear shifting, during the TM, on the engine speed is shown in Figure 6-3(h).

It is also evident from Figure 6-3(i) that the range between the two vehicles follows the desired SIVD. The SIVD is the function of preceding vehicle's velocity (Section 5.3.1). The engine speed of the ACC vehicle is initially reduced and for the first 4.6 s

it is subjected to down shifting due to lower throttle input and higher brake torque. As the TM is completed the engine speed increases smoothly tracking the engine speed of the preceding vehicle for the rest of the simulation time. The simulations in Figure 6-3 show good coordination between all the sub-models and the controllers and demonstrate a safe execution of the TM.

The response of the ACC vehicle, simulated in Figure 6-3, shows that the MPC control algorithm developed for the upper-level controller can be used for the lower-level controller and the complex ACC vehicle model. The complex ACC vehicle has successfully performed the TM within the constrained boundaries. It has been observed that during the transitional operation the ACC vehicle has strictly obeyed the physical constraints applied within the upper-level controller algorithm. Operating within the constraint boundaries while the constraints are only applied to the controller is an interesting behaviour of the ACC vehicle revealed in this analysis. The effects of transmission gear shifting on the desired acceleration and ACC vehicle acceleration (Figure 6-3(c)) has also been noticed. It has been observed that MPC control method is robust enough to cope with dynamic effects and achieves the required tasks (Section 5.1) using the complex vehicle model as well.

For the purpose of validation Figure 6-3 results have been compared with Figure 5-4 which shows the similar scenario. During the transient and steady-state operation the complex ACC vehicle response is similar to the first-order ACC vehicle response; comparing Figure 5-4(a) with Figure 6-3(b) for vehicle speeds, Figure 5-4(b) with Figure 6-3(a) for vehicle positions, Figure 5-4(c) with Figure 6-3(c) for vehicle acceleration, Figure 5-4(d) with Figure 6-3 (i) for the range. The acceleration of complex ACC vehicle (Figure 6-3(c)) shows the effects of engine and transmission dynamics which were not included in first-order vehicle model. This comparison is used for the validation of the results produced for the complex ACC vehicle. The remaining parts of Figure 6-3 show the corresponding internal complex behaviour of the vehicle's sub-models.

In the subsequent sections the ACC vehicle has been analysed for different situations which gives more confidence towards the robustness of the entire system.

6.4.2 Preceding Vehicle with Throttle Input of 50 Degrees

In Section 6.4.1, the throttle input for the preceding vehicle was 70 degrees and it has been observed that the ACC vehicle has performed the required TM successfully while tracking the desired SIVD. ACC vehicle is obeying the deceleration limit which is applied in the upper-level controller formulation and avoiding the collision with the preceding vehicle. It is important to investigate the ACC vehicle response against a different SIVD. As the SIVD is the function of preceding vehicle velocity which is in turn depends upon the throttle input, therefore, the throttle input to the preceding vehicle is varied to get a different desired SIVD. In order to examine the robustness of the controller, the throttle input to the preceding vehicle is changed to 50 degrees while the rest of the parameters and the encounter scenario are same as in Section 6.4.1.

Figure 6-4 shows the response of the ACC vehicle for a different throttle input of 50 degrees to the preceding vehicle. The similar plots for vehicle positions (Figure 6-4(a)), velocities (Figure 6-4(b)), accelerations (Figure 6-4(c)), net torques (Figure 6-4(d)), mass of air in the intake manifold (Figure 6-4(e)), throttle inputs (Figure 6-4(f)), brake torques (Figure 6-4(g)), engine speeds (Figure 6-4(h)), range (Figure 6-4(i)), and gear shifting (Figure 6-4(j)) for the two vehicles have been simulated again to analyse the behaviour of the ACC vehicle. It has been noticed that the ACC vehicle is smoothly following the preceding vehicle with a new desired SIVD and in all plots the ACC vehicle shows a very good agreement with the preceding vehicle's states during the steady-state operation. The throttle input computed for the ACC vehicle is exactly the same as for the preceding vehicle, i.e. 50 degree. The overall observations are same as what have been observed in the Section 6.4.1. The results produced in Figure 6-4 have been validated against Figure 5-4 (first-order ACC vehicle) as the simulation scenario is same. It can be observed that the complex ACC vehicle is achieving the required control objectives with the evidence that the ACC vehicle is tracking the desired SIVD Figure 6-4(i).

The difference between the scenarios considered in Section 6.4.1 and in this section is that the ACC vehicle has to follow different SIVDs during the steady-state operation (see Figure 6-3(i) and Figure 6-4(i)). Another important difference found is the gear shifting pattern. One can see in Figure 6-4(j) that the ACC vehicle is

operating in the 3rd gear during the steady-state operation, which means no disturbance in the throttle input (Figure 6-4(f)). Whereas, in Section 6.4.1, due to the higher throttle input (70 degrees) the ACC vehicle has performed gear transmission from 3rd to 4th gear Figure 6-3(j). This gear up-shifting has created disturbance in desired acceleration (Figure 6-3(c)) computed by the upper-level controller which in turns affects the throttle input (Figure 6-3(f)) for the ACC vehicle.
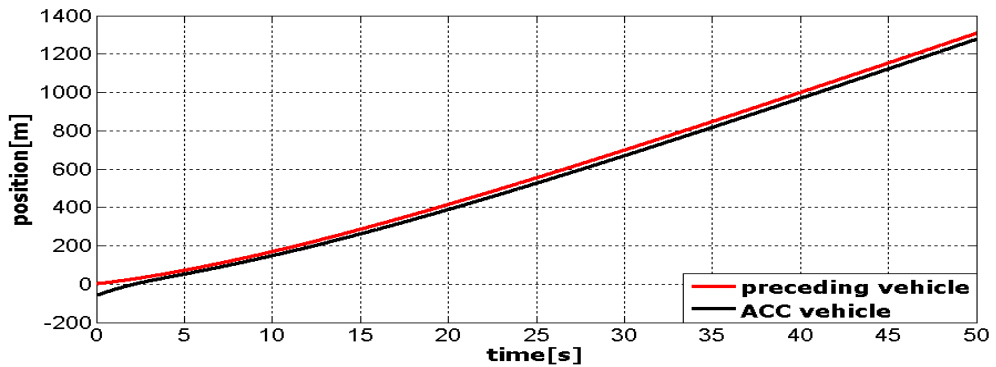

(a) Vehicle positions
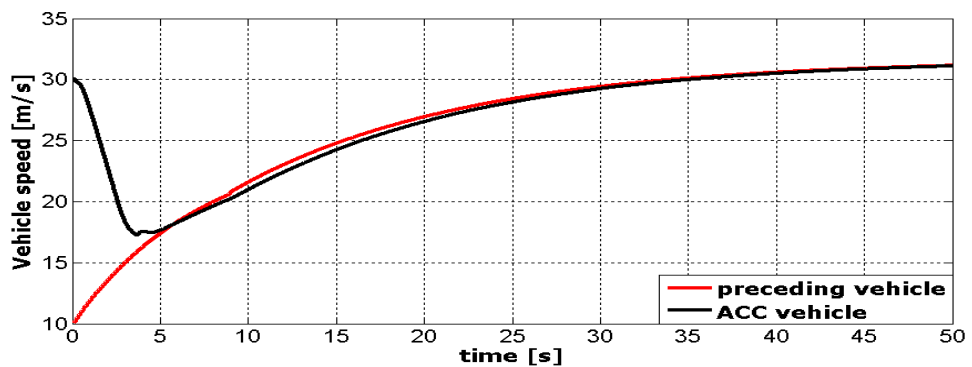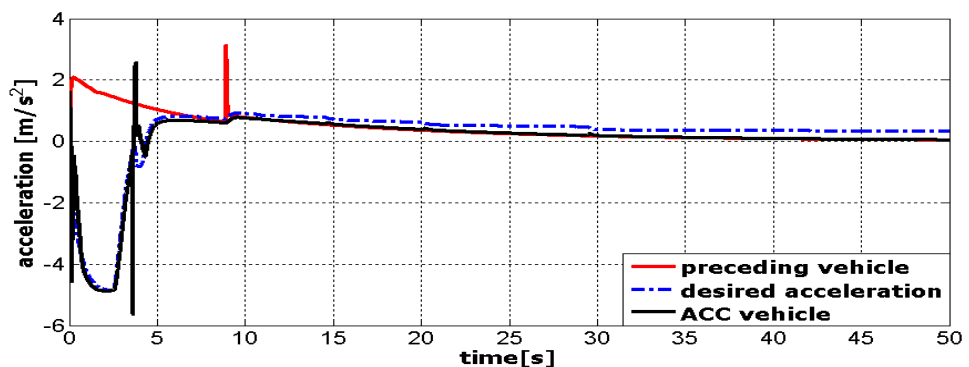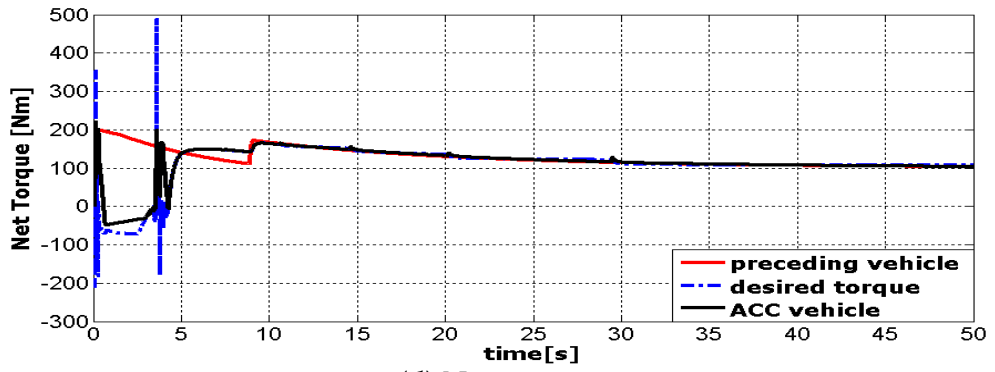
(b) Vehicle velocities

(c) Vehicle accelerations

185

(d) Net torque
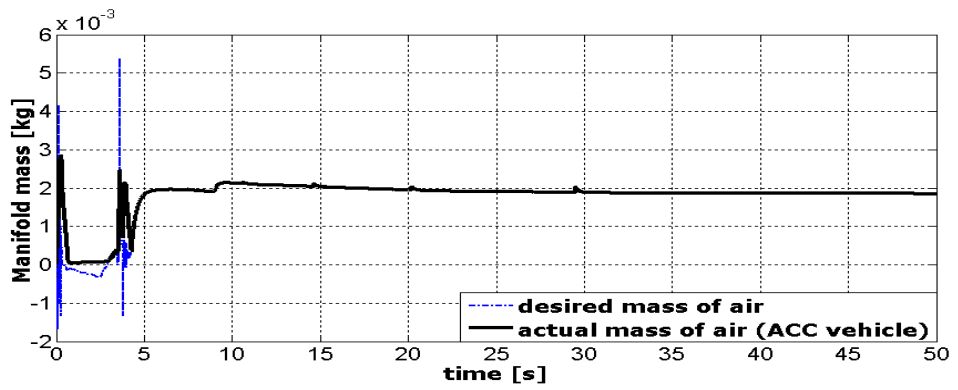
(e) Mass of air in the intake manifold
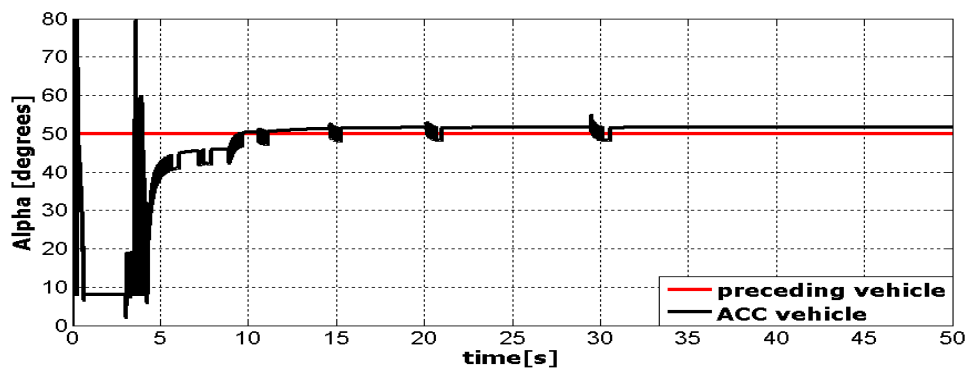
(f) Throttle input
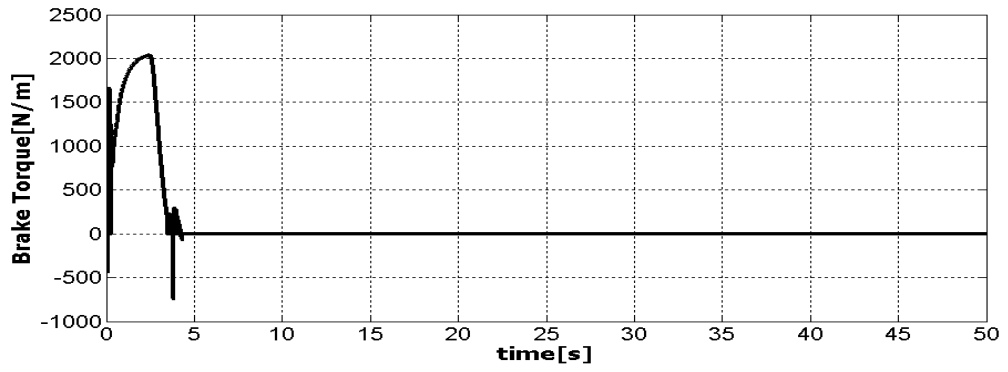
(g) Brake torque
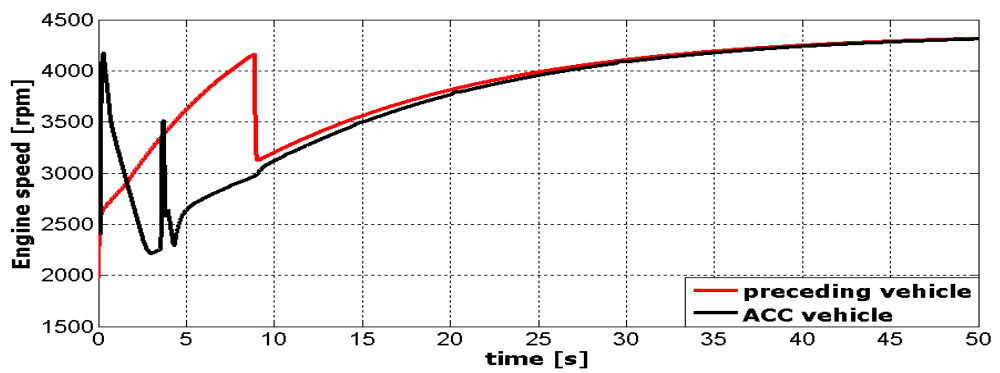
(h) Engine speed
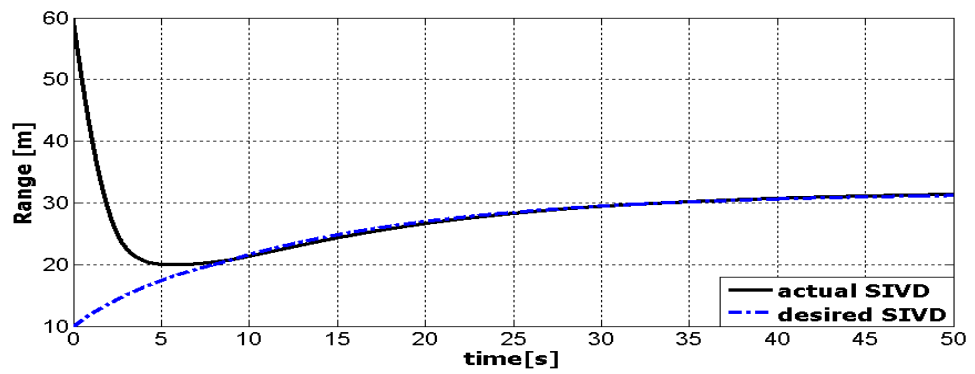
(i) Range
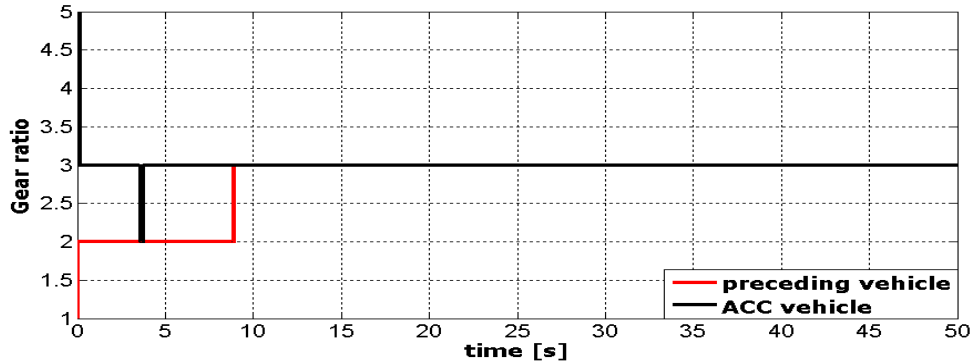
(j) Gear shifting

Figure 6-4   Response of ACC vehicle to the TM described in Section 6.4.2

6.4.3 Parametric and Sensitivity Analyses

In Chapter 5, a sensitivity analysis of the first-order ACC vehicle model was carried out for different initial ranges, different lengths of control horizon (N_C), and different values of control input cost weighting (**R**). It has been examined how the variation in these parameters affects the first-order ACC vehicle model. For example, it was found that with the higher values of **R** the control is tight control, with higher control horizon (N_C) the control input energy is distributed over a longer period of future time which causes instability in the system, and the system can be stabilized by using the higher values of **R**. The complex vehicle dynamics during the TM were not considered in that stability analysis. It is, therefore, necessary to analyse the ACC vehicle behaviour under these parametric changes when a complex longitudinal dynamic model is used for the ACC vehicle. It is necessary to analyse how these parametric changes would affect the engine dynamics, transmission gear shifting (up-shifting or down-shifting), throttle input, brake input, etc.

6.4.3.1   Sensitivity analysis for different values of control horizon (N_C)

The length of the control horizon (N_C) is defined as after a certain interval (number of instants in future time) there should be no variation in the future control signal (Camacho and Bordons, 2004). N_C considered in this study is 3 samples. In this section the complex ACC vehicle is analysed for two different lengths of N_C: 5

188

samples and 10 samples. The corresponding effects on engine and transmission dynamics have been noticed because the desired control input is distributed over a longer period of future time. In Figure 6-5, N_C = 5 samples and **R** =1 have been used, and it has been noticed that due to the distribution of the control input energy the engine dynamics (Figure 6-5(d)) is severely affected causing a delayed response from the engine model during the transitional operation. It has also been noticed that the transmission down-shifting and up-shifting has also been delayed and during the transitional operation the range between the two vehicles is reduced to less than 10 m which is a quite dangerous and can lead to severe consequences. The response of the ACC vehicle during the steady state operation is unaffected as the ACC vehicle is maintaining the desired SIVD (Figure 6-5(e)). In order to overcome all these shortcomings caused by a higher value of N_C different values of **R** have been used. It has been found that using **R** = 5 stabilizes the ACC vehicle response during the transitional operation. Because the higher value of **R** penalizes the control input signal which restores the ACC vehicle response. The engine response has been significantly improved and the transmission down-shifting and up-shifting is taking place when required (when compared to the Figure 6-4). It has been investigated from this analysis that variation in MPC control parameter N_C has significant effect on the overall performance of the ACC vehicle. It was also found that performance of the ACC vehicle in this condition can be improved by using a higher value of control input cost weighting (**R**). For the situation considered **R** = 5 is a suitable value which can be observed in Figure 6-5.
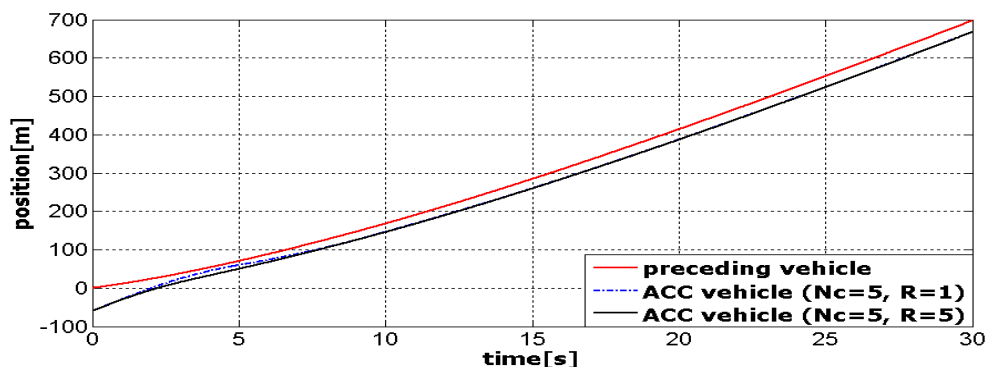

(a) Vehicle positions
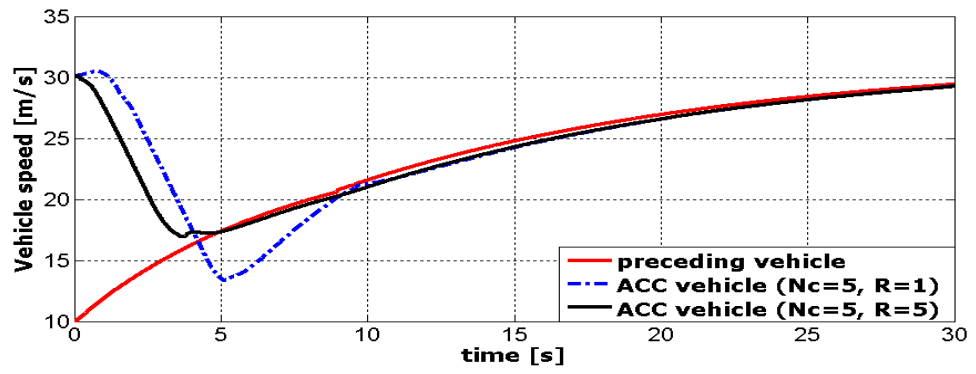
(b) Vehicle velocities
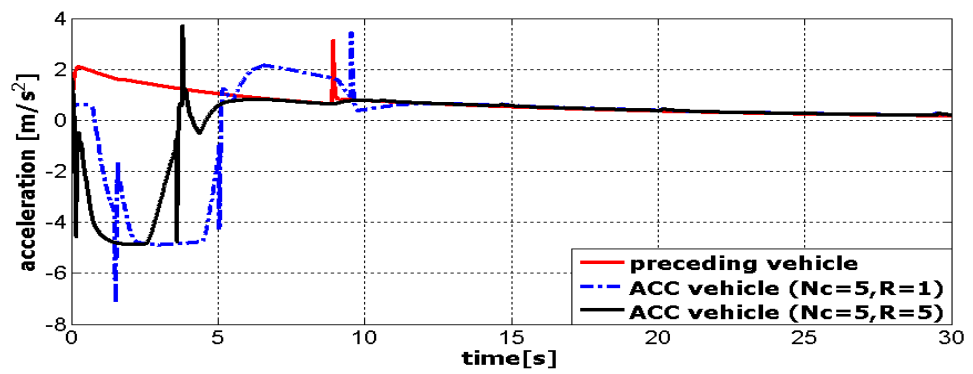
(c) Vehicle acceleration
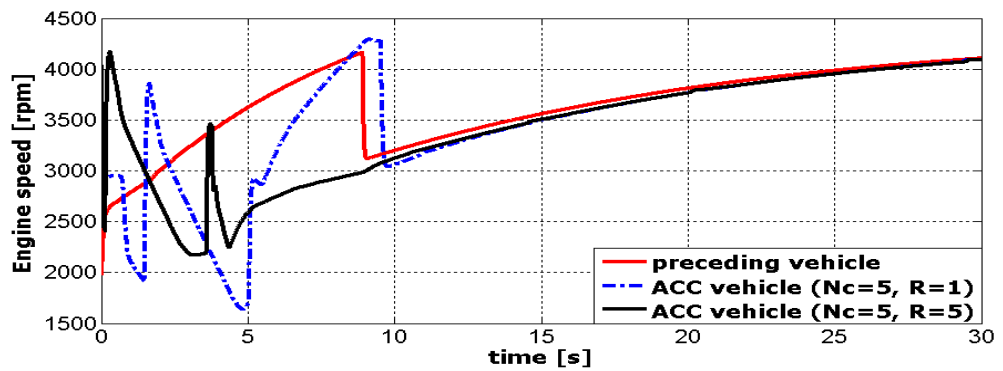
(d) Engine speed
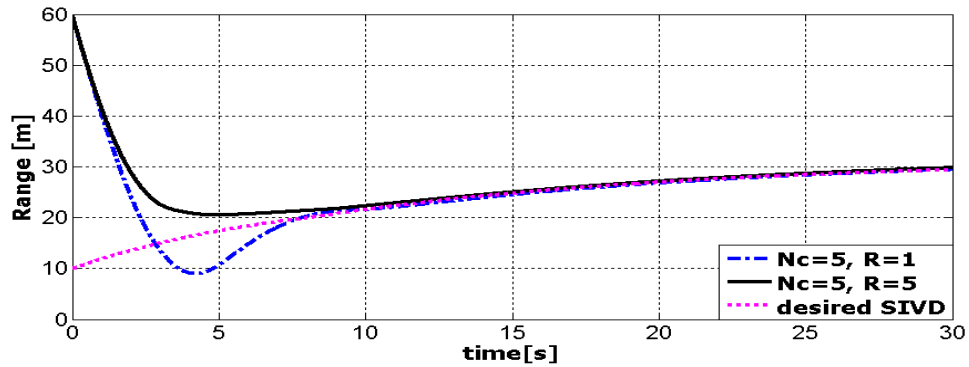
(e) Range

Figure 6-5   Response of ACC vehicle for N_C = 5 and different values of $\mathbf{R}$

The simulation results of Figure 6-5 have been validated against Figure 5-10 under the same situation. It is clear from the comparison the complex ACC vehicle shows a similar response when the length of N_C was increased by the same number. Using the complex ACC vehicle model also shows the effects of N_C length on the vehicle sub-models and how the sub-model's dynamics is affected by these parameters changes.

The sensitivity analysis of the ACC vehicle has also been carried now for N_C = 10 samples. Initially, the control input cost weighting function ($\mathbf{R}$) is assumed as 1. N_C = 10 samples means that the control input energy is distributed for 10 future sampling instants (where each time step is 0.1 s). The simulation results show that due to a higher value of N_C the ACC vehicle response is getting worse than the previous condition (N_C = 5 samples). The range between the two vehicles is getting very small and it may cause a collision with the preceding vehicle (Figure 6-6(a)). The ACC vehicle is initially accelerating (Figure 6-6(c)) due to the acceleration commands computed by the MPC control law, whereas it should initially decelerate to avoid the collision. The engine and transmission dynamics have also been disturbed (Figure 6-6(d)) and it takes longer to achieve the steady state operation. Again to overcome these problems different higher values of $\mathbf{R}$ has been used and it has been determined that using $\mathbf{R}$ = 8 ACC vehicle achieves the desired control objectives and perform the TM successfully by establishing a SIVD with zero range-rate. After using different higher values of N_C it can be concluded that higher the length of N_C higher the instability in the response of the ACC vehicle and in order to

191

restore the response of the ACC vehicle a higher value of **R** is required. The restored behaviour of the complex ACC vehicle can be compared with Figure 6-4 to examine the stability of the ACC vehicle.
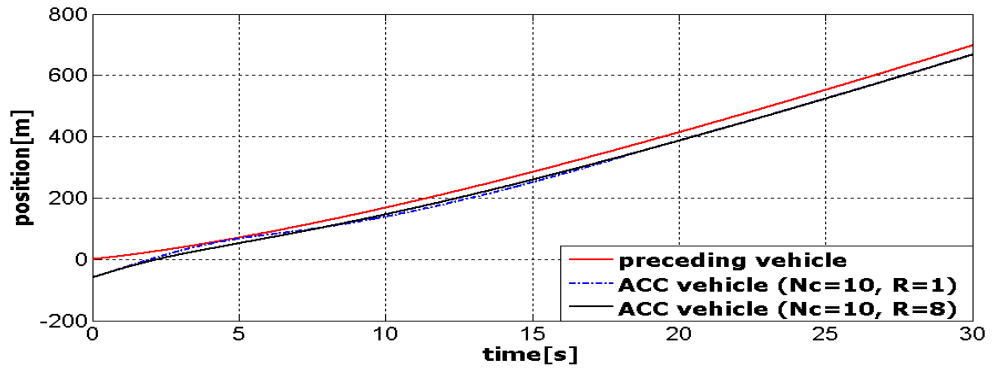

(a) Vehicle positions
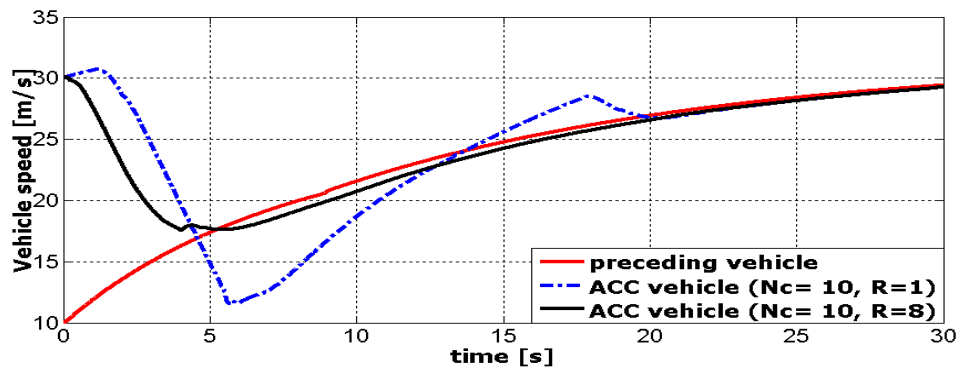
(b) Vehicle velocities
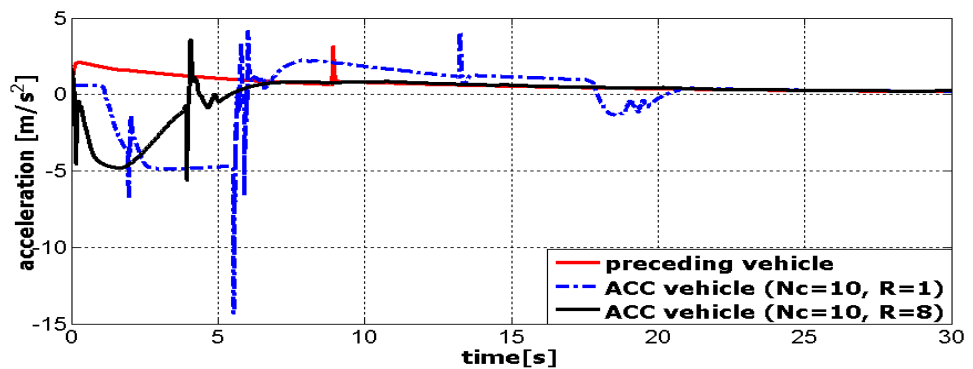
(c) Vehicle accelerations
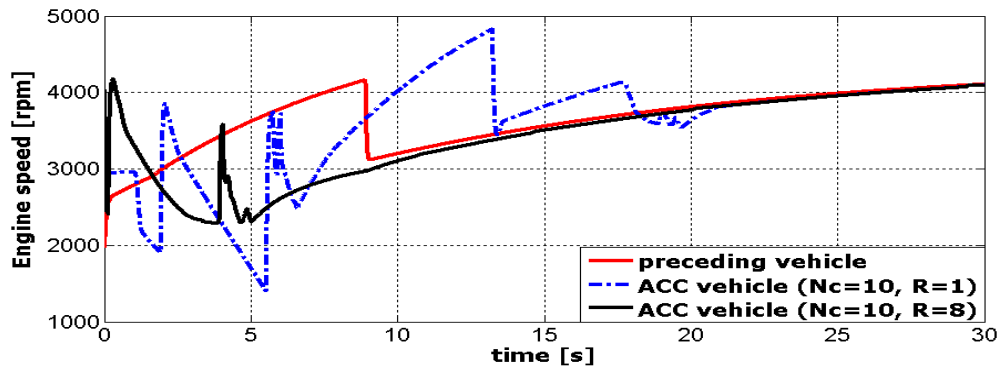
(d) Engine speed
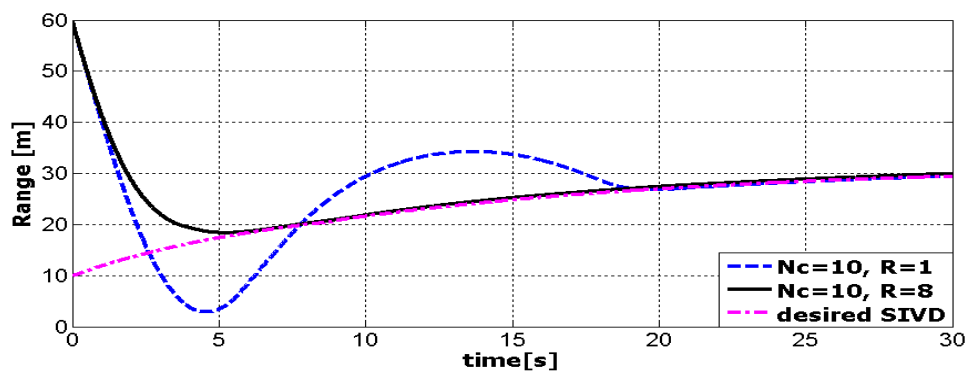
(e) Range

Figure 6-6   Response of ACC vehicle for N_C = 10 and different values of **R**

6.4.3.2   Sensitivity analysis for different control input cost weighting coefficient (R)

In this section the sensitivity of the ACC has been analysed for different values of control input cost weighting (**R**). The main purpose of this analysis is to analyse how the ACC vehicle will response for different values of **R** and how its values affects the engine and transmission dynamics. Two different values of R other than 1 are used for the sensitivity analysis purpose; **R** = 0.1 and **R** = 20. The lower value of **R** represents a looser control and the higher value of **R** represents a tighter control. Results for different values of **R** have been shown in Figure 6-7; in the case of lower value the ACC vehicle response shows a higher disturbance in the ACC vehicle's response. The ACC vehicle is unable to establish a SIVD (Figure 6-7(e)) and cannot setup a zero range-rate (Figure 6-7(b)). Figure 6-7(c) shows that the ACC vehicle is able to maintain the deceleration limit (-0.5g) but it cannot avoid the collision with the preceding vehicle. The engine and transmission response (Figure

6-7(d)) are not catching up with the preceding vehicle response at all. Figure 6-7(e) shows that during the transitional operation the ACC vehicle has collided with the preceding vehicle and during the steady-state operation it is travelling far behind the preceding vehicle. This analysis with lower value of **R** (**R** = 0.1) shows the computed control input signal is not enough to control the dynamic behaviour of the ACC vehicle.

In the case of higher **R**=20 value the ACC vehicle response is quite satisfactory. It has been precisely observed that during the transitional and steady-state operation the response of the ACC vehicle has not been delayed but has been prolonged. This is because of the higher influence of the cost weighting on the optimal control input. The ACC vehicle can successfully perform the TM and can achieve the desired control objectives. The analysis carried out in this section shows that a lower value of **R** (**R** < 1) for input is not suitable for the ACC vehicle at all when using the MPC control algorithm, however, a higher value up to 20 can be used for the ACC vehicle in order to improve the performance of the ACC vehicle.
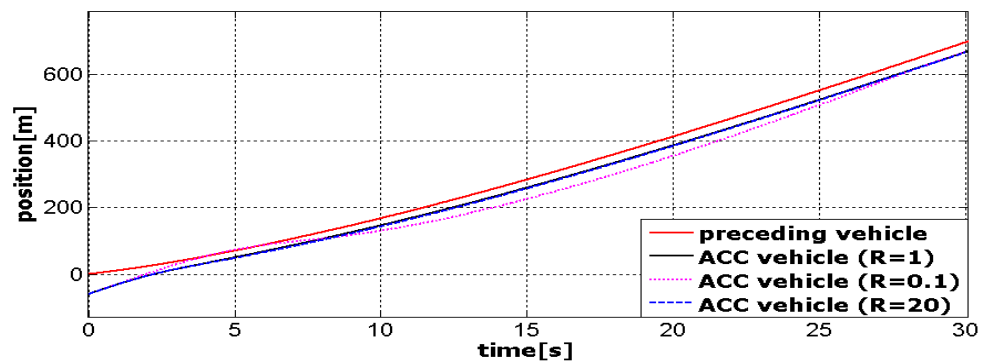

(a) Vehicle positions

(b) Vehicle velocities

194
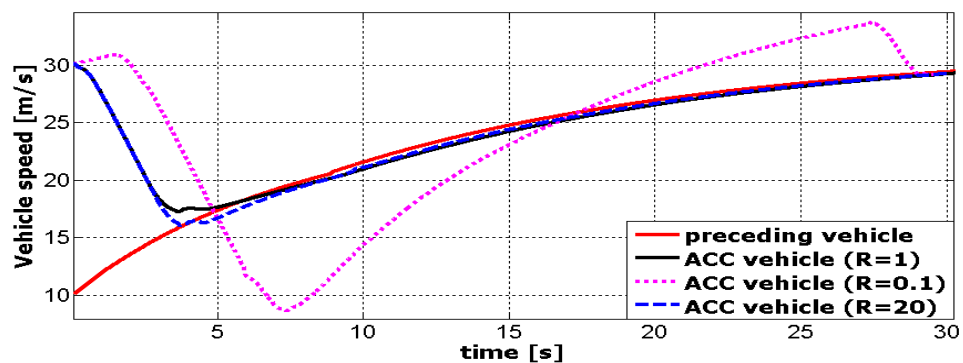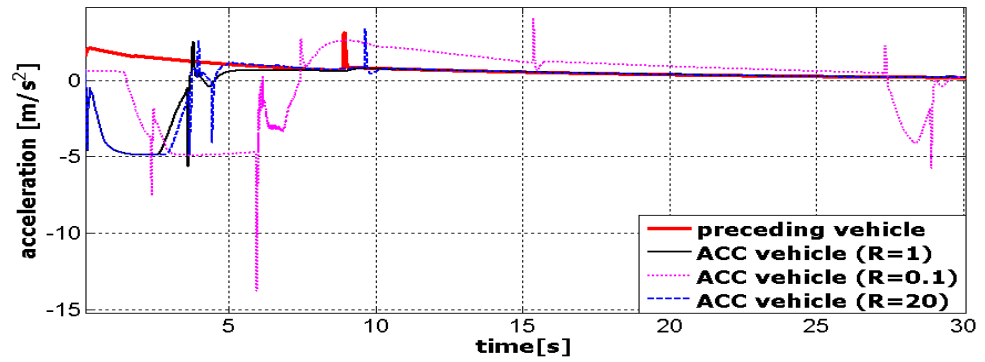
(c) Vehicle accelerations
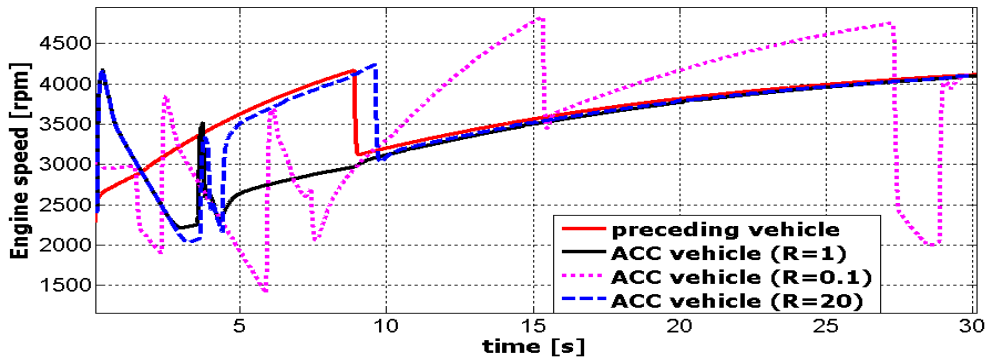
(d) Engine speed
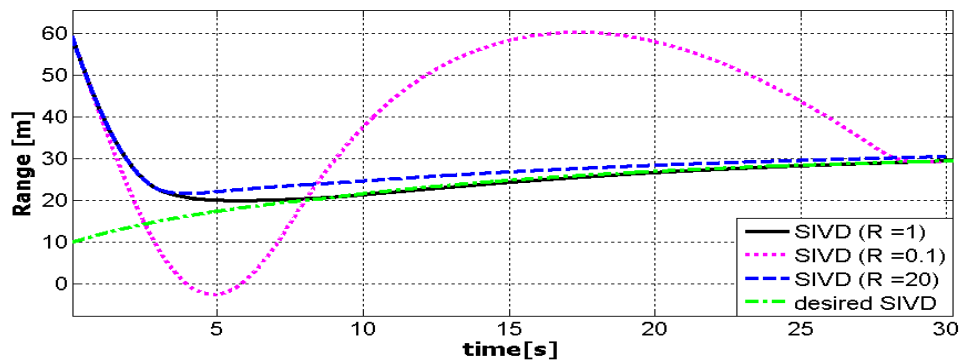
(e) Range

Figure 6-7   Response of ACC vehicle for different values of **R**

195

6.4.3.3 ACC vehicle analysis for different vehicle masses

The dynamic response of the vehicle can be greatly influenced by variation in the mass of the vehicle. For example, various numbers of passengers, different sizes of the engine, different models, etc can vary the inertia of a vehicle. This can possibly affect the controller performance and in turn affect the ACC vehicle performance. Therefore, it is essential to investigate the ACC vehicle's response for different values of mass. In this section the ACC vehicle analysis has been carried out for different vehicle masses while rest of the model and its parameters are same. The vehicle mass for both vehicles considered in this study is 1644 kg. In this analysis the preceding vehicle's mass remains the same while for the ACC vehicle masses chosen are 1400 kg, 1800 kg, and 2000 kg. The results obtained from these changes have been compared with the actual mass considered, i.e. 1644 kg.

The encounter scenario between the two vehicles is same as used in Figure 6-4. Figure 6-8 shows the ACC vehicle analysis for different masses and the comparison shows that the ACC vehicle's response is hardly affected by the mass variations. The ACC vehicle's position, longitudinal speed, acceleration, engine speed, and the range between the two vehicles have been simulated. This comparison shows that MPC control method is robust enough to cope with mass variations of the ACC vehicle and can be used for a complex ACC vehicle model analysis.
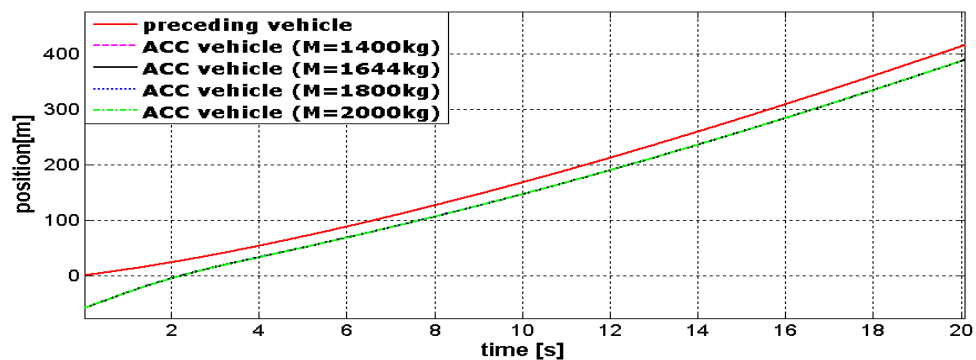
(a) Vehicle positions
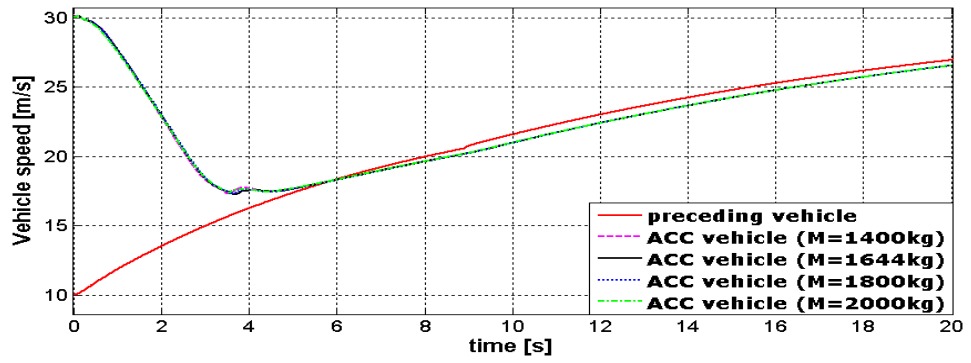
(b) Vehicle velocities
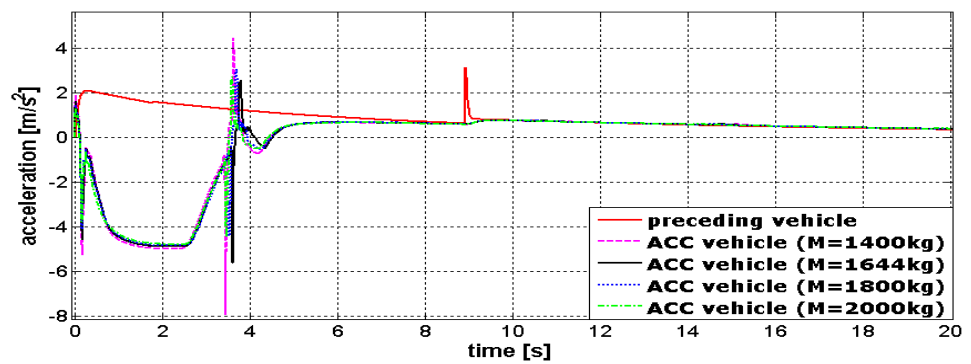
(c) Vehicle accelerations
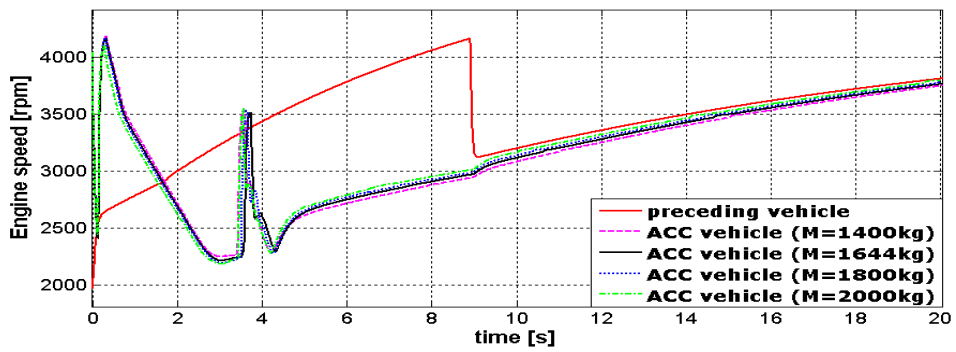
(d) Engine speed
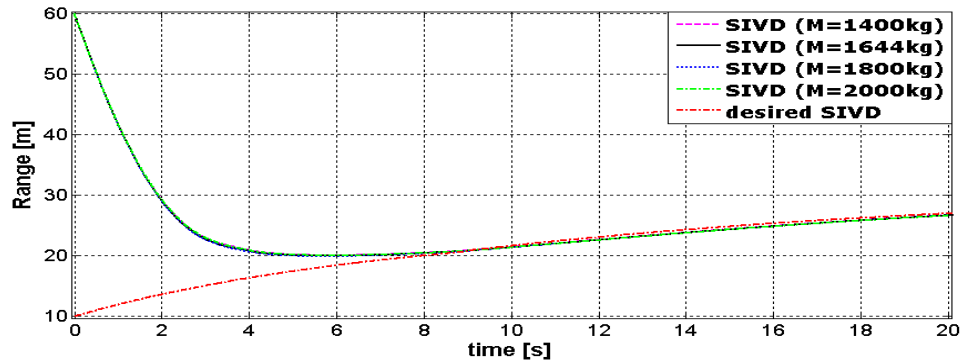
(e) Range

Figure 6-8   Response of the ACC vehicle for different ACC vehicle mass.

6.4.3.4   ACC vehicle analysis for different values of headway time (*h*)

One of the main objectives for the ACC vehicle is to maintain a SIVD behind the preceding vehicle. The SIVD varies linearly with the velocity of the preceding vehicle such that the headway time (*h*) between the vehicles remains constant. The headway time can be significantly influenced by road gradient (uphill or downhill), by the gust of air, by the weather conditions (raining, snow fall), by the road conditions, error in the radar sensor, etc. It is also necessary to investigate the ACC vehicle performance for different values of headway time (*h*).

In this section the sensitivity analysis of the ACC vehicle has been carried out for different headway times (*h*). The headway time (*h*) assumed in this study is 1 s and other values assumed for *h* are 0.5 s and 1.5 s. It can be seen from Figure 6-9 that variation in *h* has greatly affected the response of the ACC vehicle. In the case of *h* = 0.5 s the ACC vehicle picks up the preceding vehicle quicker (Figure 6-9(b)) than for *h* = 1 s, and the range between the two vehicles has also significantly reduced (Figure 6-9(d)). This means that the distance between the two vehicles is not sufficient to avoid a collision if a severe emergency occurs. On the contrary, in the case of *h* = 1.5 s it takes longer for the ACC vehicle to reach the preceding vehicle velocity (Figure 6-9(b)), resulting a delayed response and a higher range (Figure 6-9(d)) between the two vehicles. It can be observed that the higher *h* value significantly delays the engine, transmission and brake responses and the ACC vehicle will no longer respond quickly to any emergency situation. Also due to higher range between the two vehicles another vehicle can jump in the spacing

between the two vehicles. Due to this the link between the two vehicles will be interrupted and at this point this new vehicle will become the new preceding vehicle for the ACC vehicle. A similar scenario has been considered in the next section to investigate the ACC vehicle's response under the step input.
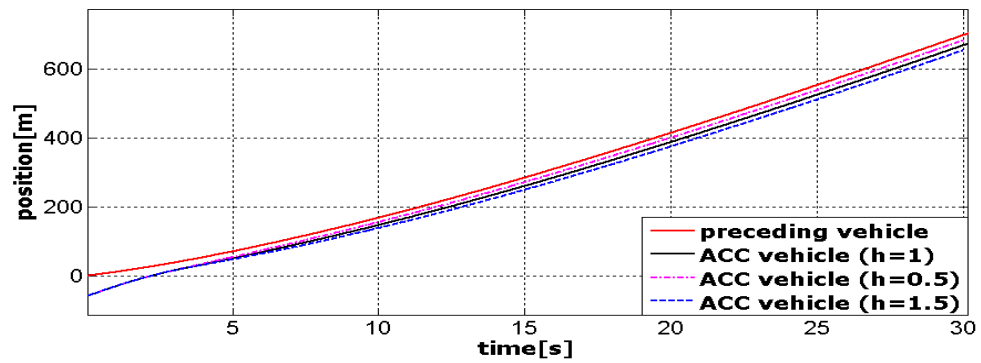
(a) Vehicle positions
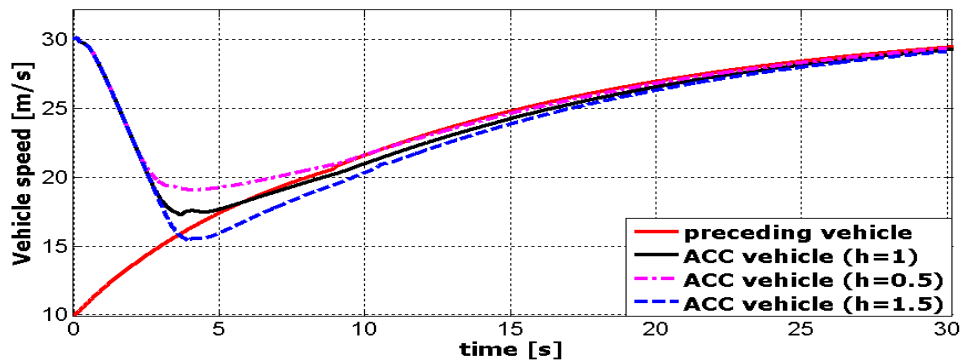
(b) Vehicle velocities
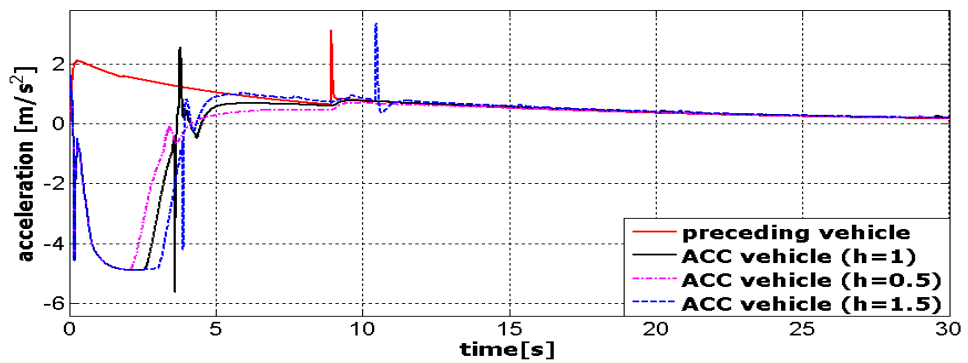
(c) Vehicle accelerations
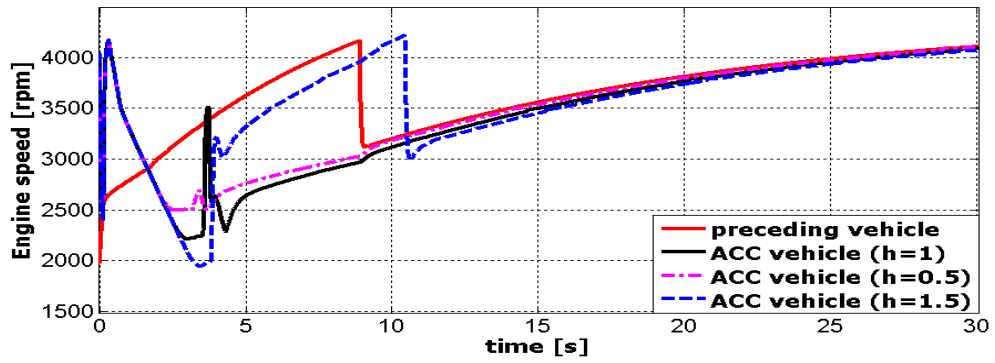
(d) Engine speed
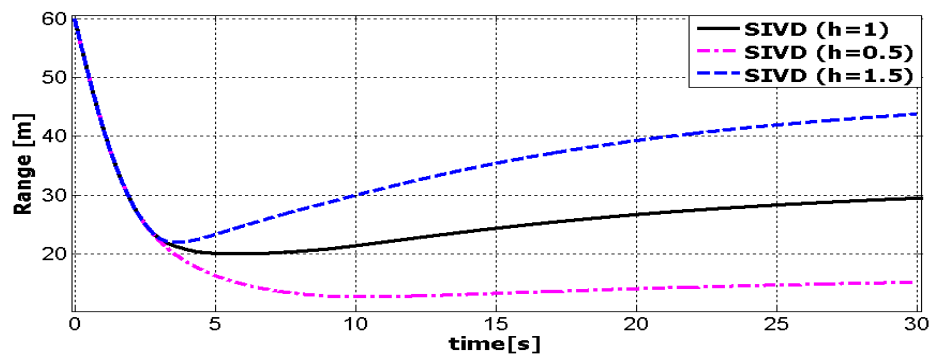
(e) Range

Figure 6-9   Response of the ACC vehicle for different headway times (*h*).

6.4.3.5   A vehicle coming in between (cut-in) the vehicles during the ACC vehicle's spacing following mode

In this section a scenario has been considered where another vehicle comes between the two vehicles while the ACC vehicle operating in the vehicle following mode during steady state operation, Figure 6-10. The purpose of this scenario is to apply a sudden disturbance (step input) to the ACC vehicle.
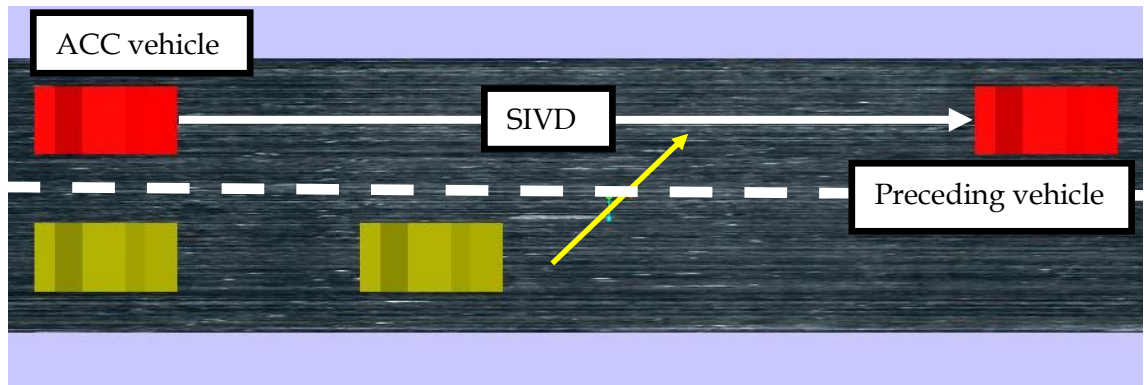
Figure 6-10   Another vehicle coming in between the two vehicles

The scenario considered is at t = 20 s the SIVD between two vehicles is 26.6 m while both vehicles are accelerating. At the same time another vehicle comes between the two vehicles at a distance of 10 m from the ACC vehicle (Figure 6-11), it is assumed that the velocity of this new vehicle is same as the preceding vehicle. At this point the range between ACC and the new vehicle has gone down to 10 m (Figure 6-11(d)). After merging in between the two vehicles this vehicle becomes the new preceding vehicle as the link between the ACC vehicle and the older preceding vehicle is interrupted. The response of the ACC vehicle against this disturbance is shown in the results in Figure 6-11. Due to this disturbance the ACC vehicle has immediately decelerated (Figure 6-11(c)) to safe speed and has accelerated again to track the desired SIVD with zero range-rate (Figure 6-11(b)). Under this transition input the engine speed has also gone down and has restored back to the required speed (Figure 6-11(e)). After this analysis it can be observed that the MPC control method is robust enough to cope with any sudden changes and can steer the ACC vehicle to a safe position.
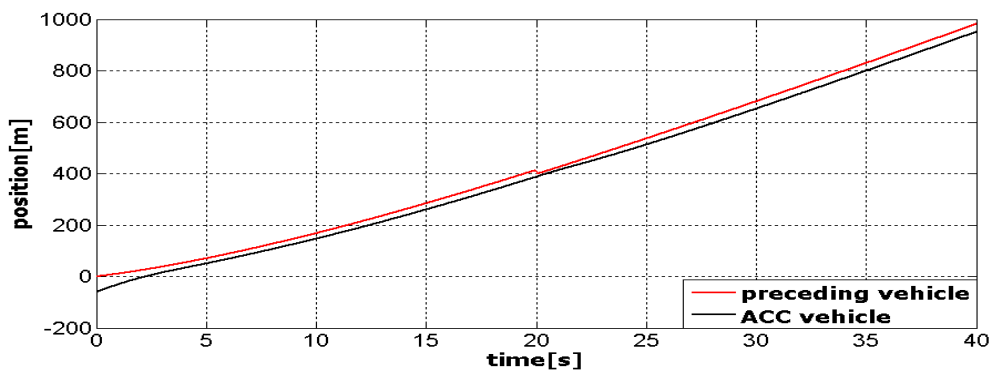

(a) Vehicle positions
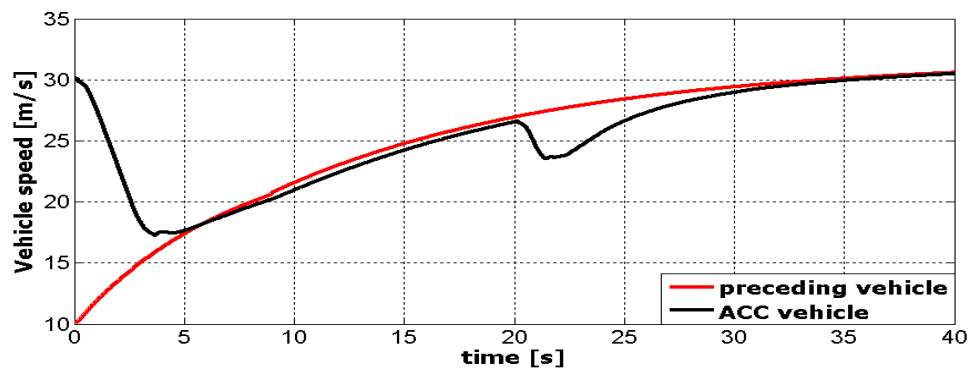
(b) Vehicle velocities
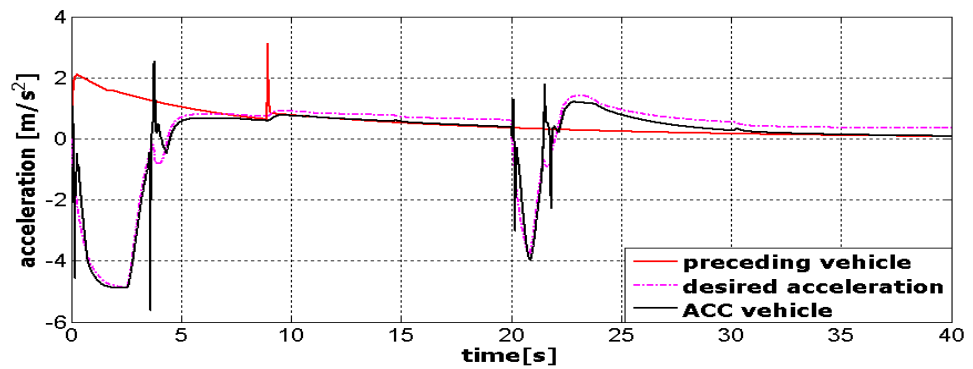
(c) Vehicle accelerations
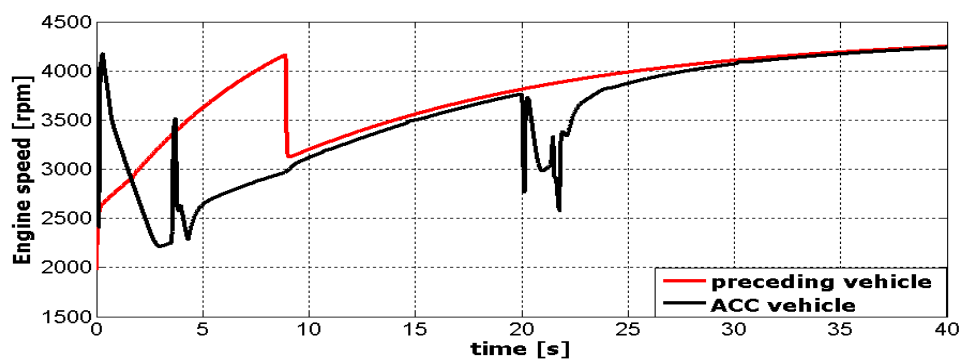
(d) Engine speed
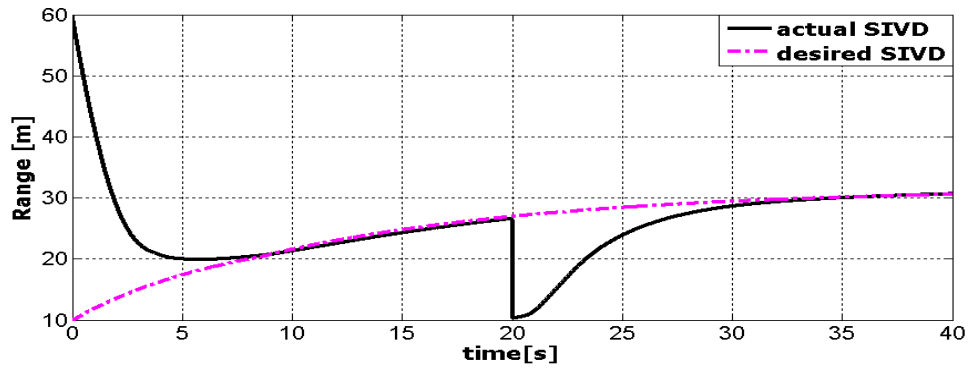
(e) Range

Figure 6-11   Response of the ACC vehicle for the scenario of Section 6.4.3.5

6.4.3.6   Vehicle's analysis for a different set of transmission gear ratios

In this section an ACC vehicle is analysed using a set of different transmission gear ratios. The gear ratios for the preceding vehicle remain same as in the previous cases. A different set of gear ratios will affect the engine speed and gear shifting pattern. For the sake of parametric analysis it is necessary to analyse the ACC vehicle behaviour for a different transmission shifting pattern. A new set of gear ratios is given in Table 6-2 which are used for the ACC vehicle.

Gear ratio	Original	New
R_1 = 1st gear speed reduction ratio	0.3184	0.333
R_2 = 2nd gear speed reduction ratio	0.505	0.4
R_3 = 3rd gear speed reduction ratio	0.73	0.667
R_4 = 4th gear speed reduction ratio	1	1
R_5 = 5th gear speed reduction ratio	1.3157	1.333
R_d = final drive speed reduction ratio	0.3257	0.333

Table 6-2   Transmission gear ratio

The response of the ACC vehicle for the different gear ratios is shown in Figure 6-12, and it can be seen that the ACC vehicle successfully performs the TM even with different transmission ratios. The throttle input for the preceding vehicle is 60 degrees; it means a different desired SIVD for the ACC vehicle to track. The simulation has been run for 100 s and it can be seen that the ACC vehicle smoothly achieves the control objectives. Due to the different gear shifting pattern the change in the engine speed can be seen clearly (Figure 6-12(d)) but still the ACC vehicle maintains the required engine speed for the rest of the simulation time. The ACC vehicle is smoothly executing the required TM, establishing the desired SIVD (Figure 6-12(e)), and maintaining the same velocity as preceding vehicle. This analysis shows the stability and robustness of MPC control algorithm and the ACC vehicle model used. It can be concluded that this vehicle model can be used for different types of vehicles because it is generically adaptable.
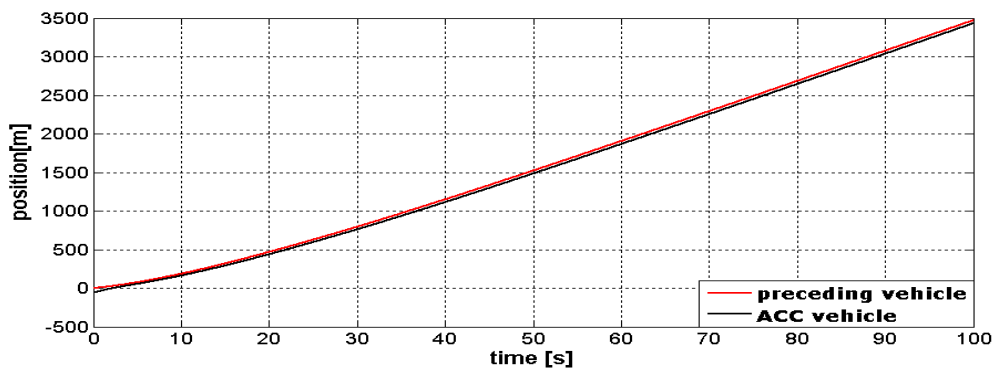

(a) Vehicle positions
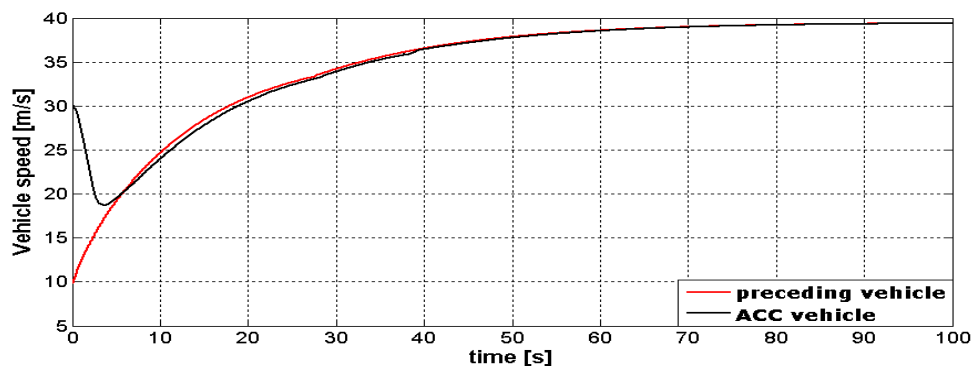
(b) Vehicle velocities
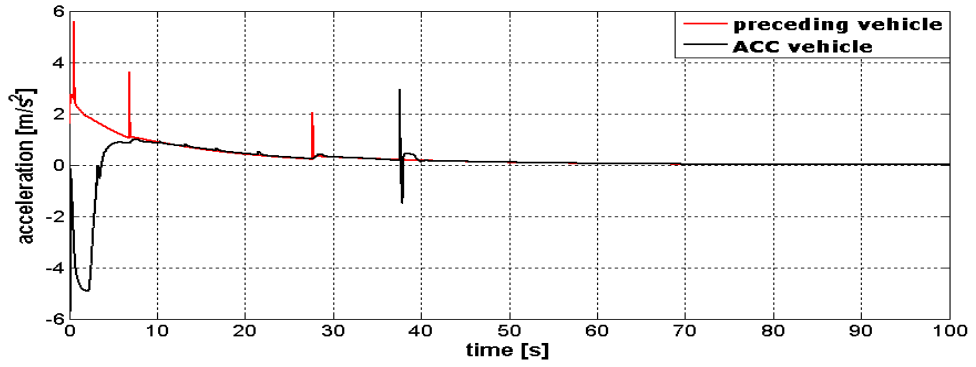
(c) Vehicle accelerations
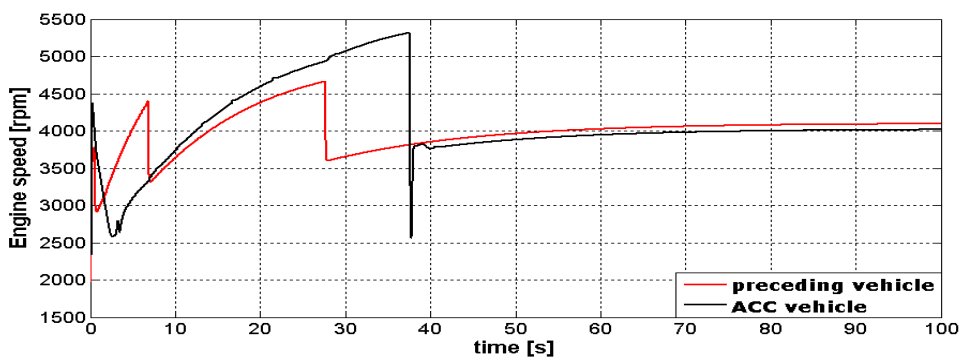
(d) Engine speed
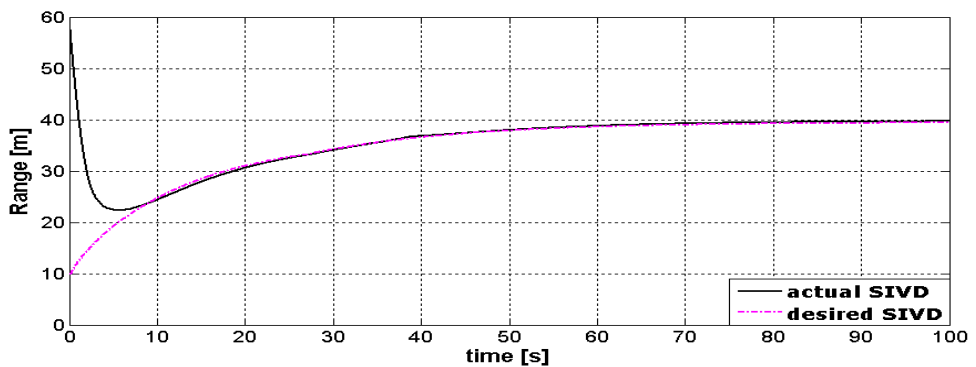
(e) Range

Figure 6-12   Response of the ACC vehicle for different transmission gear ratios

6.4.3.7   ACC vehicle analysis for a road gradient of 15 degrees

In the previous sections the sensitivity analysis of the ACC vehicle has been carried out by varying internal parameters of the MPC control algorithm and ACC vehicle model. In this section the ACC vehicle response is analysed by changing an external

parameter. The external parameter considered is positive gradient of the road and for the purpose of analysis 15 degrees road gradient has been chosen. The gradient will consequently affect the desired SIVD as the velocity of the preceding vehicle reduces down.

The simulation results for this scenario are shown in Figure 6-13. Using the same encounter scenario as in Section 6.4.2, the simulation is run for 100 s. At t = 40 s the preceding vehicle is subjected to a 15 degrees slope. It should be noted that the ACC vehicle should not be subjected to that slope at the same time and it is important to calculate at what time the slope should be introduced to the ACC vehicle. A precise observation can be made by determining the speed of the ACC vehicle and the distance between the two vehicles which will help to compute the exact time to introduce the slope to the ACC vehicle. At t = 40 s the speed of the ACC vehicle is 30 m/s and the corresponding SIVD between the two vehicles is also 30 m, therefore, the slope to the ACC vehicle should be introduced after 1 s of the preceding vehicle slope introduction. At t = 80 s and t = 81 s the road gradient is removed from preceding and ACC vehicle respectively, and they travel on a flat road for the rest of the simulation time. At t = 40 s both vehicles are travelling in 3rd gear (Figure 6-13(f)).

It can be closely observed from Figure 6-13(b) that when preceding vehicle decelerates at t = 40 s the control input commands computed for the ACC vehicle are to decelerate (Figure 6-13(b), dashed-dotted line) until the ACC vehicle reaches to the slope (till t = 41 s). These deceleration commands are due to the error in the range-rate (relative velocity) between the two vehicles. Due to this deceleration in the preceding vehicle, the ACC vehicle is subjected to the brake torque (Figure 6-13(e)). At t = 41 s the ACC vehicle further decelerates due to the road slope. The control input commands now for the ACC vehicle are to accelerate (Figure 6-13(b), dashed-dotted line). These acceleration commands are due to the effect of acceleration of the ACC vehicle in the error vector (Equation (5.24)).

On the slope, the control input commands for the ACC vehicle are to accelerate but it can be seen that the ACC vehicle is unable to track the desired SIVD (Figure 6-13(d)). The reason found is the computation of the desired net torque (T_{net_des}), as given in Equation (6.4), for the ACC vehicle does not take into account the road

gradient information in its formulation. The desired net torque (Figure 6-13(g)) is not sufficient to track the desired SIVD (Figure 6-13(d)) while travelling on the slope. Therefore, it is necessary to incorporate the road gradient information in the lower-level controller formulation in order to achieve the control objectives.

While travelling on the slope both vehicles are subjected to transmission down-shifting (Figure 6-13(f)) which affects the MPC controller performance. When the slope is removed then both vehicles accelerate again and MPC control laws achieve the required control objectives. The corresponding engine speeds and longitudinal velocities for both vehicles are shown in Figure 6-13(c) and Figure 6-13(a) respectively.

Based on this analysis, it can be concluded that this kind of response cannot be simulated using a first-order ACC vehicle model, therefore, it is necessary to use the complex ACC vehicle for a detailed analysis under the TMs. However, a first-order ACC vehicle model can be used for the upper-level controller design.
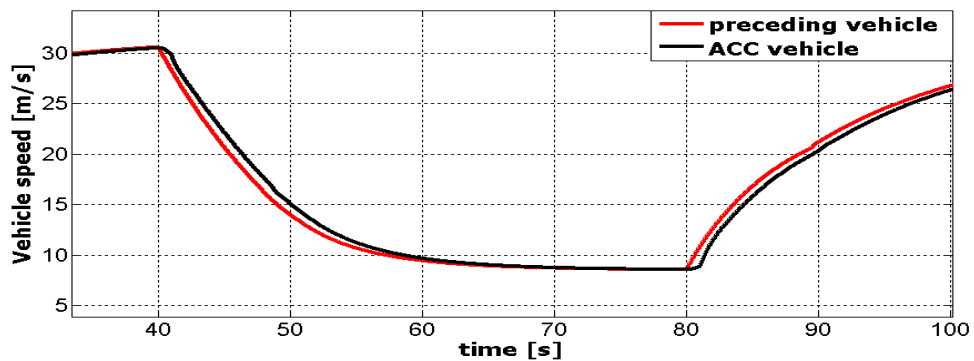
(a) Vehicle velocities
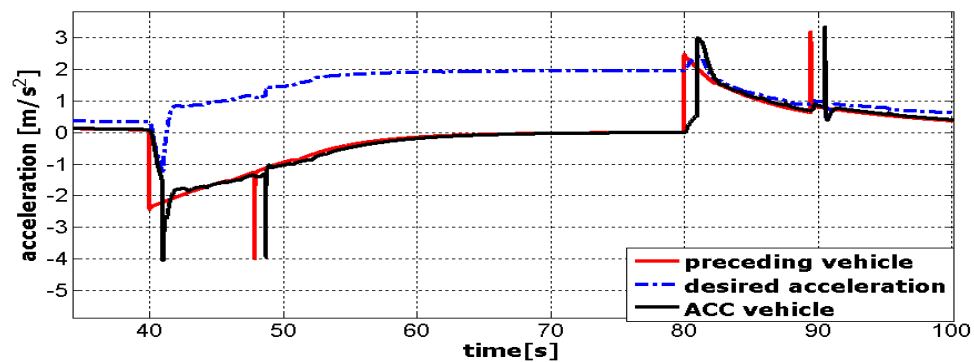
(b) Vehicle accelerations

207
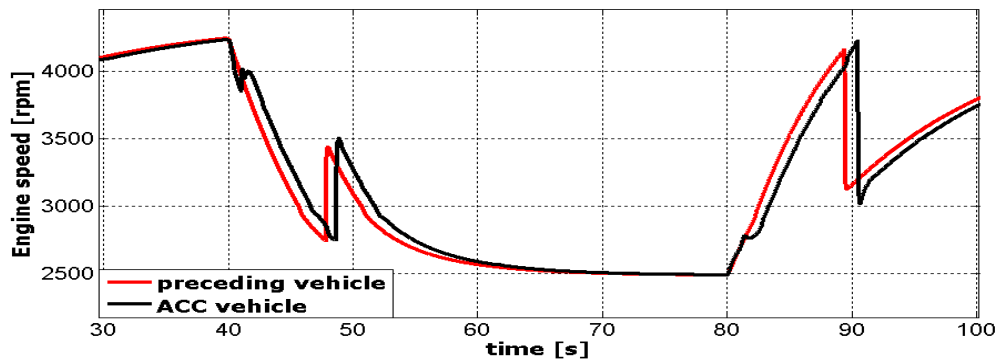
(c) Engine speed
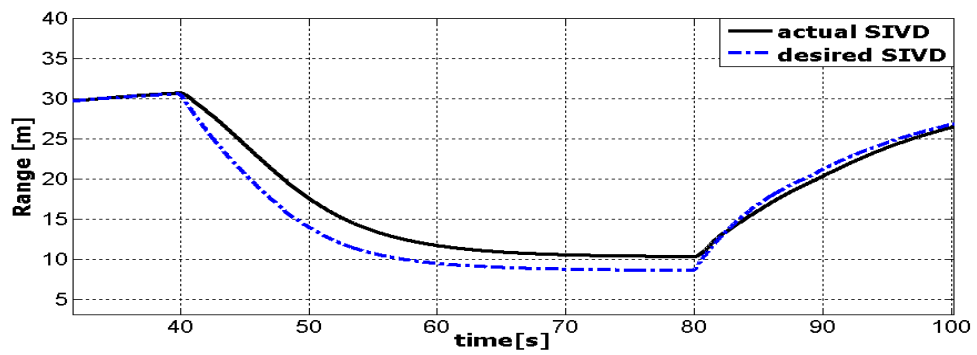
(d) Range
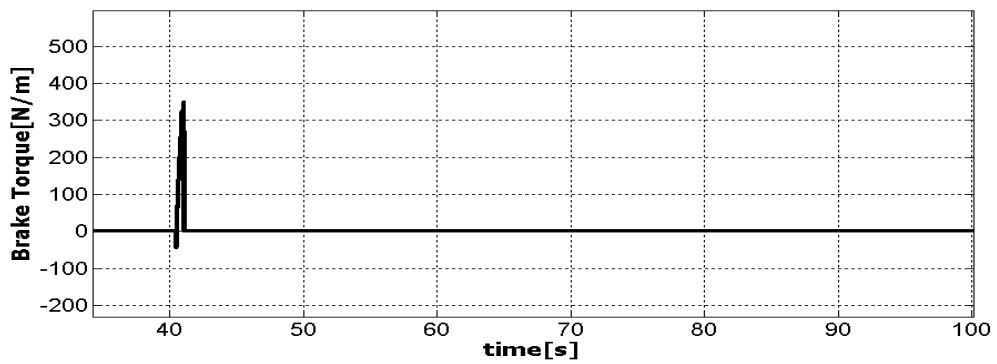
(e) Brake torque
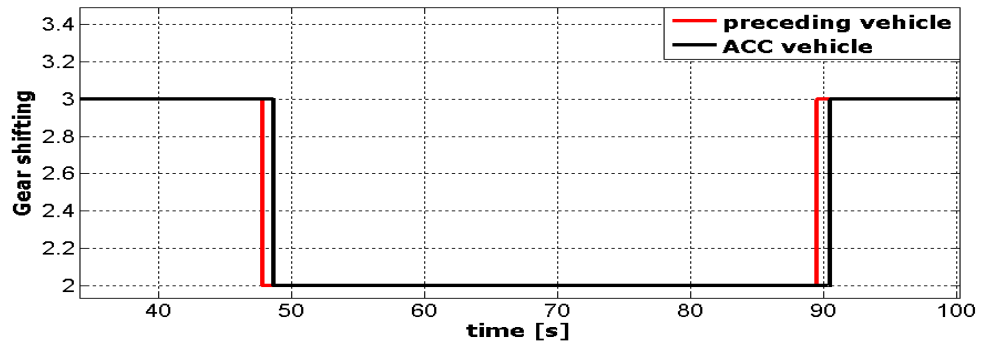
(f) Gear shifting
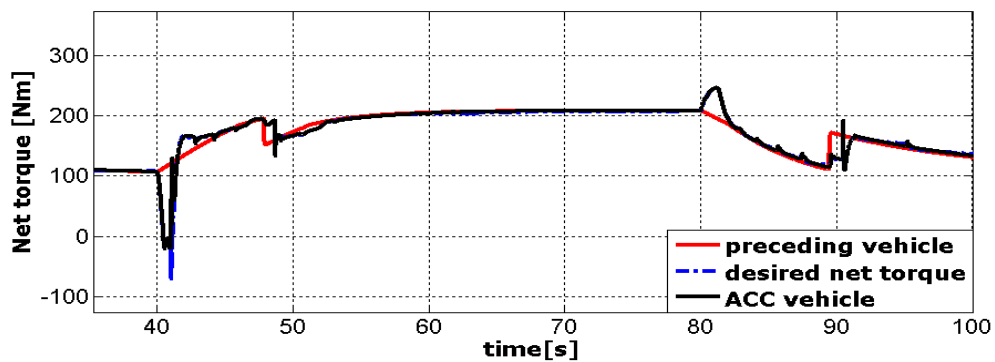
(g) Net torque

Figure 6-13   Response of ACC vehicle on a road gradient of 15 degrees.

6.4.3.8   ACC vehicle analysis against a halt preceding vehicle

In the previous sections encounter scenarios were considered where the preceding vehicle was travelling, either accelerating or travelling with constant velocity. In each case the desired SIVD was always greater than zero and it was always travelling with the coordinate frame of the transitional manoeuvre. In this section the ACC vehicle's analysis is carried out against a halt preceding vehicle. Out of all encounter scenarios and situations considered in this chapter, this encounter scenario is the most critical encounter scenario. The ACC vehicle has to perform a TM where the preceding vehicle is at rest which implies that the desired SIVD for this situation is zero throughout the simulation time.

The following simulations have been carried out to evaluate the performance of the MPC controller and the complex vehicle model for a scenario where an ACC vehicle

travelling at a speed of 30 m/s detects a preceding vehicle at rest. The initial range between the two vehicles is 110 m. The objective of the TM for the ACC vehicle is to establish the SIVD maintaining a zero-range-rate during its entire manoeuvre avoiding the collision with the preceding vehicle. The initial engine speed, throttle input, and gear ratio for the ACC vehicle are 4040 rpm, 50 degrees, and 5th gear, respectively.

Figure 6-14 shows that the ACC vehicle successfully performs the required TM, avoids the collision with the preceding vehicle, and establishes the desired SIVD with zero range-rate. It should be noted that the ACC vehicle is obeying all the applied constraints during this TM i.e. control input, states, and collision avoidance while the constraints are applied in the upper-level controller formulation. It can be seen that the ACC vehicle is not executing a negative velocity.

Figure 6-14(c) shows that ACC vehicle is initially accelerating while the desired initial acceleration commands (dash-dotted blue line) for the ACC vehicle are to decelerate. This is an undesirable response of the complex ACC vehicle, but still it is achieving the control objectives. Figure 6-14(e) shows that the ACC vehicle is performing down-shifting from 5th to 3rd gear at t = 0.6 s and from 3rd to 1st gear at t = 4.1 s. Due to this transmission down-shifting the engine speed Figure 6-14(d) gets affected which in turn effects the acceleration Figure 6-14(c) of the ACC vehicle.

For the purpose of validation ACC vehicle position (Figure 6-14(a)), speed (Figure 6-14(b)), and acceleration (Figure 6-14(c)) have been compared with the same scenario conducted for simple ACC vehicle model (Figure 5-6). The comparison shows that the complex ACC vehicle response matches well with the simple ACC vehicle. Figure 6-14(c) shows the engine and transmission dynamic effects on the acceleration of the complex ACC vehicle which were not included in the simple ACC vehicle modelling. The comparison shows that the complex ACC vehicle is initially accelerating while the simple ACC vehicle is decelerating (Figure 5-6(c)) straight away.

Based on this analysis it can be concluded that the upper-level controller analysis alone in not sufficient and it cannot be recommended for a real ACC vehicle. Therefore, it is necessary to analyse the complex ACC vehicle in the simulated environment under these transitional manoeuvres.
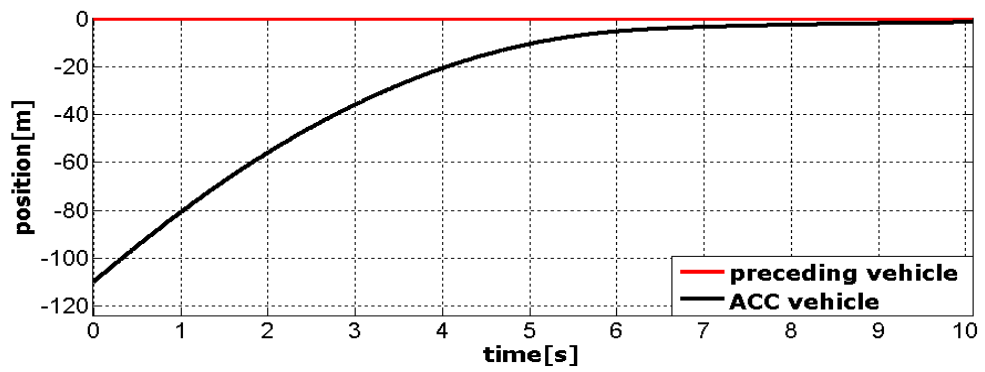
(a) Vehicle positions
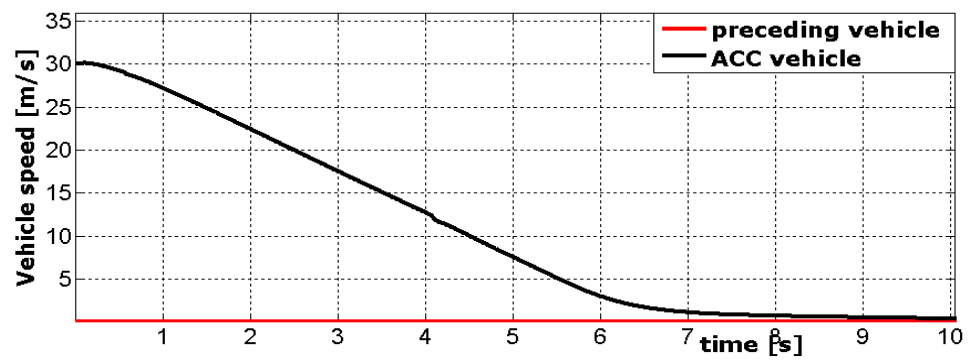
(b) Vehicle velocities
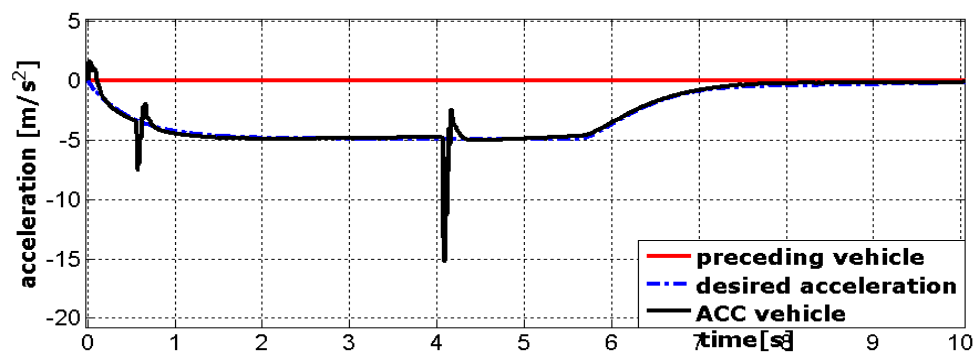
(c) Vehicle accelerations
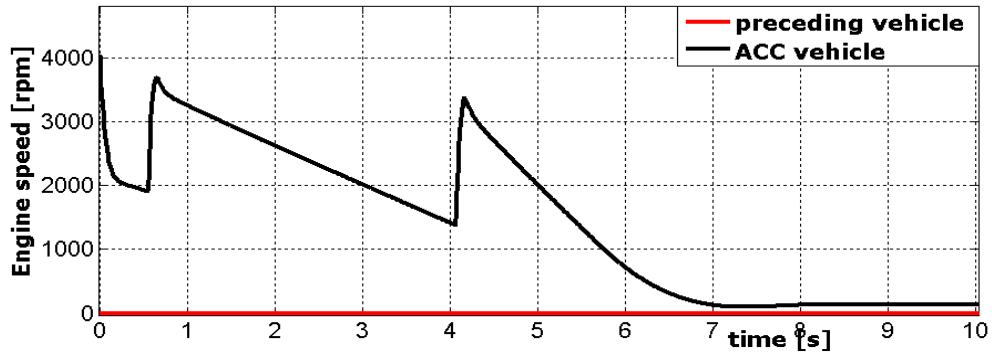
(d) Engine speed
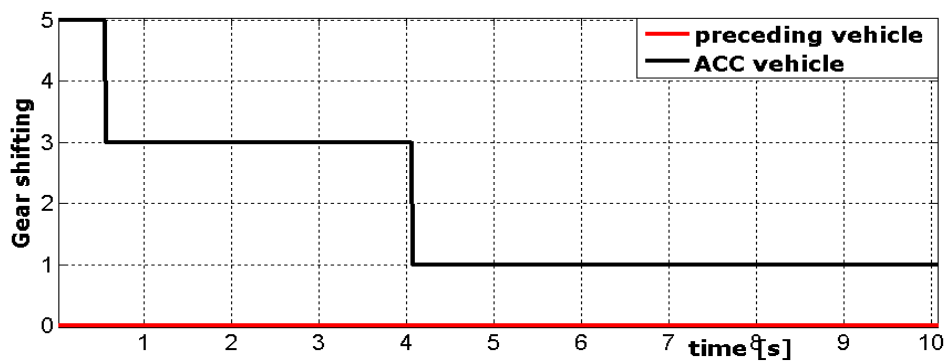
(e) Gear shifting

Figure 6-14   Response of ACC vehicle for Section 6.4.3.8 scenario.

The analyses and observations conducted in this chapter are the major findings of this study. The two-vehicle model, where both vehicles are based on complex vehicle model, has been simulated for different critical encounter scenarios and different parameter sets and in all situations the complex ACC vehicle model has produced satisfactory and expected results using the MPC control algorithm while taking in account the operational constraints and in the presence of internal complexities of the vehicle dynamics.

6.5   Conclusions

In this chapter a lower-level controller model has been developed to compute the throttle and brake input commands for the complex ACC vehicle model. Before conducting the two-vehicle system analysis, the lower-level controller and ACC

vehicle model were analysed using a sinusoidal input as the desired acceleration for the ACC vehicle to track (Figure 6-2). The simulation results show that the lower-level controller is computing the required throttle and brake input commands for the complex ACC vehicle and tracking the desired acceleration commands smoothly. After this satisfactory response, it was concluded that the lower-level controller and the complex ACC vehicle can be used in the two-vehicle system.

For the two-vehicle system, the upper-level controller has been used (based on MPC control algorithm) to compute the desired acceleration commands for the lower-level controller. The lower-level controller then computed the required throttle and brake input commands for the complex ACC vehicle.

The simulation results in Figure 6-3 show that the complex ACC vehicle is smoothly executing the high deceleration manoeuvre, tracking the desired acceleration commands, within the deceleration limit of -0.5g and avoiding collision with the preceding vehicle. Without the deceleration limits the ACC vehicle would have decelerated to -8.1 m/s^2 (Figure 5-4(c)). The acceleration limits has been formulated as the control input constraint and the collision avoidance has been formulated as a state constraint. It was interesting to observe that the ACC vehicle is operating within these constraints, although these constraints were only incorporated within the MPC algorithm in the upper-level controller. The complex ACC vehicle has successfully established the desired safe inter-vehicle distance (SIVD) with zero range-rate behind the preceding vehicle.

It should be noted that due to the deceleration limit (applied on the control input signal), the ACC vehicle was not allowed to apply the necessary brake torque to avoid the collision. The brake input signal was expected to saturate at certain level which has been observed during the transitional manoeuvre (TM). The brake torque for the ACC vehicle is maintained at the required level to avoid the collision with the preceding vehicle.

The simulation results, Figure 6-3, for the complex ACC vehicle have been compared against the first-order ACC vehicle simulation results (Figure 5-4) for the same encounter scenario. The velocity, acceleration, and range of the complex ACC vehicle show a good agreement with the first-order ACC vehicle. The difference between the two results found was the effect of engine and transmission dynamics

on the upper-level controller and the ACC vehicle itself. It has been found that the proposed MPC algorithm is robust enough to cope with nonlinearities in engine and transmission dynamics. This comparison forms a firm basis for further investigations into the MPC controller and ACC vehicle parameter studies.

This chapter also covers parametric and sensitivity analyses of the complex ACC vehicle towards the variation in certain parameters of the ACC vehicle and MPC controller. Some interesting features have been found from this parameter studies. The parameters for which the sensitivity analysis has been carried out are as follows:

a. By varying the throttle input to the preceding vehicle.

b. By varying the length of the control horizon (N_C) and using different values of control input cost weighting (**R**) to restore the controlled behaviour.

c. By varying the control input cost weighting (R) in order to have the entire system under a loose control and a tight control.

d. By changing the mass of the ACC vehicle.

e. By introducing a 15 degree road gradient to both vehicles.

f. By changing the headway time.

g. By applying the step input to the ACC vehicle.

h. By using a different set of transmission gear ratios for the ACC vehicle.

i. During a cut-in manoeuvre.

j. ACC vehicle analysis against a halt preceding vehicle

For each analysis simulation results have been produced and it has been observed that the ACC vehicle has successfully executed the required critical TMs and achieved the control objectives within the constrained boundaries. It has been observed that in each analysis the ACC vehicle is obeying the SIVD policy with zero range-rate.

The simulation results show that the above parameters have serious influence on the engine and transmission dynamics and can lead to some serious consequences. It has been observed that length of control horizon (N_C) greater than 4 samples seriously influences the engine dynamics and transmission dynamics during the transitional and the steady-state operations. The ACC vehicle was unable to minimize the steady-state error. The ACC vehicle takes longer to establish the SIVD with the zero range-rate. It has been found that with higher values of N_C, the control objective can be achieved by using higher values of control input cost weighting (**R**). For N_C = 5 the value of **R** found to restore the controlled response was 5, and for N_C = 10 the value of **R** found to restore the controlled response was 8. The simulation results (Figure 6-5) using N_C = 5 for complex ACC vehicle has been validated against the similar results for the first-order ACC vehicle (Figure 5-10). The comparison of both shows a good agreement.

The sensitivity of the complex ACC vehicle has been analysed for different values of **R.** In the case of **R** = 0.1 ('loose' control) the ACC vehicle cannot meet the required objectives either during the transitional operation or the steady-state operation. The engine dynamics and transmission dynamics result in higher errors, the SIVD could not be established, and the ACC vehicle is not responsive enough to achieve the zero range-rate. On the contrary, in the case of **R** = 20 ('tight' control) the response of the ACC vehicle is prolonged but the control objectives have been still achieved. The higher value of **R** has affected the ACC vehicle response during the transitional operation while during the steady-state operation the response is satisfactory.

It has been observed that the complex ACC vehicle can follow the preceding car using any throttle input for the preceding vehicle. The throttle inputs used for the preceding vehicle were 70 and 50 degrees which means two different behaviours from the transmission gear shifting pattern, engine dynamics, and a different desired SIVD to achieve. In each case the ACC vehicle has smoothly followed the preceding vehicle with the required throttle input and has achieved the control objectives. Both vehicles have also been analysed for a 15 degree road gradient and it has been observed that the complex ACC vehicle is unable to achieve the control objectives while moving on a slope. The reason found is the lower-level controller does not take into account the gradient of the road.

The analysis of the ACC vehicle for different headway time (h) shows that using h = 0.5 s, the range between the two vehicle has significantly reduced and the distance between the two vehicles is not sufficient to avoid a collision if a severe emergency occurs. On the contrary, using h = 1.5 s resulted in a delayed response and a higher range between the two vehicles. It can be observed that the higher h value significantly delays the engine, transmission and brake response. Also, due to higher range another vehicle can jump in the spacing between the two vehicles and could be a reason for severe consequences.

The analysis of the ACC vehicle for different vehicle masses indicates that a mass within the range of 1400-2000 kg is suitable for the ACC vehicle, and the MPC controller is robust enough to cope with the mass variations. Another interesting feature analysed was for a different set of transmission gear ratios. The ACC vehicle's longitudinal motion was unaffected by a different gear shift pattern which means different gear ratios can be used for this vehicle model. During the step input (cut-in scenario) the ACC vehicle has performed remarkably well and manoeuvred to safe speed in order to avoid collision. The important feature of the controller developed is the sudden response to the step input and then restoring back to the desired control objectives. The results show that the complex ACC vehicle operates within the deceleration limits, does not execute a negative velocity, and avoids a collision with the preceding vehicle.

The complex ACC vehicle analysis against the halt preceding vehicle shows that the ACC vehicle is initially accelerating while it should decelerate because the desired commands are to decelerate. Based on this analysis it can be concluded that the upper-level controller analysis alone in not sufficient and it cannot be recommended for a real ACC vehicle. Therefore, it is necessary to analyse the complex ACC vehicle in the simulated environment under transitional manoeuvres.

Based on the comparison of first-order ACC vehicle and the complex ACC vehicle simulation results, it is concluded that the response of the complex ACC vehicle model shows a good level of agreement with the first-order ACC vehicle model response. This implies that one can design the upper-level controller, using the first-order vehicle model, without considering the internal complexities of the vehicle sub-models. The first-order ACC vehicle model has been used for the complex

vehicle validation; whereas the complex ACC vehicle model can be used for the experimental validation in future work. Also, the above analyses were not possible using the first-order ACC vehicle model. Therefore, it is recommended that a complex vehicle model should be used for a detail ACC vehicle analysis.

The proposed complex ACC vehicle model can be used for different applications, e.g. obstacle avoidance, for pedestrian safety measures, lateral dynamic control (if lateral dynamic model is included), driver behaviour model analysis, and hybrid vehicle analysis (if the powertrain model is modified). This two-vehicle model can be further extended for more than two vehicles in order to analyse the string stability of a platoon of ACC vehicles. The model can help to understand the ACC behaviour in other critical situations, e.g. sensor failure. It can help to understand the behaviour of brake actuators and how the operational constraints control the ACC vehicle dynamic behaviour.

Chapter 7.   Conclusions and Future Work

7.1   Introduction

An application of a model predictive control (MPC) algorithm to control the longitudinal dynamics of an adaptive cruise control (ACC) system equipped vehicle is presented in this thesis using Matlab to simulate the system. A two-vehicle system (Figure 3-34) has been developed which consists of a preceding vehicle and an ACC vehicle. This study has been carried out in order to investigate the response of a complex ACC vehicle model during critical transitional manoeuvres (TMs) and under the operational constrained boundaries to avoid a collision with the preceding vehicle. Before analysing the complex ACC vehicle, the analyses of upper-level-controller using four control methods (proportional-integral-derivative (PID), sliding mode, constant-time-gap (CTG), and MPC) have been carried out. For the upper-level controller analysis, a first-order ACC vehicle model has been used. It has been found (in the upper-level controller analysis) that MPC is the most appropriate control method among the four control methods due to its prediction model and online optimization characteristics. Another advantage of using the MPC control method is that it can incorporate, by nature, the operational constraints in its formulation while the other control methods were unable to take them into account.

Using a first-order ACC vehicle model to analyse the upper-level controller response under the critical TMs is not sufficient to investigate the dynamic characteristics of a real vehicle. Because the first-order ACC vehicle model does not consider the dynamic effects of the vehicle's sub-models, i.e. engine, transmission,

and brake dynamics. In order to investigate the dynamic characteristics of these sub-models, a detailed complex vehicle model has been developed for the ACC vehicle's analysis (Chapter 3). A lower-level controller model has also been presented (Chapter 6) to determine the throttle and brake input commands for the complex vehicle model to track the desired acceleration commands computed by the upper-level controller. It should be noted that a first-order lag is considered between the upper-level and lower-level controllers. This lag in the lower-level controller performance comes from brake or engine actuation lags and sensor signal processing lags. A number of simulations have been conducted to investigate parametrically the complex ACC and the simple first-order ACC vehicle model against vehicle's and controller's parameter changes. The identification of knowledge gaps, the contribution of each chapter towards the development/analysis of the two-vehicle system, and the findings of this study are as follows.

7.2 Contributions and Conclusions from Thesis

The literature review conducted in Chapter 2 presents a significant amount of research work in the area of ACC vehicles. A number of ACC vehicle models and controller approaches have been developed which cover a wide range of ACC vehicle applications. Most of the work has been done, so far, for the unconstrained response of an ACC vehicle which provides new directions to investigate the constrained ACC vehicle response. The gaps in the reported research area were described in Section 2.4. The study objectives to fill these gaps were proposed in Section 2.5. The aims of the research are to obtain deeper understanding of the ACC system and to model and simulate the interaction between vehicle and the vehicle controllers.

The contribution of this thesis is towards the enhancement of the existing ACC systems. A simulation-based approach is used in this thesis, with initial experimental data adopted from the existing literature. The development of the overall system model includes the following stages of activity: vehicle modelling, controllers modelling, and their interaction. This analysis helps to improve the

219

vehicle model and controller design parameters and provides directions for the further research to improve the ACC vehicle performance.

An important aspect of this study is developing a complex vehicle model for the ACC system analysis. In Chapter 3, a 5-speed automatic transmission powertrain model has been developed for the longitudinal dynamic control of a vehicle. The complex nature of the vehicle model refers to the effects of engine, transmission and brake models on the overall behaviour of the vehicle. A simplified approach for gear up-shifting and down-shifting using the gear schedule maps (Figure 3-8) has been used where the transmission gear up-shifting and down-shifting is triggered using the look-up maps using the throttle angle and vehicle's longitudinal speed information (Kulkarni *et al.*, 2006). Simulation results have been produced using the complex vehicle model and have been validated against previous studies (Cho and Hedrick, 1989; (Yi and Chung, 2001). For the computation of the desired throttle or brake input in the lower-level controller (Chapter 6), engine maps are required. Usually, the engine maps are provided by the manufacturers (based on the experimental testing). In this study, the engine maps have been constructed off-line which correspond to the proposed engine model. The simulation results obtained from the engine-map models have been validated with the complex vehicle model to ensure that these engine maps can be used for the lower-level controller calculations. After the satisfactory response, it can be concluded that this complex vehicle model can be used for the ACC vehicle analysis for longitudinal dynamic control. This complex vehicle model has been used for both vehicles in the two-vehicle system in Chapter 6, which consists of a preceding vehicle and an ACC vehicle (following vehicle).

Chapter 3 also presents a simple first-order ACC vehicle model which is used for the upper-level controller analysis under the critical TMs using the four well-known control methods (Chapter 4 and 5). A first-order lag has been incorporated in this simple vehicle model. This lag comes from brake or engine actuation lags and sensor signal processing lags.

Four control methods: PID, sliding mode, CTG, and MPC have been used for the upper-level controller analysis using the first-order ACC vehicle model (Chapter 4

& 5). Based on their analysis and comparison, the most suitable control algorithm was used for the upper-level controller.

The main tasks for these control methods to perform on the ACC system are:

1 Track smoothly desired acceleration commands

2 Reach and maintain a safe inter-vehicle distance (SIVD) in a comfortable. manner and at the same time react quickly in the case of dangerous scenarios.

3 System performance optimization.

4 Optimize the system performance within defined constrained boundaries.

In Chapter 4, the fundamentals of an ACC system as a whole have been discussed. The formulation and analyses of three control methods (PID, sliding mode, CTG) have been covered in Chapter 4. It has been found after the comparison of these three control methods that none of these control algorithms can compute the required spacing-control laws for the ACC vehicle during the critical TMs and cannot cope with the operational constraints of the ACC system. The operational constraints refer to the control input, states and collision avoidance constraints. In the case of PID and CTG analyses during TMs (situation 3), the ACC vehicle is executing a negative velocity and cannot avoid the collision with the preceding vehicle. It has been found that the sliding mode control method is not suitable for the two-vehicle system due to the first-order lag in the simple vehicle model. The reason found is the lag amplifies the chattering characteristics of the sliding mode method. A parametric analysis for the CTG control law has also been carried out by changing its two parameters: weighing factor and headway time. The analysis shows that the CTG is more sensitive to headway time than the weighing factor.

In Chapter 5 MPC control algorithm has been used for the two-vehicle system. Basic features of MPC method and the formulation of the prediction model to obtain the optimal control input using a linear single-input-single-output (SISO) system have been explained. The MPC algorithm is then applied to the two-vehicle system for the first-order ACC vehicle analysis under TMs. A discrete-time state-space model is developed which is used to predict the future error vector between the two vehicles.

This error vector consists of spacing error between the two vehicles, relative velocity between the two vehicles, and the absolute acceleration of the ACC vehicle. This error vector model is developed such that the control objectives assigned to the controllers are achieved. The prediction model is then used compute the future control input for the first-order ACC vehicle.

Simulation results, under the same situations, obtained from MPC control method have been compared with the control methods presented in chapter 4. Some of the advantages of using MPC method over the other control strategies are the operational constraints (control input, states and collision avoidance) can be incorporated in the control algorithm during the analysis process and an online optimization can be achieved. The control input constraints are fully applied on all the components of $\Delta\mathbf{U}_k$ and have been translated as six linear inequalities Equation (5.31).

The main difference between the MPC and PID control strategies is that the MPC control strategy uses the desired reference trajectory which is computed using the prediction model, the MPC controller then uses the plant characteristics in order to follow the desired reference trajectory. Whereas, the control action taken by the PID control strategy is based on the past errors which can be viewed as if the driver is driving the vehicle using the rear view mirror. Similarly, in the sliding mode control method, the control objectives are designed as a sliding surface using the previous plant's states (off-line computation). The CTG control algorithm is based on the previous plant's states which is not robust enough in comparison with the MPC control method. The on-line optimization is not possible and the operational constraints cannot be included in the formulation of CTG control algorithm. After comparing these all control methods it has been found that the MPC control algorithm is the most appropriate for the ACC vehicle analysis.

The dynamic behaviour of the ACC vehicle, using the MPC controller technique, has been analysed for different TMs. The response of the first-order ACC vehicle model has been analysed with constraints and without constraints and results have been compared and discussed. The shortcoming occurred without using the constraints has also been highlighted. It has been observed that with a first-order

model the ACC vehicle successfully establishes the desired SIVD with the zero range-rate with all constraints included in the MPC controller formulation.

A sensitivity analysis of the ACC vehicle has been carried out for MPC in Chapter 5 for different initial conditions, different ranges, different control input cost weighting function ($\mathbf{R}$) and different control horizon (N_C).

It has been noticed that ACC has performed the TM successfully regardless of the initial conditions, provided the initial conditions are selected within the range of Bageshwar, *et al.* (2004) model. Because, a lower initial range for a given range-rate has been analysed and it has been found that the ACC vehicle cannot avoid the collision with the preceding vehicle. Higher values of initial range (more than for a given range-rate) provides ample time to the ACC vehicle to achieve the control objectives within the given constraints boundaries. It is, therefore, can be concluded that the initial values computed by Bageshwar, *et al.* (2004) are appropriate and can be used for the two-vehicle encounter scenario in this study.

It has been observed that the higher values of control input cost weighting ($\mathbf{R}$) correspondingly penalize the control input magnitude which can also be termed as a 'tight' control. In this situation the control objectives are not violated but it results in a delayed response. Therefore, it should be noted that for a best performance of the system an appropriate value of $\mathbf{R}$ should be selected which neither relax the control input to have a 'loose' control nor effect excessively the control input to have a 'tight' control.

The effect of different lengths of control horizon (N_C) has been analysed in Chapter 5. For a stable response of the ACC vehicle the value of N_C chosen is 3 samples. It has been observed in the analysis that using a higher value of N_C ($N_C > 4$) causes the control input to be distributed for a higher control horizon, resulting in an error in the desired objectives. This error due to a higher value of N_C has been reduced by increasing the cost weighting function ($\mathbf{R}$). It has been observed that for a higher value of N_C a higher corresponding value of $\mathbf{R}$ is required to achieve the required control objectives.

In Chapter 6 the lower-level controller model was developed to compute the throttle and brake input commands for the complex vehicle model used for the ACC

vehicle. Before conducting the two-vehicle system analysis the lower-level controller and ACC vehicle model were analysed using an arbitrary sinusoidal input and the results have proven that the proposed lower-level controller and ACC vehicle model are tracking the desired input command as required.

In Chapter 5, the ACC vehicle analyses were based on a first-order model which does not consider the internal dynamics of the vehicle sub-models. In Chapter 6, the ACC vehicle was based on a complex vehicle model and covers the effects of engine dynamics, transmission dynamics, and the brake model. It should be noted that in this study these effects have been taken into account in the error vector prediction model for the two-vehicle system which have not been covered in the previous studies. The absolute acceleration of the ACC vehicle is affected due to transmission gear shifting. Due to the transmission effects, the error vector gets affected which in turn affects the upper-level controller performance. The disturbance in the upper-level controller performance de-stabilizes the complex ACC vehicle response during the gear shifting (see Figure 6-4(c)).

Figure 6-3 shows the complex ACC vehicle has established the desired SIVD with zero range-rate within the operational constraints boundaries. This TM has been performed under the effects of engine and transmission dynamics. This shows the robustness of the MPC control algorithm which at the same time can cope with these nonlinearities and internal complexities of the vehicle dynamics. The complex ACC vehicle has performed the higher deceleration manoeuvre, tracking the desired acceleration commands, under the deceleration limit of -4.9 m/s^2. Without the deceleration limits the ACC vehicle would have decelerated to -8.1 m/s^2 (Figure 5-4c). It was also interesting to find that the ACC vehicle is operating within the operational constraints, although the operational constraints were only incorporated within the MPC control algorithm in the upper-level controller, and the complex ACC vehicle and its throttle and brake actuators are strictly following it.

It has been found the lengths of prediction and control horizon plays important role in the stable close-loop performance. Using a higher length of prediction horizon (N_P = 230) a good acceleration has been achieved. Smaller control horizon (N_C < 4) gives a controlled response and using N_C > 4 seriously affects the controller performance and vehicle response.

Chapter 6 also covers the important analysis which is termed as parametric and sensitivity analysis of the complex ACC vehicle towards the variation in certain parameters of the complex ACC vehicle and MPC controller. Some interesting features have been found from this parametric and sensitivity analysis. The parameters for which the sensitivity analysis has been carried out are as follows:

a. By varying the throttle input to the preceding vehicle.

b. By varying the length of the control horizon (N_C) and using different values of control input cost weighting (**R**) to restore the controlled behaviour.

c. By varying the control input cost weighting (**R**) in order to have the entire system under a loose control and a tight control.

d. By changing the mass of the ACC vehicle.

e. By introducing a 15 degree road gradient to both vehicles.

f. By changing the headway time.

g. By applying the step input to the ACC vehicle.

h. By using a different set of transmission gear ratios for the ACC vehicle.

i. During a cut-in manoeuvre.

j. ACC vehicle analysis against a halt preceding vehicle

The simulation results with these variations have been produced and it has been found that most of these parameters have serious influence on the engine and transmission dynamics and can lead to some serious consequences. The sensitivity analysis discussion is as follows.

It has been observed that the complex ACC vehicle can follow the preceding vehicle using different throttle input for the preceding vehicle. The throttle inputs used for the preceding vehicle are 70 degree and 50 degree which means two different behaviours from the transmission gear shifting pattern, engine dynamics, and a different desired SIVD to achieve. In each case the ACC vehicle has smoothly

followed the preceding vehicle with the required throttle and brake inputs and has achieved the required control objectives.

It has been found that using a length of control horizon (N_C) greater than 4 seriously influences the engine dynamics and transmission dynamics during the TM and the steady-state operations. With the higher values of N_C the required control objectives have been achieved by using the higher values of control input cost weighting (**R**). For example, for N_C = 5 the value of **R** used to restore the controlled response is 5, and for N_C = 10 the value of **R** used to restore the controlled response is 8.

It has been found that using **R** = 0.1 ('loose' control) the ACC vehicle cannot meet the required objectives either during the transitional or the steady-state operation. On the contrary **R** = 20 ('tight' control) has affected the ACC vehicle response during the transitional operation while during the steady-state operation the response is satisfactory.

The analysis of the ACC vehicle for different headway time (h) shows using h = 0.5 s the range between the two vehicle has significantly reduced and the distance between the two vehicles is not sufficient to avoid a collision if a severe emergency occurs. On the contrary, using h = 1.5 s resulted in a delayed response and a higher range between the two vehicles. It can be observed that the higher h value significantly delays the engine, transmission and brake response. Due to higher range another vehicle can jump in the spacing between the two vehicles and could be a reason for severe consequences. It can be recommended that, the constant headway time is not suitable; therefore, a variable headway time should be used for the spacing policy.

The analysis of the ACC vehicle for different vehicle masses indicates that a mass within the range of 1400-2000 kg is suitable for the ACC vehicle, and the MPC controller is robust enough to cope with these variations.

Both vehicles have also been analysed for a 15 degree road gradient and it has been observed that the complex ACC vehicle is unable to achieve the control objectives while moving on a slope. The reason found is the lower-level controller does not take into account the gradient of the road.

Another interesting feature analysed was using a different set of transmission gear ratios. The ACC vehicle's longitudinal motion was unaffected by a different gear shift pattern which means different gear ratios can be used for this vehicle model. During the step input (cut-in scenario) the ACC vehicle has performed remarkably well and manoeuvred to the safe speed in order to avoid the collision with the new preceding vehicle. The important feature of the controller developed is the sudden response to the step input and then restoring back to the desired control objectives.

The complex ACC vehicle analysis against the halt preceding vehicle shows that the ACC vehicle is initially accelerating while it should decelerate because the desired commands are to decelerate. Based on this analysis it can be concluded that the upper-level controller analysis alone in not sufficient and it cannot be recommended for a real ACC vehicle. Therefore, it is necessary to analyse the complex ACC vehicle in the simulated environment under these transitional manoeuvres.

For each analysis the simulation results have been produced and it has been observed that the ACC vehicle has successfully executed the required critical TMs and has achieved the required control objectives within the operational constraints and the same time obeying the SIVD policy.

The simulation results of the complex ACC vehicle (Section 6.4.1 and Section 6.4.3.1) have been validated against simulation results of the first-order ACC vehicle (Section 5.4.1 and Section 5.5.4). The validation shows the complex ACC vehicle matches well the first-order ACC vehicle. The difference between the two results found were the effects of engine and transmission dynamics on the upper-level controller and the ACC vehicle itself. It has been found that the proposed MPC algorithm is robust enough to cope with these nonlinearities of engine and transmission dynamics and all the vehicle parameters changes considered.

Based on the comparison of first-order ACC vehicle and the complex ACC vehicle simulation results, it is concluded that one can design the upper-level controller, using the first-order vehicle model, without considering the internal complexities of the vehicle sub-models. The first-order ACC vehicle model has been used for the complex vehicle validation, whereas, the complex ACC vehicle model can be used for the experimental validation of future work. The reasons for which the complex ACC vehicle is recommended are as follows.

1. The analysis of effects of engine and transmission dynamic on the upper-level controller and ACC vehicle.

2. Analysis of the ACC vehicle's brake and throttle actuators response during the critical TMs and under the constraint boundaries.

3. ACC vehicle's sensitivity analyses against vehicle parameters.

4. Effects of MPC controller parameters on the complex vehicle dynamics response.

5. Analysis of ACC vehicle against external parameters, e.g. road gradient, cut-in manoeuvre.

The above analyses were not possible using the first-order ACC vehicle model. Therefore, a complex vehicle model should be used for the detail ACC vehicle analysis.

7.3 Future Work

The research work presented in this thesis provides further direction to improve vehicle models and controller design. Some limitations and recommendations for the vehicle model and the controllers design are pointed out. Although, the ACC vehicle performance with some assumptions was satisfactory, its performance can be further improved with the following considerations.

The transmission gear shifting in the complex vehicle model takes place using look-up tables. The vehicle response can be further improved if automatic transmission systems or dual-clutch transmission systems are used for the proposed vehicle model. The advantage of using these complicated systems is the transmission gear shifting takes place smoothly, therefore, the effects on the vehicle's acceleration can be reduced and the performance of the upper-level controller and the ACC vehicle can be improved.

In this study, the traction force has been modelled as a function of slip ratio within the linear region (small slip ratio) which assumes that the friction coefficient of the

tyre-road interface is 1 and the normal force is constant. It is assumed that the longitudinal force is generated instantaneously while in practice the generation of longitudinal force longitudinal force is not instantaneous but is subjected to a delay generally referred to as 'tyre lag'. The lag is closely related to the rotation of the tyre, typically taking between half and one full revolution of the tyre to effectively reach the steady-state force condition. With the application of throttle or brake input the tyre must roll through a certain distance before the longitudinal deflection and force build up. This distance is usually referred as 'relaxation length'. Also, in the transitional manoeuvres considered, a higher slip ratio is expected where the traction force and the slip ratio relation is no longer linear. Therefore, the consideration of relaxation length, a transient tyre model, and a nonlinear tyre model need to be used to calculate the tyre forces (e.g. the Pacejka "Magic Formula" model (Wong, 2008)) in this case. The inclusion of the anti-lock braking systems (ABS) can be very useful during vehicle skidding and wheels locking. These important features of a tyre model are recommended for future work.

It was found that while travelling on a slope (vehicle following mode) the ACC was unable to achieve the control objectives. The reason found that the road gradient information was not considered in the lower-level controller formulation. Therefore, it is suggested for the future work that road gradient should be taken in account in order to compute the required throttle or brake commands.

The proposed complex vehicle model can be further analysed for the lateral dynamic control if a lateral model is included. But, in this case the proposed tyre model will not be suitable because only a small slip ratio is considered in the tyre modelling. Furthermore, an advance brake system, anti-lock brake system, is recommended in this case to control the steering and braking at the same time under the TMs.

The proposed complex ACC vehicle model can be used for different applications, e.g. obstacle avoidance, for pedestrian safety measures, the driver behaviour model analysis, and hybrid vehicle analysis (if the powertrain model is modified). This two-vehicle model can be further extended for more than two vehicles in order to analyse the string stability of a platoon of ACC vehicles. It can help to understand the ACC behaviour in other critical situations, e.g. sensor failure, under bad weather

conditions (raining, snow). It can help to understand the behaviour of brake actuators and how the operational constraints control the ACC vehicle dynamic behaviour.

In the MPC algorithm, a linear prediction model has been considered. A higher length of prediction horizon results in the best closed-loop performance and an increased weighting on the control input reduce the errors. It has been considered that the reference path is equal to the set path trajectory. For a superior path following a nonlinear prediction model is recommended, although the linear model is computationally efficient and the nonlinear model requires higher sampling time (T) for the online computation but due to nature of the vehicle model a nonlinear prediction should be used. The nonlinear characteristics of the prediction model can compensate for the nonlinearities neglected in the lower-level controller which can give a more realistic response. This is recommended for future work.

Bibliography:

Ali, Z, Popov, A, A and Charles, G (2010). Transition Controller for Adaptive Cruise Control System. AVEC 10, 10th International Symposium on Advanced Vehicle Control. Loughborough, UK.

Bageshwar, V.L., Garrard, W.L. and Rajamani, R. (2004). "Model Predictive Control of Transitional Maneuvers for Adaptive Cruise Control Vehicles." IEEE Transactions on Vehicular Technology **53**(5): 1573-1585.

Bertrand, D. (2006). "Estimating maximum friction coefficient based on knowledge of the loads and self-alignment torque generated in a tire contact zone." from www.freepatentsonline.com/7069135.html.

Bhatti, A. I., Spurgeon, S. K., Dorey, R. and Edwards, C. (1999). "Sliding mode configuration for automotive engine control." International Jounal of Adaptive Control and Signal Processing **13**: 49-69.

Bleek, R. (2007). Design of a Hybrid Adaptive Cruise Control Stop-&-Go system, Technische Universiteit Eindhoven.

Camacho, E.F. and Bordons, C. (2004). Model Predictive Control. London, Springer.

Canudas de Wit, C. and Brogliato, B. (1999). Stability Issues for Vehicle Platooning in Automated Highway Systems. Proceedings of the IEEE International

Conference on Control Applicalions, Kohala Coast-Island of Hawai'i, Hawai'i, USA.

Chaing, W., Zhu, L. and Patankar, R. (2007). "Mean Value Engine Modeling and Validation for a 4-stroke, Single Cylinder Gasoline Engine." Trends in Applied Sciences Research **2**(2): 124-131.

Chen, C-K. and Shih, M-C. (2004). "PID-Type Fuzzy Control for Anti-Lock Brake Systems with Parameter Adaptation." JSME International Journal **47**(2): 675-685.

Cho, D. and Hedrick, J.K. (1989). "Automotive Powertrain Modeling for Control." Transactions of the ASME **111**: 568-576.

Connolly, T.R. and Hedrick, J.K. (1999). "Longitudinal Transition Maneuvers in an Automated Highway System." Journal of Dynamic Systems, Measurement, and Control **121**: 471-478.

Cook, J.A. and Powell, B.K. (1988). "Modelling of an Internal Combustion Engine for Control Analysis." IEEE Control Systems Magazine: 20-26.

Corona, D. and Schutter, B.D. (2008). "Adaptive Cruise Control for a SMART Car: A Comparison Benchmark for MPC-PWA Control Methods." IEEE Transactions on Control Systems Technology **16**(2): 365-372.

Dorf, R.C. and Bishop, R.H. (2001). Modern Control Systems. New Jersey, Prentice Hall

Edwards, C. and Spurgeon, S.K. (1998). Sliding Mode Control: Theory and Applications. London, Taylor & Francis

Feng, Q., Yin, C. and Zhang, J. (2005). "A Transient Dynamic Model for HEV Engine and its implementation for Fuzzy-PID Governor." IEEE Robotics and Automation Magazine: 73-78.

Fenton, R.E. (1994). "IVHS/AHS: Driving into the Future." IEEE Control Systems **14**(6): 13-20.

Ferrara, A. and Vecchio, C. (2007). "Collision Avoidance Strategies and Coordinated Control of Passenger Vehicles." Nonlinear Dynamics **49**( ): 475-492.

Fling, R.T. and Fenton, R.E. (1981). "A Describing-Function Approach to Antiskid Design." IEEE Transactions on Vehicular Technology **30**(3): 134-144.

Franklin, G.F., Powell, J.D. and Emami-Naeini. (2006). Feedback Control of Dynamic Systems, Pearson Prentice Hall.Fifth Edition

Ganguli, A. and Rajamani, R. (2004). "Tractable model development and system identification for longitudinal vehicle dynamics." Proc. Instn Mech. Engrs Part D Automobile Engineering **218**: 1077-1084.

Gerdes, J.C. and Hedrick, J.K. (1996). Brake System Requirements for Platooning on an Automated Highway. Proceedings of the American Control Conference. Washington.

Gerdes, J.C. and Hedrick, J.K. (1997). "Vehicle speed and spacing control via coordinated throttle and brake actuation." Control Eng. Practice **5**(11): 1607-1614.

Girard, A.R., Spry, S. and Hedrick, J.K. (2005). "Intelligent Cruise-Control Applications." IEEE Robotics and Automation Magazine: 22-28.

Goetz, M., Levesley, M, C. and Crolla, D, A. (2005). "Dynamics and control of gearshifts on twin-clutch transmissions." Proc. IMechE, Automobile Engineering **219**: 951-963.

Gorski, E. (2008). "2008 Formula SAE Detailed Design Document."

Han, W. and Yi, S-J. (2003). "A study of shift control using the clutch pressure pattern in automatic transmission." Proc Instn Mech Engrs, Automobile Engineering **217**: 289-298.

Haney, P.R. and Richardson, M.J. (2000). "Adaptive Cruise Control, System Optimisation and Development for Motor Vehicles." The Journal of Navigation **53**(01): 42-47.

Harris, W. and Beckman, J. (2010). "How Dual-clutch Transmissions Work." from http://auto.howstuffworks.com/dual-clutch-transmission.htm.

Hedrick, J.K., Gerdes, J.C., Maciuca, D.B. and Swaroop, D. (1997). Brake system Modeling, Control And Integrated Brake/throttle Switching Phase I. California PATH Research Report. California, Berkeley, University of California, Berkeley.

Hedrick, J.K., McMahon, D.H. and Swaroop, D. (1993). Vehicle Modeling and Control for Automated Highway System. California PATH Program, Institute of Transportation Studies. Berkeley, University of California.

Heywood, J.B. (1988). Internal Combustion Engine Fundamentals, McGraw-Hill

Hong, C-W. (1996). "Dynamic simulation of road vehicle performance under transient accelerating conditions." Proc Instn Mech Engrs **210**: 11-21.

Huang, A-C. and Chen, Y.J. (2001). "Safe Platoon Control of Automated Highway Systems." Proc Instn Mech Engrs Part I **215**(5): 531-543.

Ioannou, P. (2003). "Guest Editorial Adaptive Cruise Control Systems Special Issue." IEEE Transactions on Intelligent Transportation Systems **4**(3): 113-114.

Kato, S., Tsugawa, S., Tokuda, K., Matsui, T. and Fujii, H. (2002). "Vehicle Control Algorithms for Cooperative Driving with Automated Vehicles and

Intervehicle Communications." IEEE Transactions on Intelligent Transportation Systems **3**(3): 155-161.

Kulkarni, M., Shim, T. and Zhang, Y. (2006). "Shift dynamics and control of dual-clutch transmissions " Mechanism and Machine Theory **42**: 168-182.

Lee, Y., Park, S., Lee, M. and Brosilow, C. (1998). "PID Controller Tuning for Desired Closed-Loop Responses for SI/SO Systems." AIChE Journal **44**(1): 106-115.

Li, S., Li, k., Rajamani, R. and Wang, J. (2010). "Model Predictive Multi-Objective Vehicular Adaptive Cruise Control." IEEE Transactions on Control Systems Technology **18**(6): 1-11.

Li, S., Li, K. and Wang, J. (2010). Development and Verification of Vehicular Multi-Objective Coordinated Adaptive Cruise Control Systems. AVEC 10. Loughborough University, UK.

Liang, C-Y. and Peng, H. (1999). "Optimal Adaptive Cruise Control with Guaranteed String Stability." Vehicle System Dynamics **31**: 313-330.

Liang, H., Chong, K.T., No, S, T. and Yi, S-Y. (2003). "Vehicle longitudinal brake control using variable parameter sliding control." Control Eng. Practice **11**: 403-411.

Maciejowski, J.A. (2002). Predictive Control with Constraints, Prentice Hall

Maciuca, D.B., Gerdes, J.C. and Hedrick, J.K. (1994). Automatic Braking Control for IVHS. Proceedings International Symposium on Advanced Vehicle Control (*AVEC 94)*. Tsukuba, Japan.

Maciuca, D.B. and Hedrick, J.K. (1995). Advanced nonlinear brake system control for vehicle platooning. Proceedings of the third European Control Conference, Rome, Italy.

Magni, L., Raimondo, D.M. and Allgower, F. (2009). Nonlinear Model Predictive Control. Berlin, Springer

Martinez, J-J. and Canudas de Wit, C. (2007). "A Safe Longitudinal Control for Adaptive Cruise Control and Stop-and-Go Scenarios." IEEE Transactions on Control Systems Technology **15**(2): 246-258.

Mayne, D.Q., Rawlings, J.B., Rao, C.V. and Scokaert, P.O.M. (1999). "Constrained Model Predictive Control: Stability an Optimality." Automatica **36**: 789-814.

Murdocco, V., Albero, D. and Carrea, Paola. (2000). "Control of longitudinal vehicle motion for adaptive cruise control and Stop & Go applications." Proc. ITS, Torino.

Naranjo, J.E., Gonzalez, C., Reviejo, J., Garcia, R. and Pedro, T. (2003). "Adaptive Fuzzy Control for Inter-Vehicle Gap Keeping." IEEE Transactions on Intelligent Transportation Systems **4**(3): 132-142.

Ni, D. and Henclewood, D. (2008). "Simple Engine Models for VII-Enabled In-Vehicle Applicationss." IEEE Transactions on Vehicular Technology **57**(5): 2695-2702.

O'Dwyer, A. (2009). Handbook of PI and PID Controller Tuning Rules. London, Imperial College Press.3rd

Peppard, L.E. (1974). "String Stability of Relative-Motion PID Vehicle Control Systems." IEEE Transactions on Automatic Control **19**(5): 579-581.

Powell, B, K. (1979). "A Dynamic Model for Automotive Engine Control Analysis." Proc. 18th IEEE Conf. Decision and Control.

Puleston, P.F., Spurgeon, S. K. and Monsees, G. (2001). "Automotive Engine Speed Control: A Robust Nonlinear Control Framework." IEE Proc.-Control Theory Appl. **148**(1): 81-87.

Rajamani, R. (2006). Vehicle Dynamics and Control. Mechanical Engineering Series. New York, Springer.

Rajamani, R., Choi, S.B., Law, B.K., Hedrick, J.K., Prohaska, R. and Kretz, P. (2000). "Design and Experimental Implementation of Longitudinal Control for a Platoon of Automated Vehicles." Transactions of the ASME **122**: 470-476.

Rajamani, R. and Zhu, C. (2002). "Semi-Autonomous Adaptive Cruise Control Systems." IEEE Transactions on Vehicular Technology **51**(5): 1186-1192.

Ramli, M.Md. and Morris, A.A. (1991). A nonlinear mathematical engine model for the development of dynamic engine control. Eigth International Conference on Automotive Electronics. London, UK.

Report. (1992). United States Department of Transportation, *NHTSA, FARS and GES*, "Fatal Accident Reporting System (FARS) and General Estimates System (GES), ".

Richard, A. and How, J.P. (2005). "Model Predictive Control of Vehicle Maneuvers with Guaranteed Completion Time and Robust Feasibility." Proceedings of the American Control Conference.

Rowell, S. (2007). Modelling the Control Strategies for Riding a Motorcycle. Nottingham, PhD thesis, University of Nottingham.

Rowell, S., Popov, A. A. and Meijaard, J.P. (2008). Parameter Study of Motorcycle Riding by Model Predictive Control AVEC 08, 9th International Symposium on Advanced Vehicle Control. Japan.

Runde, J, K. (1984). Modelling and control of an automatic transmission. Massachusetts, B.S.M.E, Purdue University.

Sheikholeslam, S. and Desoer, C.A. (1993). "Longitudinal Control of a Platoon of Vehicles with no Communication of Lead Vehicle Information: A System Level Study." IEEE Transactions on Vehicular Technology **42**(04): 546-554.

Shladover, S.E. (1991). "Longitudinal Control of Automative Vehicles in Close-Formation Platoons." Journal of Dynamic Systems, Measurement, and Control **113**( ): 231-241.

Shladover, S.E. (2005). "Automated Vehicles for Highway Operations (Automated Highway Systems)." Proc. IMechE Systems and Control Engineering **219**: 53-75.

Short, M., Pont, M, J. and Huang, Q. (2004). Simulation of Vehicle Longitudinal Dynamics. Safety and Reliability of Distributed Embedded Systems. Leicester, University of Leicester.

Solyom, S., Rantzer, A. and Ludemann, J. (2004). "Synthesis of a Model-Based Tire Slip Controller." Vehicle System Dynamics **41**(6): 475-499.

Sun, M., Lewis, F.L. and Ge, S.S. (2004). Platoon-Stable Adaptive Controller Design. 43rd IEEE Conference on Decision and Control. Atlantis, Paradise Island, Bahamas**:** 5481-5486.

Swaroop, D. (1997). String Stability of Interconnected Systems: An Application to Platooning in Automated Highway Systems. Berkeley, University of Cailfornia.

Swaroop, D. and Hedrick, J.K. (1999). "Constant Spacing Strategies of Platooning in Automated Highway Systems." Transactions of the ASME **121**: 462-470.

Swaroop, D., Hedrick, J.K. and Choi, S.B. (2001). "Direct Adaptive Longitudinal Control of Vehicle Platoons." IEEE Transactions on Vehicular Technology **50**(1): 150-161.

BIBLIOGRAPHY

Terzano, D.O. (2001). Simulation of Flow Control Algorithm for Multi-Lane Automated Highway Systems. Florida, University of Florida.

Troppmann, R. and Hoger, A. (2006). "Driver Assistance Systems, an introduction to Adaptive Cruise Control: Part 1." from http://www.eetimes.com/design/automotive-design/4011081/Tech-Tutorial-Driver-Assistance-Systems-an-introduction-to-Adaptive-Cruise-Control-Part-1.

Unknown. (2008). "Use of Advanced In-Vehicle Technology by Young and Older Early Adopters: Survey Results on Adaptive Cruise Control Systems." from www.aaafoundation.org.

Unknown. (2009). "Department for Transport, Regional Transport Statistics in Great Britain." from www.dft.gov.uk.

Utkin, V (2008). Sliding Mode Control: Mathematical Tools, Design and Applications. Nonlinear and Optimal Control Theory. USA, Spinger Berlin/Heidelberg. **1932/2008:** 289-347.

Utkin, V., Guldner, J. and Shi, J. X. (1999). Sliding Mode Control in Electromechanical Systems. London, Taylor & Francis

Visioli, A. (2006). Practical PID Control. London, Springer

Wang, J. and Rajamani, R. (2004). "The impact of adaptive cruise control systems on highway safety and traffic flow." Proc Instn Mech. Engrs **218**: 111-130.

Wang, L. (2009). Model Predictive Control System Design and Implementation Using Matlab, Springer.

Wong, J.Y. (2001). Theory of Ground Vehicles, John Wiley & Sons.3rd Edition

Wong, J.Y. (2008). Theory of Ground Vehicles, John Wiley & Sons.Fourth Edition

Wu, S., Zhu, E., Li, Q., Xie, J. and Peng, X. (2008). Study on Intelligent Shift Control Strategy of Automobile Based on Genetic-fuzzy Algorithm. The 3rd International Conference on Innovative Computing Information and Control (ICICIC'08).

Yi, J. and Horowitz, R. (2002). Macroscopic Traffic Flow Stability for Adaptive Cruise Controlled (ACC) Vehicles. Proceedings of the 41st IEEE Conference on Decision and Control, Las Vegas, Nevada USA.

Yi, K. and Chung, J. (2001). "Nonlinear Brake Control for Vehicle CW/CA Systems." IEEE/ASME TRANSACTIONS ON MECHATRONICS **6**(1): 17-25.

Yi, S-Y. and Chong, K-T. (2005). "Impedance Control for a Vehicle Platoon System." Mechatronics **15**(5): 627-638.

Zhang, N., Liu, D, K., Jeyakumaran, J, M. and Villanueva, L. (2002). "Modelling of dynamic characteristics of an automatic transmission during shift changes." Proc Instn Mech Engrs, Systems and Control Engineering **216**: 331-341.

Zlocki, A. and Themann, P. (2010). Improved energy efficiency by model based predictive ACC in hybrid vehicles based on map data. AVEC 10. Loughborough University, UK.